CELLULAR MECHANISM OF BICARBONATE REGULATION AND EXCRETION IN AN INSECT INHABITING EXTREMES OF ALKALINITY

by

KEVIN STRANGE

B.Sc., University of California, Davis, 1977

M.A., University of California, Davis, 1978

A THESIS SUBMITTED IN PARTIAL FULFILMENT OF

THE REQUIREMENTS FOR THE DEGREE OF

DOCTOR OF PHILOSOPHY

in

THE FACULTY OF GRADUATE STUDIES

DEPARTMENT OF ZOOLOGY

We accept this thesis as conforming to

the required standard

THE UNIVERSITY OF BRITISH COLUMBIA

May 1983

In presenting this thesis in partial fulfilment of the requirements for an advanced degree at the University of British Columbia, I agree that the Library shall make it freely available for reference and study. I further agree that permission for extensive copying of this thesis for scholarly purposes may be granted by the head of my department or by his or her representatives. It is understood that copying or publication of this thesis for financial gain shall not be allowed without my written permission.

Department of Zoology

The University of British Columbia
1956 Main Mall
Vancouver, Canada
V6T 1Y3

Date July 4, 1983

ABSTRACT

The saltwater mosquito larva, Aedes dorsalis, is one of the only organisms capable of inhabiting hypersaline lakes composed almost entirely of high concentrations of $NaHCO_3$ and Na_2CO_3 salts. Under laboratory conditions larvae survived and developed normally in saline media with pH values up to 10.5, HCO_3^- concentrations up to 250 mM, or CO_3^{2-} concentrations up to 100 mM. Despite ingestion of these alkaline media at rates equivalent to 130% of larval body weight per day, these insects regulated hemolymph pH (7.55-7.70) and HCO_3^- concentrations (8.0 - 18.5 mM) within narrow physiological limits. Micropuncture and microcannulation studies on the rectal salt gland demonstrated that this organ was an important site of pH and HCO_3^- regulation. Microcannulated salt glands secreted a strongly hyperosmotic fluid containing 402 mM HCO_3^- and 41 mM CO_3^{2-} at a rate of 38 $nl \cdot h^{-1}$. Lumen-to-bath HCO_3^- and CO_3^{2-} gradients of 21:1 and 241:1, respectively, were generated by the salt gland epithelium against a transepithelial potential of -25 mV (lumen negative) demonstrating clearly the active nature of HCO_3^- secretion.

To study the mechanisms of HCO_3^- transport, an in vitro microperfused rectal salt gland preparation was developed. Net total CO_2 transport ($J_{net}^{CO_2}$) as measured by microcalorimetry in perfused salt glands was unaffected by bilateral Na^+ or K^+ and serosal Cl^- substitutions, or by serosal addition of 1.0 mM ouabain, 2.0 mM amiloride or 0.5 mM SITS. Removal of luminal Cl^- inhibited $J_{net}^{CO_2}$ by 80%, while serosal addition of 1.0 mM acetazolamide or 0.5 mM DIDS inhibited $J_{net}^{CO_2}$ by 80% and 40%, respectively.

Perfusion of the anterior and posterior rectal segments demonstrated clearly that the anterior rectum was the site of CO_2 secretion in

the microperfused salt gland. Net Cl^- reabsorption in the anterior segment was measured by electron microprobe analysis and was equivalent to the rate of CO_2 secretion. In addition, Cl^- reabsorption in the anterior segment was completely inhibited by bilaterally replacing CO_2 and HCO_3^- with a phosphate or HEPES buffered saline. These data provide strong quantitative evidence for the presence of a 1:1 Cl^-/HCO_3^- exchange mechanism located in the anterior rectal salt gland segment.

Microcannulation studies on the individual salt gland segments demonstrated that both rectal segments are capable of secreting a hyperosmotic fluid containing Na^+, Cl^- and HCO_3^-. Based on these results and the results of studies in which the effects of serosal ion substitutions on salt gland fluid secretion were examined, it has been suggested tentatively that both segments secrete a NaCl-rich fluid and that fluid secretion is driven by coupled NaCl transport. It is further suggested that once this fluid enters the salt gland lumen its composition is modified by ion exchange and reabsorptive processes which are dependent upon the ionic regulatory needs of the animal. In larvae inhabiting low Cl^-, $NaHCO_3$-CO_3 lakes, this modification involves a 1:1 exchange of luminal Cl^- for serosal HCO_3^-.

The cellular mechanisms of anterior salt gland HCO_3^- and Cl^- transport were examined using ion and voltage-selective microelectrodes in conjunction with a microperfused anterior segment preparation which allowed complete changes in serosal and mucosal saline composition to be made in <5-10 seconds. Addition of DIDS or acetazolamide to or removal of CO_2 and HCO_3^- from the serosal bath caused large, 20-50 mV hyperpolarizations of V_a and had little effect on V_{bl}. Rapid changes in luminal Cl^- concentration altered V_a in a rapid, step-wise manner. The slope of the

relationship between V_a and luminal Cl^- activity was 42.2 mV/decalog $a^l_{Cl^-}$ ($r = 0.992$). Intracellular Cl^- activity was 23.5 mM and was approximately 10 mM lower than that predicted for a passive distribution at the apical membrane. Changes in serosal Cl^- concentration had no effect on V_{bl} indicating an electrically silent basolateral Cl^- exit step. Intracellular pH in anterior rectal cells was 7.67 and the calculated $a^c_{HCO_3^-}$ was 14.4 mM. These results show that under control conditions HCO_3^- enters the anterior rectal cell by an active mechanism against an electrochemical gradient of 77.1 mV and exits the cell at the apical membrane down a favorable electrochemical gradient of 27.6 mV. Based on these results, a tentative cellular model has been proposed in which Cl^- enters the apical membrane of the anterior rectal cells by passive, electrodiffusive movement through a Cl^--selective channel, and HCO_3^- exits the cell by an active or passive electrogenic transport mechanism. The electrically silent nature of basolateral Cl^- exit and HCO_3^- entry, and the effects of serosal addition of the Cl^-/HCO_3^- exchange inhibitor DIDS on $J^{CO_2}_{net}$ and V_{te} suggest strongly that the basolateral membrane is the site of a direct coupling between Cl^- and HCO_3^- movements via a Cl^-/HCO_3^- exchange mechanism.

TABLE OF CONTENTS

	Page
ABSTRACT	i
TABLE OF CONTENTS	iv
LIST OF TABLES	vi
LIST OF FIGURES	vii
LIST OF ABBREVIATIONS	x
ACKNOWLEDGEMENTS	xii
CHAPTER I: GENERAL INTRODUCTION	1
A. Acid-Base Regulation	1
1. Vertebrate Acid-Base Excretion	2
2. Invertebrate Acid-Base Excretion	8
B. Organization of Larval Excretory System	11
CHAPTER II: BICARBONATE REGULATION AND EXCRETION	17
A. Introduction	17
B. Materials and Methods	20
Animals	20
Capillary pH Electrodes	23
Hemolymph pH Measurements	26
Hemolymph HCO_3^- Measurements	26
Rectal Micropuncture Studies	27
Cannulated *in vitro* Rectal Preparation	27
Analysis of Rectal Secretions	31
Transepithelial Potential	31
Calculations	32
C. Results	32
D. Discussion	50
1. Rectal HCO_3^- Secretion	53
CHAPTER III: IONIC REQUIREMENTS OF CO_2 TRANSPORT IN THE MICROPERFUSED RECTAL SALT GLAND	56
A. Introduction	56
B. Materials and Methods	57
Animals	57
Microperfusion System	58
Determination of Net Total CO_2 Flux	61
Salines	62
Inhibitor Studies	65

Page

C. Results..... 66

D. Discussion..... 78

CHAPTER IV: SITE OF CL^-/HCO_3^- EXCHANGE AND FUNCTION OF ANTERIOR AND POSTERIOR SALT GLAND SEGMENTS..... 83

A. Introduction..... 83

B. Materials and Methods..... 84
Animals..... 84
Microperfusion and Microcannulation Studies..... 84
Sample Analysis..... 85
Salines..... 85

C. Results..... 89

D. Discussion..... 102
1. Site of Cl^-/HCO_3^- Exchange..... 102
2. Excretory Functions of Anterior and Posterior Segments.... 103

CHAPTER V: CELLULAR MECHANISM OF BICARBONATE AND CHLORIDE TRANSPORT... 110

A. Introduction..... 110

B. Materials and Methods..... 110
Animals..... 110
Microperfusion System..... 110
Bath and Luminal Solution Changes..... 111
Electrical Measurements..... 115
Microelectrode Impalements..... 118
Salines..... 118

C. Results..... 120
1. Microelectrode Impalements..... 120
2. Electrogenic HCO_3^- Transport..... 128
3. Electrogenic Cl^- Reabsorption..... 149

D. Discussion..... 158
1. Cellular Entry and Exit Steps..... 158
2. Electrochemical Gradients..... 173

CHAPTER VI: GENERAL DISCUSSION..... 179

REFERENCES..... 197

LIST OF TABLES

		Page
Table 2.1	Composition of artificial lake waters in which larvae were reared or acclimated.	21
Table 2.2	Composition of hemolymph and physiological salines for larvae acclimated to different artificial lake waters.	22
Table 2.3	Values of pK_1', pK_2' and S used for calculation of CO_2, HCO_3^- and CO_3^{2-} concentrations.	33
Table 2.4	Concentrations of Ca^{2+}, Mg^{2+}, total sulfur and total phosphorus, and pH in rectal secretions collected by micropuncture.	46
Table 3.1	Composition of physiological salines.	63
Table 3.2	Changes in total CO_2 and Cl^- concentrations in collected perfusates.	64
Table 3.3	Summary of chitinase experiments.	81
Table 4.1	Composition of physiological salines.	88
Table 4.2	Measured fluid secretion rates for whole, cannulated rectal salt glands bathed in various salines.	98
Table 4.3	Ionic composition of rectal secretions.	99
Table 4.4	Calculated rates of Na^+ and Cl^- excretion for cannulated anterior and posterior segments.	105
Table 5.1	Composition of physiological salines.	119
Table 5.2	Calculated Cl^- electrochemical gradients for apical and basolateral cell membranes bathed by control serosal and mucosal salines.	156
Table 5.3	Calculated HCO_3^- electrochemical gradients for apical and basolateral cell membranes bathed by control serosal and mucosal salines.	176
Table 5.4	Intracellular pH and calculated apical membrane electrochemical gradients for H^+ and HCO_3^-.	177

LIST OF FIGURES

		Page
Figure 1.1	Organization of larval gut and excretory system.	12
Figure 1.2	Organization and ultrastructure of rectal salt gland.	14
Figure 2.1	Ultramicro internal capillary pH electrode.	25
Figure 2.2	Microcannulated rectal preparation.	30
Figure 2.3	Survival and development of fourth instar larvae in alkaline environments.	35
Figure 2.4	Drinking rates estimated by ^{14}C-inulin ingestion for fourth instar larvae acclimated to alkaline environments.	38
Figure 2.5	Hemolymph pH regulation in fourth instar larvae during acclimation to high HCO_3^- and CO_3^{2-} media.	40
Figure 2.6	Hemolymph HCO_3^- concentration.	42
Figure 2.7	Osmolality and concentrations of major ions in rectal secretions collected by micropuncture from larvae acclimated to three different alkaline media.	45
Figure 2.8	Osmolality and concentrations of major ions in rectal secretions collected from cannulated recta of animals acclimated to 250 mM HCO_3^- medium.	49
Figure 2.9	Transepithelial potential across cannulated recta from animals acclimated to 250 mM HCO_3^- medium.	52
Figure 3.1	Microperfused rectal salt gland preparation.	60
Figure 3.2	Transepithelial potential and time course determinations of $J_{net}^{CO_2}$ in microperfused rectal salt gland.	68
Figure 3.3	Effects of bilateral Na^+ or K^+ substitutions on $J_{net}^{CO_2}$.	70
Figure 3.4	Effects of luminal and serosal Cl^- substitutions on $J_{net}^{CO_2}$.	73
Figure 3.5	Effects of serosal addition of 1.0 mM ouabain or 2.0 mM amiloride on $J_{net}^{CO_2}$.	75
Figure 3.6	Effects of serosal addition of 0.5 mM SITS, 0.5 mM DIDS or 1.0 mM acetazolamide on $J_{net}^{CO_2}$.	77

		Page
Figure 4.1	Arrangement of pipets and ligatures for microperfusion and microcannulation of individual salt gland segments.	87
Figure 4.2	Changes in perfusate total CO_2 concentration for whole salt glands and individual segments.	91
Figure 4.3	Effects of luminal Cl^- substitution on the change in perfusate total CO_2 concentration from whole salt glands and anterior segments.	93
Figure 4.4	Changes in anterior segment perfusate total CO_2 and Cl^- concentrations and effects of bilateral CO_2 and HCO_3^- substitution with HEPES or phosphate buffered salines on Cl^- reabsorption.	95
Figure 4.5	Rates of fluid secretion in whole, microcannulated salt glands and anterior and posterior segments.	101
Figure 4.6	Summary of major excretory and transport functions of individual salt gland segments.	107
Figure 5.1	Schematic diagram of microperfused anterior rectal salt gland segment and double perfusion pipet arrangement.	113
Figure 5.2	Examples of acceptable cellular impalements obtained with voltage-selective microelectrodes.	122
Figure 5.3	Examples of acceptable impalements obtained with H^+ and Cl^--selective microelectrodes.	125
Figure 5.4	Distribution of V_{bl} and intracellular pH and Cl^- activity in anterior rectal salt gland cells.	127
Figure 5.5	Effects of rapid addition of 1.0 mM acetazolamide to the serosal bathing saline on V_{te}.	130
Figure 5.6	Effects of addition of 0.5 mM DIDS to the serosal bathing saline on V_{te} in 4 separate anterior rectal salt gland preparations.	132
Figure 5.7	Effects of serosal CO_2 and HCO_3^- replacement with a 5.0 mM HEPES buffered saline on V_{te}.	135
Figure 5.8	Effects of replacing serosal CO_2 and HCO_3^- with the lipid soluble buffer, glycodiazine, on V_{te}.	138
Figure 5.9	Transepithelial potential and V_{bl} during and after addition of 1.0 mM acetazolamide to the serosal bathing saline.	140

Page

Figure 5.10 Effects of serosal CO_2 and HCO_3^- replacement with the lipid soluble buffer, glycodiazine, on V_{bl} and V_{te}. 142

Figure 5.11 Changes in V_{bl} and V_{te} during and after replacement of serosal CO_2 and HCO_3^- with a 5.0 mM HEPES buffered saline. 144

Figure 5.12 Effects of high serosal HCO_3^- concentration at constant pH on V_{bl} and V_{te}. 146

Figure 5.13 Effects of luminal Na^+ or K^+ substitutions on V_{te} and V_{bl}. 148

Figure 5.14 Effect of serosal CO_2 and HCO_3^- substitution on V_{bl} and V_{te} during perfusion of salt gland lumen with Cl^--free salines. 151

Figure 5.15 Effects of rapid changes in luminal Cl^- concentration on V_{te} and V_{bl}. 153

Figure 5.16 Relationship between the log of the luminal Cl^- activity and V_a. 155

Figure 5.17 Effects of rapid changes in serosal Cl^- concentration on V_{bl}. 160

Figure 5.18 Effects of rapid changes in serosal K^+ concentration on V_{bl}. 162

Figure 5.19 Tentative cellular model of HCO_3^- and Cl^- entry and exit steps in anterior rectal salt gland cells. 164

Figure 5.20 Effects of bilateral CO_2 and HCO_3^- replacement with either a phosphate, HEPES or glycodiazine buffered saline on the change in anterior segment perfusate Cl^- concentration. 169

Figure 5.21 Tentative scheme showing proposed proton shuttling effects of glycodiazine buffer. 172

LIST OF ABBREVIATIONS

PCO_2	- partial pressure of CO_2 gas.
Δ	- read as, change in.
$[i]$	- concentration of "i".
a_i	- chemical activity of an ion ("i").
a_i^l, a_i^s, a_i^c	- chemical activity of an ion in the luminal, serosal and intracellular compartments, respectively.
pH_c	- intracellular pH.
J_{net}^i	- net flux of an ion ("i").
V_{te}	- transepithelial electrical potential (Ψmucosa - Ψserosa).
V_{bl}	- basolateral membrane potential (Ψcell - Ψserosa).
V_a	- apical membrane potential (Ψcell - Ψmucosa).
$\Delta\tilde{\mu}_i$	- electrochemical gradient for an ion ("i").
$\Delta\tilde{\mu}_i^a$, $\Delta\tilde{\mu}_i^{bl}$	- electrochemical gradient for an ion ("i") at the apical and basolateral membranes, respectively.
V_i	- voltage output from an ion-selective microelectrode.
Ω	- ohms.
μ	- micron.
nl	- nanoliter.
mV	- millivolt.
K_1'	- the overall apparent equilibrium constant between dissolved CO_2 and $H^+ + HCO_3^-$.
pK_1'	- the negative logarithm of K_1'.
pK_2'	- the negative logarithm of the apparent equilibrium constant between HCO_3^- and $CO_3^{2-} + H^+$.
S	- CO_2 solubility coefficient.
I.D.	- inner diameter.
O.D.	- outer diameter.

SITS	- 4-acetamido-4'-isethiocyanostilbene-2, 2'-disulfonic acid (an inhibitor of anion exchange mechanisms).
DIDS	- 4, 4'-diisothiocyano-2, 2'-disulfonic acid (an inhibitor of anion exchange mechanisms).
HEPES	- N-2-hydroxyethyl piperazine-N'-2-ethanesulfonic acid (a weak acid buffering compound).

ACKNOWLEDGEMENTS

I would like to thank my research supervisor, Dr. John Phillips, for providing me with the academic freedom and financial means to pursue my own ideas and for useful comments and discussion throughout the course of this work.

I am also indebted to and would like to thank the following people:

Dr. Walter Boron for valuable instruction in microelectrode techniques and the many individuals at Yale University who shared with me their extensive knowledge of *in situ* and *in vitro* microperfusion methods;

Dr. G.G.E. Scudder for purchasing and allowing me exclusive use of the Picapnotherm;

Dr. Tom Mommsen for many useful discussions and for suggesting the use of and collecting spider digestive juices;

Dr. Mary Chamberlin for her invaluable distortions of reality, for making the laboratory a stimulating environment during the first three years of my stay at U.B.C., and for introducing me to Mr. P. Head;

Mr. P. Head for his technical support and exceptionally wise counsel;

Joan Martin for useful comments and discussion, for suggesting the use of the 10 μ ligatures, and for her companionship;

My research committee, Drs. B. Milsom, J. Gosline and D. Randall for useful comments concerning the final form of this manuscript;

Christine McCaffrey and Dr. G.A. Quamme for electron microprobe analyses;

Mr. Ken Pope of Vancouver General Hospital for his truly superb job and craftsmanship in constructing the microperfusion pipet holder described in Chapter V;

Don Brandys and Fergus O'Hara for building me countless pieces of equipment;

Kathy Gorkoff for her outstanding job in typing this manuscript and for helping me finish on time;

Bob Latrace for being here and having Stores open at 7:30 a.m.!

Finally, I would particularly like to thank Tom Baumeister, Katy Farley, Matt and Joey Jones, Rich Moore, Terri Scemons and Lynn Vasington for their friendship and support, and for providing me with the all-too-infrequent incentives to play instead of work.

CHAPTER I. GENERAL INTRODUCTION

A. Acid-Base Regulation

Almost every biochemical reaction that occurs in a living organism is affected by the H^+ concentration of the surrounding medium. The acid-base status of both intracellular and extracellular fluids must be maintained within a very narrow range in order for these reactions to proceed at optimal rates and to allow their integration into complex physiological functions.

Short-term defense against changes in acid-base balance is provided first by intracellular and extracellular buffers. In addition, buffering by organ systems such as bone (Robinson, 1975), calcareous exoskeletons (Henry, Kormanik, Smatrisk and Cameron, 1981; Randall and Wood, 1981), the lime sacs of frogs (Robertson, 1972) and calcareous shells of molluscs (Dugal, 1939; Burton, 1976) and turtles (Jackson and Ultsch, 1982) aid in correcting acid-base disturbances. Long-term pH regulation, however, must be mediated by elimination of acids and bases. In single celled organisms and individual cells this process is carried out by well defined membrane transport mechanisms and possibly by specific metabolic pathways (Cohen and Iles, 1975; Roos and Boron, 1981; Sanders and Slayman, 1982). Long-term extracellular acid-base homeostasis in multicellular organisms is maintained by the respiratory and excretory systems, and perhaps by metabolic functions of the gut, muscle, and liver or analogous organs.

The individual roles played by these various organ and buffer systems in acid-base regulation are highly complex and dependent upon an organism's physiological state. Attempts to summarize these mechanisms are beyond the scope of the current work and instead, only a discussion of excretory acid-base regulation is warranted.

1) Vertebrate Acid-Base Excretion

The role of the mammalian kidney in acid-base homeostasis has been studied extensively (for recent reviews see Malnic and Giebisch, 1979; Warnock and Rector, 1979, 1981; Malnic, 1981; Berry and Warnock, 1982) and the kidney has been shown clearly to respond to conditions of acidosis and alkalosis in a compensatory manner (reviewed by Cogan, Rector and Seldin, 1981). Controlled reabsorption of filtered HCO_3^- by the nephrons and concomitant urine acidification is quantitatively the most important means of urinary acid-base excretion. The bulk (80-90%) of HCO_3^- reabsorption occurs in the proximal convoluted tubule while smaller amounts are reabsorbed in the proximal straight and distal tubules. The collecting tubule also plays a role in acid-base regulation and is capable of acidifying (McKinney and Burg, 1977a, 1978a; Lombard, Jacobson and Kokko, 1979; Richardson and Kunau, 1981; DuBose, 1982; Koeppen and Helman, 1982) or alkalinizing (McKinney and Burg, 1977a, 1978b) the final urine depending upon physiological conditions.

The kidney additionally functions in acid-base regulation by excreting protons bound to nonvolatile buffers such as phosphate and ammonia. Indeed, this is thought to be quantitatively far more important than excretion of unbound H^+ since the maximal urine to blood pH gradient generated by mammalian kidneys is only approximately 2.0 pH units.

As originally suggested by Pitts (1948), ammonia is the primary buffer involved in urinary acid-base excretion. Ammonia is synthesized in the tubule cell as NH_3 from glutamine and other amino acids. Because of its small size and lack of charge, NH_3 is thought to diffuse freely into the urine and peritubular blood. Since the urine is more acidic than either the blood or cell interior, NH_3 is trapped in the tubule lumen as it rapidly buffers secreted H^+ to form NH_4^+. This 'acid trapping' of NH_3 as NH_4^+

maintains a constant downhill gradient for NH_3 diffusion at the luminal cell membrane and results in net NH_4^+ excretion (reviewed by Pitts, 1974; Rector, 1976; Warnock and Rector, 1981).

Recently, the concept of ammoniagenesis and 'acid trapping' has been questioned by Atkinson and Camien (1982). These authors were apparently unaware of an extensive literature describing several decades of intense research on the subject (reviewed by Balagura-Baruch, 1971; Cohen and Kamm, 1976; Hems, 1975; Stoff, Epstein, Narins and Relman, 1976; Klahr and Schoolwerth, 1977; Tannen, 1978; Warnock and Rector, 1981) and instead have based their criticism on the simple observation that glutamine catabolism to glutamate produces equivalent amounts of NH_3 and H^+. As such, the authors point out that there can be no net acid excretion by the kidney and they claim the kidney plays little role in acid-base regulation. These authors failed to consider, however, the obvious possibility of further glutamine metabolism. In reality, glutamine is first converted to glutamate and then to α-ketoglutorate producing two NH_3 and two H^+. Alpha-ketoglutorate is metabolized primarily to glucose or catabolized to CO_2 and H_2O (see for example, Krebs and Vinay, 1975; Cheema-Dhadli and Halperin, 1978; Venay, Lemieux and Gorugoux, 1979). During the process the two H^+ are consumed resulting in net NH_3 synthesis and providing the basis for net urinary ammonia and acid excretion as NH_4^+.

Acid-base excretion in amphibians depends on the coordinated functions of the kidney, urinary bladder, skin and in some cases, the gills. Little is known about the role of the amphibian kidney in acid-base regulation which is surprising given the utility of this organ in studies of cellular mechanisms of renal transport. Early micropuncture studies in the frog and Necturus (Montgomery and Pierce, 1937; Walker, 1940) suggested that

the kidney was involved in urinary acidification and ammonia excretion. Yoshimura, Yata, Yuasa and Wolbach (1961) have shown that the frog kidney responds in a compensatory manner to acidosis. More recently, O'Regan, Malnic and Giebisch (1982) have shown urinary acidification in Necturus proximal tubule and Boron and Boulpaep (1983a,b) have described a cellular mechanism in Ambystoma proximal tubule which they believe is involved in both intracellular pH regulation and urinary acidification (discussed in Chapter VI).

The role of the amphibian skin in acid-base balance can be inferred from its ability to excrete H^+ (Huf, Parrish and Weatherford, 1951; Fleming, 1957; Garcia-Romeu, Salibian and Pezzani-Hernandez, 1969; Emilio, Machado and Menano, 1970; Ehrenfeld and Garcia-Romeu, 1977), NH_4^+ (Fanelli and Goldstein, 1964; Vanatta and Frazier, 1980) and HCO_3^- or OH^- (Garcia-Romeu, 1971; Ehrenfeld and Garcia-Romeu, 1978; Vanatta and Frazier, 1981), and by the ability of the animal to alter this excretion in response to acid-base disturbances (Vanatta and Frazier, 1980, 1981). Amphibian gills are similarly capable of excreting NH_4^+ and HCO_3^- or OH^- (Dietz and Alvarado, 1974) and may also be involved in acid-base homeostasis.

The most extensively studied acid-base excretory organ in amphibians is the toad urinary bladder (reviewed by Steinmetz, 1974; Leaf, 1982). This organ excretes H^+, NH_4^+ and HCO_3^- or OH^- (Frazier and Vanatta, 1971, 1972, 1973; Ludens and Fanestil, 1972; Fitzgerrel and Vanatta, 1980), and compensatory changes in the excretion of these ions are observed during acid-base imbalances (Frazier and Vanatta, 1971, 1973; Fitzgerrel and Vanatta, 1980). In addition, acid and base excretion may be under hormonal and neural control (Frazier and Zachariah, 1979; Frazier and

Vanatta, 1980) in the bladder further implicating it as an important pH regulatory site.

Only a few indirect studies have examined renal acid and base excretion in reptiles and the results suggest that the kidney may be involved in acid-base homeostasis. For example, in the alligator and crocodile kidneys, NH_4^+ and HCO_3^- are secreted in exchange for Na^+, K^+ and Cl^-, and the major salt in the final urine is NH_4HCO_3 (Coulson and Hernandez, 1959; Schmidt-Nielsen and Skadhauge, 1967). The excretion of NH_4HCO_3 is thought to be involved primarily in elimination of excess water and in salt conservation since the renal tubules of these animals have a limited capacity for establishing and maintaining a high urine-to-plasma osmotic gradient (Schmidt-Nielsen and Skadhauge, 1967). Observations of Coulson and Hernandez (1959, 1961) suggest, however, that excretion of NH_4HCO_3 may also be linked to acid-base regulation. Dantzler (1969) has observed patterns of urinary acidification in freshwater snakes similar to those observed in mammalian nephrons and he has suggested that the tubule cells play an important role in H^+ excretion and HCO_3^- reabsorption. In addition, Minnich (1972) has provided evidence which suggests that urinary acid excretion in reptiles is influenced by diet in a pattern similar to that observed for mammals (Long and Giebisch, 1979).

Uric acid is the most important end product of nitrogen metabolism in reptiles (Dantzler, 1978) and the pH of the uric acid/urate buffer system (ca. 5.8) suggests that it could play a role in urinary acid-base excretion. In support of this idea, Dantzler (1968) found that induced alkalosis in the freshwater snake Natrix sipedon increased urate secretion in the form of monobasic urate. Excretion of this form of urate would serve to eliminate excess base from the blood and regulate pH.

Other organs that may be involved in reptilean acid-base homeostasis are the cloaca which excretes both urate and uric acid (House, 1974, cited in Minnich, 1979) and acidifies the final urine (Green, 1969, cited in Minnich, 1979), and the salt gland of herbivorous reptiles which may be a major site for the excretion of dietary base (see Minnich, 1979).

In the turtle kidney the renal medulla and distal nephron are poorly developed and urine acidification and salt and water balance are instead carried out by the urinary bladder. The bladder of freshwater turtles has been the most extensively studied reptilean acid-base excretory organ and is the primary site of urine acidification (reviewed by Steinmetz, 1974) or alkalinization (Brodsky, Durham and Ehrenspeck, 1980; Satake, Durham and Brodsky, 1982) depending on the animal's acid-base status. In addition, in vitro preparations of the bladder have provided the bulk of current information on molecular and cellular mechanisms of urinary acid transport (reviewed by Al-Awqati, 1978; Steinmetz and Anderson, 1982; discussed in Chapter VI).

Only a few studies have been conducted on renal acid and base excretion in birds. Final urine to blood pH gradients generated by the avian kidney are similar to those observed in mammals (Long, 1982) and urinary acidification has been shown to be influenced by the animal's acid-base status (Wolbach, 1955; Sauveur, 1968; Simkiss, 1970) and diet (Okumura and Tasaki, 1968). The avian kidney may also contribute to acid-base balance by excretion of H^+ bound to nonvolatile buffers. Some bird species have been shown to have high urinary ammonia excretion rates, but the major end product of nitrogen metabolism is uric acid (Long, 1982) which may be involved in excretion of acids and bases in a manner similar to that suggested for reptiles (see previous discussion). Prashad and Edwards (1973) have suggested that excretion and titration of phosphate may be a means of acid

excretion in birds during acidosis induced by eggshell calcification.

Acid-base regulation has been studied extensively in fish. The gills perform both acid-base excretory and respiratory functions and the branchial epithelium appears to be the major site of acid, base and ammonia elimination (reviewed by Evans, 1975, 1980; Kirschner, 1979; Evans, Claiborne, Farmer, Mallery and Krasny, 1982; Heisler, 1982). Furthermore, branchial acid and base movements respond to acidotic and alkalotic conditions in a compensatory manner (reviewed by Cameron, 1978a; Heisler, 1980, 1982) indicating that the function of the gills is crucial for acid-base homeostasis.

Comparatively little work has been done on the function of other fish organ systems in acid and base excretion. The skin and the rectal gland appear to play negligible roles in acid-base regulation although few studies have been conducted on these organs (see Heisler, 1982). The function of the kidney in pH balance may vary considerably between species. For example, in the marine teleost, Opsanus beta, Evans (1982) found that the kidney plays a negligible role in acid extrusion. In the freshwater catfish, however, Cameron (1980) and Cameron and Kormanick (1982) demonstrated that renal elimination of acid and base was crucial for recovery from acid-base disturbances. Similarly, Wood and Caldwell (1978) suggested that renal excretion of acid in the freshwater trout could account completely for the observed recovery from a fixed acid load. These species differences may be related to the fact that marine teleosts generally have lower urine flow rates than freshwater fish and have a fixed urine pH which prevents Mg^{2+} precipitation and allows continued Mg^{2+} excretion (see for example, Pitts, 1934; Smith, 1939).

2) Invertebrate Acid-Base Excretion

The only group of invertebrates in which the excretory regulation of acid-base balance has been systematically studied are the Crustacea. In crustaceans, as in fishes, the branchial epithelium performs both respiratory and acid-base excretory functions. Net excretion of acid (Kirschner, Greenwald and Kerstetter, 1973; Ehrenfeld, 1974; Truchot, 1979), base (Ehrenfeld, 1974; Truchot, 1979) and ammonia (Mangum, Sliverthorn, Harris, Towle and Kroll, 1976; Pressley and Graves, 1980; Kormanick and Cameron, 1981; Pequeux and Gilles, 1981) occurs at the gill and fluxes of acid and base change in a compensatory manner dependent upon the acid-base status of the animal (Cameron, 1978b, 1979; Truchot, 1979). The role played by the antennal gland in acid-base regulation may vary considerably between species. For example, in the antennal glands of Callinectes (Cameron and Batterton, 1978) and Carcinus (Truchot, 1979), acid, base and ammonia excretion are negligible. In the Dungeness crab, however, the antennal gland excretes large quantities of HCO_3^- and ammonia, and this organ may be critically important in pH regulation (Wheatly, 1982).

In insects, the mechanisms of acid-base regulation are essentially unknown. The few previous studies of insect acid-base physiology were mainly concerned with determining hemolymph pH, buffering capacity and CO_2 content under a single physiological condition (Craig and Clark, 1938; Hastings and Pepper, 1943; Levenbook, 1950a,b).

The insect excretory system most likely plays the predominant role in acid-base homeostasis. Unlike the vertebrate lung and branchial gill of aquatic organisms, the insect respiratory system outwardly appears to be poorly designed for acid-base regulatory functions. A series of air-filled tubes, the trachae, deliver O_2 directly to insect tissues and cells. The

trachae open on the external surface of the animal through the spiracles and gas exchange in the tracheal system is effected by mass flow down pressure gradients and diffusion along concentration gradients (reviewed by Scheid, Hook and Bridges, 1981). Gas exchange in large insects is also mediated by ventilatory movements of the abdomen wall.

Insect hemolymph plays no direct role in gas transport and exchange. Hemolymph circulation in insects is relatively slow and the circulatory system is 'open' with a single, dorsally located vessel which functions as a heart. Furthermore, insects possess no structures analagous to erythrocytes which are essential for gas transport and respiratory maintenance of acid-base balance in vertebrates.

Respiratory pigments are also lacking in most insects. Noted exceptions are a few species of endoparasitic insects, chironomid larvae and some diving Hemipterans such as Anisops and Buenoa which possess various types of hemoglobin. In the endoparasite, Gastrophilus intestinalis, hemoglobin functions as an O_2 store under anoxic conditions (Keilin and Wang, 1946), while in Chironomus hemoglobin functions as an O_2 store and transporter at low O_2 tensions (Ewer, 1942; Walshe, 1950). Hemoglobin in the backswimmer, Anisops assimilis, functions uniquely in the maintenance of neutral buoyancy during prolonged dives by releasing O_2 into and regulating the size of the external gas bubble (Wells, Hudson and Brittain, 1981).

Acid and base excretion have been studied only very superficially in insects. A few indirect observations suggest that the rectum and Malpighian tubules may be acid-base regulatory sites. For example, Waterhouse (1940) found that in Lucilia the Malpighian tubule fluid was slightly alkaline compared to the hemolymph while the rectum had a pH between 4.8 to 5.3. Similar observations were made on Dixippus (Ramsay, 1956) where

the rectal fluid had a pH of 3.5 to 4.5. In the desert locust the pH of Malpighian tubule fluid is about the same as hemolymph pH (Speight, 1967), however, Phillips (1961) and Speight (1967) found that the rectum actively maintains an acid pH gradient of 2-3 units. Hanrahan (1982) has shown luminal alkalinization in short-circuited locust recta stimulated with cAMP. Recently, Szibbo and Scudder (1979) have shown that segment II of the Malpighian tubules of Cenocorixa bifida produces an alkaline fluid during cAMP stimulation. Martin and Strange (unpublished observations) demonstrated that this alkalinization is due to HCO_3^- secretion and suggested that this may represent an important acid-base regulatory mechanism since this species is normally found in $NaHCO_3$-CO_3 salt lakes (Scudder, 1969). An acid-base regulatory role of the insect excretory system can also be inferred from its ability to transport titratable buffers such as ammonia (Prusch, 1971, 1972, 1975; Chamberlin, 1982; Hanrahan, 1982), phosphate (reviewed by Maddrell, 1977; Phillips, 1980) and uric acid (Wiggelsworth, 1931; O'Donnell, Maddrell and Gardiner, 1983).

The major goal of the present work was to study the problem of insect acid-base regulation at the whole animal, organ and cellular levels, and to study fundamental mechanisms of epithelial H^+ and HCO_3^- transport. Larvae of the saltwater mosquito Aedes dorsalis were chosen for this study for two reasons. First, A. dorsalis normally inhabits hypersaline $NaHCO_3$-CO_3 waters (Scudder, 1969; Strange, Phillips and Quamme, 1982) clearly requiring the animal to possess powerful acid-base regulatory mechanisms. And second, the excretory system of saltwater mosquito larvae has been fairly well characterized (discussed below).

B. Organization of Larval Excretory System

Saltwater mosquito larvae can survive in a range of environments from fresh water to 300% sea water, and in athalassohaline salt lakes where the predominant salts may be mixtures of $MgSO_4$, Na_2SO_4 or $NaHCO_3$ and Na_2CO_3. Under these environmental conditions hemolymph ionic and osmotic concentrations are regulated within narrow limits by the coordinated functions of the Malpighian tubules, anal papillae and rectal salt gland (Fig. 1.1).

The Malpighian tubules of saltwater larvae function much the same as those in other insects by producing a primary, isosmotic secretion or 'filtrate' of the hemolymph which is important for waste excretion. In addition, the Malpighian tubules of Aedes campestris have the unique ability to actively secrete SO_4^{2-} (Maddrell and Phillips, 1975) and Mg^{2+} (Phillips and Maddrell, 1974), which is an important adaptation for larvae inhabiting Na_2SO_4 and $MgSO_4$ lakes. Active SO_4^{2-} secretion has also been demonstrated in the Malpighian tubules of Aedes taeniorhynchus (Maddrell and Phillips, 1978).

The anal papillae of saltwater larvae inhabiting dilute media have been shown to be sites of Na^+, Cl^- (Phillips and Meredith, 1969) and K^+ (Scherer, 1977) uptake. The function of these organs in saline water, however, is uncertain. Balance sheets of whole animal ion and water movements (Phillips and Bradley, 1977; Phillips, Bradley and Maddrell, 1978) and ultrastructural studies on the anal papillae of larvae inhabiting hyperosmotic media (Meredith and Phillips, 1973a,b) suggest indirectly that these organs may play a role in ion excretion. In addition, these organs could be involved in the uptake of ions present in low concentrations in athalassohaline media.

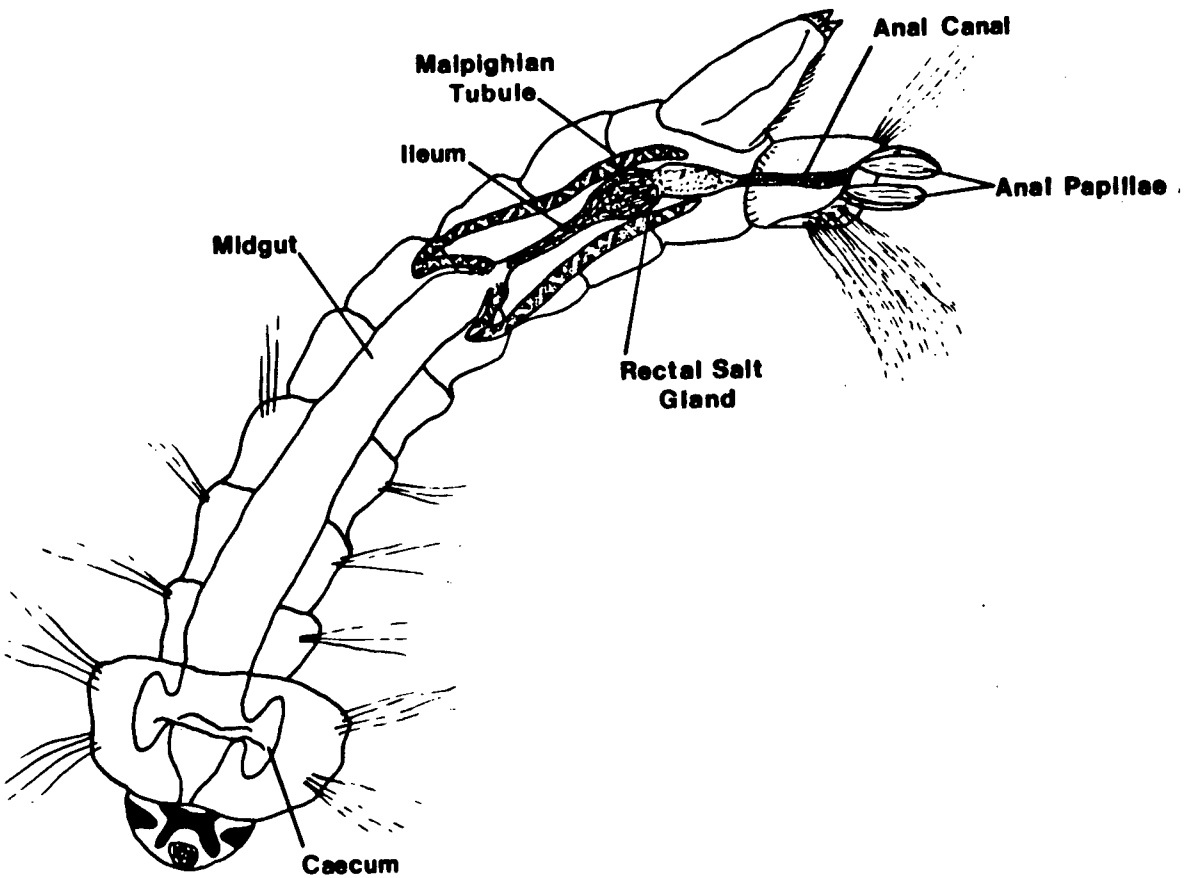

Figure 1.1 Organization of larval gut and excretory system.

Both terrestrial (Phillips, 1980, 1981) and saltwater (Stobbart and Shaw, 1974) insects excrete a final urine which is strongly hyperosmotic to the hemolymph. Production of hyperosmotic excreta in terrestrial insects is an important means of water conservation and is carried out by the rectum which selectively reabsorbs water and solutes from the isosmotic Malpighian tubule fluid (reviewed by Phillips, 1980, 1981). Saltwater mosquito larvae, on the other hand, ingest large quantities of hyperosmotic media (reviewed by Phillips and Bradley, 1977) to replace water lost by osmosis and diffusion across the cuticle. As such, saltwater mosquito larvae are not faced with the problem of water conservation, but instead, of ridding themselves of ingested ions.

The first studies on the function of the rectum in saltwater mosquito larvae were carried out by Meredith and Phillips (1973c). These investigators examined rectal ultrastructure in the freshwater larva, Aedes aegypti, and in the saltwater species, A. campestris. In A. campestris it was found that the rectum lacked the elaborately folded lateral cell membranes that are associated with hyperosmotic urine formation in terrestrial insects. Instead, the rectum was divided into two distinct segments, each consisting of a single cell type. Cells of the anterior rectal segment, which resembled rectal cells in the freshwater species, A. aegypti, had well developed apical and basal membrane infoldings and mitochondria distributed evenly throughout the cytoplasm (Fig. 1.2). The ultrastructure of the posterior segment found only in the saltwater species was considerably more elaborate, however. Cells of this segment were shown to be approximately twice as thick as those of the anterior rectum and most of the mitochondria were associated with the apical infoldings which extended across 60% of the cell. Based on these observations, Meredith and Phillips (1973c) postulated

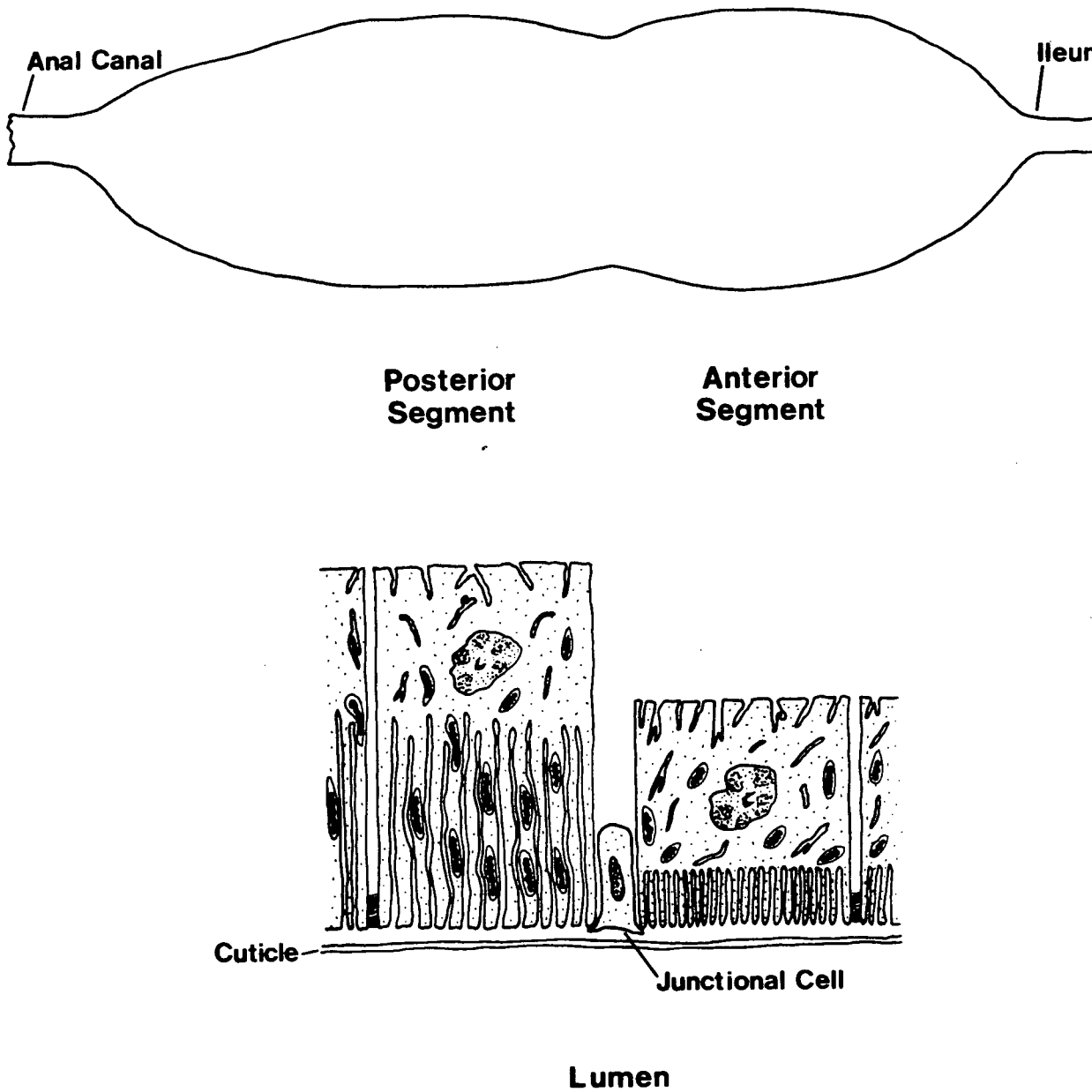

Figure 1.2. Organization and ultrastructure of rectal salt gland.

that saltwater mosquito larvae produce a hyperosmotic urine by secretion of ions or a concentrated fluid across the wall of the rectum.

Direct confirmation of this hypothesis was provided by Bradley and Phillips (1975) using A. taeniorhynchus larvae and elaborated upon in further studies (Bradley and Phillips, 1977a,b,c). Briefly, if the animal is ligated posteriorly and anteriorly to the rectum, the organ swells with a strongly hyperosmotic secretion. Na^+, K^+, Cl^- and Mg^{++} are all secreted into the rectum against 2- to 18-fold concentration gradients. This observation plus measurements of transepithelial potential differences indicated that all four ions are transported by active mechanisms (Bradley and Phillips, 1977c).

The role played by the rectum in ionic regulation during acclimation of saltwater mosquito larvae to different external media was examined by Bradley and Phillips (1977a,b). In general, the concentrations of Na^+, Mg^{++} and Cl^- secreted into the rectum tended to resemble the concentrations of these ions in the external medium to which the animal had been acclimated. Rectal K^+ concentrations, however, were always more concentrated than those in the animal's environment. These authors also noted that when larvae were reared in hyposmotic media, the rectum failed to swell with secretion. Only very small amounts of hyposmotic urine could be collected under these conditions. Since no ultrastructural changes were observed in recta of larvae acclimated to hyposmotic or hyperosmotic conditions (Meredith and Phillips, 1973c), these studies indicated an elaborate reorganization of membrane carriers and/or neural and hormonal control of transport processes.

Bradley and Phillips (1977c) studied indirectly the functions of the anterior and posterior rectal segments. The results of their work and ultrastructural studies of Meredith and Phillips (1973c) suggested that the posterior rectum was the site of hyperosmotic fluid secretion and that the anterior rectum was a site of selective ion reabsorption.

The present work is organized into six chapters with the experimental results presented in Chapters II through V. In Chapter II the degree of hemolymph pH and HCO_3^- regulation in larvae inhabiting extremes of alkalinity is examined. This chapter also demonstrates clearly that the rectal salt gland is an important site of active HCO_3^- excretion and acid-base regulation. Chapter III examines the ionic requirements for HCO_3^- secretion using a new microperfused salt gland preparation in conjunction with conventional ion substitution and transport inhibitor studies. Chapter IV provides further evidence on the mechanism of HCO_3^- secretion, demonstrates the site of HCO_3^- secretion in the microperfused salt gland and describes the function of both anterior and posterior rectal segments. In Chapter V the cellular mechanism of HCO_3^- secretion is studied using intracellular ion and voltage-sensitive microelectrodes in conjunction with a microperfused anterior rectal segment preparation which permitted rapid changes in bath and luminal fluid composition. A summary of the results is presented in Chapter VI along with a comparative discussion of cellular mechanisms of acid-base transport in vertebrate epithelia.

CHAPTER II. BICARBONATE REGULATION AND EXCRETION

A. Introduction

Hypersaline lakes found in arid regions of the world are among the most extreme natural aquatic environments known. The ionic composition of these lakes varies widely and can range from saturated brines with ion ratios similar to sea water to athalassohaline $MgSO_4$, Na_2SO_4 and $NaHCO_3$-CO_3 lakes (Topping and Scudder, 1977). Organisms inhabiting such environments are potentially valuable model systems for studying fundamental physiological and biochemical processes. Halophilic organisms can provide important insights into molecular structure and metabolic functions by revealing underlying biochemical differences in these parameters which allow the organism to withstand the environmental stress of salt lakes. Salt-loving bacteria, for example, have been used extensively to study protein and cell membrane structure and function (reviewed by Hochachka and Somero, 1973; Langworthy, 1982). Clearly, the value of an organism such as Halobacterium halobium in studies of photosynthetic mechanisms, membrane protein structure and H^+ transport cannot be overestimated (see for example, Stoeckenius, 1976; Stoeckenius, Lozier and Bogomolni, 1979; Krumm and Dwivedi, 1982; Haines, 1983).

Halophilic organisms make good model systems also by virtue of the fact that many of their physiological processes are exaggerated and therefore easily studied. For example, virtually nothing is known about the mechanisms of transepithelial Mg^{2+} transport and attempts to study this phenomenon in conventional model epithelia such as the mammalian kidney have been thwarted by extremely low tubular Mg^{2+} fluxes (Sutton, Quamme and Dirks, 1979). Certain species of saltwater mosquito larvae, however, normally

inhabit hypersaline $MgSO_4$ lakes and by necessity must excrete large quantities of Mg^{2+}. This excretion is carried out by both the Malpighian tubules (Phillips and Maddrell, 1974) and rectal salt gland (Bradley and Phillips, 1977a,b), epithelia which can now be isolated completely *in vitro* (Williams and Beyenbach, 1982; Strange, this study) and which are composed of homogeneous, relatively large transporting cells that greatly simplify transport studies.

For saltwater organisms, $NaHCO_3$-CO_3 lakes present both ionic and acid-base regulatory problems. Soda lakes often have pH values exceeding 10 and HCO_3^- and CO_3^{2-} concentrations as high as 1 to 2.4 M (Blinn, 1969; Topping and Scudder, 1977). Only a few organisms are capable of surviving under these severe alkaline conditions, the most prominent of which are insects, crustaceans, halophilic bacteria and algea (Blinn, 1969; Scudder, 1969).

Little is known about the physiological adaptations which allow organisms to survive in these alkaline environments. Acid-base and ionic regulation have been studied previously in the fish *Tilapia grahami* which normally inhabits alkaline Lake Magadi in Kenya's Rift Valley (Reite, Maloiy and Aasehaug, 1974; Johansen, Maloiy and Lykkeboe, 1975; Maetz and DeRenzis, 1978, Maloiy, Lykkeboe, Johansen and Bamford, 1978). The functional characteristics and adaptations of *Tilapia* hemoglobin have been investigated by Lykkeboe, Johansen and Maloiy (1975). These authors demonstrated that *Tilapia* hemoglobin had a very low sensitivity to changes in pH and ionic strength which permitted normal hemoglobin function over the high and variable range of pH and ionic strength found in the animal's plasma. A very high temperature sensitivity of the oxy-hemoglobin equilibrium was

additionally observed which facilitates both O_2 loading and unloading in the highly variable Lake Magadi environment.

Physiological studies have also been conducted on several species of alkalophilic bacteria. These organisms have been shown to possess extraordinarily high levels and complex assortments of membrane cytochromes which may represent an important adaptation to the bioenergetic costs of life at highly alkaline pH values (Lewis, Prince, Dutton, Knoff and Krulwich, 1981; Krulwich, 1982). In addition, alkalophilic bacteria have evolved Na^+/solute cotransport mechanisms (Bonner, Mann, Guffanti and Krulwich, 1982) similar to those observed in eukaryotic tissues (Schultz and Curran, 1970; Aronson, 1981) for ion coupled solute transport. This form of solute uptake is unique to alkalophilic bacteria as most other bacterial species utilize H^+/solute cotransport systems which are energized by an inwardly directed proton gradient such that $[H^+]out > [H^+]in$ (see for example, Flagg and Wilson, 1977; Konings and Boonstra, 1977). The need of alkalophilic bacteria to maintain cytoplasmic pH acidic to external pH, however, reverses the gradient (i.e. $[H^+]in > [H^+]out$) and thus prevents it from energizing solute uptake.

To study the cellular mechanisms of insect acid-base regulation, larvae of the mosquito Aedes dorsalis were chosen. Aedes dorsalis is a common saltwater species found throughout much of western North America and in one of the only metazoan organisms capable of inhabiting hypersaline $NaHCO_3$-CO_3 lakes. In the present chapter the extremes of alkalinity under which larvae can develop normally and the extent of hemolymph pH and HCO_3^- regulation in these environments is examined. It is also shown that the rectal salt gland is an important site of HCO_3^- excretion and pH

regulation, and rectal HCO_3^- secretion is demonstrated to occur by an energy-requiring mechanism.

B. Materials and Methods

Animals. *Aedes dorsalis* eggs were obtained from the Department of Biomedical and Environmental Health Sciences, University of California, Berkeley. Eggs were hatched as described previously (Bradley, 1976) and larvae were reared at 25°C in an alkaline rearing medium (Table 2.1) resembling natural lake waters (Topping and Scudder, 1977). Larvae were fed daily with dry fish food (Tetramin Staple Food) and the rearing media were aerated gently and changed periodically to prevent stagnation. Maintenance of the colony was otherwise similar to that described by Bradley (1976).

Survival studies were conducted by abruptly transferring third and fourth instar larvae four days after hatching to media with high HCO_3^- and CO_3^{2-}/Cl^- ratios. Mortality and development of larvae were observed for four days after transfer. Based on these results, three experimental media were chosen for use in the remainder of this study and are referred to as Rearing medium, 250 mM HCO_3^- medium, and 100 mM CO_3^{2-} medium (Table 2.1). All experiments were conducted on fourth instar larvae acclimated to these artificial lake waters for at least three days.

Larval drinking rate was estimated at 25°C using the ^{14}C-inulin uptake method of Bradley and Phillips (1975). Samples of larval hemolymph were collected and Na^+, K^+, Mg^{2+}, Ca^{2+}, Cl^- and osmotic concentrations were measured as described by Bradley and Phillips (1975, 1977b).

Physiological salines (Table 2.2) used to bathe isolated recta were based on measured ionic and osmotic concentrations of natural hemolymph. Free amino acid concentrations in larval hemolymph were determined using a

Table 2.1 Composition of artificial lake waters in which larvae were reared or acclimated.

Constituent (mM)	Rearing Medium	250 mM HCO_3^- Medium	100 mM CO_3^{2-} Medium
Na^+	361.50	361.50	398.00
K^+	2.50	2.50	2.50
Ca^{2+}	0.03	0.03	0.03
Mg^{2+}	0.50	0.50	0.50
Cl^-	246.06	39.56	97.06
SO_4^{2-}	10.00	10.00	10.00
HCO_3^-	43.50	250.00	87.00
CO_3^{2-}	29.00	29.00	100.00
pH	9.50	8.85	9.75
mOsm	638.00	597.00	576.00

Table 2.2 Composition of hemolymph (mean ± S.E., n = 6-10) and physiological salines for larvae acclimated to different artificial lake waters. All three salines also contained the following (in mM): proline 20, alanine 5, glycine 3, glutamine 4, succinate 7.4, citrate 2.5, glucose 10.

Constituent (mM)	Larval Acclimation Medium[a]					
	Rearing Medium		250 mM HCO_3^- Medium		100 mM CO_3^{2-} Medium	
	Hemolymph	Saline	Hemolymph	Saline	Hemolymph	Saline
Na^+	163±2.4	164.5	191±7.2	189.5	182±2.0	180
K^+	9.5±0.7	9	9.4±0.9	9	11.7±0.5	9
Mg^{2+}	3.8±0.2	4	4.8±0.4	4	5.5±0.4	4
Ca^{2+}	8.7±0.5	4	12.7±0.8	4	14.2±0.9	4
SO_4^{2-}	---	5	---	5	---	5
Cl^-	56±1.8	56	39.1±2.3	39	49±1.6	49
cylcamate$^-$	---	89	---	125	---	108.5
HCO_3^-	8.1±0.5	12.5	18.5±0.6	18.5	12.1±0.3	15.5
pH	7.55±0.03	7.51	7.70±0.02	7.70	7.70±0.02	7.60
mOsm	359±1.5	380	432±3.0	427	401±12	420

[a]See Table 2.1 for composition of artificial lake waters.

Beckman 118 C automatic amino acid analyzer and the four major hemolymph amino acids were included in the salines at physiological concentrations. The large anion deficit observed in larval hemolymph was simulated by including sodium cyclamate in the salines. All salines were gassed with 98% O_2 - 2% CO_2 to give a CO_2 concentration similar to that measured in hemolymph (see Results).

Capillary pH Electrodes. To minimize CO_2 loss from samples of hemolymph and rectal secretion during pH measurements, ultramicro internal capillary pH electrodes were used (Fig. 2.1). These electrodes were modified from Khuri, Agulian and Harik (1968) and required a total sample volume of 10 to 30 nl.

Electrodes were calibrated at 25°C in four buffers (pH 6.4 to 9.0) of constant ionic strength similar to that of natural hemolymph or rectal secretion. The pH of these buffers was determined before each experiment using a Radiometer Model 27 pH meter and Radiometer pH electrode calibrated with Radiometer buffers at 25°C. Only electrodes with full response times of less than 60 seconds and a calibration curve slope of 55 to 61 mV/pH Unit were used. The mean (±S.E.) calibration curve slope and correlation coefficient for all electrodes used throughout this study were 58.32±0.19 and 1.00±0.00 (n=34), respectively.

One difficulty experienced with these electrodes was a small downward drift of the voltage recorded in any calibration buffer after pH measurements on biological fluids. The cause of this drift was uncertain and could not be corrected by rinsing with chromic acid or by repeatedly 'exercising' the electrode in two buffers. To monitor this problem, electrodes were recalibrated in two buffers following each pH measurement. Subsequent pH measurements on hemolymph or rectal secretion samples were then

Figure 2.1 Ultramicro internal capillary pH electrode.

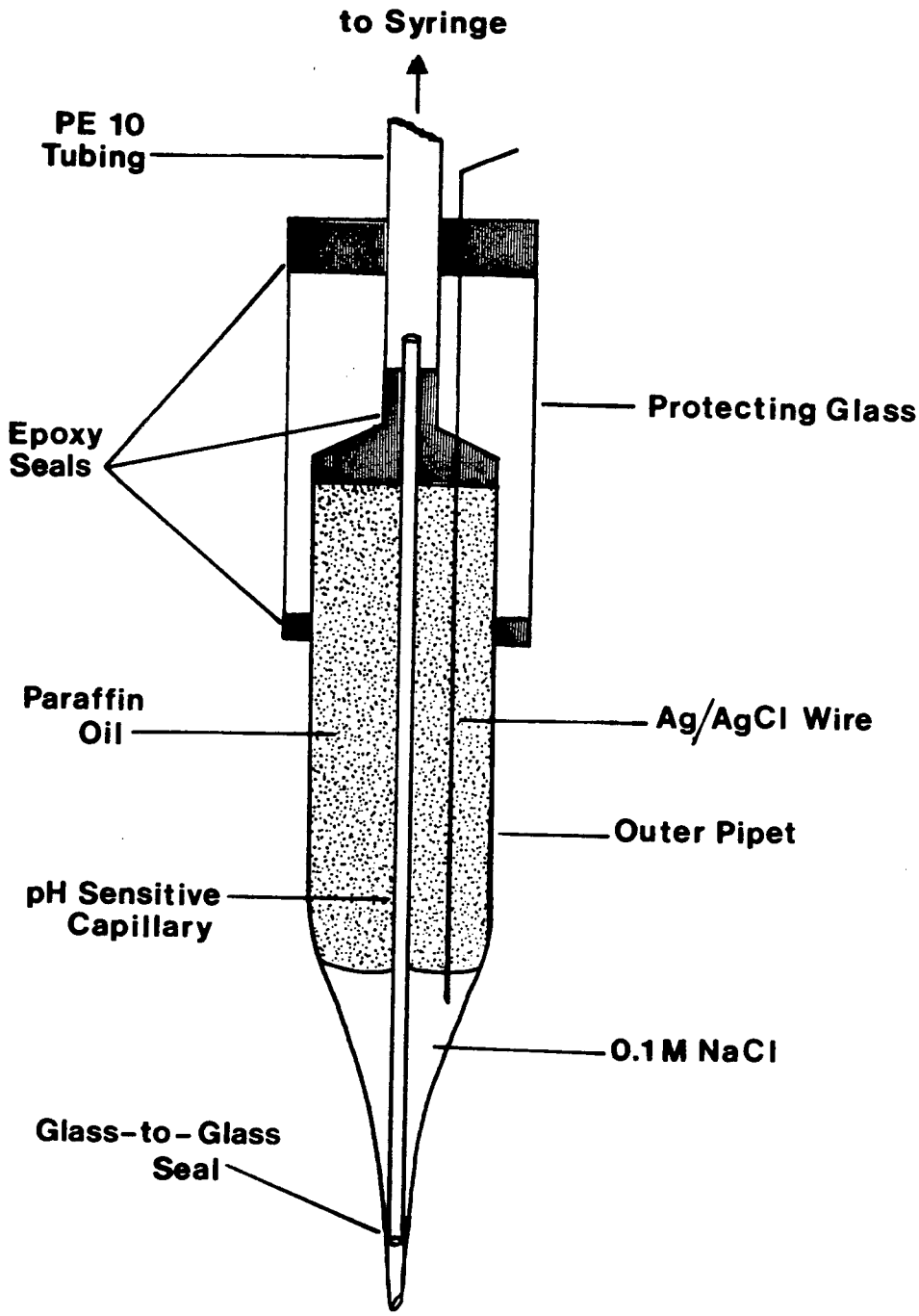
to Syringe
PE 10
Tubing
Epoxy
Seals
Protecting Glass
Paraffin
Oil
Ag/AgCl Wire
Outer Pipet
pH Sensitive
Capillary
0.1 M NaCl
Glass-to-Glass
Seal

corrected for this drift using the new calibration curve. Electrodes showing deviations in calibration slope of more than ± 2mV/pH unit were discarded.

Hemolymph pH Measurements. Regulation of hemolymph pH was examined by transferring third and fourth instar larvae to high HCO_3^- and CO_3^{2-} media four days after hatching. Hemolymph samples were collected by briefly rinsing larvae in distilled water, blotting them dry and placing them under heavy paraffin oil (MCB Reagents; Saybolt viscosity 340-355). The cuticle was then torn with forceps and the drop of exuded hemolymph collected immediately in a mercury-filled micropipet. This sample was transferred rapidly to a heavy paraffin oil bath (25°C) and a capillary pH and 3M KCl microelectrode were lowered into the hemolymph drop visualized under a dissecting microscope. The potential difference between the electrodes was measured with a Kiethley Model 602 electrometer and Model 6013 pH electrode adaptor and the voltage recorded on a Fisher Series 5000 Recordall.

Hemolymph HCO_3^- Measurements. Hemolymph HCO_3^- was measured using the ultramicro Astrup method of Karlmark and Sohtell (1973). To equilibrate paraffin oil baths with gasses of different CO_2 content, high gas flow rates (2-3 $l.min^{-1}$) and an equilibration time of at least one hour were used before samples were added. Karlmark and Sohtell (1973) found that a minimum gas flow rate of 450 $ml.min^{-1}$ and a 30 minute equilibration time were necessary for complete gas to oil equilibration. This was confirmed using an Orion PCO_2 electrode, but the higher flow rates were chosen to assure complete equilibration under all conditions. In addition, it was found that complete gas to oil equilibration at 25°C was only obtained when light paraffin oil (MCB Reagents; Saybolt viscosity 90) was used.

Samples of hemolymph were collected for determination of HCO_3^- as described above and allowed to equilibrate with CO_2 under oil for 20 to 30 minutes before pH measurements were made with capillary electrodes at 25°C. Gas flow was turned off briefly (less than 1 min) during sample loading and pH measurements. Different hemolymph samples were equilibrated with four gasses of varying CO_2 content (0.5 to 10% CO_2, balance N_2; Canadian Liquid Air Company, certified analysis). Resulting pH versus log PCO_2 titration curves were plotted using the least squares method of linear regression.

Rectal Micropuncture Studies. The micropuncture preparation used in this study was modified considerably from that described by Bradley and Phillips (1975). Briefly, the rectum was isolated by ligating a larva just anterior to the seventh abdominal segment and also at the terminal anal segment. The portion of the larva anterior to the first ligature, the cuticle over the rectum, and the tracheal connections were then dissected away. Using the terminal ligature, the rectum was suspended in 10 to 15 ml of the appropriate physiological saline maintained at 25°C and gassed with 98% O_2 - 2% CO_2. After 90 minutes the rectum had swollen noticeably with secretion and was removed gently from the bath, touched lightly to bibulous paper to remove adhering external fluid, and placed under paraffin oil. Ten to 40 nl of rectal secretion were collected by puncturing recta with sharpened and bevelled acid-washed micropipets filled with Sudan black-stained paraffin oil. Micropuncture pipets were bevelled at an angle of 30° to a tip diameter of 10-15 μ using a K.T. Brown type microelectrode beveler (Sutter Instrument Company, San Francisco, California).

Cannulated In Vitro Rectal Preparation. To examine rectal HCO_3^- secretion in greater detail, a microcannulated preparation was

developed which permitted rapid and complete collection of secreted rectal fluid. Diagrams of the Sylgard resin (Dow Corning) bathing chamber and the cannulated rectum are shown in Figure 2.2. All cannulation experiments were conducted at room temperature (21-23°C) using larvae acclimated to 250 mM HCO_3^- medium.

Microcannulae were pulled from glass tubing over a small flame to yield tip diameters of 35 to 50 μ. The tips of the pipets were broken to the appropriate length with forceps and the broken end heat-polished with a microforge. Pipets were siliconized with Dow Corning 1107 fluid, filled with Sudan black-stained paraffin oil and mounted on a Narishige micromanipulator using a micropipet holder (Leitz, Wetzlar, Germany) attached to a 50 ml syringe.

Recta were isolated by placing a larva in the bathing chamber and tying a fine ligature around the terminal anal segment. The bathing chamber was filled and perfused continuously with physiological saline and the rectum, ileum and a portion of the midgut were dissected free from the larva. Approximately 20 to 30 nl of saline were then drawn up into a microcannula and the pipet inserted down the midgut and into the rectum. The saline was injected into the rectum and then withdrawn completely and expelled into the bath. After assuring that the rectum was completely empty the microcannula was reinserted and tied into place using two ultrafine ligatures (diameter ca. 10 μ; see Fig. 2.2B).

During the course of these experiments the bathing chamber was perfused with saline gassed with 98% O_2 - 2% CO_2 and recta were allowed to swell with secretion for 90 minutes before fluid was drawn into the cannula using the attached syringe. At the end of the experiments the bath

Figure 2.2 Microcannulated rectal preparation. A) Sylgard resin bathing chamber. B) Cannulated rectal salt gland.

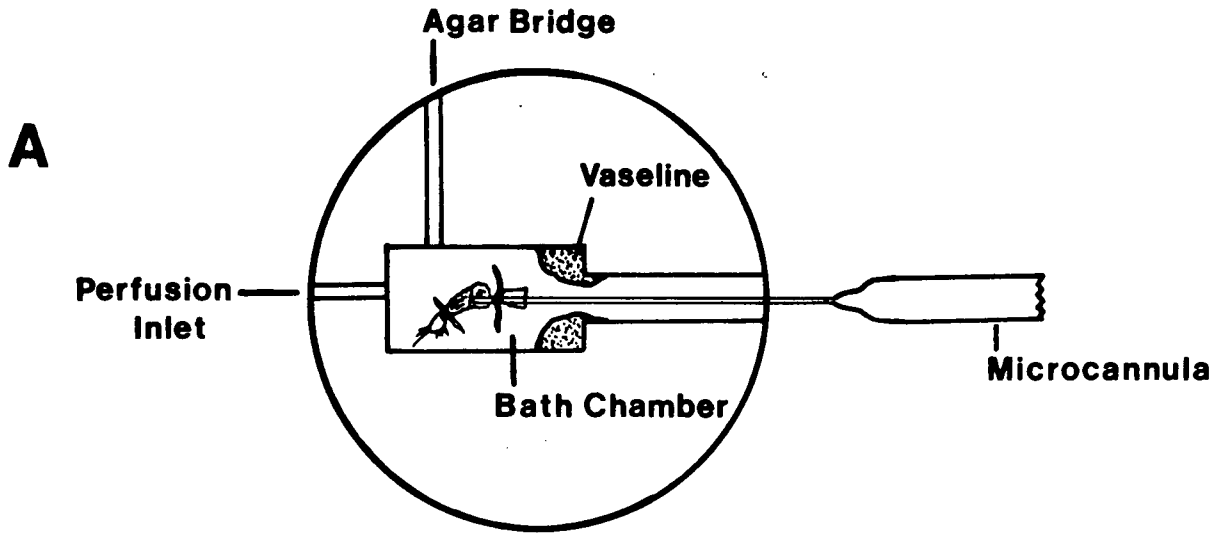
A
Agar Bridge
Vaseline
Perfusion Inlet
Bath Chamber
Microcannula

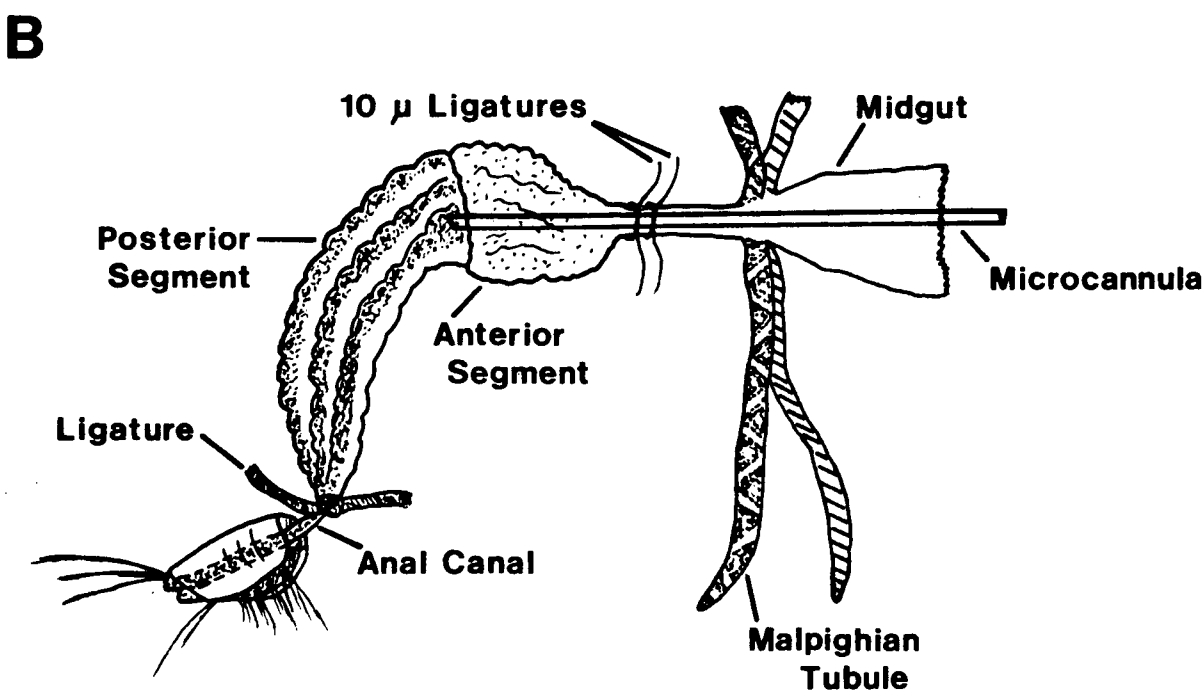
B
10 µ Ligatures
Midgut
Posterior Segment
Microcannula
Anterior Segment
Ligature
Anal Canal
Malpighian Tubule

was drained, the rectum removed from the pipet and the sample of secretion prepared for analysis.

Analysis of Rectal Secretions. Rectal secretion volume was determined by measuring drop diameters under paraffin oil as described by Bradley and Phillips (1975). Osmotic concentrations of rectal secretions were measured with a Clifton nanoliter osmometer. Concentrations of Na^+, K^+, Mg^{2+}, Ca^{2+}, Cl^-, total phosphorous and total sulfur were measured in each sample of secretion by electron microprobe analysis using a Cameca model MBX microprobe and methods described previously (Morel and Roinel, 1969; Roinel, 1975). Because of the high ion concentrations in rectal fluid, samples were diluted two to three times with distilled water before preparation for microprobe analysis. Chloride concentrations were also measured by the electrometric titration procedure of Ramsay, Brown and Croghan (1955) on rectal secretions pooled from four to five animals.

Bicarbonate concentrations in rectal secretions collected by micropuncture were estimated by measuring the pH of samples equilibrated under paraffin oil at 25°C with 98% O_2 - 2% CO_2 according to the methods described above. In later experiments, total CO_2 and pH were measured in rectal secretions collected by microcannulation. Secretion pH was measured at 25°C immediately after collection while total CO_2 concentrations were determined by microcalorimetry (Picapnotherm; Microanalytic Instrumentation, Bethesda, Maryland) as described by Vurek, Warnock and Corsey (1975). Aliquots of rectal secretion were transferred to the Picapnotherm by constant volume nanoliter pipets (2 to 3 nl) similar to those of Prager, Bowman and Vurek (1965).

Transepithelial Potential. Rectal transepithelial potential (TEP) was measured using a microcannula (see above) with 3M KCl-Agar in the tip and

the remainder of the pipet filled with 3M KCl solution. The microcannula and bath chamber made contact via salt bridges with calomel electrodes and TEP was measured using a Kiethley Model 602 electrometer. Transepithelial potential was recorded continuously for 90 minutes on a Fisher Series 5000 Recordall with subsequent corrections for junction and asymmetry potentials.

Calculations. Concentrations of CO_2, HCO_3^- and CO_3^{2-} were calculated from the Henderson-Hasselbalch equation after correcting pK_1', pK_2', and CO_2 solubility coefficients (S) for ionic strength using the equations of Hastings and Sendroy (1925) and McGee and Hastings (1948). Values of pK_1', pK_2' and S used throughout this study are shown in Table 2.3. Statistical analyses were conducted using paired or unpaired t-tests in this chapter and throughout the thesis.

C. Results

In preliminary studies I examined the ability of A. dorsalis larvae to survive in saline media buffered with low concentrations of HCO_3^- and CO_3^{2-} at high pH values. Larval survival and development were normal in media with pH values up to 10.5. A pH 11.0 survival was still normal but pupation and pupal-to-adult eclosion were greatly reduced. Since the pH of alkaline lakes rarely rises above 10.5 due to the inherent nature of their buffering systems, factors other than pH per se must limit the distribution of larvae in natural alkaline waters. Further survival studies were therefore conducted by replacing NaCl in the Rearing medium with different concentrations of $NaHCO_3$ and/or Na_2CO_3. Figure 2.3 demonstrates that survival and development are normal in media containing 250 mM HCO_3^- or 100 mM CO_3^{2-}. Slightly higher concentrations of these two ions (300 mM HCO_3^- and 150 mM CO_3^{2-}) resulted in greatly reduced survival (32 to

Table 2.3 Values of pK_1', pK_2' and S used for calculation of CO_2, HCO_3^- and CO_3^{2-} concentrations.

	Larval Acclimation Medium[a]		
Constant	Rearing Medium	250 mM HCO_3^- Medium	100 mM CO_3^{2-} Medium
Hemolymph pK_1'	6.12	6.11	6.11
Hemolymph S	0.0340	0.0338	0.0339
Secretion[b] pK_1'	6.04	6.04	6.04
Secretion[b] S	0.0329	0.0329	0.0329
Secretion[c] pK_1'	---	6.00	---
Secretion[c] pK_2'	---	9.64	---

[a] See Table 2.1 for composition of acclimation media.

[b] Rectal secretion collected by micropuncture.

[c] Rectal secretion collected by microcannulation.

Figure 2.3. Survival and development of fourth instar larvae in alkaline environments. Refer to Table 2.1 for media composition.

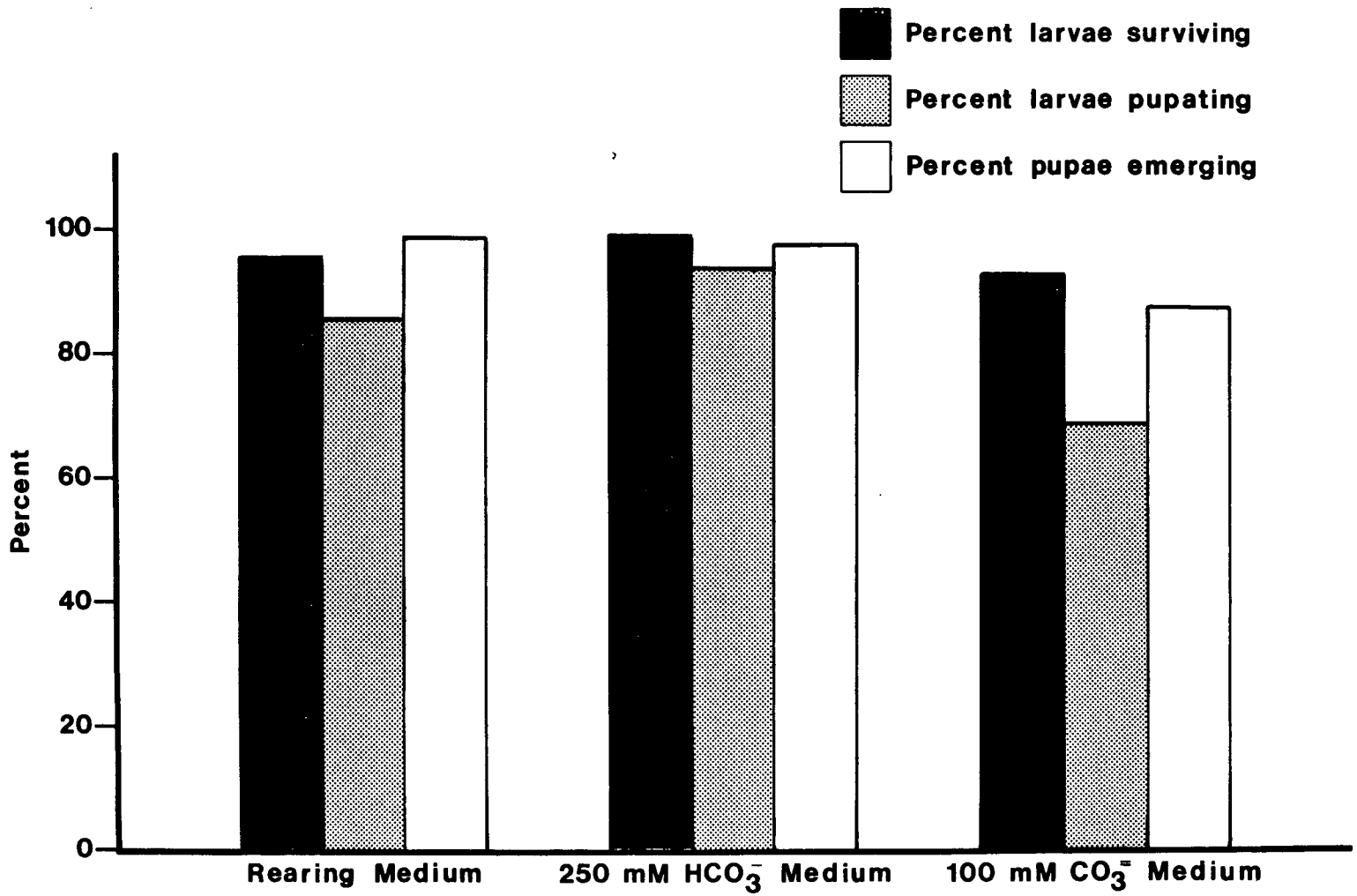
Percent larvae surviving
Percent larvae pupating
Percent pupae emerging
Percent
100
80
60
40
20
0
Rearing Medium
250 mM HCO_3^- Medium
100 mM $CO_3^=$ Medium

46% after four days) and failure of any of the larvae to develop past the pupal stage.

Ionic and osmotic concentrations of hemolymph from animals acclimated to high HCO_3^- and CO_3^{2-} environments are shown in Table 2.2. Hemolymph osmotic concentrations increased slightly but significantly ($0.005 < P < 0.01$) from 359 mOsm to 401-432 mOsm following transfer of larvae from the Rearing medium to either 250 mM HCO_3^- or 100 mM CO_3^{2-} medium. In addition, hemolymph Na^+ concentration increased significantly ($P< 0.001$) from 163 mM to 181-190 mM, while Ca^{2+} increased from 8.5 mM to 12.5-14.0 mM ($P < 0.001$). Hemolymph Cl^- concentration decreased slightly but significantly ($0.001 < P < 0.005$) as external Cl^- was replaced by HCO_3^- and CO_3^{2-}.

Fluid ingestion rate was measured to estimate the load imposed on pH and HCO_3^- regulatory mechanisms in the larvae and to determine whether larvae could reduce this load by reducing drinking rate. Figure 2.4 shows that drinking rate (53-56 $nl.mg^{-1}.h^{-1}$) was independent of external HCO_3^- and CO_3^{2-} levels.

To determine how well larvae regulate hemolymph acid-base status when faced with such high ingestion rates, hemolymph pH was measured for four consecutive days following transfer of larvae from the Rearing medium to either high HCO_3^- or high CO_3^{2-} environments (Fig. 2.5). Hemolymph pH increased only slightly from 7.55 to 7.70 during the first day and remained constant thereafter.

Hemolymph HCO_3^- concentration was determined in larvae acclimated to all three artificial lake waters (Fig. 2.6). A typical titration curve of hemolymph pH versus log hemolymph PCO_2 is shown in Fig. 2.6A. Titration curves for the three groups of larvae were linear with correlation coefficients varying between -0.98 and -0.99. Hemolymph PCO_2 was

Figure 2.4 Drinking rates estimated by ^{14}C-inulin ingestion for fourth instar larvae acclimated to alkaline environments (mean $\pm$ S.E., n = 10-12). Refer to Table 2.1 for media composition.

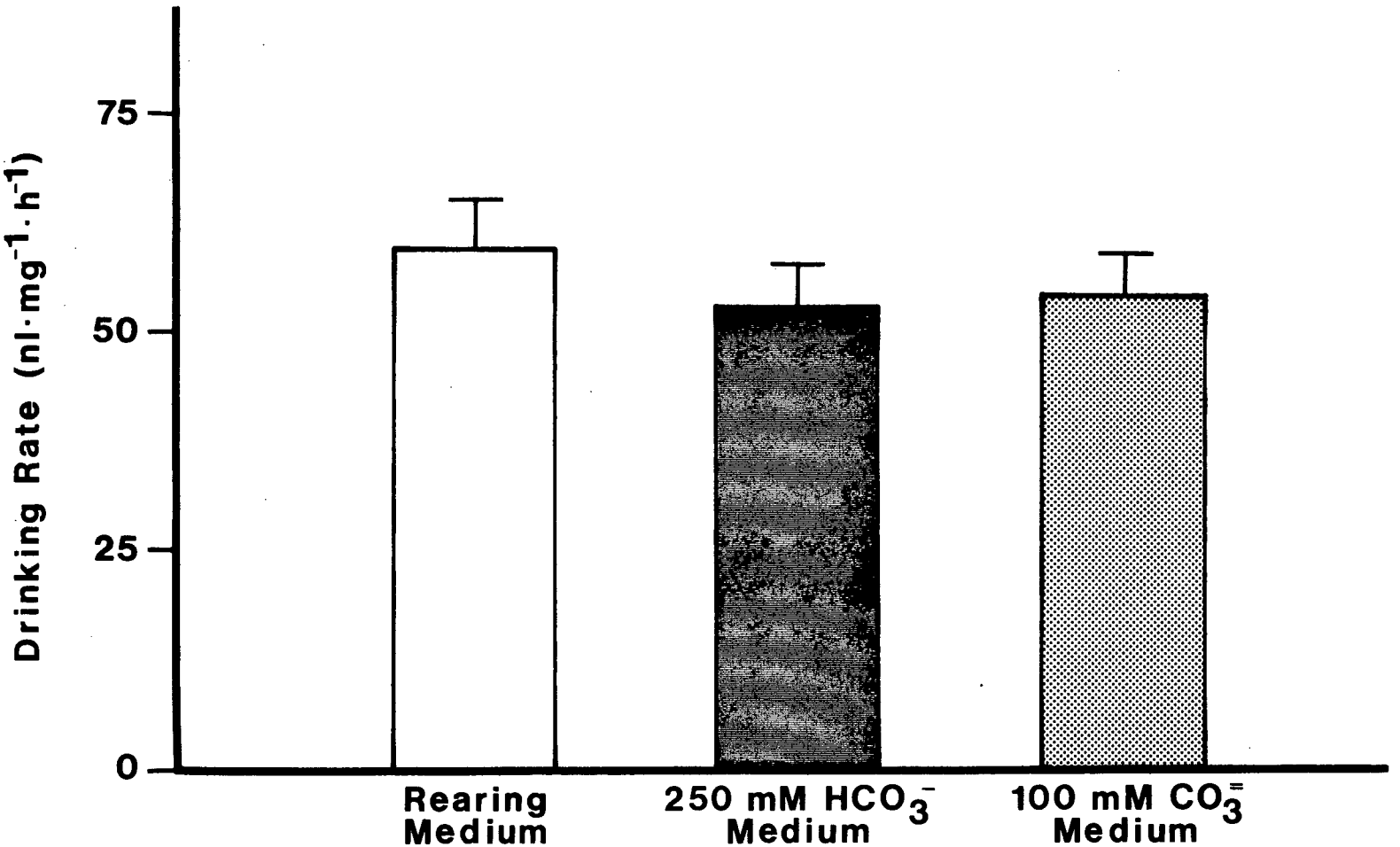
Drinking Rate (nl·mg⁻¹·h⁻¹)
75
50
25
0
Rearing Medium
250 mM HCO3⁻ Medium
100 mM CO3⁼ Medium

Figure 2.5 Hemolymph pH regulation in fourth instar larvae during acclimation to high HCO_3^- and CO_3^{2-} media. Animals were transferred from the Rearing medium to 250 mM HCO_3^- or 100 mM CO_3^{2-} media at zero time (means $\pm$ S.E., n = 6-9). Refer to Table 2.1 for media composition.

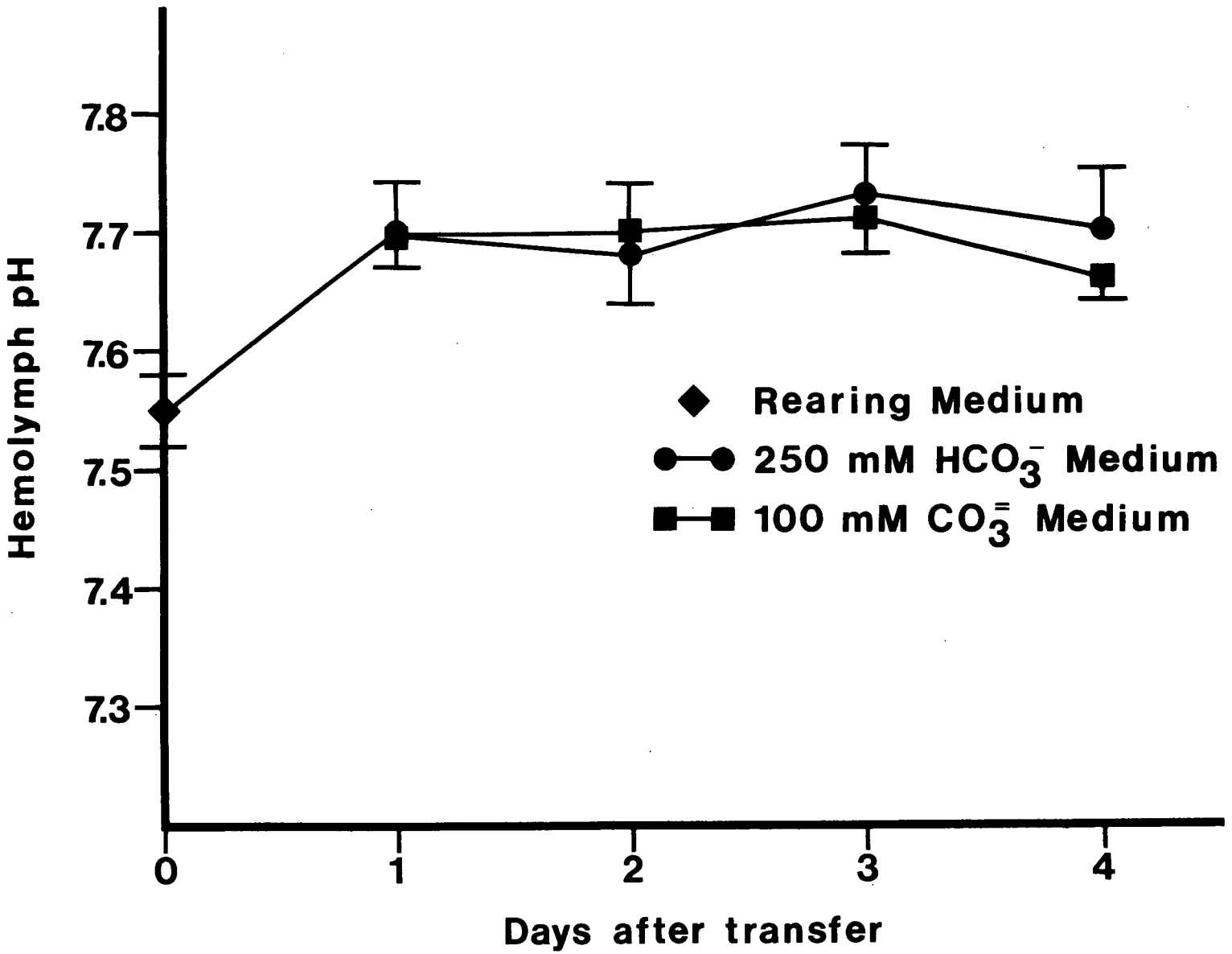
Hemolymph pH
7.8
7.7
7.6
7.5
7.4
7.3
0
1
2
3
4
Days after transfer
Rearing Medium
250 mM HCO_3^- Medium
100 mM $CO_3^=$ Medium

Figure 2.6 Hemolymph HCO_3^- concentration. A) pH vs. log PCO_2 titration curve for hemolymph from animals acclimated to the Rearing medium. Solid circles are means ± S.E. (n = 8-9) of hemolymph samples titrated with one of four different CO_2-N_2 gas mixtures. The line is the linear regression calculated for these points ($y = -0.51x + 8.03$; $r = -0.994$). Solid squares are pH values of native hemolymph (see Fig. 2.5). The values were fitted to the line using the calculated regression equation. B) Concentration of hemolymph HCO_3^- in animals acclimated to alkaline media. PCO_2 values were obtained from pH vs. log PCO_2 titration curves and HCO_3^- concentration calculated using the Henderson-Hasselbalch equation (means ± S.E., n = 9-29). Refer to Table 2.1 for media composition.

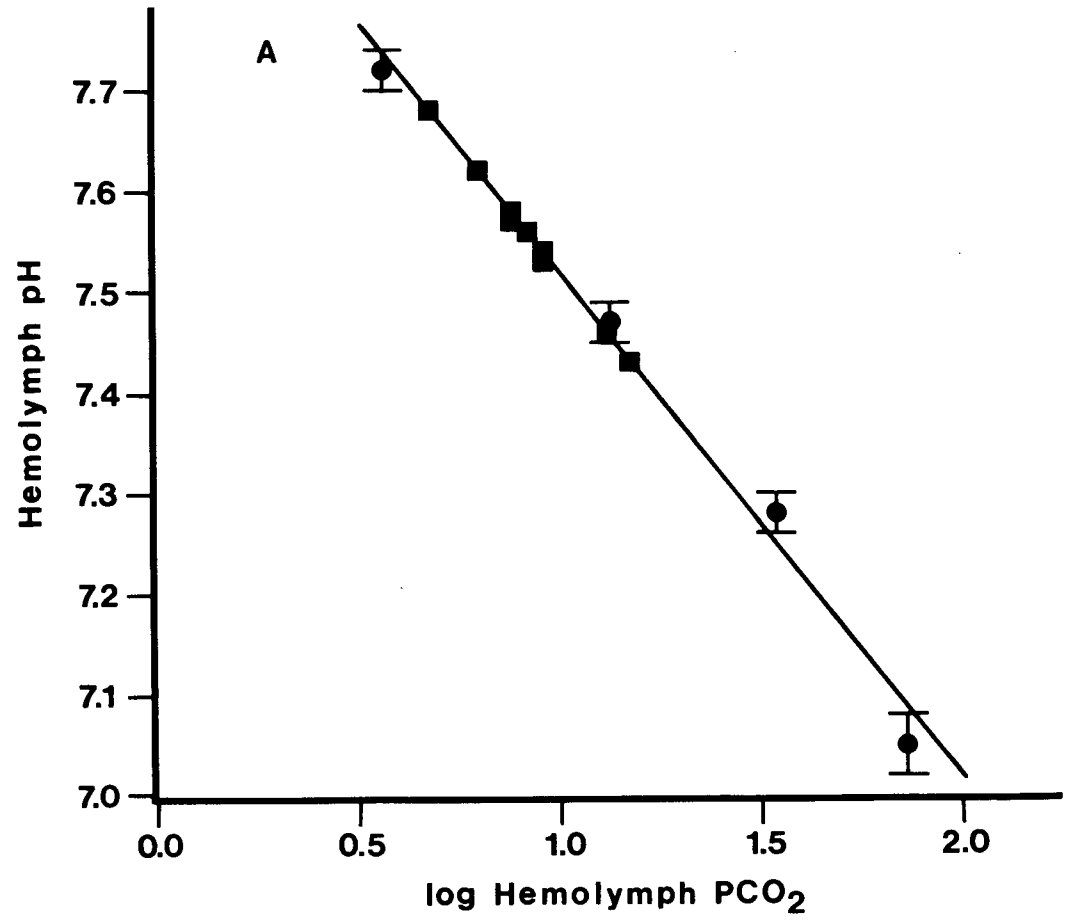
A
Hemolymph pH
7.7
7.6
7.5
7.4
7.3
7.2
7.1
7.0
0.0
0.5
1.0
1.5
2.0
log Hemolymph PCO_2

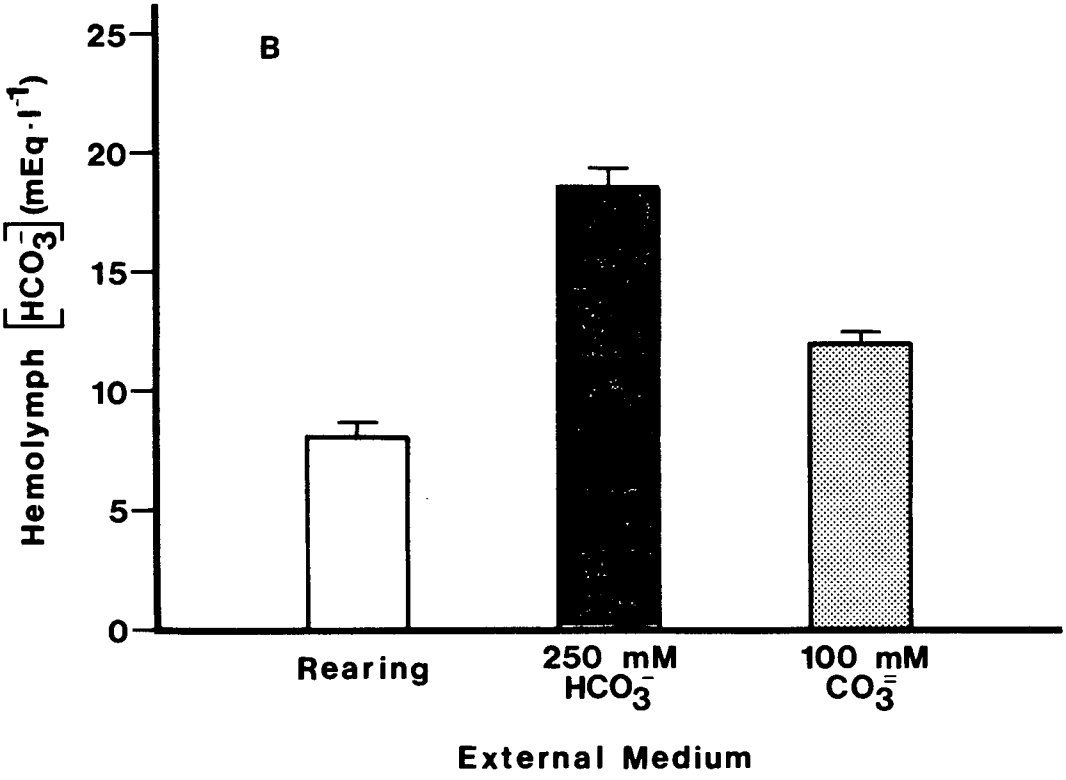
B
Hemolymph $[HCO_3^-]$ (mEq·l^{-1})
25
20
15
10
5
0
Rearing
250 mM HCO_3^-
100 mM $CO_3^=$
External Medium

determined using these titration curves and the measured hemolymph pH values in Fig. 2.5. PCO_2 values were (in mm Hg, mean $\pm$ S.E., n = 9-29) 9.05 $\pm$ 1.10, 14.79 $\pm$ 1.33 and 9.44 $\pm$ 0.50 for animals acclimated to the Rearing, 250 mM HCO_3^- and 100 mM CO_3^{2-} media, respectively. Hemolymph PCO_2 was significantly higher ($P<0.0001$) in animals acclimated to 250 mM HCO_3^- medium. Bicarbonate concentrations calculated from these data are shown in Fig. 2.6B. Despite large increases in external HCO_3^- and CO_3^{2-} levels, hemolymph HCO_3^- concentrations remain low and only increase from 8.0 to 12.0-18.5 mM.

As previously described by Bradley and Phillips (1975, 1977a) for Aedes taeniorhynchus and A. campestris larvae from other hypersaline waters, the ligated rectum of A. dorsalis also swells with secretion when bathed in artificial hemolymphs. The osmotic and ionic concentrations of secretions collected by micropuncture of isolated recta are shown in Fig. 2.7. Mean Na^+ (270-300 mM) and osmotic (700-735 mOsm) concentrations were essentially the same for larvae acclimated to the three external media. Mean chloride concentrations in rectal secretions increased from 50 mM to 135 mM, being lowest in animals acclimated to high HCO_3^- and CO_3^{2-} media. Concentrations of K^+ in rectal secretions were between 27 and 46.5 mM. Ca^{2+} and Mg^{2+} concentrations in secretions were very low (0.3 - 1.0 mM) while total phosphorus varied from 1.5 to 4.6 mM and total sulfur was ca. 8.0 mM (Table 2.4).

Osmotic and ionic concentrations of rectal secretions collected from microcannulated recta of larvae acclimated to 250 mM HCO_3^- medium are shown in Fig. 2.8 and were significantly higher than those of secretions collected by micropuncture (cf. Fig. 2.7). Mean osmotic concentration was 1030 mOsm, while mean Na^+, K^+ and Cl^- concentrations were 413 mM, 31.4 mM and 44.9 mM, respectively, Concentrations of Ca^{2+} and Mg^{2+} were

Figure 2.7 Osmolality and concentrations of major ions in rectal secretions collected by micropuncture from larvae acclimated to three different alkaline media (means ± S.E., n = 5-12). See Tables 2.1 and 2.2 for composition of acclimation media and physiological salines.

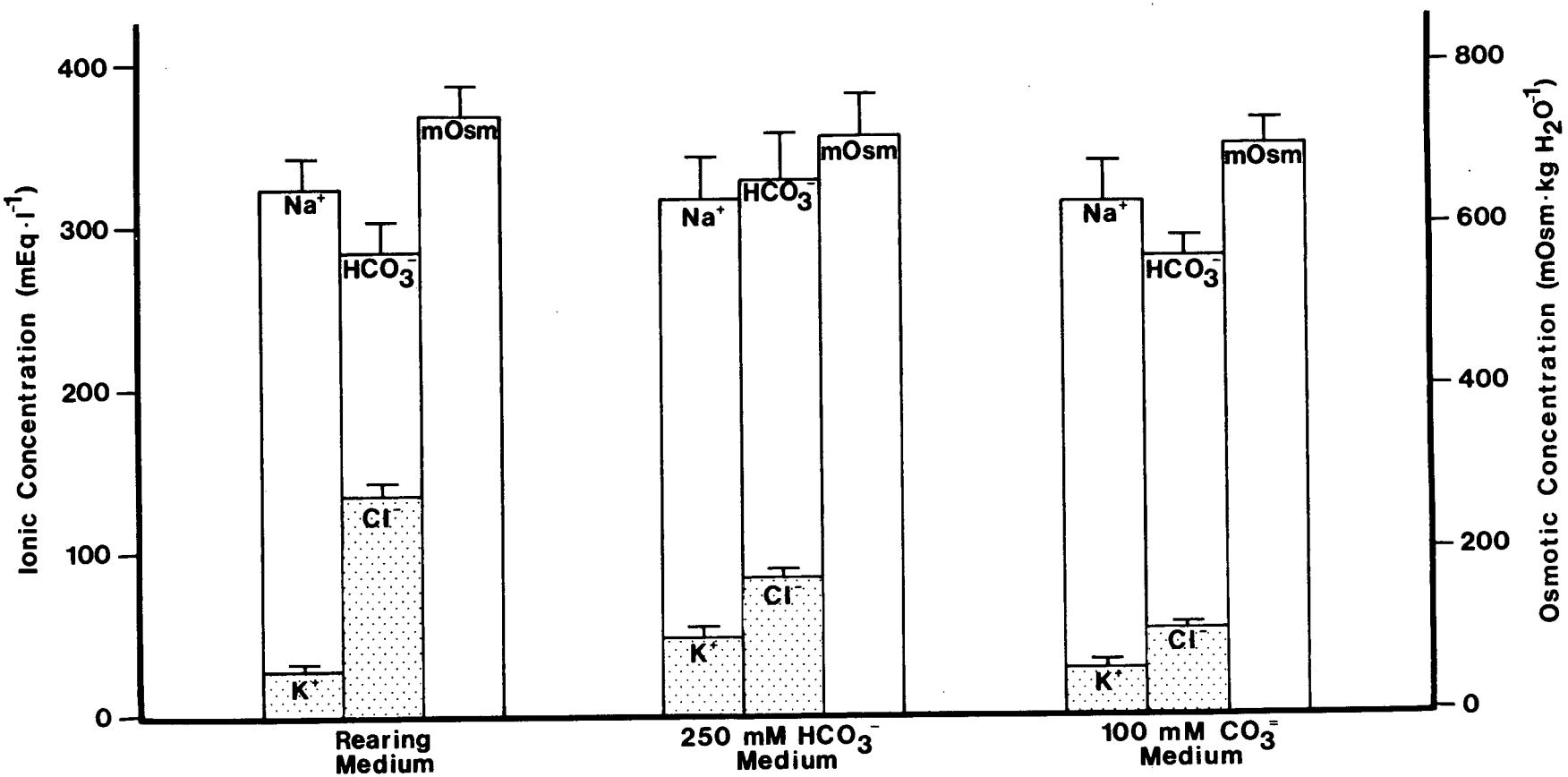
Ionic Concentration (mEq·l⁻¹)
Osmotic Concentration (mOsm·kg H₂O⁻¹)
400
300
200
100
0
800
600
400
200
0
Na⁺
HCO₃⁻
mOsm
Cl⁻
K⁺
Rearing Medium
250 mM HCO₃⁻ Medium
100 mM CO₃⁼ Medium

Table 2.4 Concentrations of Ca^{2+}, Mg^{2+}, total sulfur and total phosphorus and pH in rectal secretions collected by micropuncture. pH values were determined on secretions equilibrated with 2% CO_2 (mean ± S.E., n = 7-11).

	Larval acclimation medium[a]		
Constituent (mM)	Rearing Medium	250 mM HCO_3^- Medium	100 mM CO_3^{2-} Medium
Mg^{2+}	0.77±0.11	1.04±0.26	---
Ca^{2+}	0.34±0.04	0.76±0.22	---
Total Sulfur	7.85±0.81	8.90±1.84	---
Total Phosphorus	4.63±1.03	3.61±1.64	1.49±0.30
pH	8.43±0.04	8.72±0.05	8.72±0.03

[a] See Table 2.1 for composition of acclimation media.

again very low (0.5-0.8 mM) while total phosphorus levels were 2.4 mM and total sulfur was 13.4 mM (data not shown).

The major objective of the micropuncture studies was simply to determine whether the rectum was an important site of HCO_3^- excretion and regulation. Bicarbonate concentrations were thus initially estimated by measuring the pH at a known CO_2 tension of rectal secretions collected by micropuncture. This method is the same as that used in early work on the kidney (Gottschalk, Lassiter and Mylle, 1960; Viera and Malnic, 1968) and pancreas (Swanson and Solomon, 1973) and is based on the assumption that luminal PCO_2 is the same as that in the hemolymph (i.e. 2.0% CO_2). The concentrations of HCO_3^- calculated from the Henderson-Hasselbalch equation using the measured pH and known PCO_2 are shown in Fig. 2.7 and ranged between 150 to 240 mM.

It must be stressed here that the calculated HCO_3^- levels shown in Fig. 2.7 are slight overestimates of actual concentrations. At the pH values of the rectal secretions (8.4 - 8.7; Table 2.4), a significant fraction of the total CO_2 pool is present as CO_3^{2-} which cannot be calculated directly from the Henderson-Hasselbalch equation using only known pH and PCO_2 values. To determine actual HCO_3^- and CO_3^{2-} concentrations in rectal secretion then, and to calculate transepithelial HCO_3^- and CO_3^{2-} gradients across the rectal wall, I subsequently measured total CO_2 in secretions collected from cannulated recta of animals acclimated to 250 mM HCO_3^- medium. The total CO_2 concentration in these secretions was 444 $\pm$ 25 mM (mean $\pm$ S.E., n = 6) while pH was 8.65 $\pm$ 0.05 (mean $\pm$ S.E., n = 7). Using these measured values, concentrations of CO_2, HCO_3^- and CO_3^{2-} were calculated from the Henderson-Hasselbalch equation and were 0.90 mM, 402 mM and 41 mM, respectively (see Fig. 2.8).

Figure 2.8 Osmolality and concentrations of major ions in rectal secretions collected from cannulated recta of animals acclimated to 250 mM HCO_3^- medium (see Table 2.1). Values are means ± S.E., n = 8-9. Concentrations of HCO_3^- and CO_3^{2-} are calculated from measurements of total CO_2 and pH as described in the text.

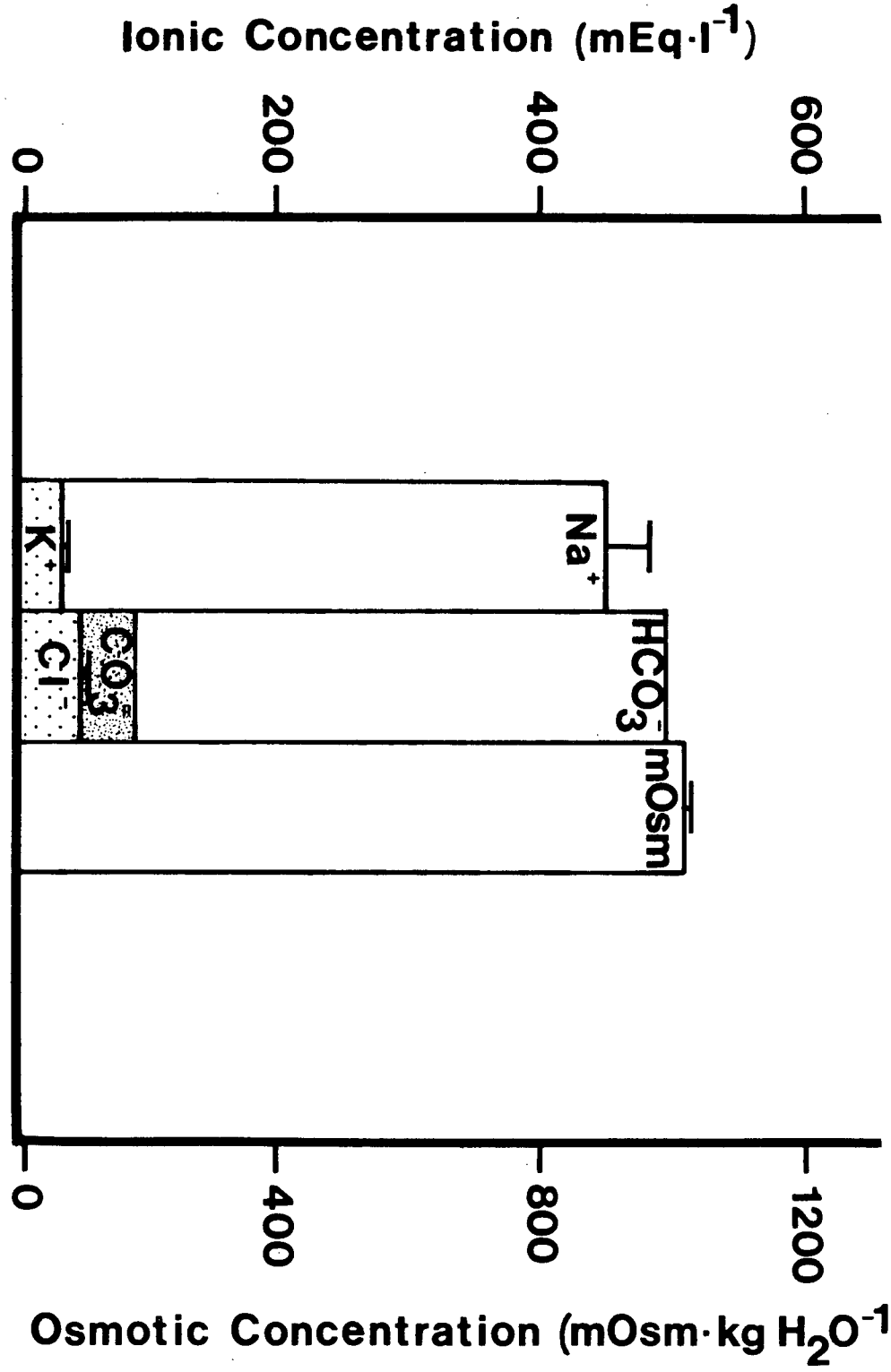
Ionic Concentration (mEq·l^{-1})
0
200
400
600
K$^+$
Na$^+$
Cl$^-$
CO$_3^-$
HCO$_3^-$
mOsm
0
400
800
1200
Osmotic Concentration (mOsm·kg H$_2$O^{-1})

Secretion rate was estimated in cannulated recta by measuring the volume of collected fluid and was 37.6 $\pm$ 6.4 $nl.h^{-1}.rectum^{-1}$ (mean $\pm$ S.E., n = 6). The calculated total CO_2 secretion rate in cannulated recta was 16.7 nMoles total $CO_2.h^{-1}.rectum^{-1}$.

Transepithelial potentials across cannulated recta are shown in Fig. 2.9. Immediately after ligation, mean TEP was -14.2 mV (lumen negative). During the course of the experiment TEP gradually increased as the rectum swelled with secretion and reached a value of -25.3 mV (lumen negative) after 90 minutes.

D. Discussion

The results of survival studies indicate that A. dorsalis larvae survive and develop normally in concentrated $NaHCO_3$-CO_3 media and that the distribution of this species in alkaline lakes is limited not by high pH per se, but instead by the concentrations of HCO_3^- and CO_3^{2-} in these environments. Larvae inhabiting alkaline waters ingest the external medium at a rate equivalent to ca. 130% of their body weight per day. Previous studies (Wiggelsworth, 1933a,b; Kiceniuk and Phillips, 1974; Maddrell and Phillips, 1975) have shown that the bulk of ingested fluid and ions is absorbed into the hemolymph across the midgut and caecae. The degree of hemolymph pH and HCO_3^- regulation exhibited by these insects (Figs. 2.5 and 2.6) is remarkable considering the acid-base regulatory problems which must be imposed by such high rates of fluid ingestion.

The elevated hemolymph PCO_2 observed in animals acclimated to 250 mM HCO_3^- medium (see Results) is difficult to explain at present, but may represent an attempt of the larvae to retain CO_2 so as to lower hemolymph pH. This could be a valuable regulatory response especially if the excretory system is not capable of eliminating HCO_3^- rapidly enough to maintain

Figure 2.9 Transepithelial potential (lumen relative to haemocoel side) across cannulated recta from animals acclimated to 250 mM HCO_3^- medium (see Table 2.1). Values are means $\pm$ S.E., n = 6.

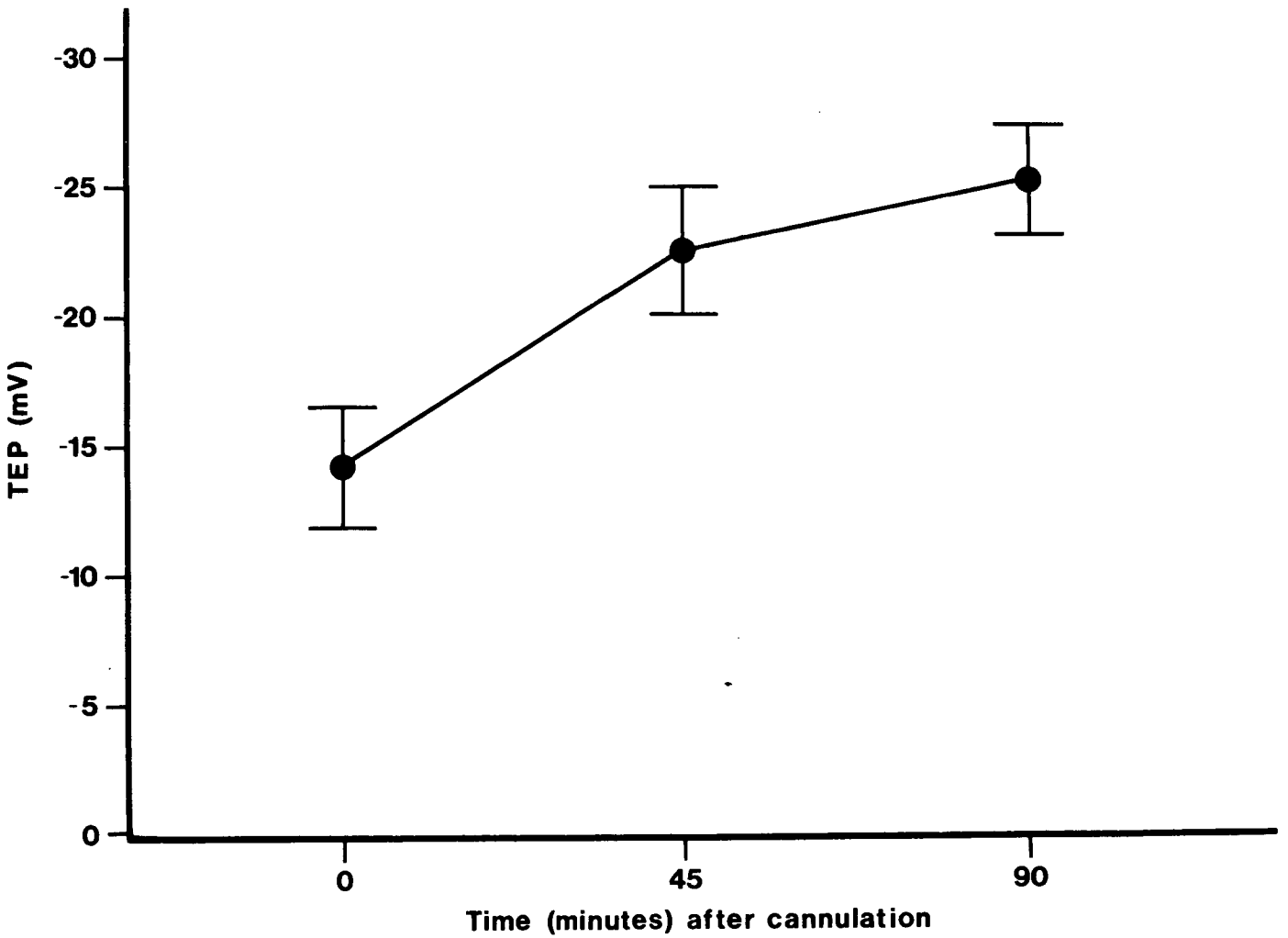
-30
-25
-20
-15
-10
-5
0
TEP (mV)
0
45
90
Time (minutes) after cannulation

hemolymph pH within physiological limits. Alternatively, this elevated PCO_2 value could arise from passive processes and largely be a result of a leftward shift of the CO_2-HCO_3^- equilibrium as ingested HCO_3^- rapidly enters the hemolymph.

Larval hemolymph exhibits a large inorganic anion deficit (Table 2.2) which is characteristic of dipteran hemolymph and is due to the presence of large concentrations of organic acids (Florkin and Jeuniaux, 1964). This inorganic anion deficit increased as hemolymph Na^+ concentrations increased and Cl^- levels dropped when larvae were acclimated to high HCO_3^- and CO_3^{2-} media (Table 2.2). If organic acids account for this deficit then an increase in these compounds would not only maintain hemolymph electroneutrality, but may also enhance hemolymph buffering capacity necessary to counter short-term alkaline shifts in hemolymph pH.

Hemolymph Ca^{2+} concentrations (Table 2.2) also increased when larvae were acclimated to 250 mM HCO_3^- or 100 mM CO_3^{2-} media. The rise in Ca^{2+} levels may reflect changes in the amount of Ca^{2+} bound to organic molecules. In addition, elevated hemolymph pH may increase Ca^{2+} complexation and precipitation, making it necessary for larvae to increase total hemolymph Ca^{2+} concentration as a means of regulating Ca^{2+} activity.

1) Rectal HCO_3^- Secretion

The function of the rectum of saline water mosquito larvae in osmoregulation was discussed in Chapter I. Briefly, the rectum is composed of two ultrastructurally distinct segments (Meredith and Phillips, 1973c; cf. Fig. 2.2B) and is functionally analogous to avian and reptilean salt glands. When larvae are acclimated to hypersaline media, the rectal salt gland produces strongly hyperosmotic secretions with ion ratios and total osmotic

concentrations reflecting those found in the external environment (Bradley and Phillips, 1975, 1977a,b). This organ is believed to be the major site of Na^+, Mg^{2+} and Cl^- regulation in saline waters (Bradley and Phillips, 1977a).

Data from micropuncture studies (Fig. 2.7 and Table 2.4) demonstrate that the rectal salt gland is also an important site of HCO_3^- excretion and regulation as postulated by Bradley and Phillips (1977a). Larvae acclimated to 250 mM HCO_3^- and 100 mM CO_3^{2-} media produce rectal secretions with significantly higher concentrations of HCO_3^- than animals acclimated to the Rearing medium.

The total osmotic and ionic concentrations of secretions collected by microcannulation were considerably higher than those of secretions collected by micropuncture (cf. Figs. 2.7 and 2.8). The most likely explanation for this discrepancy is related to the differences between the two isolated rectal preparations used. With the micropuncture preparation it is possible that small amounts of relatively dilute midgut and Malpighian tubule fluid remain in the rectum after ligation even though the larvae normally empty the rectum when handled (Bradley and Phillips, 1975; Strange, unpublished observations). When using the cannulated preparation, however, it was always possible to rinse and then empty the rectum completely before the start of any experiment. This presumably results in the collection of pure rectal secretion.

Data from microcannulation studies allowed determination of transrectal HCO_3^- and CO_3^{2-} gradients. Lumen-to-hemocoel side HCO_3^- and CO_3^{2-} ratios of 21:1 and 241:1, respectively, were calculated using results shown in Fig. 2.8. In addition, the calculated luminal CO_2 concentration (see Results) was slightly higher than that in the bath giving a

lumen-to-hemocoel CO_2 ratio of 1.8:1.

To generate the observed HCO_3^- and CO_3^{2-} gradients by passive mechanisms, a transepithelial potential of +69 mV to +76 mV (lumen positive) would be required as calculated from the Nernst equation. The measured rectal TEP (Fig. 2.9) varied between -14 mV to -25 mV (lumen negative) demonstrating clearly that HCO_3^- transport occurs by an energy-dependent process.

In conclusion, it is clear that A. dorsalis larvae can inhabit extremes of alkalinity and yet regulate their acid-base status within narrow physiological limits. The rectal salt gland mediates a large component of acid-base regulation by excreting HCO_3^- against remarkably large electrochemical gradients. In the following chapter the epithelial mechanism of HCO_3^- excretion is examined using a microperfused salt gland preparation.

CHAPTER III - IONIC REQUIREMENTS OF CO_2 TRANSPORT IN THE MICROPERFUSED RECTAL SALT GLAND

A. Introduction

Mechanisms of H^+/OH^- and HCO_3^- transport have been studied in a wide variety of vertebrate epithelia including fish gills, pancreas, renal tubules, salivary glands, amphibian and reptilean urinary bladders, gastric mucosa, intestines, amphibian skin, gall bladder and choroid plexus. Detailed cellular mechanisms of acid and base movements have been most extensively studied in the turtle urinary bladder (reviewed by Steinmetz, 1974; Steinmetz and Anderson, 1982; see also Gluck, Cannon and Al-Awqati, 1982), gastric mucosa (reviewed by Forte, Machen and Öbrink, 1980; Sachs, Faller and Rabon, 1982) and proximal tubule (reviewed by Warnock and Rector, 1979, 1981; see also Boron and Boulpaep, 1983a,b; Ives, Yee and Warnock, 1983; Sasaki and Berry, 1983). Studies in single cells such as sea urchin eggs, snail and squid neurons, and crayfish and barnacle muscle fibers (reviewed by Roos and Boron, 1981) have provided detailed information on invertebrate acid and base transport mechanisms. Virtually nothing is known, however, about H^+/OH^- and HCO_3^- transport in invertebrate epithelia. Indirect studies on Libbellula and Aeschna nymphs (Krogh, 1939), freshwater bivalves (Dietz and Branton, 1975; Dietz, 1978; Scheide and Dietz, 1982), anal papillae of freshwater mosquito larvae (Stobbart, 1967, 1971), earthworm integument (Dietz and Alvarado, 1970; Dietz, 1974) and snail integument (de With, Witteveen and van der Woude, 1980; de With and van der Schors, 1982) suggest the presence of Na^+/H^+ (or NH_4^+) and Cl^-/HCO_3^- exchange mechanisms in these tissues. In crustacean gills the direct measurement of both acid and base, and Na^+ and Cl^- fluxes, and the demonstration of the interdependence of these fluxes has provided good evidence for the presence

of Na^+/H^+ and Cl^-/HCO_3^- exchangers which mediate transepithelial acid-base movements (Kirschner, Greenwald and Kerstetter, 1973; Ehrenfeld, 1974; Pequeux and Gilles, 1981). The structural complexity of the gill epithelium and problems associated with both *in vivo* and *in vitro* studies, however, has prevented further characterization of acid and base transport mechanisms.

The mosquito larva, *Aedes dorsalis*, is one of the few organisms capable of inhabiting extremely alkaline salt lakes containing high concentrations of HCO_3^- and CO_3^{2-} and having pH values up to 10.5 (see Scudder, 1969; Topping and Scudder, 1977). In Chapter II it was demonstrated that the rectal salt gland is an important site of pH and HCO_3^- regulation in these larvae. Isolated salt glands secrete fluid containing 402 mM HCO_3^- and 41 mM CO_3^{2-} at a rate of 38 $nl \cdot h^{-1}$. Lumen-to-bath HCO_3^- and CO_3^{2-} gradients of 21:1 and 241:1, respectively, are generated by the salt gland epithelium against a transepithelial potential of -25 mV (lumen negative).

To investigate the transport mechanisms responsible for the maintenance of these exceptionally large HCO_3^- and CO_3^{2-} gradients, an *in vitro* microperfused salt gland preparation was developed. The work in the present chapter examines the ionic requirements of CO_2 transport using conventional ion replacement experiments and well-known inhibitors of acid-base transport mechanisms.

B. Materials and Methods

Animals. Larvae were reared in a low alkalinity rearing medium and the adult colony maintained as described previously (Chapter II). Three days after hatching larvae were transferred to 250 mM HCO_3^- medium containing (in mM): 361.5 Na^+, 2.5 K^+, 0.03 Ca^{2+}, 0.50 Mg^{2+}, 39.6 Cl^-, 10.0 SO_4^{2-},

250 HCO_3^-, 29.0 CO_3^{2-}, pH 8.9. All experiments were conducted at room temperature (21 - 24°C) using fourth instar larvae acclimated to this medium for three to six days.

Microperfusion System. Diagrams of the bath chamber and microperfused salt gland are shown in Fig. 3.1. Perfusion pipets were pulled from acid-washed glass tubing (1.0 mm O.D., 0.8 mm I.D.; Drummond Scientific Company, Broomall, Pennsylvania) over a small flame to yield outer diameters of 35 - 50 μ. The pipet tips were broken to an appropriate length with forceps and the tip opening reduced to a diameter of 3 - 8 μ and heat polished using a microforge.

Collection pipets were pulled from glass tubing (3.0 mm O.D., 1.8 mm I.D.) on a micropipet puller (Model PE2, Narishige Instruments, Tokyo). The tips of the pipets were broken off with forceps and a glass cannula (2.0 - 3.0 mm long, 70 - 90 μ O.D., 50 - 70 μ I.D.) was sealed into the tip with a long column of epoxy. This epoxy seal was electrically insulated and waterproofed using Sylgard 184 resin (Dow Corning).

The bath chamber was fabricated from polymerized Sylgard 184 resin molded into the bottom of a 55 mm diameter plastic petri dish. Total chamber volume was 1.5 to 1.8 ml.

Rectal salt glands were isolated by pinning a larva to the bottom of the bath chamber using a small 'staple' fashioned from an insect pin. The bathing chamber was filled and superfused continuously with oxygenated saline and the anal canal, rectal salt gland, ileum and a small portion of the midgut were dissected free. Salt glands were approximately 1.0 - 1.2 mm long and 200 - 300 μ in diameter. The total length of the preparation with midgut, ileum and anal canal attached was approximately 3.0 - 3.5 mm.

Figure 3.1 A) Diagram of Sylgard bath chamber showing arrangement of collection and perfusion pipets. Bath superfusion was in the opposite direction to luminal perfusion and the bathing saline flowed continuously over a glass lip at the bath outlet into a waste container. B) Diagram of microperfused rectal salt gland. Note anterior and posterior rectal segments.

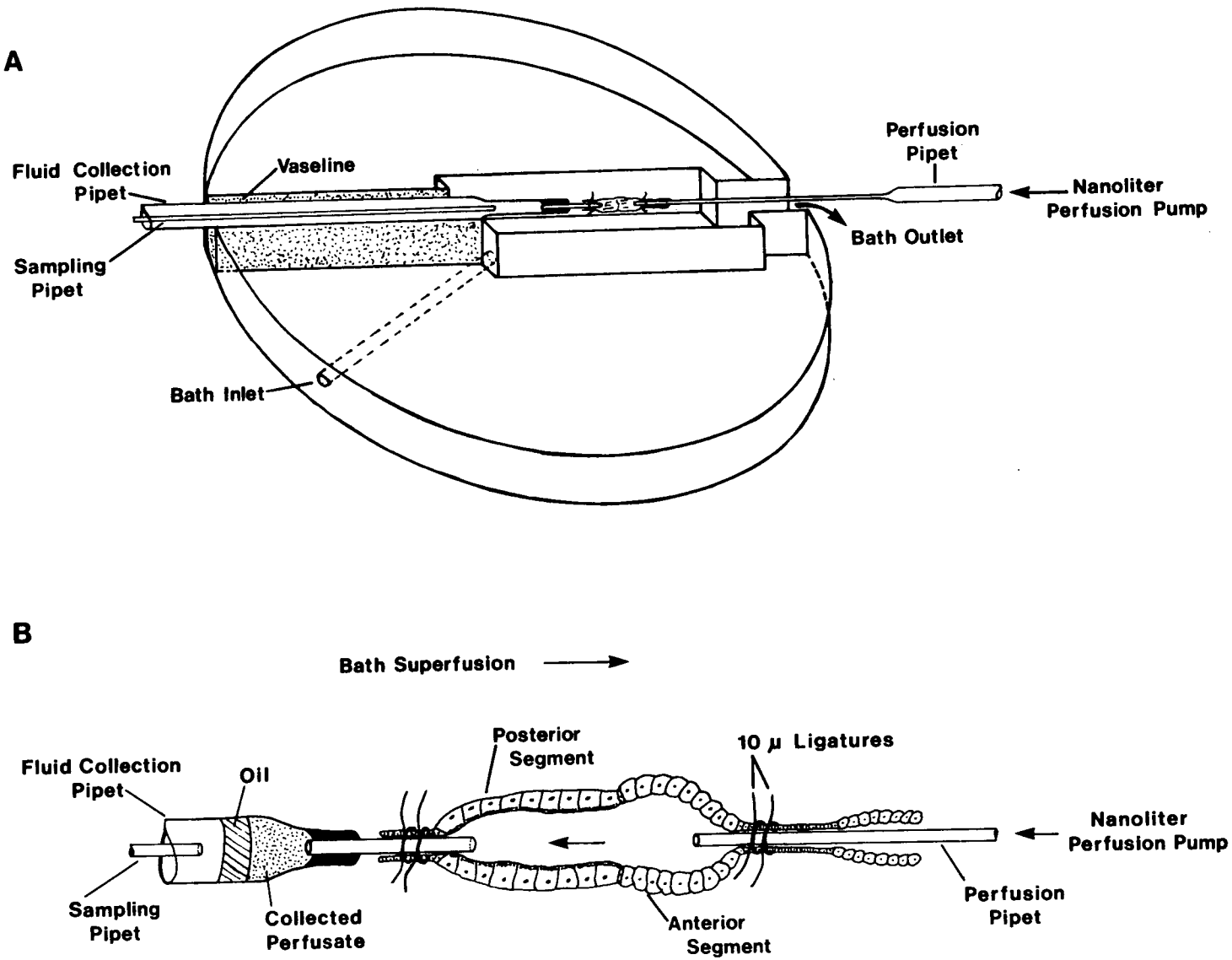
A
Fluid Collection Pipet
Vaseline
Perfusion Pipet
Nanoliter Perfusion Pump
Bath Outlet
Sampling Pipet
Bath Inlet
B
Bath Superfusion
Fluid Collection Pipet
Oil
Posterior Segment
10 μ Ligatures
Nanoliter Perfusion Pump
Sampling Pipet
Collected Perfusate
Anterior Segment
Perfusion Pipet

After an initial 2 - 2.5 hour equilibration period (see Discussion), salt glands were perfused by inserting a perfusion pipet down the midgut and ileum into the anterior segment, and by inserting a collection pipet into the posterior rectal segment via the anal canal. Both the collection pipet holder and perfusion pump (see below) were mounted on Narishige micromanipulators (Model MM-3). The salt gland was ligated onto the collection and perfusion pipets using two or three 10 μ ligatures which were made by teasing apart 5-0 silk surgical suture thread (Ethicon Inc., Somerville, N.J.) under mineral oil. These ligatures were partially tied under the oil, blotted on bibulous paper and dampened before use.

Rectal salt glands were perfused at a rate of 10 $nl \cdot min^{-1}$ using a nanoliter perfusion pump (WPI Model 1400, New Haven, CT). The bath chamber was superfused by gravity at a rate of 4 - 5 $ml \cdot min^{-1}$. During experiments and equilibration periods the bath chamber was covered with the bottom of a plastic petri dish and a stream of 98% O_2 - 2% CO_2 was directed immediately over the bathing saline.

Determination of Net total CO_2 Flux. Collected perfusates were sampled by inserting an oil-filled micropipet attached to a length of PE 100 tubing down the bore of the collection pipet. Salt glands were initially perfused for a 20 - 25 minute period after set-up and the collected perfusate discarded. Timed collections (20 - 25 minutes) of perfusate were then made for determination of total CO_2 content using microcalorimetry (Picapnotherm; Microanalytic Instrumentation, Bethesda, MD) as described by by Vurek, Warnock and Corsey (1975). Volumes of collected perfusate were determined by measuring drop diameters under oil with an eyepiece micrometer.

The net rate of total CO_2 transport ($J_{net}^{CO_2}$) was calculated according to the equation:

$$J_{net}^{CO_2} = C_c V_c - C_p V_p / L$$

where C_c and C_p are the total CO_2 concentrations in the collected and perfused fluids, respectively, V_c is the perfusion collection rate, V_p is the pump perfusion rate and L is the salt gland length.

Net fluid movement across the perfused salt gland epithelium was measured under a variety of experimental conditions using ^{3}H-inulin (New England Nuclear Corp.) as a volume marker or by determining the differences between the timed perfusate collection rate and the calibrated pump rate. Mean inulin recovery under a variety of experimental conditions was 97.0 $\pm$ 0.6% ($\pm$ S.E., n = 26) and the mean difference between V_c and V_p was -0.09 $\pm$ 0.08 nl·min^{-1} ($\pm$ S.E., n = 31). In stopped-flow microperfusion experiments the rate of salt gland fluid secretion was only 0.3 $\pm$ 0.07 nl·min^{-1} (mean $\pm$ S.E., n = 3) demonstrating that net fluid movements were clearly below accurate detection limits in glands perfused at a rate of 10 nl·min^{-1} (i.e. at these fluid secretion and perfusion rates a maximal volume change of only 3 - 4% would occur in the collected perfusates). Therefore, for all calculations V_c was assumed to be equal to V_p. For comparison, the actual changes in total CO_2 concentrations of collected perfusates are shown in Table 3.2.

Salines. The composition of physiological salines used throughout this study are shown in Table 3.1. The control bath saline was based on measured hemolymph ionic and free amino acid concentrations and on measured pH, PCO_2 and HCO_3^- values (Chapter II). The control perfusate was isosmotic to the bathing saline and had high Na^+, K^+ and Cl^- concentrations

Table 3.1. Composition of physiological salines. All salines were gassed with 98% O_2 - 2% CO_2 and contained the following (in mM): proline 20, alanine 5, glycine 3, glutamine 4, succinate 7.4, citrate 2.4, glucose 10.

Component	Bath Salines				Perfusion Salines			
(mM)	Control	Na^+-Free	K^+-Free	Cl^-Free	Control	Na^+-Free	K^+-Free	Cl^--Free
Na^+	189.5	-	198.5	189.5	148.5	-	198.5	148.5
K^+	9	9	-	9	50	50	-	50
Mg^{2+}	4	4	4	4	4	4	4	4
Ca^{2+}	4	4	4	4	4	4	4	4
Cl^-	39	39	39	-	164	164	164	-
HCO_3^-	18.5	18.5	18.5	18.5	18.5	18.5	18.5	18.5
SO_4^{2-}	4.5	4.5	4.5	4.5	5	5	5	5
Isethionate$^-$	125	-	125	148	-	-	-	-
Sucrose	-	250	-	-	-	-	-	-
Choline$^+$	-	64.5	-	-	-	148.5	-	-
Methylsulfate$^-$	-	-	-	-	-	-	-	148
NO_3^-	-	-	-	16	-	-	-	16
Lissamine Green	-	-	-	-	0.05%	-	-	-

Table 3.2. Changes in total CO_2 and Cl^- concentrations in collected perfusates. Values are means ± S.E. (n = 4-12).

Experiment	Total CO_2 (mM)	Cl^- (mM)
Control	70.6 ± 5.3	-81.6 ± 5.0
Bilateral Na^+-free	68.3 ± 4.4	-
Bilateral K^+-free	68.3 ± 5.1	-
1.0 mM serosal ouabain	75.8 ± 6.8	-
2.0 mM serosal amiloride	73.1 ± 1.3	-
Serosal Cl^--free	75.6 ± 3.4	-
Luminal Cl^--free	17.0 ± 2.4	-
Bilateral Cl^--free	17.0 ± 2.4	-
0.5 mM serosal SITS	69.7 ± 4.8	-
0.5 mM serosal DIDS	43.3 ± 4.1	-
0.1 mM serosal acetazolamide	14.5 ± 1.3	-
1.0 mM serosal acetazolamide	14.7 ± 0.9	-

similar to larval Aedes campestris Malpighian tubule fluid (Phillips and Maddrell, 1974). All perfusates were Millipore filtered (0.45 u) two times before use. Both perfusion and bathing salines were gassed with 98% O_2 - 2% CO_2 and had mean pH values of 7.64 and 7.63, respectively. Note that the large inorganic anion deficit observed in larval hemolymph (Chapter II) was simulated in the bathing salines using sodium isethionate.

Inhibitor Studies. The mechanisms of CO_2 transport were examined by adding the following inhibitors to the serosal medium (see Discussion): 2.0 mM amiloride (Merck, Sharp and Dome, Kirkland, Quebec), 0.5 mM SITS (4-acetamido-4'- isothiocyanostilbene-2, 2'-disulfonic acid, BDH Chemicals Ltd., Vancouver, British Columbia), 0.5 mM DIDS (4, 4'-diisothiocyano-2, 2'-disulfonic acid, Sigma Chemical Co., St. Louis, MO), 1.0 mM ouabain (Sigma) or 10^{-4} -10^{-3} M acetazolamide (Sigma). Salt glands were dissected and prepared for perfusion in control salines as described above. Immediately after the start of luminal perfusion, the bath was changed to control saline containing one of the inhibitors. After a 20 - 25 minute perfusion period, perfusates were collected and discarded and the salt gland perfused for an additional 25 minutes. Total exposure time to the inhibitor was 45 - 55 minutes.

Both SITS and DIDS were dissolved in amino acid-free saline (replaced with sucrose). Weighing and preparation of SITS and DIDS and perfusion experiments with SITS and DIDS salines were all carried out in a darkened room. In addition, the bath perfusion reservoir was wrapped in foil and the bath chamber was covered with a foil-wrapped petri dish. Amiloride was dissolved in bath salines in which K_2SO_4 had been replaced by KCl and $MgCl_2$ replaced by $Mg(NO_3)_2$. All inhibitors were made up fresh before each experiment.

C. Results

Results shown in Fig. 3.2 demonstrate the viability of the *in vitro* salt gland preparation. Microperfused whole salt glands maintain a high and stable transepithelial potential of -40 to -50 mV (lumen negative) for at least 7 - 8 hours and this potential is rapidly abolished by cyanide (Fig. 3.2A). In addition, microperfused salt glands secrete total CO_2 at very high and stable rates (Fig. 3.2B). Mean $J^{CO_2}_{net}$ under control conditions was 799 $\pm$ 57 pMole·min^{-1}·mm^{-1} ($\pm$ S.E., n = 9).

The contribution of metabolic CO_2 to transepithelial CO_2 flux in this tissue is negligible. Mean $J^{CO_2}_{net}$ in rectal salt glands bathed bilaterally with CO_2 and HCO_3-free salines (replaced with HEPES buffered saline) was 23.2 $\pm$ 0.7 pMole·min^{-1}·mm^{-1} ($\pm$ S.D., n = 2). The mean change in collected perfusate total CO_2 concentration was 1.9 $\pm$ 0.1 mM which is close to the limits of accurate detection using microcalorimetry (Vurek *et al.*, 1975).

Ion substitution studies were conducted to determine the ionic requirements for CO_2 transport. Rectal salt glands were equilibrated in the various ion-free salines for 2 - 2.5 hours prior to perfusion to minimize the problem of ion leakage and recycling through the epithelial cells.

Fig. 3.3 and Table 3.2 show that bilateral Na^+ or K^+ substitutions had no significant ($P > 0.25$) effect on $J^{CO_2}_{net}$. Mean $J^{CO_2}_{net}$ in Na^+ and K^+-free salines were 771 $\pm$ 54 pMole·min^{-1}·mm^{-1} ($\pm$ S.E., n = 9) and 757 $\pm$ 57 pMole·min^{-1}·mm^{-1} ($\pm$ S.E., n = 10), respectively. Qualitative, microscopic observations showed that removal of serosal and mucosal K^+ caused both anterior and posterior rectal cells to swell slightly, while bilateral Na^+ substitution caused only a small amount of swelling in anterior rectal cells. Removal of serosal Na^+ or K^+ only, caused excessive swelling of

Figure 3.2 A) Transepithelial potential recorded in microperfused rectal salt gland. The salt gland was perfused by gravity with the perfusion pipet functioning as the luminal electrode (Chapter V). B) Time course determinations of control $J^{CO_2}_{net}$ in microperfused salt glands. The open and closed squares and circles represent results obtained from individual salt gland preparations.

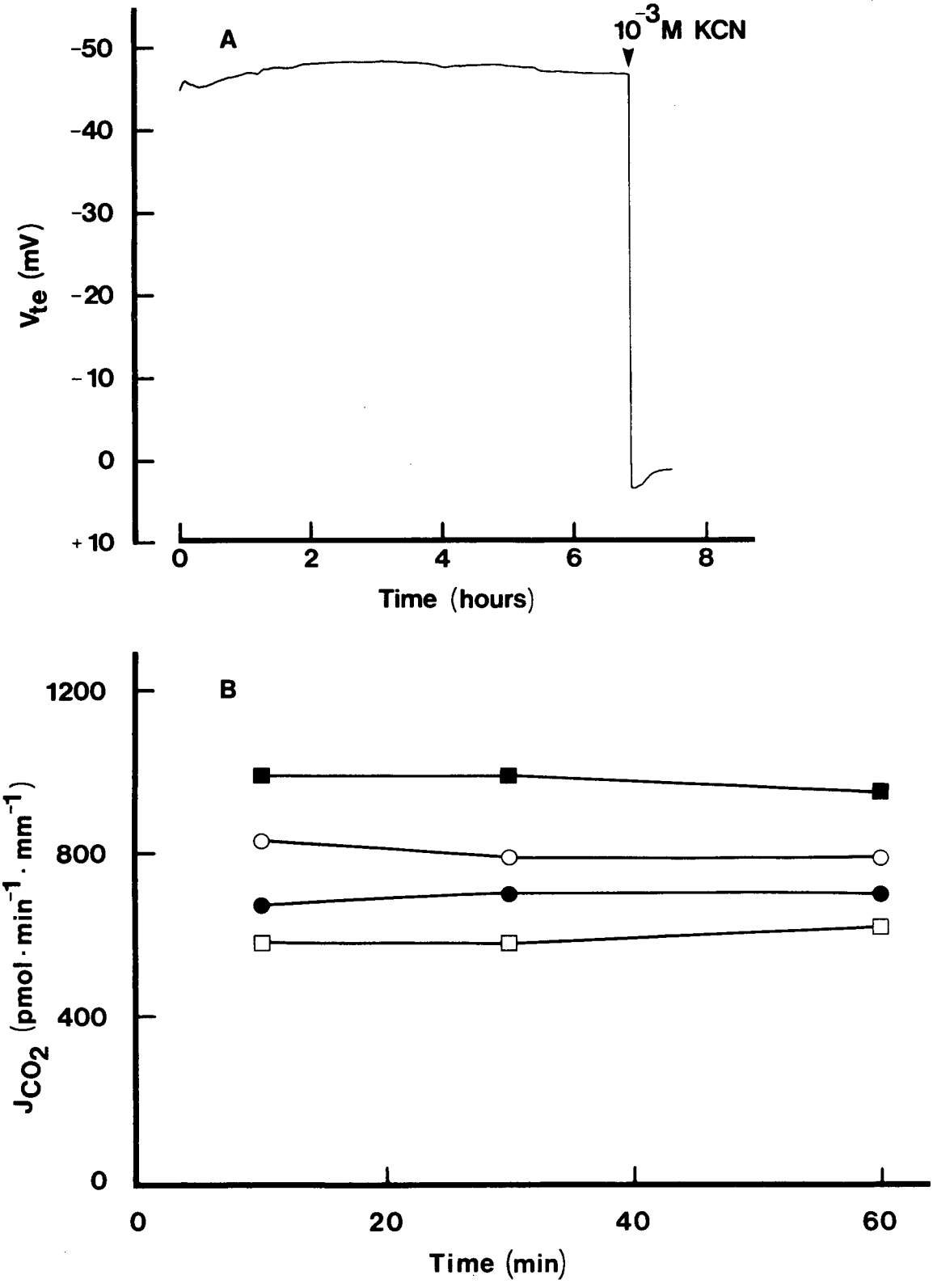
A
10^{-3}M KCN
-50
-40
-30
-20
-10
0
+10
V_{te} (mV)
0
2
4
6
8
Time (hours)
B
1200
800
400
0
J_{CO_2} (pmol · min^{-1} · mm^{-1})
0
20
40
60
Time (min)

Figure 3.3 Effects of bilateral Na^+ or K^+ substitutions on $J^{CO_2}_{net}$. Values are means $\pm$ S.E. (n = 9-10).

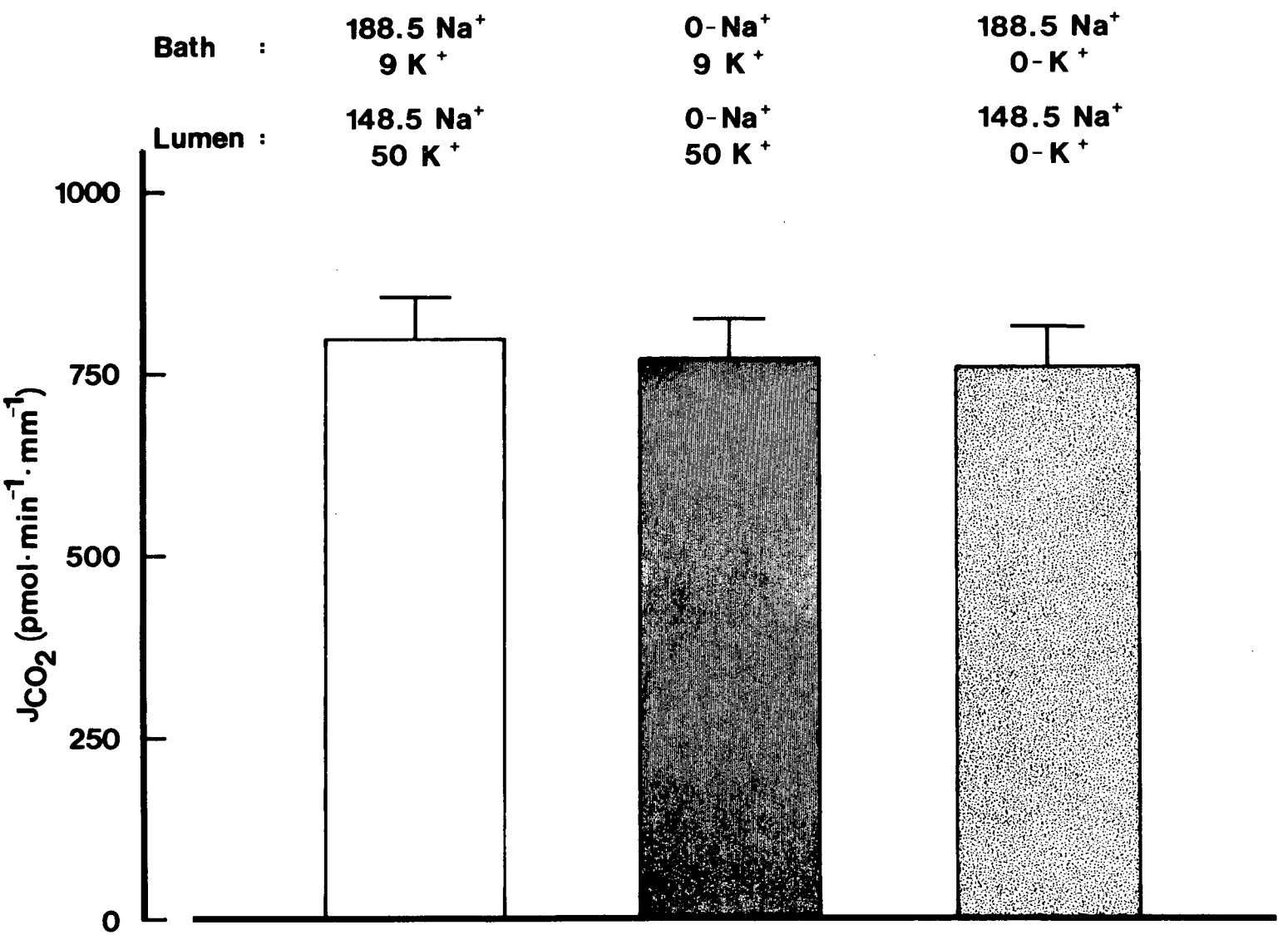
Bath :
188.5 Na+
9 K+
0-Na+
9 K+
188.5 Na+
0-K+
Lumen :
148.5 Na+
50 K+
0-Na+
50 K+
148.5 Na+
0-K+
1000
750
500
250
0
JCO2 (pmol·min-1·mm-1)

the anterior rectal cells and usually resulted in luminal occlusion.

Substitution of serosal Cl^- with isethionate or methylsulfate (Fig. 3.4, Table 3.2) had no significant ($P > 0.25$) effect on $J^{CO_2}_{net}$ ($\bar{x}\ J^{CO_2}_{net}$ = 861 $\pm$ 78 pMole·min^{-1}·mm^{-1}; $\pm$ S.E., n = 5). Removal of luminal Cl^-, however, decreased $J^{CO_2}_{net}$ by approximately 80% ($P < 0.0005$) to 178 $\pm$ 24 pMole·min^{-1}·mm^{-1} (mean $\pm$ S.E., n = 6). Substitution of both serosal and mucosal Cl^- had no further inhibitory effect on $J^{CO_2}_{net}$ ($\bar{x}\ J^{CO_2}_{net}$ = 175 $\pm$ 25 pMole·min^{-1}·mm^{-1}; $\pm$ S.E., n = 6; see Fig. 3.4 and Table 3.2).

In two experiments both Cl^- and SO_4^{2-} were removed from the serosal and mucosal salines. The mean $J^{CO_2}_{net}$ of 144 $\pm$ 44 pMole·min^{-1}·mm^{-1} ($\pm$ S.D., n = 2) was not significantly different ($0.10 < P < 0.25$) from that observed with mucosal and serosal Cl^- substitutions alone ($\bar{x}\ J^{CO_2}_{net}$ = 191 $\pm$ 69 pMole·min^{-1}·mm^{-1}; $\pm$ S.D., n = 4). These results were therefore pooled and are shown in Fig. 3.4. Removal of SO_4^{2-} and/or Cl^- had no obvious effect on cell volume in either anterior or posterior salt gland segments.

To examine the mechanisms of CO_2 transport further, well known inhibitors of acid-base transport mechanisms were added to the serosal medium. Net total CO_2 transport rates were 849 $\pm$ 80 pMole·min^{-1}·mm^{-1} and 761 $\pm$ 32 pMole·min^{-1}·mm^{-1} ($\pm$ S.E., n = 4-5) in the presence of 1.0 mM serosal ouabain or 2.0 mM serosal amiloride, respectively (Fig. 3.5 and Table 3.2), and were not significantly different ($P > 0.25$) from control $J^{CO_2}_{net}$. Similarly, addition of 0.5 mM SITS (Fig. 3.6 and Table 3.2) to the bathing saline had no effect ($P > 0.25$) on $J^{CO_2}_{net}$ ($\bar{x}\ J^{CO_2}_{net}$ = 750 $\pm$ 45 pMole·min^{-1}·mm^{-1}; $\pm$ S.E., n = 4). Addition of 0.5 mM DIDS (Fig. 3.6), however, caused a significant ($0.0025 < P < 0.005$) decrease of approximately 40% in $J^{CO_2}_{net}$ to a value

Figure 3.4 Effects of luminal and serosal Cl^- substitutions on $J^{CO_2}_{net}$. Values are means $\pm$ S.E. (n = 5-9).

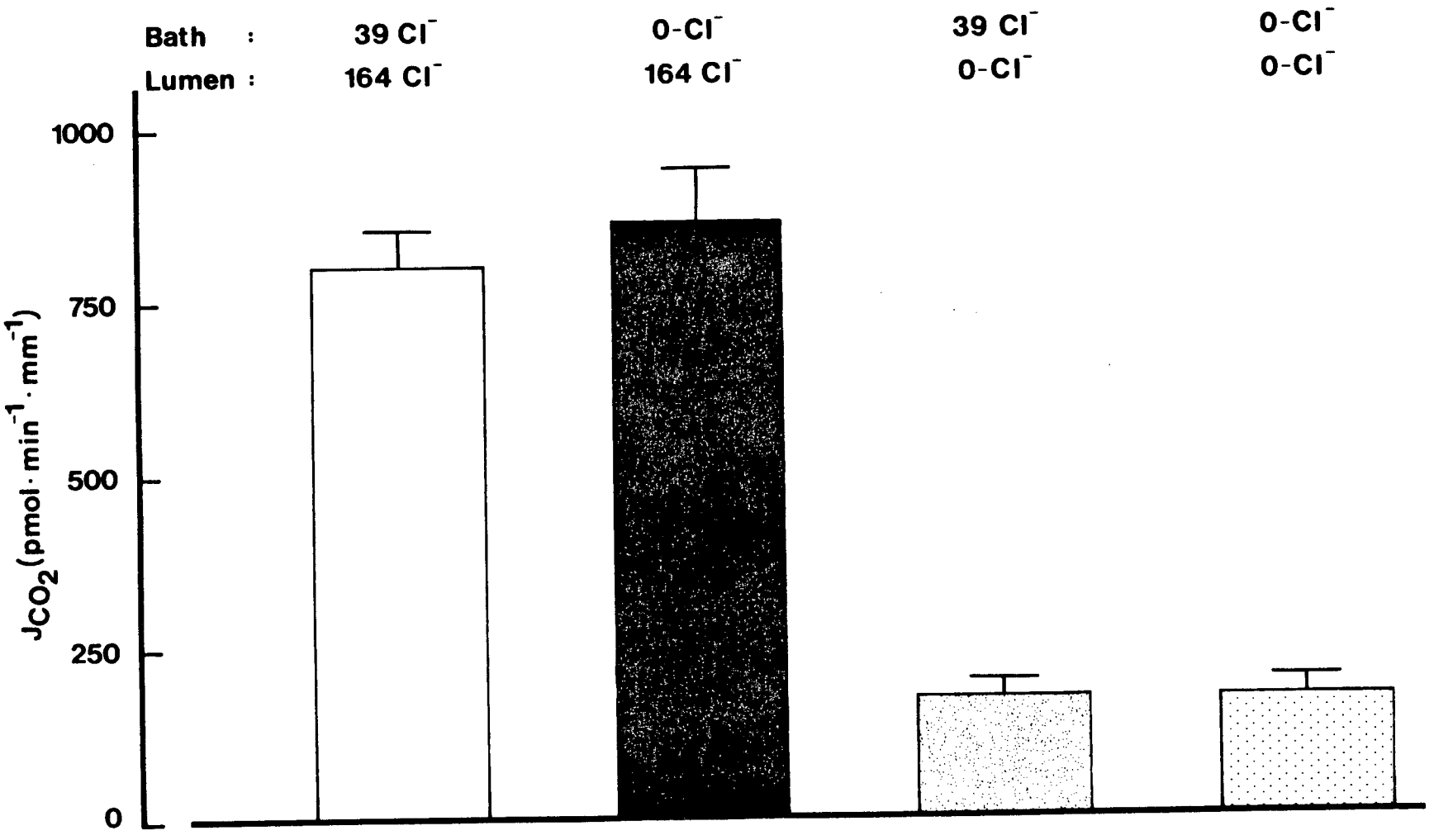
Bath :
Lumen :
39 Cl⁻
164 Cl⁻
0-Cl⁻
164 Cl⁻
39 Cl⁻
0-Cl⁻
0-Cl⁻
0-Cl⁻
1000
750
500
250
0
J_{CO_2} (pmol · min⁻¹ · mm⁻¹)

Figure 3.5 Effects of serosal addition of 1.0 mM ouabain or 2.0 mM amiloride on $J^{CO_2}_{net}$. Values are means $\pm$ S.E. (n = 4-9).

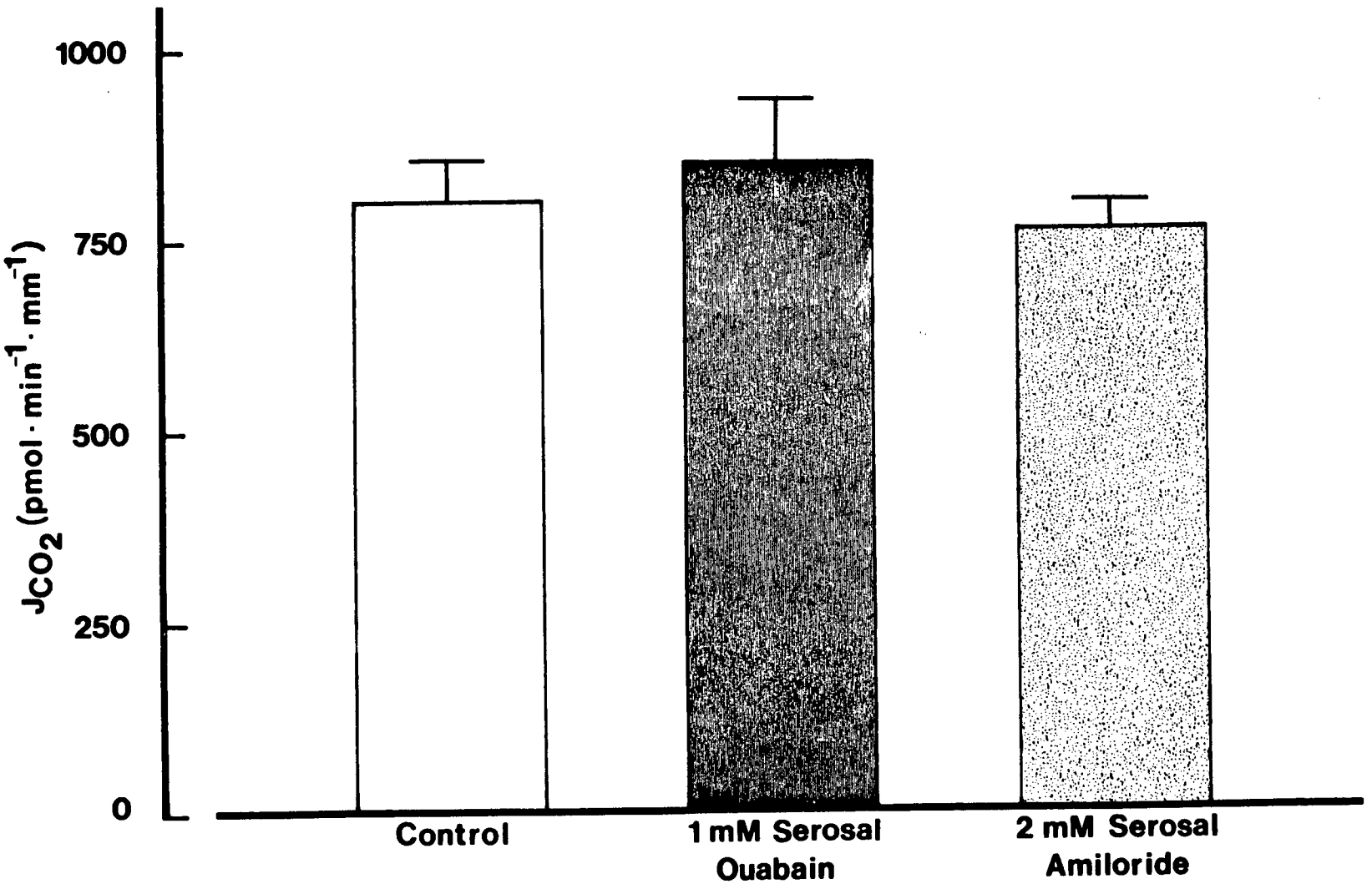
1000
750
500
250
0
J_{CO_2} (pmol · min^{-1} · mm^{-1})
Control
1 mM Serosal Ouabain
2 mM Serosal Amiloride

Figure 3.6 Effects of serosal addition of 0.5 mM SITS, 0.5 mM DIDS or 1.0 mM acetazolamide on $J^{CO_2}_{net}$. Values are means $\pm$ S.E. (n = 4-9).

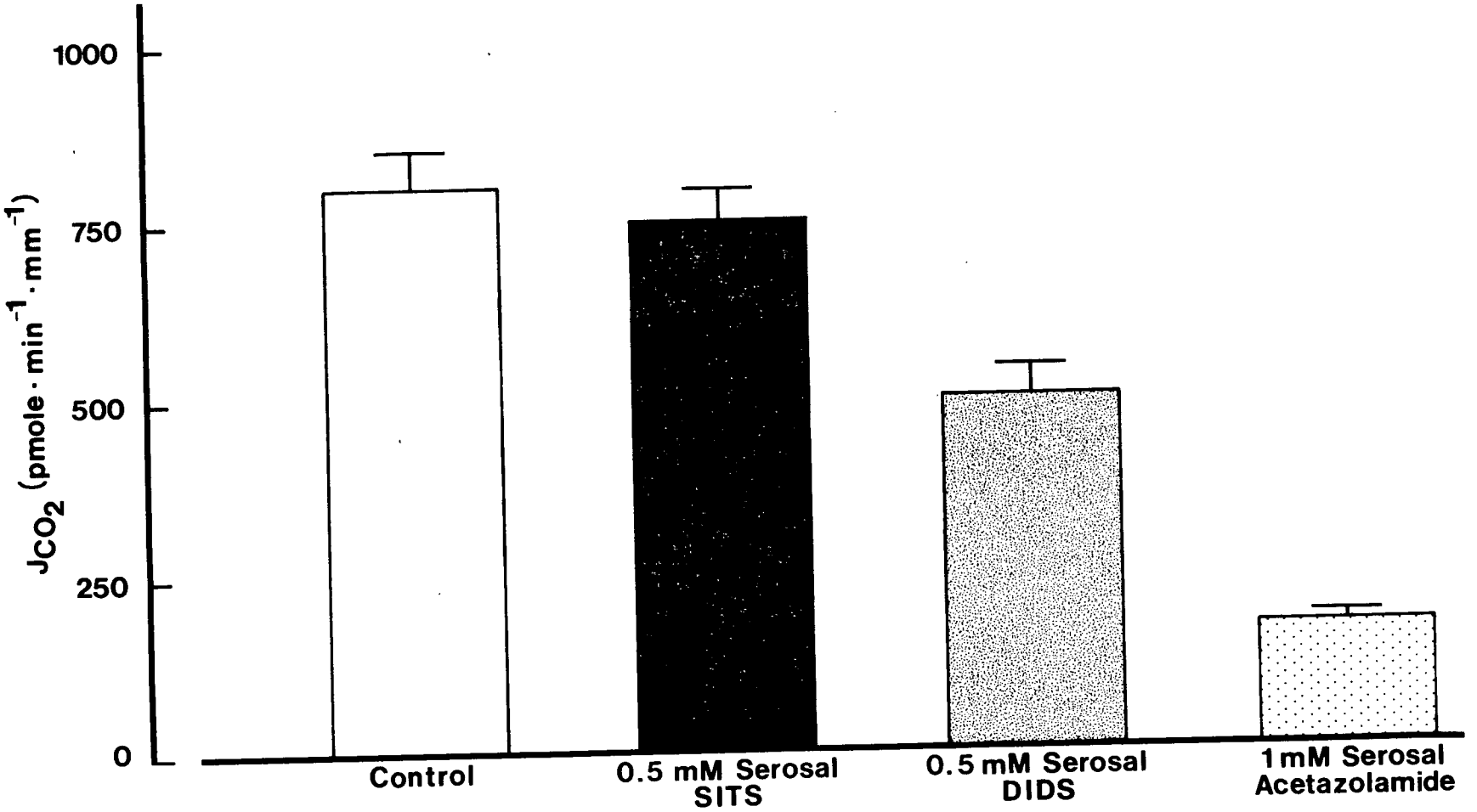
1000
750
500
250
0
J_{CO_2} (pmole · min^{-1} · mm^{-1})
Control
0.5 mM Serosal SITS
0.5 mM Serosal DIDS
1 mM Serosal Acetazolamide

of 500 ± 42 pMole·min^{-1}·mm^{-1} (± S.E., n = 4). The lack of any inhibitory effect of SITS indicated that DIDS inhibition was not due to a nonspecific effect of the amino acid-free saline (see Materials and Methods).

Net CO_2 secretion was inhibited by approximately 80% ($P < 0.0005$) when the carbonic anhydrase inhibitor, acetazolamide, was added to the bath at a concentration of 10^{-4}M (Table 3.2) or 10^{-3}M (Fig. 3.6 and Table 3.2).

D. Discussion

The microperfused rectal salt gland of A. dorsalis provides an excellent model system in which to study the mechanisms of transepithelial H^+ and HCO_3^- transport. Microperfused salt glands are remarkably viable and maintain a large and very stable transepithelial potential for at least 7 to 8 hours (Fig. 3.2A). This potential is completely poisoned by KCN demonstrating that it is due to active transport processes.

Salt glands perfused in vitro secrete total CO_2 at very high and easily measurable rates. Preliminary studies (unpublished observations) indicated that $J_{net}^{CO_2}$ declined steadily when salt glands were perfused immediately after dissection. When salt glands were equilibrated for 2 to 2.5 hours in bathing saline before perfusion, however, $J_{net}^{CO_2}$ remained stable during the 1 hour collection period (Fig. 3.2B).

The results of the present study suggest that Na^+/H^+ and K^+/H^+ exchange mechanisms play no role in transepithelial HCO_3^- movements. Complete bilateral substitution of Na^+ or K^+ (Fig. 3.3), or serosal addition of 1.0 mM ouabain (Fig. 3.5) have no effect on $J_{net}^{CO_2}$. Bicarbonate transport is also unaffected by serosal addition of 2.0 mM amiloride (Fig. 3.5), a diuretic which has been shown clearly to be a potent inhibitor of Na^+/H^+

exchange mechanisms in a wide variety of cells and epithelia (reviewed by Benos, 1982).

Removal of serosal Cl^- had no effect on $J^{CO_2}_{net}$ while luminal Cl^- removal inhibited CO_2 transport by approximately 80% (Fig. 3.4). In addition, the Cl^-/HCO_3^- exchange inhibitor, DIDS, decreased $J^{CO_2}_{net}$ by 40% when added to the serosal side of the epithelium (Fig. 3.6). These results suggested that HCO_3^- transport is mediated by a Cl^-/HCO_3^- exchange mechanism located at the basolateral cell membrane. To test this idea further, net Cl^- transport (J^{Cl}_{net}) was examined by electron microprobe analysis as described in the following chapter. A large net Cl^- absorption was observed and this J^{Cl}_{net} of -888 $\pm$ 57 pMole·min^{-1}·mm^{-1} ($\pm$ S.E., n = 12) was not significantly different ($P > 0.10$) from the rate of CO_2 secretion (see Results and Table 3.2). These results therefore provide good quantitative evidence for the presence of a 1:1 Cl^-/HCO_3^- exchange system in the rectal salt gland.

Carbonic anhydrase function has been shown to be of major importance in almost all acid-base transporting epithelia studied to date (reviewed by Maren, 1967; Parsons, 1982). The pronounced inhibitory effect of serosal acetazolamide (Fig. 3.6) indicates that carbonic anhydrase function also plays a critical role in salt gland HCO_3^- secretion. Further studies are needed to determine if carbonic anhydrase is located in the cytoplasm, and apical and basolateral cell membranes (see Dobyan and Bulger, 1982), and whether acetazolamide directly inhibits cellular HCO_3^- entry and exit steps (see for example Fromter and Sato, 1976; Boron and Fong, 1983).

Experiments designed to examine mechanisms of salt gland HCO_3^- transport using luminal ion transport inhibitors were complicated by the

presence of the luminal cuticle (Meredith and Phillips, 1973c). Studies in the locust rectum (Phillips and Dockrill, 1968; Lewis, 1971) have shown that the insect hindgut cuticle contains pores with a radius of 6.5 Å and functions as a molecular sieve preventing large molecules (> 200 M.W.) in the lumen from interacting directly with the apical cell membrane.

The permeability properties of the salt gland cuticle were examined indirectly in the present study by use of the vital dye Janus Green. This dye has a molecular weight of 511 and stains cells an intense blue. Salt glands perfused with salines containing > 1% Janus Green showed no staining, while addition of the dye to the serosal side caused cells to immediately stain a dark blue. Since Janus Green clearly could not pass through the cuticle it was apparent that the transport inhibitors used in the present study (M.W. of 222 to 724) would not likely be able to interact with carrier molecules at the apical membranes. Several attempts (summarized in Table 3.3) were therefore made to alter cuticular permeability using Janus Green as a permeability indicator. Spider digestive juices were collected as described by Collatz and Mommsen (1974) and Mommsen (1978a). These juices contain powerful chitinase enzymes specifically adapted to function on arthropod cuticle (Mommsen, 1980). In addition, the juices contain powerful proteases, carbohydrases, esterases, phosphatases, nucleases and emulsifiers (Collatz and Mommsen, 1974; Mommsen, 1978a,b,c). Unfortunately, none of the treatments described in Table 3.3 had any effect on apparent cuticular permeability and thus prevented luminal inhibitor studies. The results do suggest indirectly, however, that the structure of the hindgut cuticle may be considerably different from that of the insect exoskeleton.

Table 3.3 Summary of chitinase experiments.

- Perfusion of the lumen with saline containing high concentrations of commercially available chitinase enzymes (1-2 mg./ml.; Sigma).
- Perfusion of the lumen with saline containing small aliquots of digestive juices collected from funnel-weaver spiders (Tegenaria atrica).
- Pre-prefusion of the lumen with 1% Triton X-100 followed by a 45-55 minute perfusion with pure digestive juices collected from South American tarantulas (Dugesiella sp.).

To summarize, the rectal salt gland of A. dorsalis larvae can be successfully microperfused in vitro. Salt glands from larvae inhabiting extremely alkaline environments secrete total CO_2 at high and stable rates, and the secretion appears to be mediated primarily by a 1:1 Cl^-/HCO_3^- exchange mechanism. In the following chapter further evidence is provided for a Cl^-/HCO_3^- exchange system, the anterior rectal segment is demonstrated to be the site of this exchange and the major transport and excretory functions of the anterior and posterior rectal segments are examined.

CHAPTER IV. SITE OF CL^-/HCO_3^- EXCHANGE AND FUNCTION OF ANTERIOR AND POSTERIOR SALT GLAND SEGMENTS

A. Introduction

The rectal salt gland of saltwater mosquito larvae secretes a strongly hyperosmotic fluid (Bradley and Phillips, 1975) and is a major site of Na^+, K^+, Mg^{2+}, Cl^- (Bradley and Phillips, 1977a,b) and HCO_3^- (Chapter II) excretion and regulation. Rectal salt glands are composed of two segments linked together by a single row of small, indistinct junctional cells, and each segment is composed of a single cell type. Morphological studies on the salt gland (Meredith and Phillips, 1973c) showed that the ultrastructure of anterior rectal cells was similar to cells found in recta of obligatorily freshwater larvae which produce a hyposmotic urine by rectal solute reabsorption. The larger posterior rectal cells, found only in saltwater species, have an elaborately folded apical membrane with infoldings extending across 60% of the cytoplasm. The bulk of the posterior rectal cell's mitochondria are associated directly with these infoldings. Based on these observations Meredith and Phillips (1973c) suggested that the posterior segment was the actual site of hyperosmotic fluid secretion and that the anterior segment was involved in selective solute reabsorption.

Experimental evidence for this hypothesis was provided by Bradley and Phillips (1977c). These investigators tied relatively large ligatures around intact larvae to ablate either the anterior or posterior rectal segments. The cuticle over the segment of interest was dissected away and the segment incubated in artificial hemolymph. Photographic evidence suggested that the posterior rectum had swelled slightly with fluid although the rate of secretion was severely inhibited compared to that observed in the whole salt gland (cf. Bradley and Phillips, 1975). No swelling and fluid

secretion were apparent in anterior rectal segments. Fluid collected by micropuncture from the posterior segment was hyperosmotic, while the very small amounts of fluid collected from anterior segments was slightly hyposmotic to the bathing saline.

In the previous chapter it was shown that HCO_3^- secretion in the rectal salt gland of A. dorsalis is mediated by a 1:1 exchange of luminal Cl^- for serosal HCO_3^-. The work in the present chapter demonstrates the location of this Cl^-/HCO_3^- exchange using microperfused anterior and posterior segment preparations and describes directly the major excretory functions of anterior and posterior rectal salt gland cells.

B. Materials and Methods

Animals. Experimental animals, and rearing and acclimation media were similar to those described in the previous chapter.

Microperfusion and Microcannulation Studies. Perfusion and collection pipets were constructed, and salt glands dissected and equilibrated as described previously (Chapter III). Individual salt gland segments were perfused by cannulating with perfusion and collection pipets ligated into place using two to three 10 μ ligatures (see Chapter III) tied around the ileum, anal canal and directly between the two segments at the junctional region (Fig. 4.1A). Segments were perfused at 10 $nl \cdot min^{-1}$ using a nanoliter perfusion pump (see Chapter III). A pre-collection period of 10 minutes followed by a perfusate collection period of 10-20 minutes was used in all studies.

Microcannulation studies were performed by cannulating individual segments with microcannulae (same construction as perfusion and collection pipets) filled with Sudan Black-stained paraffin oil. Ligatures were tied

around the ileum, anal canal and one cell row (ca. 50 μ) on either side of the junctional region (see Fig. 4.1B). Both oil-filled microcannulae were mounted on Narishige micromanipulators (Model MM-3), and the anterior cannula (see Fig. 4.1B) was held in a micropipette holder (Leitz, Wetzlar, West Germany) attached to a 50 ml syringe. Fluid secreted by the individual segments was collected continuously in the anterior pipet using the attached syringe. After 60-90 minutes the bath chamber was drained, the rectum removed and the secretion sample prepared for analysis (see below). The bath chamber design and superfusion were the same as those described in the previous chapter. All experiments were conducted at room temperature (21 - 24°C)

Sample Analysis. Volumes of collected perfusates and rectal secretion were determined by measuring drop diameters under mineral oil with an eyepiece micrometer. Total CO_2 in these fluids was measured by microcalorimetry (Picapnotherm; Microanalytic Instrumentation, Bethesda, Maryland) as described by Vurek, Warnock and Corsey (1975). Concentrations of Na^+, K^+, Mg^{2+}, Ca^{2+}, Cl^-, total phosphorus and total sulfur were measured in perfusate and secretion samples by electron microprobe analysis using a Cameca model MBX microprobe and methods described previously (Morel and Roinel, 1969; Roinel, 1975). Because of the high ion concentrations in these fluids, samples were diluted two to three times with distilled water before preparation for microprobe analysis.

Salines. The composition of control and HCO_3^--free salines used in this study are shown in Table 4.1. Sodium and Cl^--free salines were the same as those described in the previous chapter. Bicarbonate-free salines were buffered with HEPES (N-2-hydroxyethyl piperazine-N'-2-ethanesulfonic acid) or phosphate and were gassed vigorously with 100% O_2

Figure 4.1 A) Arrangement of ligatures and pipets for microperfusion of individual salt gland segments. B) Arrangement of oil-filled cannulae and ligatures for collection of secretions from individual salt gland segments.

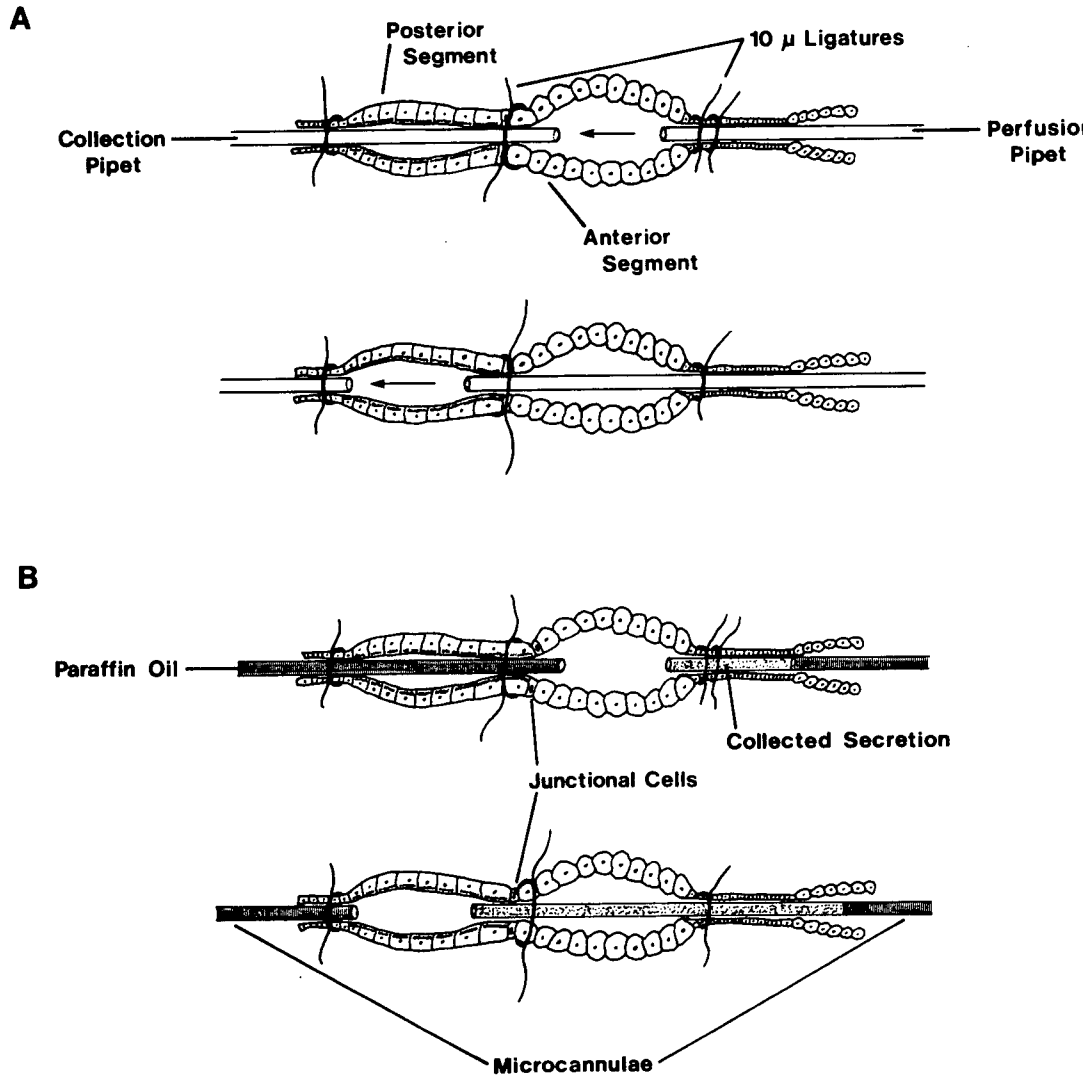
A
Posterior Segment
10 μ Ligatures
Collection Pipet
Perfusion Pipet
Anterior Segment
B
Paraffin Oil
Collected Secretion
Junctional Cells
Microcannulae

Table 4.1. Composition of physiological salines. All salines also contained the following (in mM): proline 20, alanine 5, glycine 3, glutamine 4, succinate 7.4, citrate 2.4, glucose 10.

	Bathing Salines			Perfusion Salines		
Component (mM)	Control	CO_2-Free (Phosphate)	CO_2-Free (HEPES)	Control	CO_2-Free (Phosphate)	CO_2-Free (HEPES)
Na^+	189.5	189.2	189.5	148.5	148.2	148.5
K^+	9	9	9	50	50	50
Mg^{2+}	4	4	4	4	4	4
Ca^{2+}	4	4	4	4	4	4
Cl^-	39	39	39	164	180	171
HCO_3^-	18.5	0	0	18.5	0	0
SO_4^{2-}	4.5	4.5	4.5	5	5	5
Isethionate$^-$	125	141	140	-	-	-
HEPES	-	-	10	-	-	10
$H_2PO_4^-$	-	0.2	-	-	0.2	-
HPO_4^{2-}	-	1.0	-	-	1.0	-
pH	7.7	7.7	7.7	7.7	7.7	7.7
CO_2 (%)	2	0	0	2	0	0
O_2 (%)	98.0	100	100	98	100	100

while all other salines were gassed with 98% O_2 - 2% CO_2. Saline pH was adjusted to 7.7 using concentrated HNO_3 or NaOH.

C. Results

Results in Figure 4.2 demonstrate clearly that the anterior segment is the site of CO_2 secretion in the microperfused salt gland. The increase in perfusate total CO_2 concentration during perfusion of the anterior segment was 67.4 $\pm$ 5.9 mM (mean $\pm$ S.E., n = 7) and was not significantly different ($P > 0.25$) from the value of 70.6 $\pm$ 5.3 mM (mean $\pm$ S.E., n = 9) observed during perfusion of the whole gland. Further evidence in support of this observation is shown in Figure 4.3. Removal of luminal Cl^- in perfused whole glands or perfused anterior segments inhibited total CO_2 secretion by 80-85% (see also the previous chapter). The change in perfusate total CO_2 concentration when whole salt glands were perfused with Cl^--free salines (17.0 $\pm$ 2.4 mM; mean $\pm$ S.E., n = 6) was not significantly different ($0.1 < P < 0.25$) from that of anterior segments perfused with Cl^--free salines (12.9 $\pm$ 2.6 mM; mean $\pm$ S.E., n = 4).

Note that there is also a very small and highly variable component of CO_2 secretion in the perfused posterior segment (Fig. 4.2). The mean increase in posterior perfusate total CO_2 concentration was 4.9 $\pm$ 1.7 mM ($\pm$ S.E., n = 5).

Figure 4.4 demonstrates that Cl^- reabsorption (Δ $[Cl^-]$ = -77.1 $\pm$ 6.3 mM; mean $\pm$ S.E., n = 9) in perfused anterior segments is not significantly different ($0.1 < P < 0.25$) from total CO_2 secretion as previously shown for perfused whole salt glands (Chapter III). Furthermore, equilibration of salt glands for 2.5 hours in CO_2 and HCO_3^--free bathing salines prior to perfusion of anterior segments with CO_2 and HCO_3^--free perfusates

Figure 4.2 Changes in perfusate total CO_2 concentration for whole salt glands and individual segments. Values are means $\pm$ S.E. (n = 5-9).

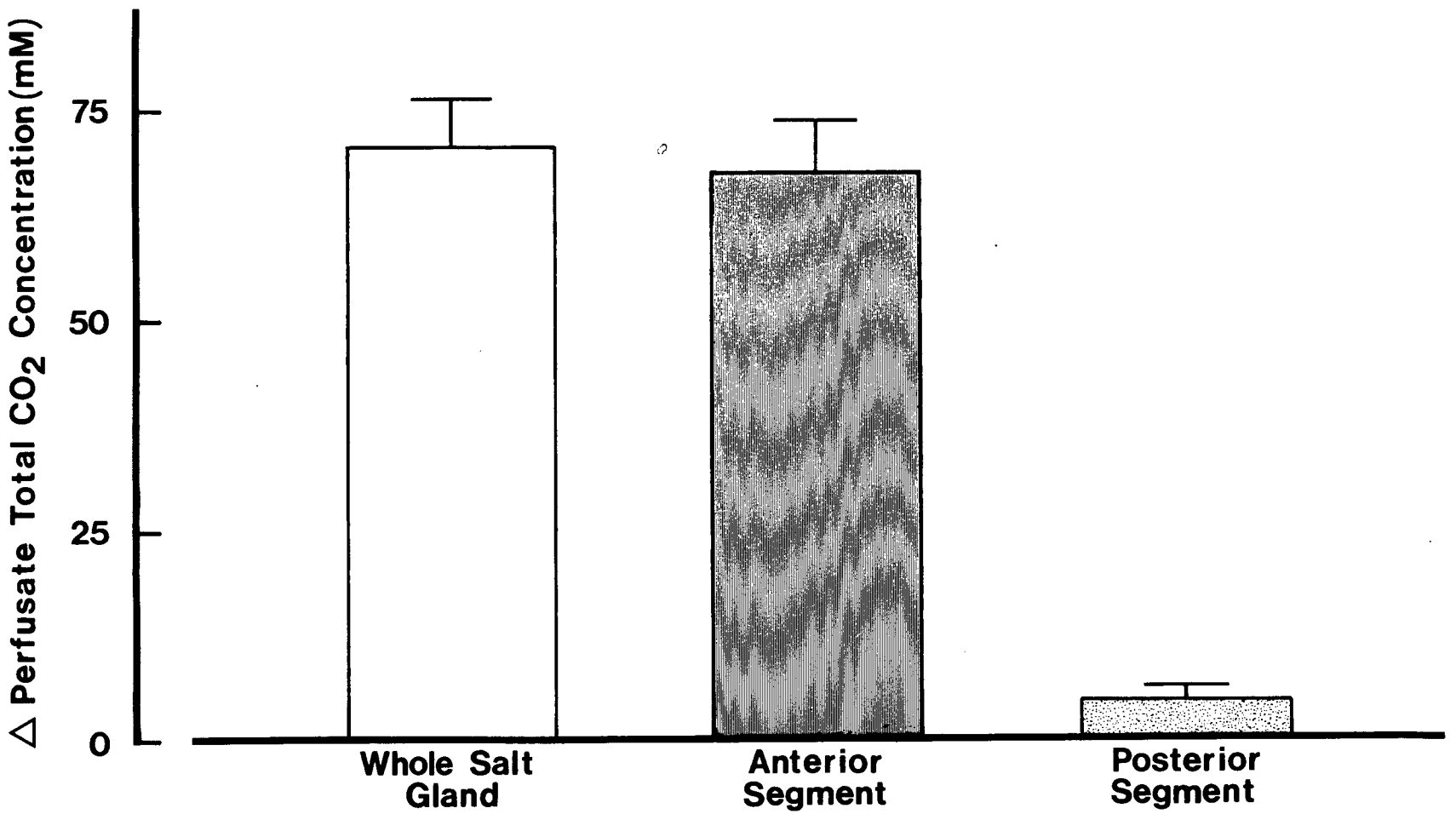
Δ Perfusate Total CO_2 Concentration (mM)
75
50
25
0
Whole Salt Gland
Anterior Segment
Posterior Segment

Figure 4.3 Effects of luminal Cl^- substitution on the change in perfusate total CO_2 concentration from whole salt glands and anterior segments. Values are means $\pm$ S.E. (n = 4-9).

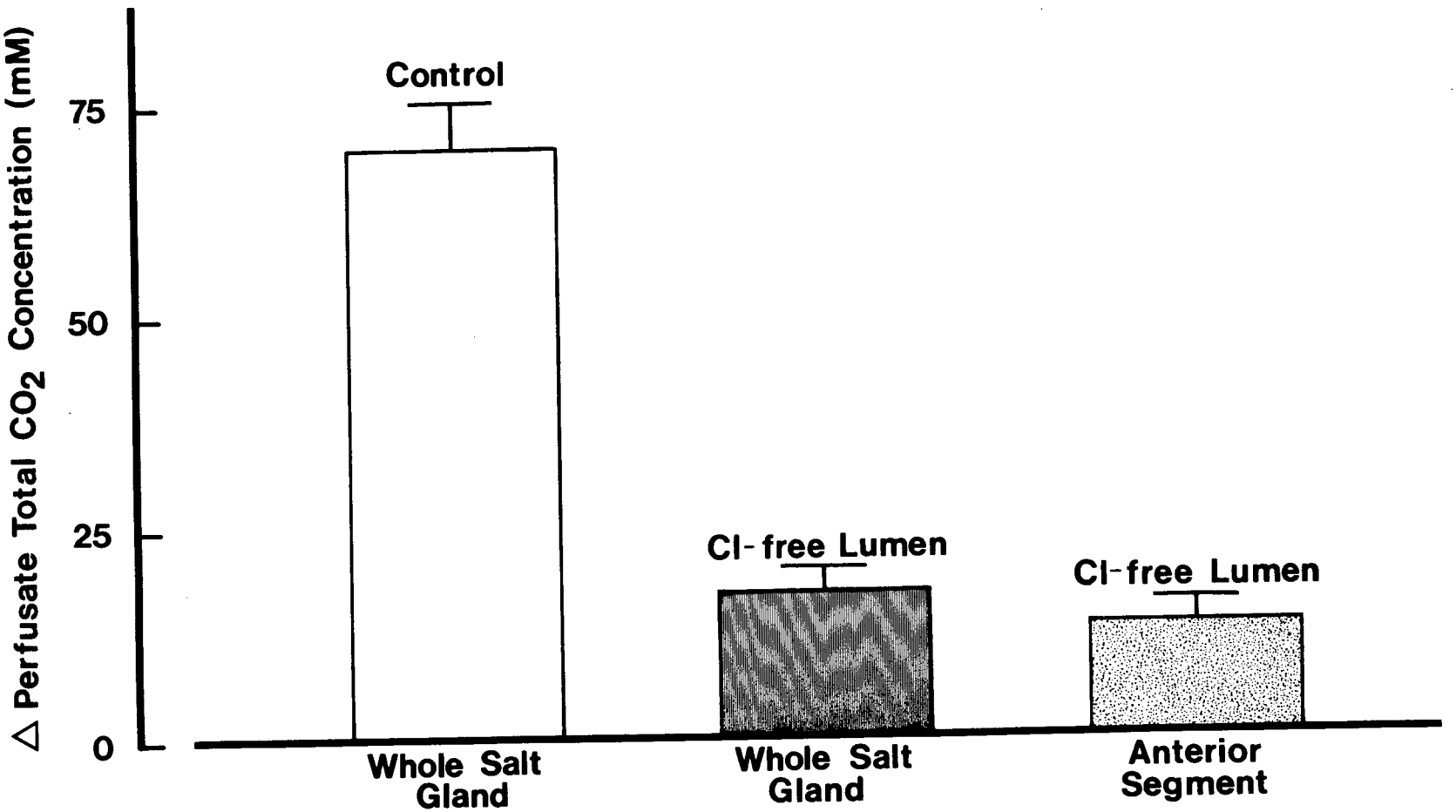
Δ Perfusate Total CO_2 Concentration (mM)
75
50
25
0
Control
Cl-free Lumen
Cl-free Lumen
Whole Salt Gland
Whole Salt Gland
Anterior Segment

Figure 4.4 Changes in anterior segment perfusate total CO_2 and Cl^- concentrations and effects of bilateral CO_2 and HCO_3^- substitution with HEPES or phosphate buffered salines (see Table 4.1) on Cl^- reabsorption. Values are means $\pm$ S.E. (n = 5-9).

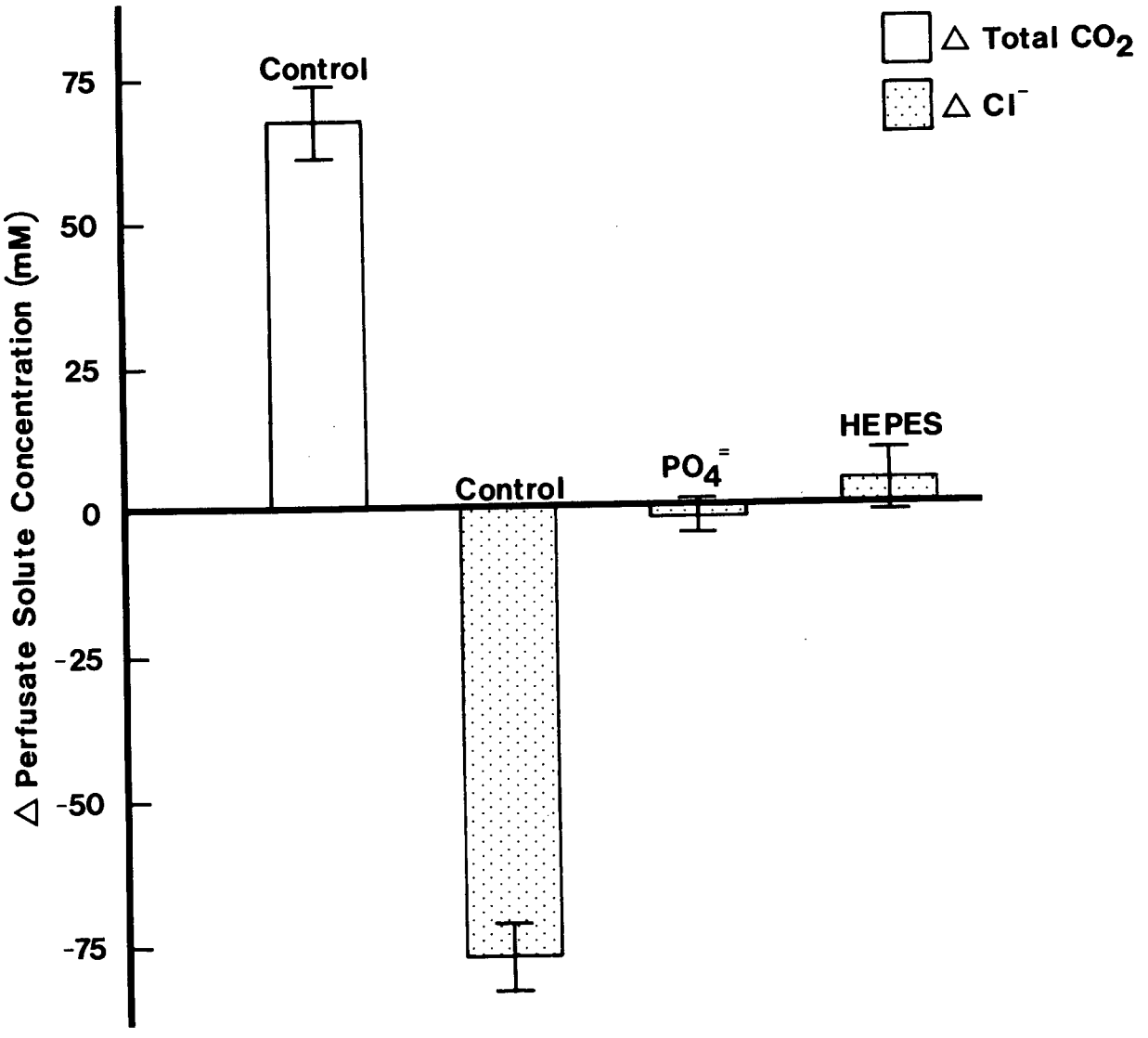
Δ Total CO_2
Δ Cl^-
Control
Control
$PO_4^=$
HEPES
75
50
25
0
-25
-50
-75
Δ Perfusate Solute Concentration (mM)

(HEPES or phosphate substitution) completely inhibited Cl^- reabsorption. The change in perfusate Cl^- concentrations with bilateral HEPES or phosphate buffered salines were 4.7 $\pm$ 5.1 mM and -1.7 $\pm$ 2.6 mM (mean $\pm$ S.E., n = 5-9), respectively, and these values were not significantly different from zero ($0.1 < P < 0.25$)

In early studies on salt gland function it was observed that fluid secretion in whole, cannulated salt glands was dependent upon the presence of Na^+ and Cl^- in the bathing saline. Rates of fluid secretion for salt glands pre-equilibrated for 30 minutes in Na^+-free (replaced by choline) or Cl^--free (replaced by isethionate or NO_3^-) salines and then cannulated with oil filled pipets are shown in Table 4.2. Fluid secretion was inhibited by 92% in Na^+-free saline and by 57-68% in Cl^--free saline. These values were significantly different from control rates of fluid secretion ($P < 0.001$). Data in Table 4.2 are consistent with coupled NaCl secretion since both ions are necessary for normal fluid secretion rates assuming high permeability of the substituted co-ion. It should be noted that secretions collected from glands bathed in Cl^--free salines still contained a significant amount of Cl^-([Cl^-] = 28.9 $\pm$ 2.1 mM) suggesting Cl^- leakage and recycling through the epithelial cells and/or a Cl^- transport mechanism with a very high Cl^- affinity.

Contrary to these results were the findings that fluid secretion was relatively independent of bath CO_2 and HCO_3^- (Table 4.2). Mean fluid secretion rates in phosphate or HEPES buffered bathing salines were 61.0 $\pm$ 1.8 $nl \cdot h^{-1}$ and 26.8 $\pm$ 3.4 $nl \cdot h^{-1}$, respectively. In addition, under CO_2 and HCO_3^--free conditions rectal secretions are almost pure, concentrated NaCl (see Table 4.3). The higher rate of fluid secretion in phosphate versus HEPES buffered saline may be due to an indirect effect of

PO_4^{2-} on cellular energy metabolism. Regardless, the rates and hypertonicity of the NaCl secretion from glands bathed in CO_2-free saline are comparable to those of $NaHCO_3$-rich secretions from glands bathed in control saline (see Table 4.3).

To determine where in the salt gland this hyperosmotic fluid secretion was occurring (see Discussion), and to examine the major excretory functions of anterior and posterior salt gland segments, the microcannulated preparations shown in Figure 4.1B were used. Fluid secretion rate in the cannulated posterior segment was 29.5 $\pm$ 3.4 $nl \cdot h^{-1}$ (mean $\pm$ S.E., n = 8), which was slightly but not significantly lower ($0.1 < P < 0.25$) than the value of 37.6 $\pm$ 6.4 $nl \cdot h^{-1}$ (mean $\pm$ S.E., n = 6; data from Chapter II) observed for whole salt glands (Fig. 4.5). Anterior segments also secrete fluid but at a much lower rate of 9.9 $\pm$ 1.7 $nl \cdot h^{-1}$ (mean $\pm$ S.E., n = 5; Fig. 4.5).

The ionic composition of secretions collected from whole salt glands (data from Chapter II) and the individual segments bathed in control saline are shown in Table 4.3. All three secretions are clearly hyperosmotic to the bathing saline (427 mOsm). The Na^+ concentrations for these three secretions were not signifiantly different ($P > 0.25$) and ranged between 384 and 413 mM. Chloride concentrations were about two to three times higher in secretions from posterior segments than either secretions from the whole salt gland ($P < 0.0005$) or the anterior segment ($P < 0.005$). In addition, posterior segment secretions had a large anion deficit indicating a significant component of CO_2 secretion by posterior rectal cells when CO_2/HCO_3^- was present in the bathing saline (see Discussion).

Table 4.2. Measured fluid secretion rates for whole, cannulated rectal salt glands bathed in various salines. Values are means ± S.E. or S.D.

Experiment	Fluid secretion rate ($nl \cdot h^{-1}$)	n
Control	37.6 ± 6.4	6
Na^+-free bath (choline)	3.0 ± 0.6	4
Cl^--free bath (NO_3^-)	16.2 ± 4.1	3
Cl^--free bath (isethionate)	12.2 ± 2.4	5
CO_2-free bath (phosphate)	61.0 ± 1.8	2
CO_2-free bath (HEPES)	26.8 ± 3.4	4

Table 4.3. Ionic composition of rectal secretions. Data for whole, cannulated salt glands are from Chapter II. Concentrations of HCO_3^- and CO_3^{2-} were calculated from measurements of total CO_2 and pH as described previously (Chapter II). Calcium and Mg^{2+} concentrations were always < 1.0 mM. Values are means ± S.E., n = 5-9 (*mean ± S.D., n = 2). All preparations were bathed in control saline (see Table 4.1) unless otherwise stated in this table.

Preparation	Na^+	K^+	Cl^-	Total Sulfur	Total Phosphorus	HCO_3^-	$CO_3^=$
Whole, cannulated salt gland	412.7 ± 31.5	31.4 ± 3.4	44.9 ± 4.7	13.4 ± 2.8	2.40 ± 0.8	402	41
Cannulated anterior segment	384.4 ± 17.0	20.9 ± 1.8	86.0 ± 4.0	14.7 ± 1.7	0.64 ± 0.4	-	-
Cannulated posterior segment	409.2 ± 42.1	5.9 ± 3.5	141.8 ± 13.8	27.3 ± 4.8	0.30 ± 0.07	-	-
*Whole, cannulated salt gland - CO_2-free bath (phosphate buffer)	640.3 ± 99.7	6.0 ± 0.9	632.6 ± 79.8	9.2 ± 4.8	0.50 ± 0.4	-	-
Whole, cannulated salt gland - CO_2-free bath (HEPES buffer)	269.6 ± 40.5	18.6 ± 4.6	298.5 ± 31.7	15.0 ± 6.4	0.48 ± 0.1	-	-

Figure 4.5 Rates of fluid secretion in whole, microcannulated salt glands and anterior and posterior segments. Values are means $\pm$ S.E. (n = 5-8).

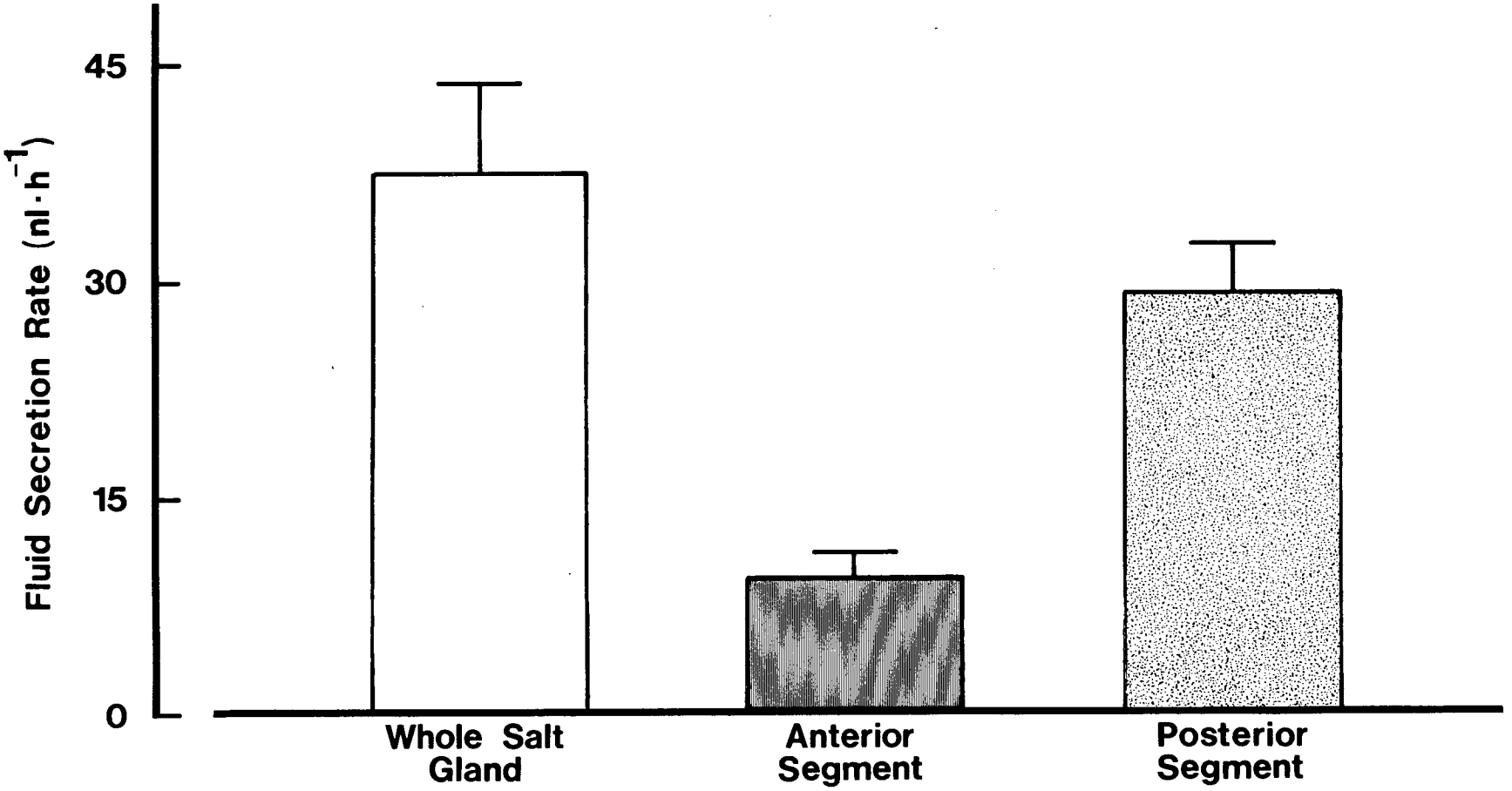
Fluid Secretion Rate (nl·h⁻¹)
45
30
15
0
Whole Salt Gland
Anterior Segment
Posterior Segment

D. Discussion

1) Site of Cl^-/HCO_3^- Exchange

During initial studies when the microperfused preparation described in the previous chapter was being developed, attempts were made to perfuse the individual salt gland segments. Transepithelial potentials in perfused anterior and posterior segments were observed to decline slowly with time suggesting that the long-term viability of these preparations was rather poor and therefore they were not ideally suited for studies of ion transport mechanisms. Despite this, the use of these preparations for the short-term experiments of the present investigation has shown clearly that the anterior rectum is the actual site of CO_2 secretion in the perfused salt gland (Figs. 4.2 and 4.3). Net Cl^- reabsorption is equivalent to total CO_2 secretion in the anterior segment (Fig. 4.4) as it is in the whole salt gland (see Chapter III). Furthermore, bilateral CO_2 substitution with either a phosphate or HEPES buffered saline completely inhibits anterior segment Cl^- reabsorption (Fig. 4.4). These results together with data presented in the previous chapter provide good evidence for the existence of a 1:1 Cl^-/HCO_3^- exchange mechanism located in the anterior salt gland.

It should be noted at this time that the actual ionic species transported (i.e. HCO_3^- and/or H^+/OH^-) during CO_2 secretion are not known. Indeed, the unequivocal demonstration of H^+/OH^- versus HCO_3^- transport in intact epithelia has not been possible (reviewed by Al-Awqati, 1978). Experiments with the lipid soluble buffer glycodiazine, discussed in Chapter V, however, suggest indirectly that H^+ and/or OH^- movements are involved in Cl^- and HCO_3^- transport.

2) Excretory Functions of Anterior and Posterior Segments

In earlier studies on whole, cannulated salt glands it was observed that fluid secretion was dependent critically on the presence of Na^+ and Cl^- in the bathing saline and relatively independent of bath CO_2 and HCO_3^- (Table 4.2). Indeed, salt glands bathed in CO_2-free salines secreted strongly hyperosmotic fluids which were almost pure NaCl (Table 4.3). This suggested indirectly that the salt gland might normally secrete a NaCl-rich fluid and that once this fluid entered the salt gland lumen its composition was modified by ion exchange and reabsorptive processes dependent upon the animal's ionic regulatory needs. In light of these observations, it was of interest to examine an hypothesis suggested recently by Bradley and Phillips (1977c; see also Meredith and Phillips, 1973c). Studies on the saltwater mosquito larva, A. taeniorhynchus, conducted by these investigators suggested indirectly that the posterior salt gland segment was the site of hyperosmotic fluid secretion and that the anterior segment was involved in selective solute and fluid reabsorption.

To study this hypothesis directly, individual salt gland segments were cannulated with oil-filled pipets. In initial studies ligatures were tied around the ileum or anal canal and directly between the two segments as shown for the perfused preparation in Fig. 4.2A. The rate of fluid secretion was found to be quite low in either anterior or posterior segments which again suggested poor long-term viability of this preparation as discussed above. To circumvent this problem, the ligature technique was refined and with great care it was possible to tie ligatures about one cell row or approximately 50 μ on either side of the junctional region (Fig. 4.2B).

Results obtained using this preparation are shown in Fig. 4.5 and Tables 4.3 and 4.4 and demonstrate clearly that the posterior segment is the

major site of hyperosmotic fluid secretion as originally suggested by Bradley and Phillips (1977c). Contrary to their original hypothesis, however, it was found that the anterior segment of A. dorsalis is also capable of secreting a hyperosmotic fluid at a rate equivalent to approximately 25% of that observed in the whole gland (Fig. 4.5, Table 4.3).

Data in Table 4.4 show that the calculated rates of Na^+ and Cl^- excretion in the cannulated posterior segment are about 3 to 5 times higher than those observed in the cannulated anterior segment. These results plus the observation that the Cl^- concentrations of posterior secretions are 2 to 3 times higher than those in either anterior or whole gland secretions (Table 4.3), suggests that one of the major functions of the posterior segment is excretion of a NaCl-rich fluid. Since fluid flow through the in vivo salt gland is not continuous and unidirectional (i.e. the in vivo rectal salt gland empties only when it becomes filled with secretion and feces) as it is in the perfused or cannulated preparation, fluid secreted by the posterior segment would come into contact with anterior rectal cells. The clear demonstration of a Cl^-/HCO_3^- exchange mechanism in the anterior salt gland (Fig. 4.4) indicates that the anterior segment is at least one site where modification of the composition of rectal secretions can occur. Figure 4.6 summarizes the major excretory functions of anterior and posterior salt gland segments. Further studies are needed to determine the ionic requirements of fluid secretion in the individual segments and to determine if both segments secrete a NaCl-rich fluid when bathed in CO_2 and HCO_3^--free saline.

The relative roles played by the individual segments in HCO_3^- excretion and pH regulation are uncertain. Data in Table 4.3 show that secretions from posterior segments bathed in control salines containing

Table 4.4. Calculated rates of Na^+ and Cl^- excretion for cannulated anterior and posterior segments.

Segment	J_{Na}	J_{Cl}
Posterior	12.1 nMole·h^{-1}	4.2 nMole·h^{-1}
Anterior	3.8 nMole·h^{-1}	0.85 nMole·h^{-1}

Figure 4.6 Summary of major excretory and transport functions of individual salt gland segments.

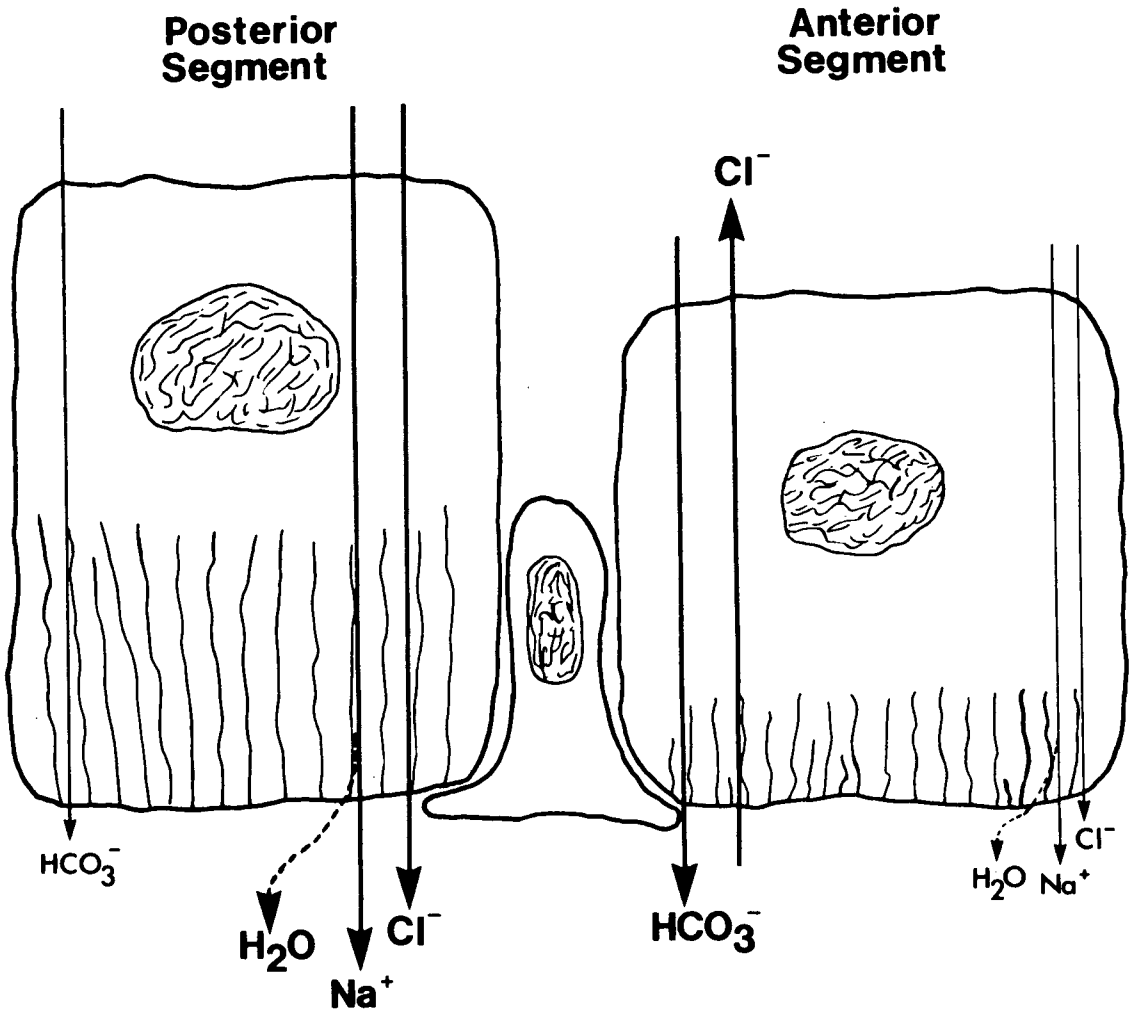
Posterior Segment
Anterior Segment
Cl⁻
HCO3⁻
H2O
Cl⁻
Na⁺
HCO3⁻
H2O
Na⁺
Cl⁻
Lumen

CO_2/HCO_3^- have a large anion deficit. Part of this deficit can be attributed to sulfur-containing compounds such as isethionate which may passively enter the lumen down a favorable electrochemical gradient (lumen TEP positive, unpublished observations) and/or a small amount of SO_4^{2-} secretion (see Bradley and Phillips, 1977a). The remainder of the deficit can most likely be attributed to HCO_3^- and CO_3^{2-} since earlier unpublished observations indicated that the small volumes of secretions collected from posterior segments ligated at the junctional region contained approximately 150 mM total CO_2. Thus, both segments are capable of excreting CO_2 at high rates. The inability to measure significant CO_2 secretion in the perfused posterior segment, however (Fig. 4.2), could indicate that the rate of posterior CO_2 transport is far lower than that in the anterior segment. Indeed, in the intact animal one can envision the posterior segment secreting a NaCl-rich fluid. Given the nature of fluid movements through the in vivo salt gland, Cl^- could be rapidly removed from the secretion in the anterior segment in exchange for serosal HCO_3^-. The generation of large transepithelial HCO_3^- and CO_3^{2-} gradients by the anterior segment would then directly affect the rate and degree of posterior segment HCO_3^- transport. Alternatively, it is entirely possible that unidirectional perfusion of the salt gland with the isosmotic salines used in this study simply inhibits posterior segment HCO_3^- secretion.

To conclude, these studies demonstrate clearly that the anterior segment is the site of Cl^-/HCO_3^- exchange in the microperfused rectal salt gland. In addition, this work has shown that both salt gland segments secrete a hyperosmotic fluid containing Na^+, Cl^- and HCO_3^-. Thus it can no longer be said with certainty that either salt gland segment is

performing one specific function *in vivo* as originally suggested by Meredith and Phillips (1973c) and Bradley and Phillips (1977c). Instead, it is tentatively suggested that both segments secrete a NaCl-rich fluid *in vivo* and that the composition of this fluid is modified once it enters the salt gland lumen by ion exchange and reabsorptive processes. To test this hypothesis further it would be valuable to examine the mechanisms of posterior and anterior segment fluid secretion in animals inhabiting a variety of environments such as $MgSO_4$, Na_2SO_4 and NaCl salt lakes.

In Chapter V the apical and basolateral membrane entry and exit steps for Cl^- and HCO_3^- are examined using intracellular ion and voltage-selective microelectrodes.

CHAPTER V - CELLULAR MECHANISM OF BICARBONATE AND CHLORIDE TRANSPORT

A. Introduction

Cellular mechanisms of H^+ and HCO_3^- transport have not previously been studied in an invertebrate epithelium. In chapters III and IV I have shown that active HCO_3^- transport in the microperfused rectal salt gland of Aedes dorsalis larvae is mediated by a 1:1 exchange of luminal Cl^- for serosal HCO_3^- and that this exchange is located in the anterior salt gland segment. The work in the present chapter examines the cellular entry and exit steps involved in HCO_3^- and Cl^- transport using intracellular ion and voltage-sensitive microelectrodes and a perfused anterior segment preparation which allowed both the bath and luminal fluid composition to be changed rapidly.

B. Materials and Methods

Animals. Larvae were reared in a low alkalinity rearing medium and the adult colony maintained as described previously (Chapter II). Three days after hatching larvae were transferred to 250 mM HCO_3^- medium containing (in mM): 361.5 Na^+, 2.5 K^+, 0.03 Ca^{2+}, 0.50 Mg^{2+}, 39.6 Cl^-, 10.0 SO_4^{2-}, 250 HCO_3^-, 29.0 CO_3^{2-}, pH 8.9. All experiments were conducted at room temperature (21-24°C) using fourth instar larvae acclimated to this medium for three to six days.

Microperfusion System. Collection pipets were constructed as described in Chapter III. Perfusion pipets were fabricated by sealing a small glass cannula (O.D. 50-60 μ, I.D. 35-40 μ, tip opening 20-25 μ) with a long column of epoxy into a glass pipet pulled from flint glass tubing (O.D. 1.0 mm, I.D. 0.8 mm; Drummond Glass Co., Broomall, PA). The epoxy seal was waterproofed and electrically insulated using cured Sylgard 184 resin (Dow

Corning). Bath chambers were constructed from molded Sylgard 184 resin and were similar to those described in Chapter III except that two superfusion inlets were positioned on either side of the salt gland preparation and the total chamber volume was reduced to approximately 0.6 ml.

Rectal salt glands were dissected as described in Chapter III. In these studies the anterior segment alone was perfused by cannulating the midgut and ileum with a perfusion pipet and the anal canal and posterior segment with a collection pipet (see Fig. 5.1). Two or three 10 μ ligatures were tied around the ileum and anal canal to ligate these pipets into place. An additional one or two 10 μ ligatures were tied one cell row or approximately 50 μ posterior to the junctional region to isolate the anterior salt gland. The transepithelial potential in perfused anterior segments was allowed to stabilize after set-up for 30-40 minutes before experiments were begun.

Bath and Luminal Solution Changes. The bath chamber was normally superfused by gravity at a rate of 3 to 5 $ml \cdot min^{-1}$. Rapid changes (< 5 secs) in bath composition were made by using a 6-way rotary valve (Altex, Rainin Instrument Co. Inc., Woburn, MA) and by increasing the rate of superfusion to 20-30 $ml \cdot min^{-1}$. While this high superfusion rate tended to cause a small amount of mechanical disturbance to the preparation, it was nevertheless possible to maintain a high number of stable microelectrode impalements during these solution changes (see Results). Bathing salines were delivered to the rotary valve and bath chamber through polyethylene tubing (PE 240).

Rapid changes in luminal solution composition were made using a double pipet arrangement shown schematically in Fig. 5.1. Perfusion pipets were sealed by a gasket arrangement into a specially designed plexiglass

Figure 5.1 Schematic diagram of microperfused anterior rectal salt gland segment and double perfusion pipet arrangement.

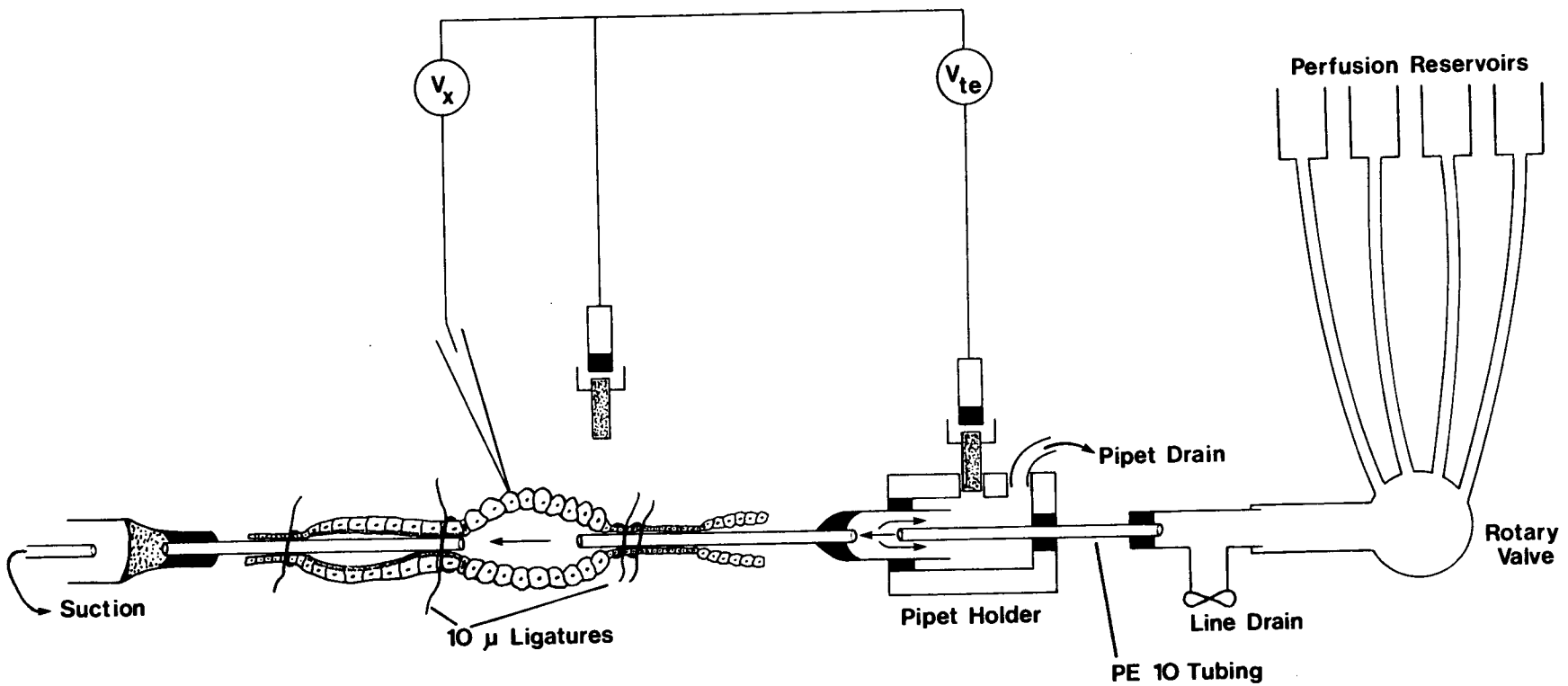
V_x
V_{te}
Perfusion Reservoirs
Pipet Drain
Rotary Valve
Suction
10 μ Ligatures
Pipet Holder
Line Drain
PE 10 Tubing

pipet holder (shown schematically in Fig. 5.1). Perfusion salines were delivered by gravity through CO_2-impermeable Saran tubing (Clarkson Equipment and Controls, Detroit, MI) to a 6-way rotary valve (Altex, Rainin). A length of polyethylene tubing (PE 240) led from the rotary valve to a plastic Y-junction. One branch of the Y-junction led to a waste container through polyethylene tubing (PE 240) which was clamped with a small serrefine clamp. This branch is referred to as a line drain (see Fig. 5.1). Approximately 1 cm of a 6 to 7 cm length of polyethylene tubing (PE 10) was sealed into the other branch of the Y-junction by a long column of epoxy. The PE 10 tubing entered the rear of the pipet holder and was inserted down the bore of the perfusion pipet to a position just behind the perfusion cannula (see Fig. 5.1). A gasket arrangement was used to seal the PE 10 tubing into the rear of the pipet holder (see Fig. 5.1). The perfusion rate through the PE 10 tubing was approximately 0.6 $ml \cdot min^{-1}$ and the bulk of perfusion solution flowed up the pipet and out a drain on the pipet holder (Fig. 5.1) to a waste container. An adjustable pinch clamp on the line draining the pipet holder allowed adjustment of luminal perfusion to rates of 150-250 $nl \cdot min^{-1}$.

Changes in luminal fluid composition were made by choosing one of four perfusates using the rotary valve and then opening the line drain for 3 to 4 seconds to flush the perfusion line. When the drain was closed a new perfusate almost instantaneously began flushing the perfusion pipet and salt gland lumen. The total time for a complete luminal solution change was < 10 seconds. Although this procedure necessarily caused very small luminal pressure transients when the line drain was opened and closed, it was possible to maintain an acceptable number of microelectrode impalements by impaling cells close to the perfusion and collection pipets.

Both the perfusion and collection pipet holders were mounted on Narishige micromanipulators (Model MM-3, Narishige Instrument Laboratories, Tokyo). Perfusates collecting in the collection pipet were continuously drawn off to waste by vacuum suction through a glass micropipet attached to a length of polyethylene tubing (PE 100; see Fig. 5.1).

Electrical Measurements. Transepithelial potential (V_{te}) was measured with reference to the bathing saline using calomel half-cells and a Kiethley Model 616 digital electrometer (Kiethley Instruments Inc., Cleveland, OH). The calomel half-cells made contact via 3 M KCl - 4% Agar bridges with the bath saline through a port in the bath chamber and with the perfusion saline through a gasket-sealed port on the perfusion pipet holder (Fig. 5.1). Changes in agar bridge junction potentials which occurred during solution changes were measured separately against a grounded calomel half-cell. Data were corrected for these changes in potential differences only when they were $\geq$ 1.0 mV. Transepithelial potential was recorded continuously on 1 channel of a 2-channel chart recorder (Model 7402A, Hewlett-Packard, San Diego, CA).

Voltage-sensitive microelectrodes were pulled on a Narishige vertical pipet puller (Model PE 2, Narishige) from capillary glass (1.0 mm O.D., Frederick Haer and Co., Brunswick, ME). These microelectrodes had resistances of either 10-12 MΩ or 30-50 MΩ. The lower resistance microelectrodes were used in later studies since they provided stabler impalements and virtually eliminated the problem of changing tip potentials which can occur during and after cell puncture. Both high and low resistance microelectrodes gave the same values for basolateral membrane potential (V_{bl}), were filled with 0.5 M or 3.0 M KCl and had tip potentials < 5.0 mV. Voltage output from these electrodes was measured using a Model M701 Microprobe

System (WP Instruments, New Haven, CT) or a differential electrometer (Model FD 223, WP Instruments), monitored on a storage oscilloscope (Model D15, Tektronix, Beaverton, OR) and recorded continuously on 1 channel of a 2-channel chart recorder (Model 7402A, Hewlett-Packard). The apical membrane potential (V_a) was determined simply as the difference between V_{bl} and V_{te}.

In my hands, I could not construct reliably double-barrelled liquid ion-exchanger microelectrodes (see Fujimoto and Kubota, 1976) with tip diameters < 1.0 μ. Microelectrodes with tip diameters this large were ineffective in impaling anterior rectal cells probably because of the presence of a rather thick basement membrane in this tissue (Meredith and Phillips, 1973c). Therefore, it was necessary to use single-barrelled ion-selective microelectrodes which had tip diameters that consistently measured $\leq$ 0.5 μ. These electrodes were pulled from acid-washed capillary glass on a Narishige vertical pipet puller, silanized by dipping their tips for 10-12 seconds into a 0.2% solution (v/v) of Dow Corning 1107 silicone oil in acetone (Aristar, BDH Chemicals Ltd., Poole, England) and baked at approximately 300°C on a hotplate for 15-25 minutes.

Chloride-sensitive microelectrodes were constructed by injecting a small column of Cl^--exchange resin (Orion 92-17102, Orion Research) into the electrode shank with a syringe and drawn-out polyethylene tubing. The microelectrodes were placed tip down into 0.5 M KCl overnight and the resin allowed to fill the electrode tip. The following day electrodes were back-filled with 0.5 M KCl and bevelled by jet stream abrasion (Ogden, Citron and Pierantoni, 1978) at a 45° angle for approximately 30 seconds. Chloride-sensitive electrodes were usually functional for 3 to 4 days.

Hydrogen-sensitive microelectrodes were constructed in a similar manner using a H^+-exchange resin which was a generous gift from Dr. W. Simon (see Ammann, Lanter, Steiner, Schulthess, Shijo and Simon, 1981). This resin was stored continuously under 100% CO_2. After filling the electrode shank with a small column of the resin, electrodes were placed tip down in a pH 7.0 buffer and left overnight in a dessicator under 100% CO_2. The microelectrodes were back-filled the next day with pH 7.0 buffer (see Ammann, et al., 1981) and bevelled as described above. The H^+-exchange microelectrodes were usually only functional for 1 day.

The voltage outputs of ion-sensitive microelectrodes were measured using a differential electrometer with $10^{15}\Omega$ input resistance (Model FD 223, WP Instruments), and the signal was filtered before recording using a low-pass filter. Electrodes were calibrated in small wells containing test solutions that made contact with the bath calomel half-cell via a 3 M KCl - 4% Agar bridge.

The Cl^--sensitive microelectrodes were calibrated in 3 to 4 solutions containing 1, 5, 50 or 150 mM KCl. Ion activities were calculated using the Debye-Hückel equation (Robinson and Stokes, 1965) and ion size parameters from Kielland (1937). These electrodes had slopes of 50-60 mV/decalog Cl^- activity and selectivities for Cl^- over HCO_3^- ranging between 3 and 5.

Hydrogen-sensitive microelectrodes were calibrated in 3 buffers (pH 6.4 - 8.3) of constant ionic strength similar to the bathing saline and had slopes of 55-60 mV/pH unit. The pH of calibration buffers was determined before each experiment using a Radiometer Model 27 pH meter (Radiometer, Copenhagen) and a Radiometer pH electrode calibrated with Radiometer buffers. As described previously (Ammann, et al., 1981), these H^+-exchanger

microelectrodes showed negligible sensitivities to Na^+ or K^+ in concentrations up to 100 mM within the pH range of 6.4 - 8.3. Both H^+ and Cl^--sensitive microelectrodes had resistances of $10^{11}\Omega$ and full response times to step changes in solution of < 5-8 seconds.

Microelectrode Impalements. The perfused anterior rectal salt gland was viewed through a dissecting microscope (Zeiss, Jena, East Germany) and illuminated from above by fiber optics (Intralux Model 150 H, Volpi AG, Urdorf, Switzerland). Electrodes were advanced manually at an angle of 45°-60° to the cell surface using a Leitz micromanipulator (Wetzlar, West Germany) until the microelectrode tip just began to touch the cell membrane. The microelectrode was allowed to 'rub' against the cell membrane for approximately 20 seconds and the cell was then impaled by tapping the table gently. In early fourth instar larvae it was possible to remotely advance microelectrodes directly into cells using a hydraulic microdrive (Model MO-8, Narishige).

Acceptable cellular impalements were characterized by an abrupt, monotonic change in microelectrode voltage, a potential which remained stable for at least 1 minute and a return of the microelectrode voltage to within $\pm$ 2.0 mV of baseline after the electrode was withdrawn from the cell.

Salines. The composition of various bathing and perfusion salines used throughout this study are shown in Table 5.1. The control bathing saline was based on measured hemolymph ionic, osmotic and free amino acid concentrations (Chapter II) while the control perfusates resembled larval Malpighian tubule fluid (Phillips and Maddrell, 1974). Note that the large anion deficit observed in larval hemolymph (Chapter II) was simulated in the bathing saline with sodium isethionate. Concentrations of Na^+, K^+ and Cl^- were varied in bath and perfusion salines by replacing these ions with

Table 5.1. Composition of physiological salines. All salines also contained the following (in mM): proline 20, alanine 5, glycine 3, glutamine 4, succinate 2.4, citrate 2.4, glucose 10.

	Bathing Salines					Perfusion Salines		
Component (mM)	Control	CO_2-free (HEPES)	CO_2-free (Glycodiazine)	65 mM HCO_3^-	113 mM HCO_3^-	Control	CO_2-free (HEPES)	Artificial Secretion
Na^+	189.5	189.5	189.5	189.5	189.5	148.5	148.5	502
K^+	9	9	9	9	9	50	50	35
Mg^{2+}	4	4	4	4	4	4	4	0.5
Ca^{2+}	4	4	4	4	4	4	4	0.5
Cl^-	39	39	39	39	39	164	164	37
HCO_3^-	18.5	-	-	65	113	18.5	-	400
CO_3^{2-}	-	-	-	-	-	-	-	40
SO_4^{2-}	4.5	4.5	4.5	4.5	4.5	5	5	-
Isethionate$^-$	125	141.5	125	78.5	30.5	-	16	-
HEPES	-	5	-	-	-	-	5	-
Glycodiazine$^-$	-	-	18.5	-	-	-	-	-
pH	7.7	7.7	7.7	7.7	7.7	7.7	7.7	8.75
CO_2 (%)	2	0	0	6	11	2	0	2
O_2 (%)	98	100	100	94	89	98	100	98
Lissamine Green (%)	-	-	-	-	-	0.05	0.05	0.05

choline$^+$, Na^+ or isethionate$^-$, respectively (see Results). Glycodiazine (sodium glymidine) was a generous gift from Mr. H. Wehner (Pentagone Labs Ltd., Vaudreuil, Quebec).

Acetazolamide (Sigma Chemical Co., St. Louis, MO) and DIDS (4-4'-diisothiocyano-2-2'disulfonic acid, Sigma) - containing bath salines were made up fresh before each experiment. DIDS was dissolved in amino acid-free saline (replaced with sucrose) and the preparation of DIDS saline was carried out in a darkened room. In addition, the bath superfusion reservoir and lines were wrapped in foil and the tissue was exposed to DIDS for 1 hour in complete darkness.

C. Results

1) Microelectrode Impalements

Examples of acceptable voltage microelectrode impalements are shown in Fig. 5.2. Mean control values for V_{te} (lumen negative), V_{bl} and V_a (cell negative) were -45.5 $\pm$ 0.5, -75.6 $\pm$ 0.2 and -30.1 $\pm$ 0.4 mV ($\pm$ S.E., n = 150 impalements on 39 preparations), respectively. Measurements of V_{bl} showed very little variation between individual cells and individual anterior segment preparations (Fig. 5.4). Basolateral membrane potential measurements were remarkably stable and it was often possible to maintain impalements with voltage electrodes for at least 60-90 minutes. In addition, any given preparation could be repeatedly impaled with voltage microelectrodes with no apparent detrimental effects to the tissue as evidenced by very stable transepithelial potentials which changed by no more than $\pm$ 3.0 mV over the course of a normal 6-8 hour experiment. Stable impalements and tissue viability are most likely facilitated by the large size of anterior rectal cells (30-40 μ in diameter, 30-40 μ long) and the extensive infolding of the

Figure 5.2 Examples of acceptable cellular impalements obtained with voltage-selective microelectrodes.

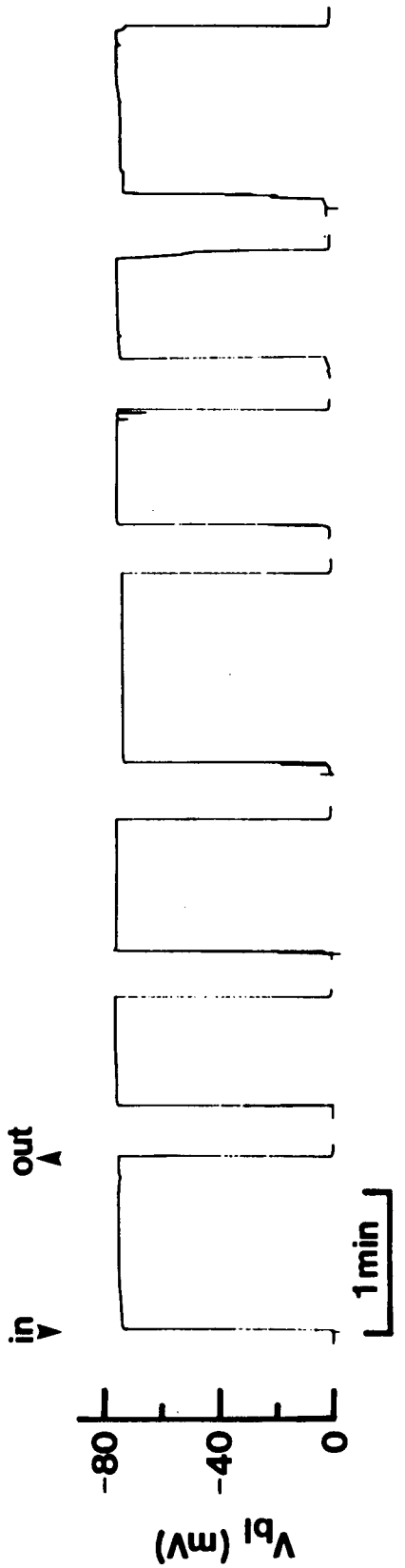
V_{bl} (mV)
-80
-40
0
in
out
1min

basal membrane which greatly increases membrane surface area (see Meredith and Phillips, 1973c).

Acceptable impalements obtained with H^+ and Cl^--sensitive electrodes are shown in Fig. 5.3. Since single-barrelled ion-selective microelectrodes were used in these studies, V_{bl} in any given preparation was determined at the beginning or end of an experiment and this value subtracted from the observed voltage outputs from either the H^+ (V_{H+}) or Cl^- (V_{Cl}-)-selective microelectrodes. Mean intracellular pH (pH_c) and Cl^- activity (a^c_{Cl} -)for preparations bathed and perfused with control salines were 7.67 $\pm$ 0.03 ($\pm$ S.E., n = 39 cells, 4 preparations) and 23.5 $\pm$ 1.4 mM ($\pm$ S.E., n = 23 cells, 7 preparations), respectively, and varied little between individual cells (Fig. 5.4).

Intracellular pH was also measured in anterior segments bathed on their luminal surfaces by high HCO_3^- solutions (Table 5.4). Mean pH_c was 7.99 $\pm$ 0.02 ($\pm$ S.E.; n = 8 cells, 2 preparations) for anterior segments perfused with an artificial, hyperosmotic secretion (see Table 5.1) and 7.84 $\pm$ 0.04 ($\pm$ S.E.; n = 14 cells, 3 preparations) for salt glands bathed on their luminal surface with their own secretions.

Attempts to impale 2 cells simultaneously with a voltage and ion-selective microelectrode generally failed and were technically very difficult to carry out. Preliminary experiments using a 'bender-type' piezoelectric electrode advancing system (Boron and Boulpaep, 1982) to impale cells were unsuccessful. This may have been due to the rather thick basement membrane present in this tissue (Meredith and Phillips, 1973c), and it may therefore be useful in future microelectrode studies to attempt impalements using faster

Figure 5.3 Examples of acceptable impalements obtained with H^+ and Cl^--selective microelectrodes. The trace marked with an asterisk shows the effect of serosal CO_2 and HCO_3^- removal (replaced with a HEPES buffered saline) on V_{H^+}. Increasing negativity of V_{H^+} indicates intracellular alkalinization. Note also that V_{H^+} becomes more positive (i.e. decreasing pH) as the H^+-electrode approaches the cell membrane. This observation is consistent with the presence of an acidic unstirred layer produced by basolateral H^+ extrusion or HCO_3^- uptake (see Results and Discussion). The actual V_{H^+} baseline is that seen upon withdrawal of the H^+-microelectrode from the cell.

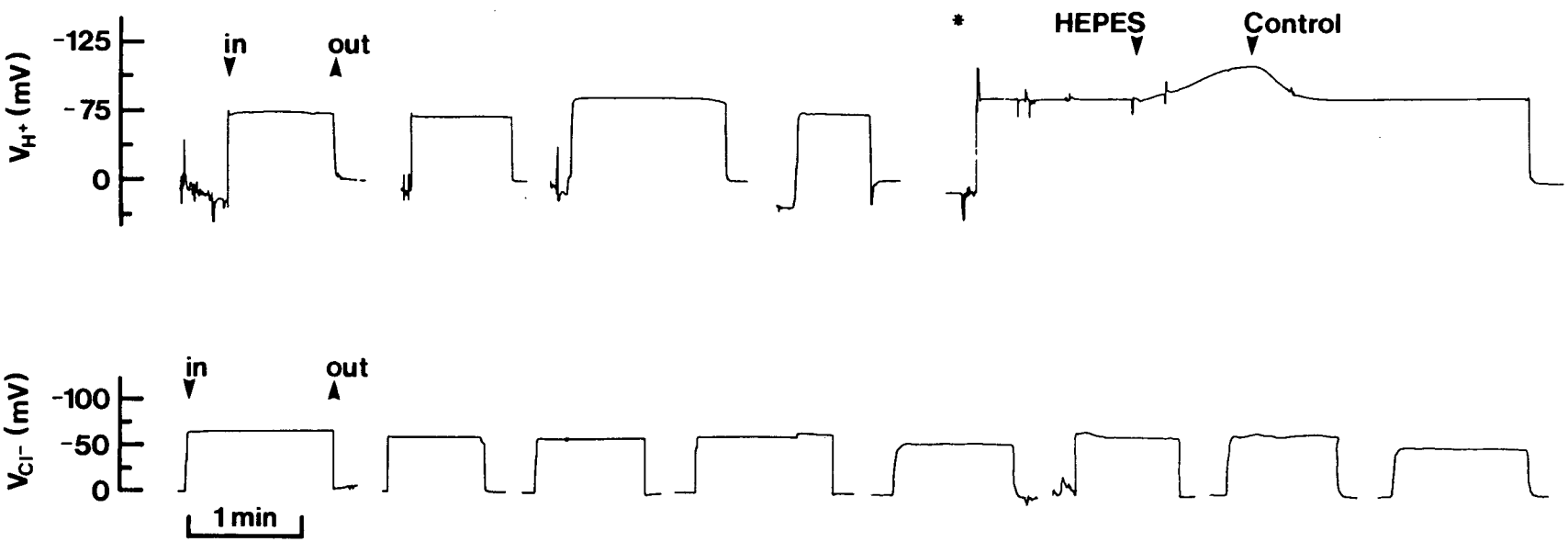
-125
-75
0
V_{H^+} (mV)
in
out
*
HEPES
Control
-100
-50
0
V_{Cl^-} (mV)
in
out
1 min

Figure 5.4 Distribution of V_{bl} and intracellular pH and Cl^- activity in anterior rectal salt gland cells. Measurements of V_{bl}, pH_c and $a^c_{Cl^-}$ were obtained from 39, 4 and 7 separate preparations, respectively.

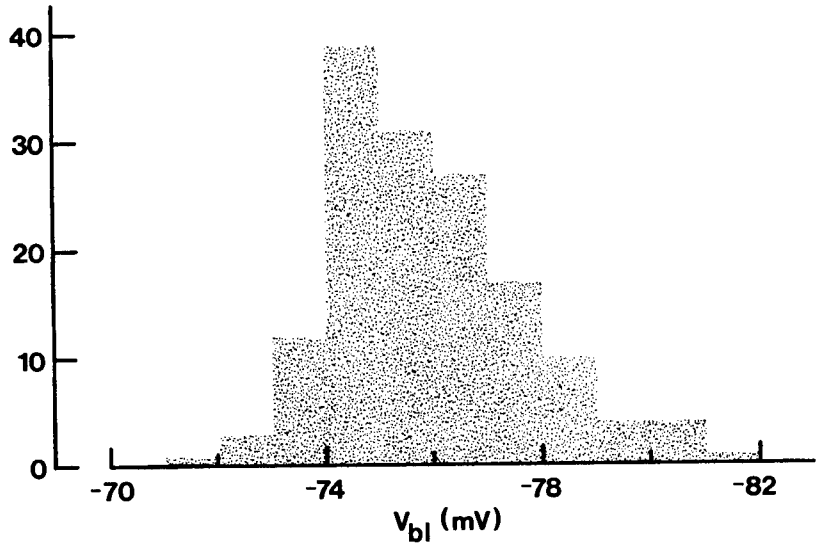
40
30
20
10
0
-70
-74
-78
-82
V_{bl} (mV)

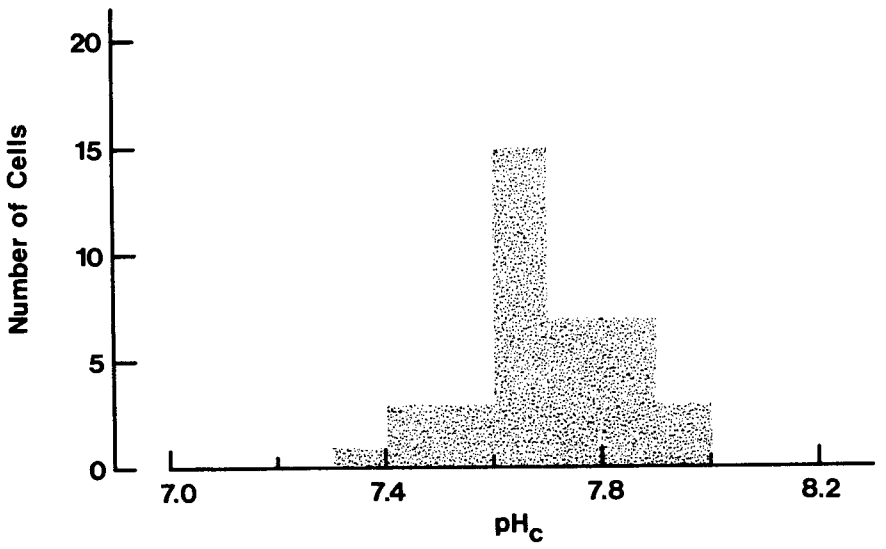
Number of Cells
20
15
10
5
0
7.0
7.4
7.8
8.2
pH_c

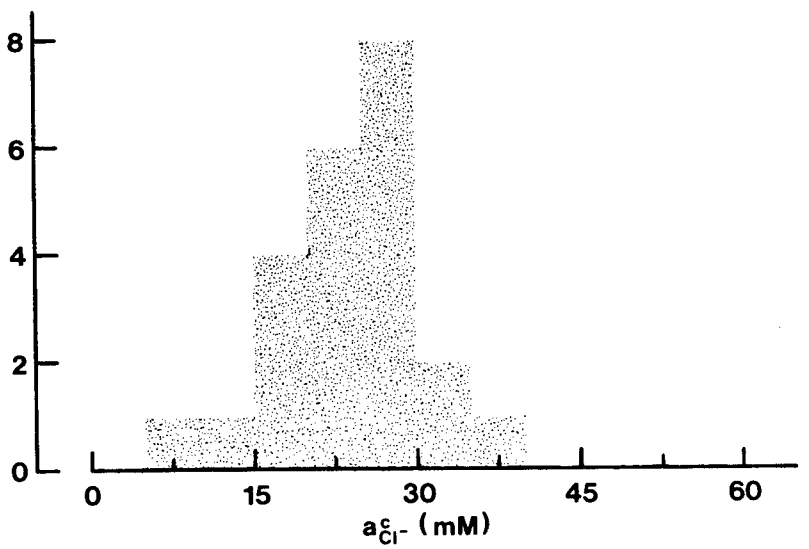
8
6
4
2
0
0
15
30
45
60
$a^c_{Cl^-}$ (mM)

and more powerful piezoelectric drive systems such as the 'stack-arrangement' described by Boron and Boulpaep (1982).

As with the voltage microelectrodes discussed above, cells could be repeatedly impaled with H^+-sensitive microelectrodes with no apparent deleterious effects to the tissue. The results obtained with Cl^--sensitive electrodes, however, were considerably different. In general, it was possible to make only 5-6 attempts at impalements, successful or unsuccessful, on any given preparation before V_{te} would start to rapidly depolarize. Since the problem never occurred with voltage or H^+-selective microelectrodes, which had the same tip dimensions as Cl^--electrodes, the only likely explanation is a direct effect of the Cl^--exchange resin on the tissue itself. This effect could be the result of resin toxicity to cellular metabolism or intriguingly, to a direct effect of the resin on electrogenic HCO_3^- transport or apical Cl^- conductance (see below). Any preparation which displayed this rapidly depolarizing V_{te} or had a V_{te} which dropped below -40 mV was immediately discarded.

2) Electrogenic HCO_3^- Transport

Several observations suggested that HCO_3^- transport in the anterior rectal salt gland was electrogenic in nature. Rapid addition of 1.0 mM acetazolamide to the bath, which inhibits $J_{net}^{CO_2}$ in this tissue (Chapter III), caused a large depolarization of V_{te} (Fig. 5.5). After a 60 minute exposure to acetazolamide V_{te} had stabilized at a new value of -7.3 $\pm$ 3.9 mV (mean $\pm$ S.E., n = 5). Removal of acetazolamide from the bathing saline caused V_{te} to return to control values within 30 minutes (Fig. 5.5).

The effects of 0.5 mM serosal DIDS on V_{te} are shown in Fig. 5.6. In 3 of the 4 preparations studied, the tissue was initially exposed to amino

Figure 5.5 Effects of rapid addition of 1.0 mM acetazolamide to the serosal bathing saline on V_{te}. Values are means $\pm$ S.E. (n = 5 preparations).

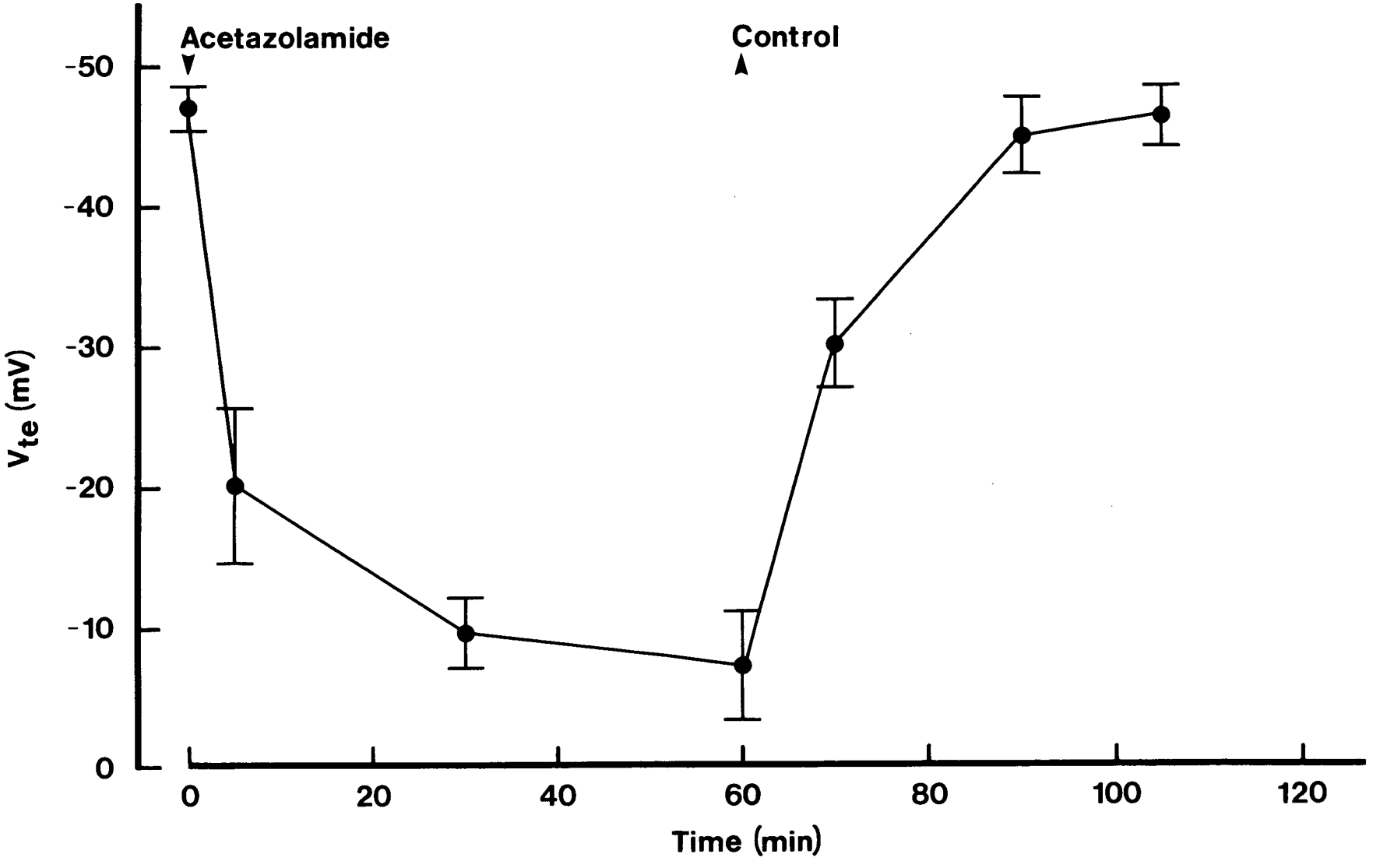
Acetazolamide
Control
-50
-40
-30
-20
-10
0
V_{te} (mV)
0
20
40
60
80
100
120
Time (min)

Figure 5.6 Effects of addition of 0.5 mM DIDS to the serosal bathing saline on V_{te} in 4 separate anterior rectal salt gland preparations. Anterior segments were exposed to DIDS saline for 60 minutes and then returned to control saline for 30 minutes. The inset shows the effects of amino acid-free saline (0-AA; see Materials and Methods) alone on V_{te} in 3 of the 4 preparations studied. Tissues were first exposed to amino acid-free saline for 60 minutes and then returned to control saline for 30 minutes before exposure to DIDS (see Results). The open and closed squares and circles represent results obtained from a single preparation.

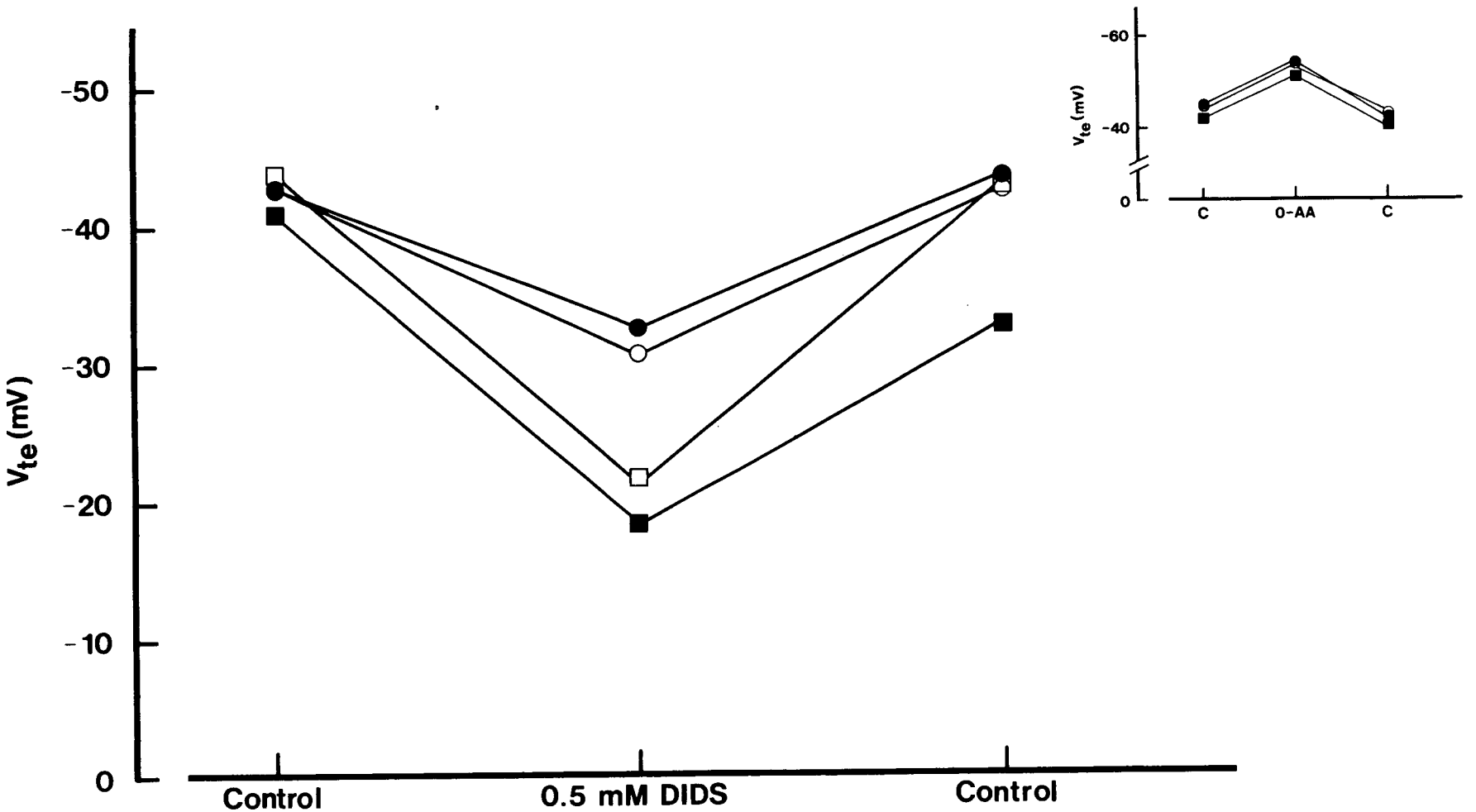
-50
-40
-30
-20
-10
0
V_{te} (mV)
Control
0.5 mM DIDS
Control
-60
-40
0
V_{te} (mV)
C
0-AA
C

acid-free bathing saline (see Materials and Methods) for 60 minutes and then returned to control saline for 30 minutes before addition of 0.5 mM DIDS to the bath. The inset in Fig. 5.6 shows that V_{te} hyperpolarized by approximately 8-10 mV in amino acid-free bathing salines and then returned to control values in control salines. Exposure of the salt gland to serosal DIDS inhibited $J_{net}^{CO_2}$ (Chapter III) and caused a depolarization of V_{te} (Fig. 5.6). The time course of this depolarization varied considerably between individual preparations and was complicated by the hyperpolarizing effects of the amino acid-free saline. In addition, V_{te} was not stable after the 60 minute DIDS exposure period and was in all cases continuing to decline rapidly. Nevertheless, the mean V_{te} of -25.8 $\pm$ 3.5 mV ($\pm$ S.E., n = 4) at this time was significantly different ($0.005 < P < 0.01$) from the control value of -44.1 $\pm$ 0.8 mV ($\pm$ S.E., n = 4). In 3 of the preparations, V_{te} returned to values near control after DIDS was removed from the bath (Fig. 5.6).

Rapid removal of CO_2 and HCO_3^- from the bath and replacement with a 5.0 mM HEPES buffered saline caused a rapid and large 30-40 mV depolarization of V_{te} (Fig. 5.7). This depolarization was complete within 1 minute (V_{te} = -12$\pm$ 1.7, mean $\pm$ S.E., n = 6; cf. Fig. 5.11) and was then followed by a partial repolarization of variable time course (cf. Fig. 5.14). After anywhere from 10-90 minutes V_{te} stabilized at a new mean value of -31.0 $\pm$ 1.1 mV ($\pm$ S.E., n = 6) which was significantly lower ($P < 0.0005$) than the control V_{te} of -44.6 $\pm$ 1.1 mV (mean $\pm$ S.E., n = 6). This repolarization phase could have been due to continued electrogenic HCO_3^- secretion since CO_2 and HCO_3^- were still present in the mucosal saline in this experiment. Removal of luminal CO_2 and HCO_3^- and replacement with HEPES saline, however, caused only a very small 1-3 mV hyperpolarization of V_{te} irrespective of the

Figure 5.7 Effects of serosal CO_2 and HCO_3^- replacement with a 5.0 mM HEPES buffered saline on V_{te}. Values are means ± S.E. (n = 6). Removal of serosal CO_2 and HCO_3^- caused a rapid depolarization of V_{te} which was complete within 1 minute (T_1; cf. Fig. 5.11). This depolarization was followed by a partial repolarization until a new stable V_{te} was reached after anywhere from 10-90 minutes (T_{10-90}; see Results and Discussion).

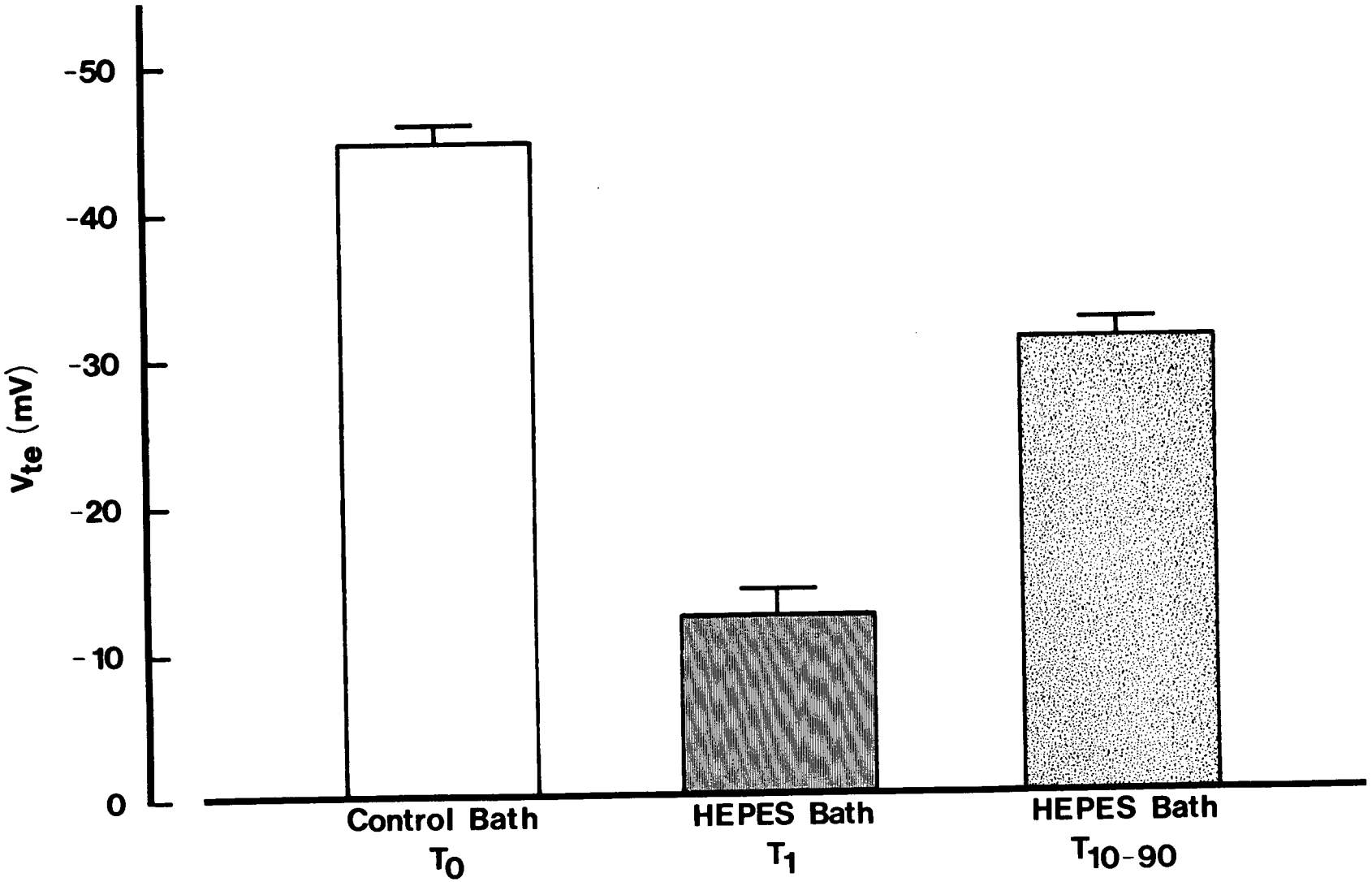
-50
-40
-30
-20
-10
0
V_{te} (mV)
Control Bath
T_0
HEPES Bath
T_1
HEPES Bath
T_{10-90}

presence or absence of CO_2 and HCO_3^- in the serosal medium (data not shown). These experiments indicate that the repolarization phase is not due to apical CO_2 recycling and continued electrogenic HCO_3^- transport. Transepithelial potentials hyperpolarized transiently by approximately 10 mV and then returned to control values after CO_2 and HCO_3^- were added back to the bath (data not shown).

Replacement of CO_2 and HCO_3^- with the lipid soluble buffer, glycodiazine, caused V_{te} to rapidly depolarize and to reverse (i.e. lumen positive; Fig. 5.8). This new positive V_{te} of 2.2 $\pm$ 2.6 mV (mean $\pm$ S.E., n = 3) remained stable for at least 60 minutes (V_{te} = 1.4 $\pm$ 1.2 mV after 60 min; mean $\pm$ S.E., n = 3). Addition of CO_2 and HCO_3^- back to the bath caused V_{te} to repolarize rapidly and usually hyperpolarize by 5-10 mV (Fig. 5.8; cf. Fig. 5.10).

To determine at which cell membrane the electrogenic HCO_3^- transport step was located, the experiments with acetazolamide, HEPES and glycodiazine were repeated while simultaneously measuring V_{bl}. Addition of acetazolamide to the bath or replacement of serosal CO_2 and HCO_3^- with glycodiazine caused V_{bl} to hyperpolarize slightly by 1-3 mV (Figs. 5.9 and 5.10). Replacement of CO_2 and HCO_3^- with HEPES caused a small, transient (2-4 mV) depolarization of V_{bl} (Fig. 5.11). Rapid increases of serosal CO_2 and HCO_3^- concentrations at constant pH caused V_{bl} to depolarize slightly by 2-4 mV and had a small hyperpolarizing effect on V_{te} of 3-4 mV (Fig. 5.12). Taken together these results indicate that HCO_3^- entry into the cell at the basolateral membrane is largely an electrically silent process, and that HCO_3^- exit at the apical membrane is mediated by an electrogenic mechanism.

Data shown in Figure 5.13 demonstrate that the observed effects of these experimental perturbations on V_a cannot be explained by an indirect

Figure 5.8 Effects of replacing serosal CO_2 and HCO_3^- with the lipid soluble buffer, glycodiazine, on V_{te}. Values are means $\pm$ S.E. (n = 3).

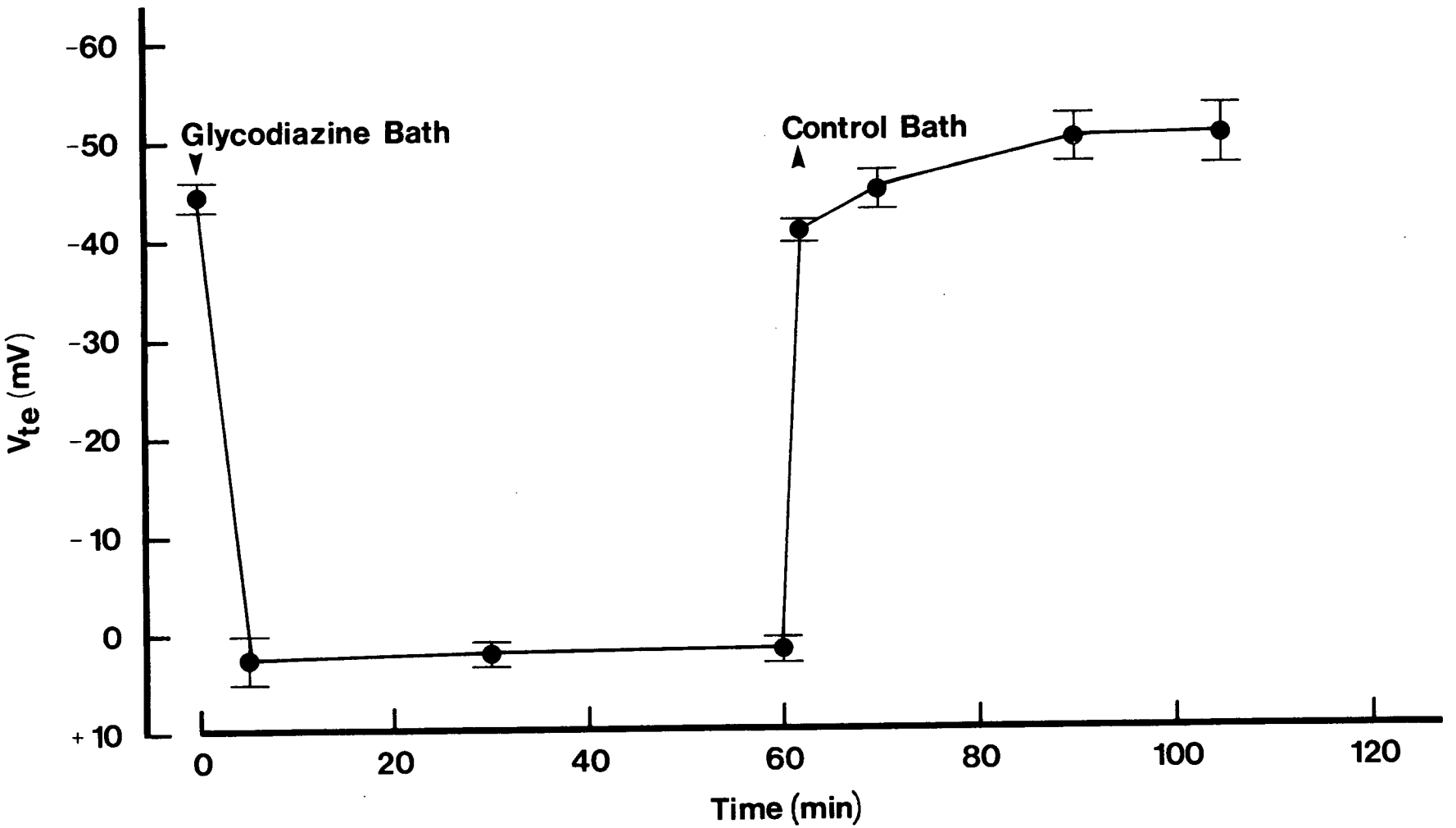
-60
-50
-40
-30
-20
-10
0
+10
V_{te} (mV)
Glycodiazine Bath
Control Bath
0
20
40
60
80
100
120
Time (min)

Figure 5.9 Transepithelial potential and V_{bl} during and after addition of 1.0 mM acetazolamide to the serosal bathing saline. A total number of 12 similar experiments were conducted on 4 separate anterior segment preparations.

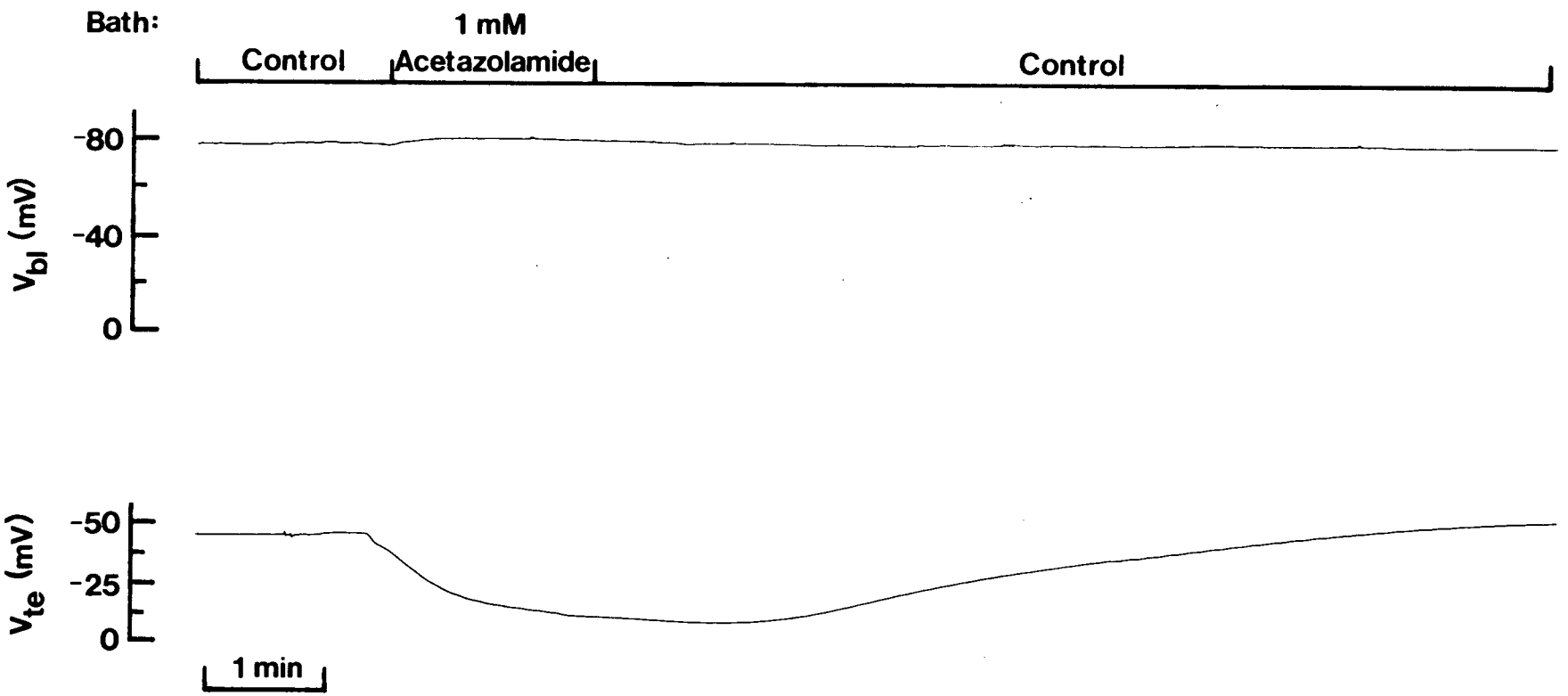
Bath:
1 mM
Control
Acetazolamide
Control
-80
-40
0
V_{bl} (mV)
-50
-25
0
V_{te} (mV)
1 min

Figure 5.10 Effects of serosal CO_2 and HCO_3^- replacement with the lipid soluble buffer, glycodiazine, on V_{bl} and V_{te}. Eight similar experiments were conducted on 3 separate anterior segment preparations.

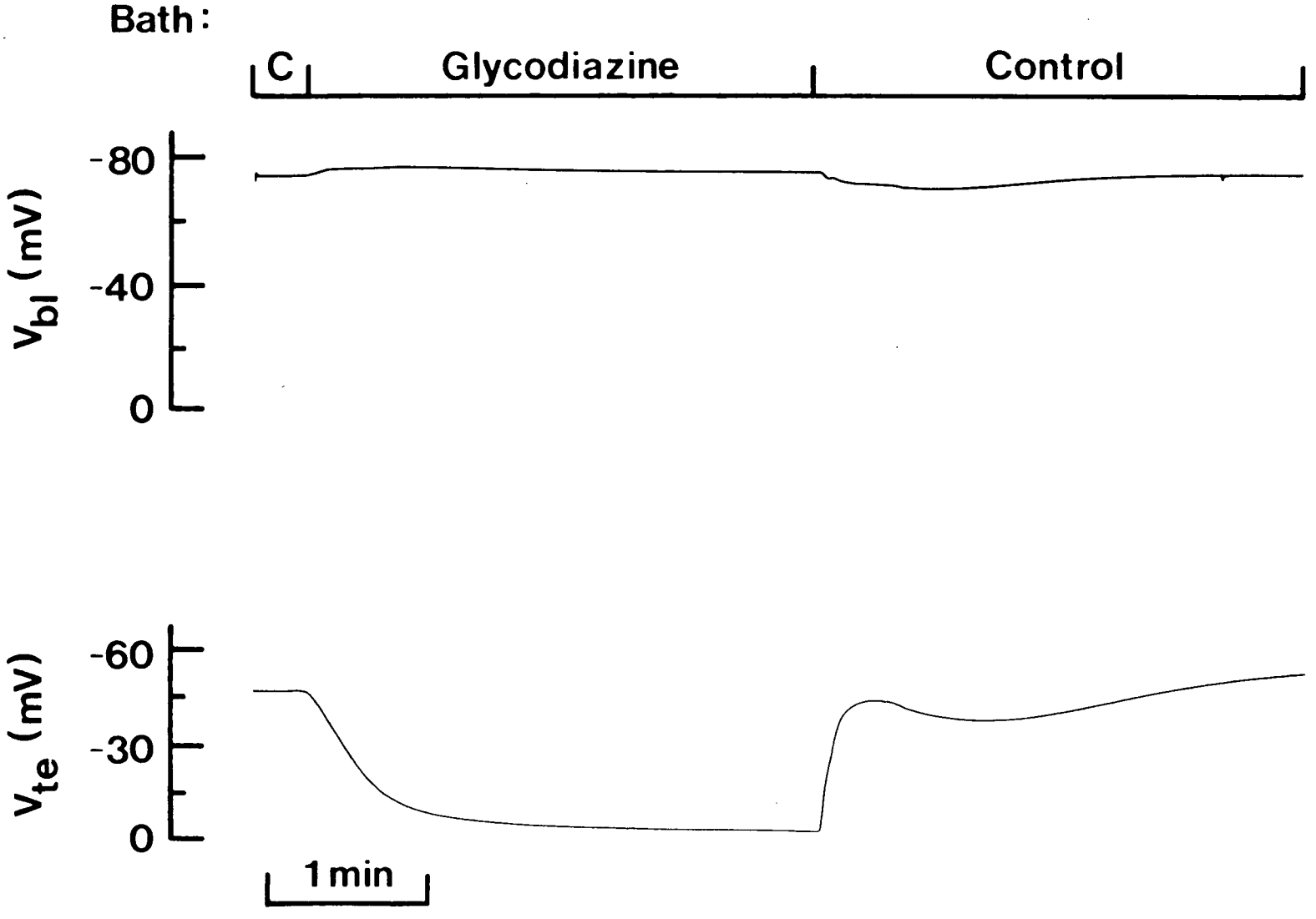
Bath:
C
Glycodiazine
Control
-80
-40
0
V_{bl} (mV)
-60
-30
0
V_{te} (mV)
1 min

Figure 5.11 Effects of replacement of serosal CO_2 and HCO_3^- with a 5.0 mM HEPES buffered saline on V_{bl} and V_{te}. Seventeen similar experiments were performed on 5 separate anterior segment preparations.

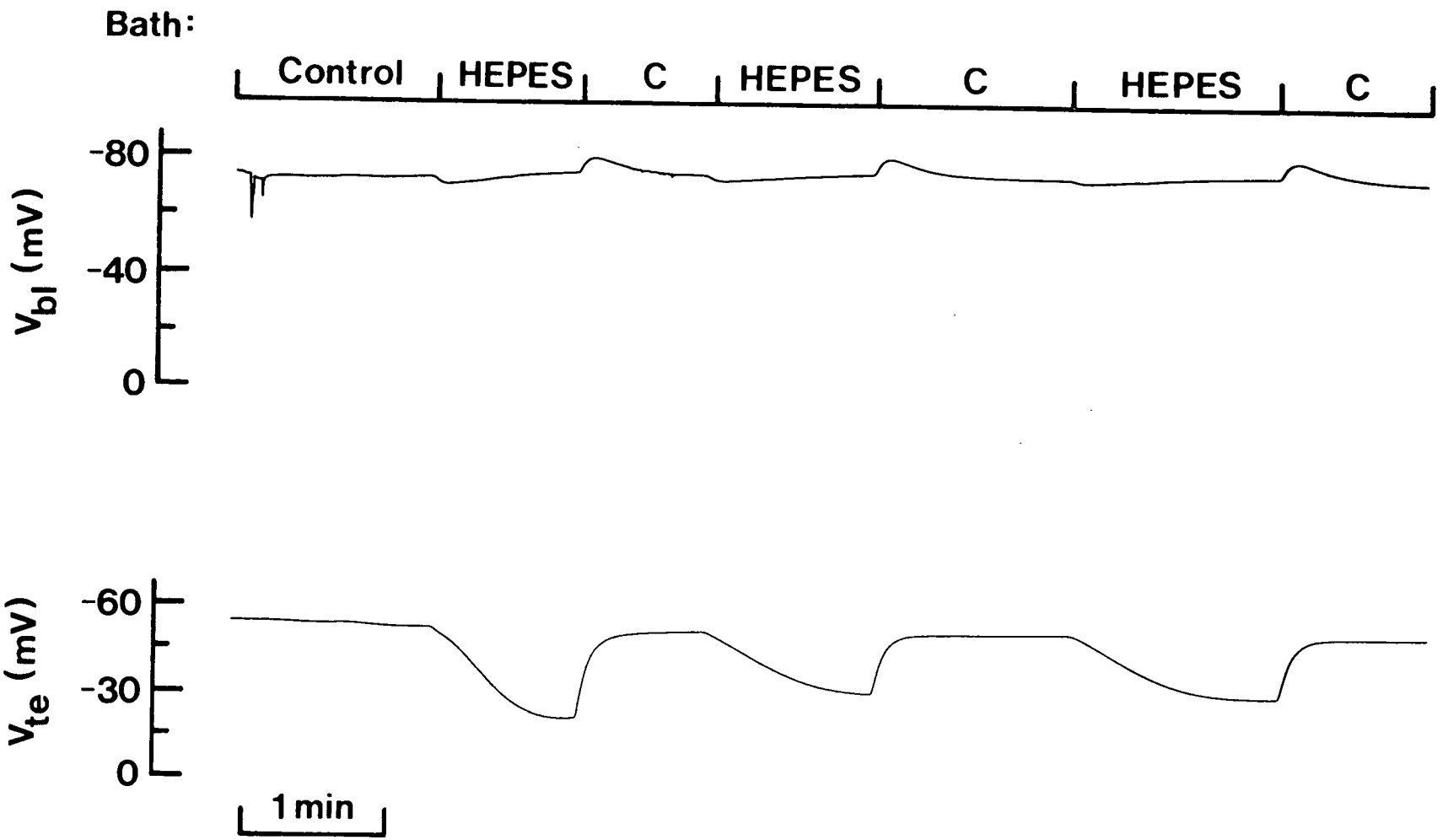
Bath:
Control
HEPES
C
HEPES
C
HEPES
C
-80
-40
0
V_{bl} (mV)
-60
-30
0
V_{te} (mV)
1 min

Figure 5.12 Effects of high serosal HCO_3^- concentration at constant pH on V_{bl} and V_{te}. Five similar experiments were conducted on 2 separate anterior segment preparations.

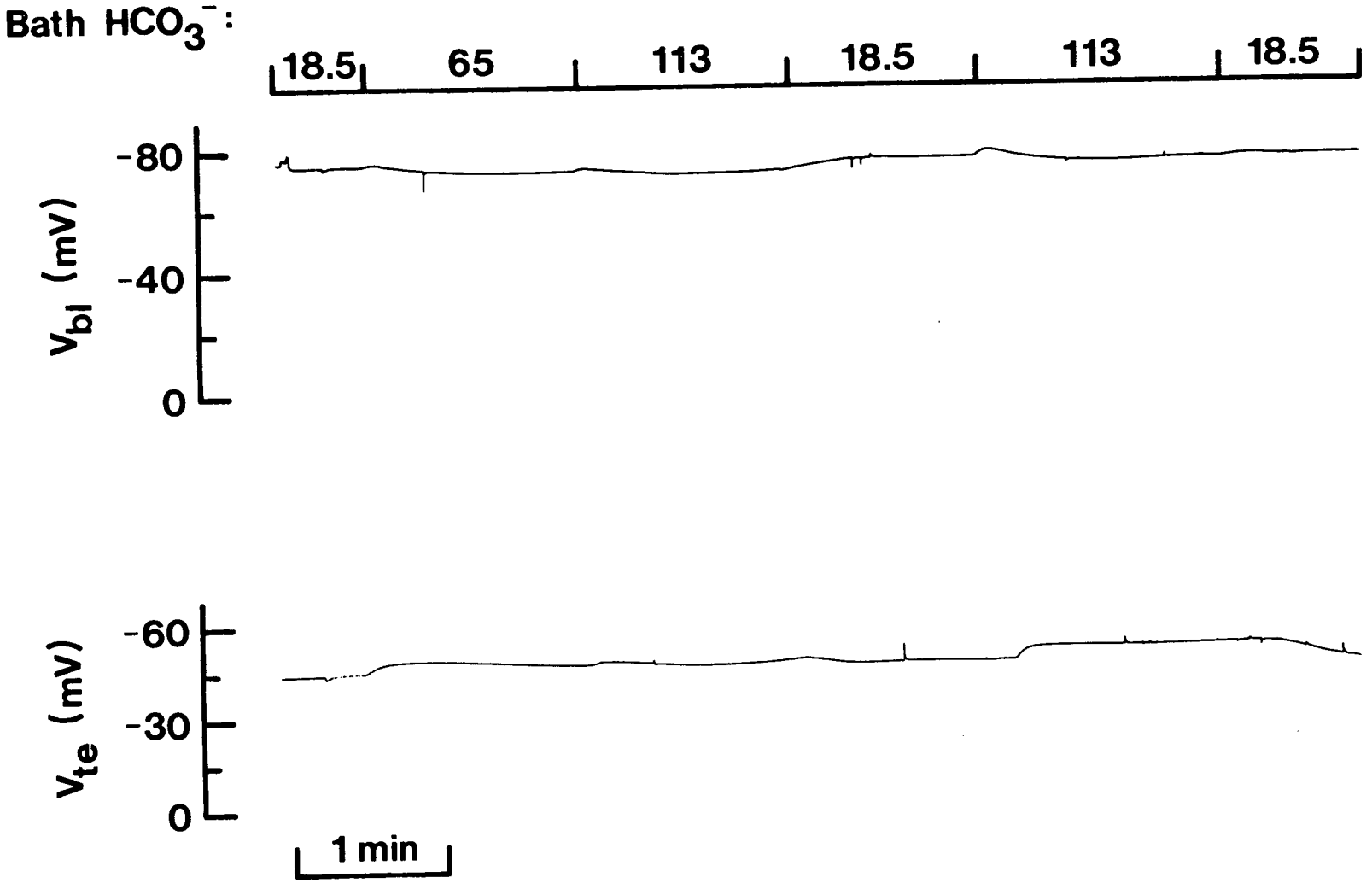
Bath HCO_3^-:
18.5
65
113
18.5
113
18.5
-80
-40
0
V_{bl} (mV)
-60
-30
0
V_{te} (mV)
1 min

Figure 5.13 Effects of luminal Na^+ or K^+ substitutions on V_{te} and V_{bl}. A total of 4-5 similar experiments were conducted on 2 separate anterior segment preparations for either the Na^+ or K^+ substitution studies.

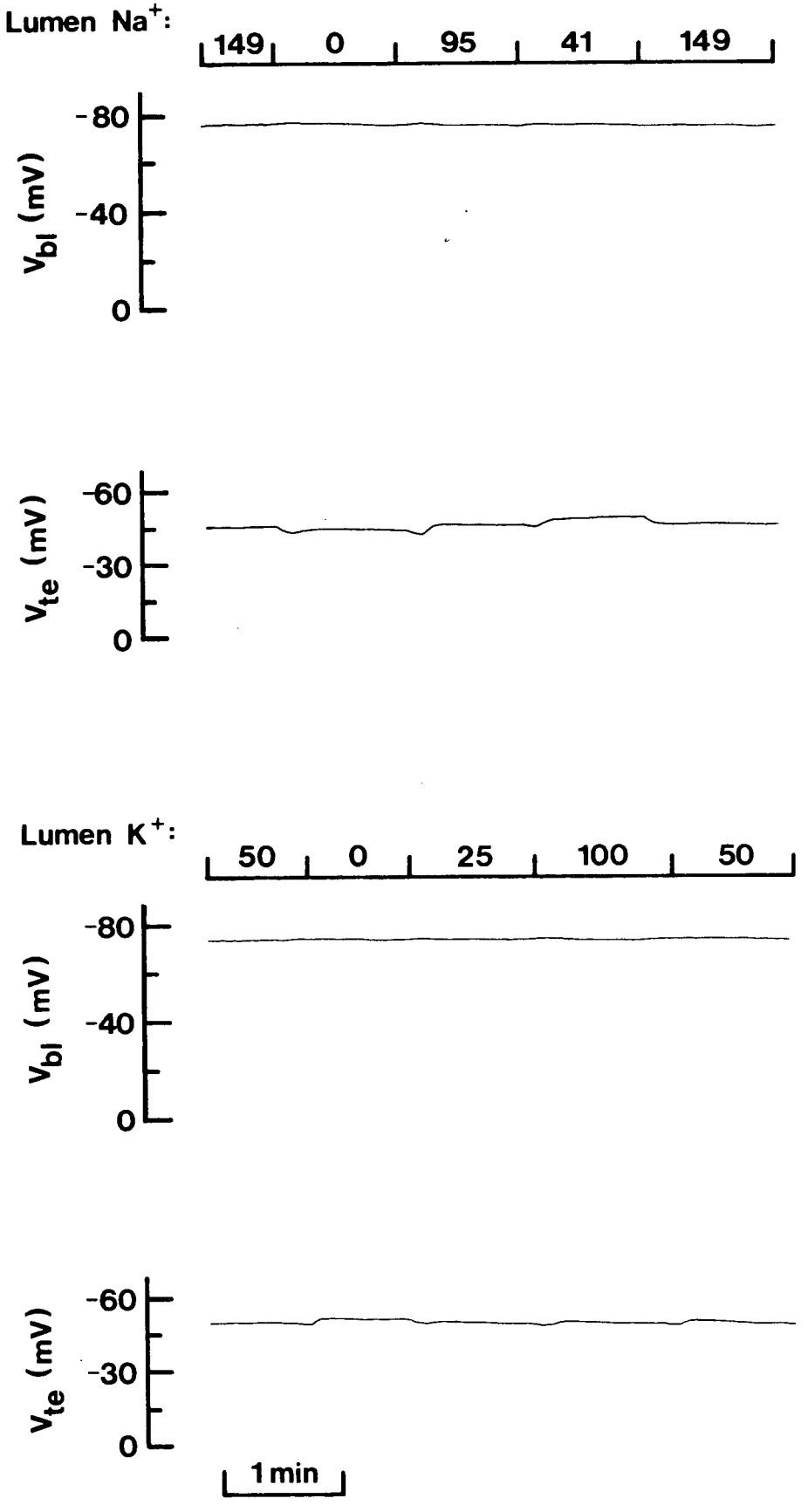
Lumen Na^+:
149
0
95
41
149
-80
-40
0
V_{bl} (mV)
-60
-30
0
V_{te} (mV)
Lumen K^+:
50
0
25
100
50
-80
-40
0
V_{bl} (mV)
-60
-30
0
V_{te} (mV)
1 min

inhibitory effect of changes in pH_c on an apical, electrogenic cation reabsorptive process. Rapid decreases in luminal Na^+ or K^+ concentrations, or complete removal of luminal Na^+ or K^+ have virtually no effect on V_a or V_{bl} indicating that the apical membrane has a very low cation conductance. Similarly, the observed alterations in V_a cannot be due to an increased apical Cl^- conductance (see below) arising from changes in pH_c. Perfusion of the lumen with Cl^--free saline followed by removal of CO_2 and HCO_3^- from the serosal bath has the same hyperpolarizing effect on V_a as observed in glands perfused with control salines (Fig. 5.14; cf. Fig. 5.11).

3) Electrogenic Cl^- Reabsorption

Data in Figure 5.15 show that rapid decreases in luminal Cl^- concentration cause a rapid, step-wise hyperpolarization of V_{te}. Simultaneous measurements of V_{bl} indicated that these potential changes were located almost entirely at the apical membrane (Fig. 5.15). The relationship between the logarithm of the luminal Cl^- activity $a^l_{Cl^-}$ and V_a was found to be linear between Cl^- concentrations of 16 to 164 mM (Fig. 5.16). The slope of the line for experiments conducted on 11 different preparations was 42.2 mV/decalog $a^l_{Cl^-}$ and the correlation coefficient was 0.992. Chloride concentrations below 16.0 mM caused a repolarization of V_a. At a luminal Cl^- concentration of 4.0 mM, mean V_a was 0.01 $\pm$ 1.1 mV ($\pm$ S.E.; n = 17 impalements, 4 preparations; see Fig. 5.16). Mean V_a in the presence of Cl^--free mucosal saline was 0.2 $\pm$ 1.1 mV ($\pm$ S.E.; n = 5 impalements, 1 preparation).

These results suggested that the apical membrane had a high Cl^- permeability and that Cl^- enters the cell, at least in part, by a passive, electrodiffusive mechanism. To test this idea further, $a^c_{Cl^-}$ was measured under control conditions. Calculated Cl^- electrochemical gradients ($\Delta\tilde{\mu}_{Cl^-}$)

Figure 5.14 Effects of serosal CO_2 and HCO_3^- removal (replaced with HEPES buffered saline) on V_{bl} and V_{te} during perfusion of the anterior segment with Cl^--free salines. Seven similar experiments were conducted on 4 anterior segment preparations.

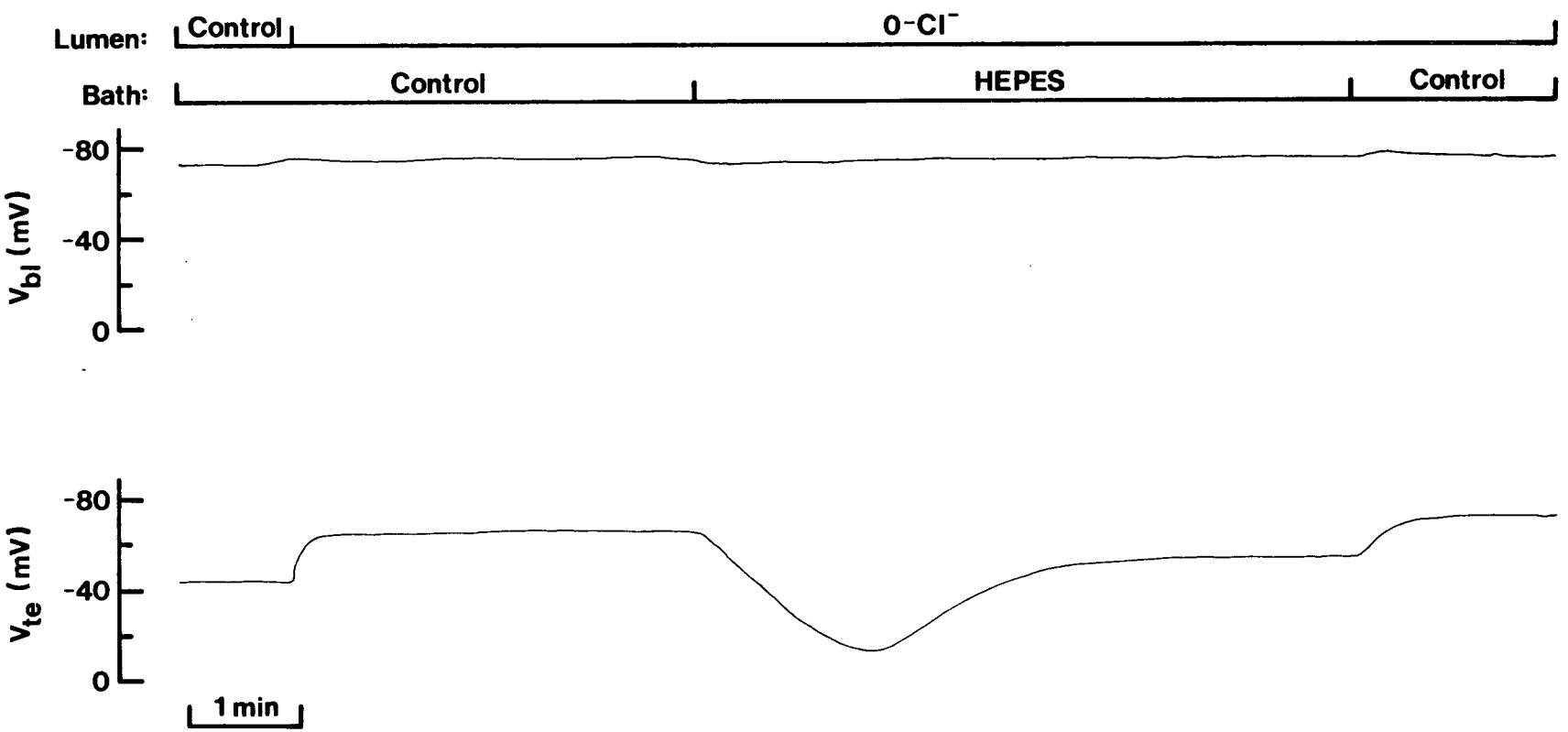
Lumen:
Control
0-Cl⁻
Bath:
Control
HEPES
Control
-80
-40
0
V_{bl} (mV)
-80
-40
0
V_{te} (mV)
1 min

Figure 5.15 Effects of rapid changes in luminal Cl^- concentration on V_{te} and V_{bl}. Similar experiments were conducted on a total of 11 separate anterior segment preparations.

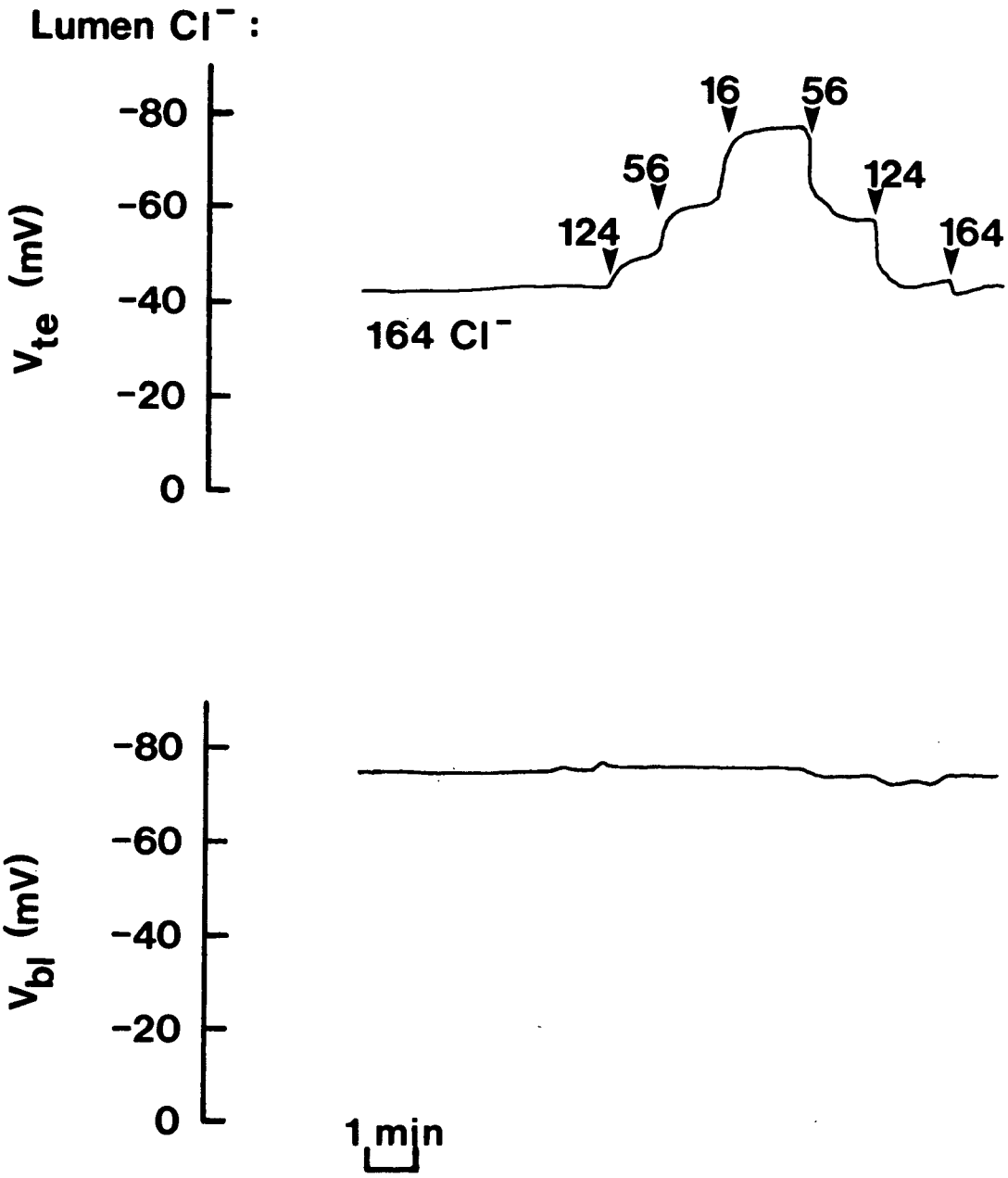
Lumen Cl⁻ :
-80
-60
-40
-20
0
V_{te} (mV)
16
56
56
124
124
164
164 Cl⁻
-80
-60
-40
-20
0
V_{bl} (mV)
1 min

Figure 5.16 Relationship between the log of the luminal Cl^- activity ($a^l_{Cl^-}$) and V_a. Each point is the mean $\pm$ S.E. of 9-17 impalements obtained from at least 2 separate anterior segment preparations. A total of 11 anterior segment preparations were used in these studies. The straight line drawn through the points was determined using the least squares method of linear regression. The point at the arrow is the value of V_a in the presence of 4 mM luminal Cl^- (see Results).

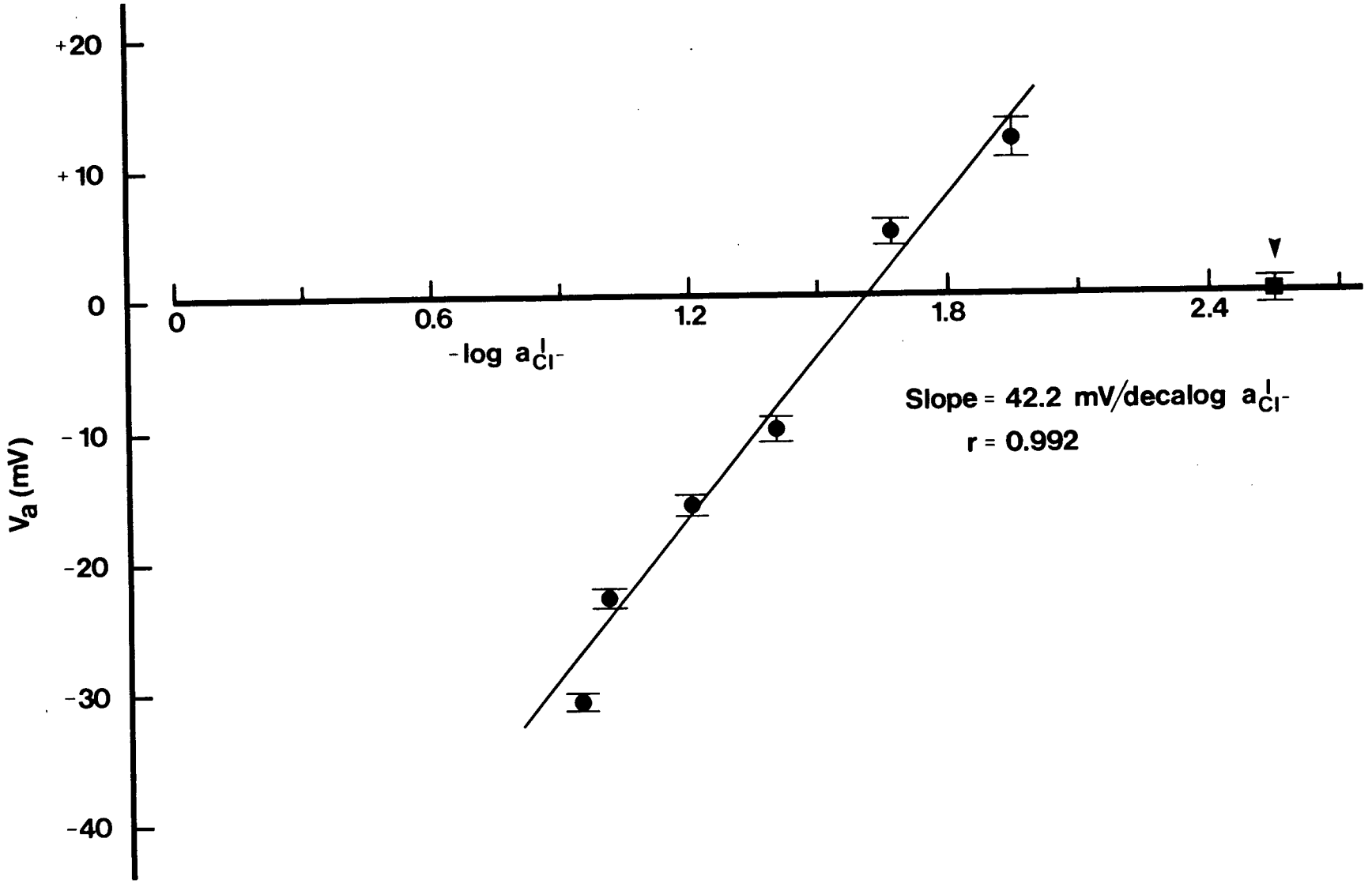
+20
+10
0
-10
-20
-30
-40
V_a (mV)
0
0.6
1.2
1.8
2.4
$-\log a^{I}_{Cl^-}$
Slope = 42.2 mV/decalog $a^{I}_{Cl^-}$
r = 0.992

Table 5.2 Calculated Cl^- electrochemical gradients for apical and basolateral cell membranes bathed by control serosal and mucosal salines Net Cl^- flux is from lumen to bath (Chapter III and IV). Negative signs indicate a favorable $\Delta\tilde{\mu}_{Cl^-}$ for passive Cl^- movement. The $\Delta\tilde{\mu}^{bl}_{Cl^-}$ was calculated using the mean V_{bl} of -75.6 mV (see Results) and a serosal Cl^- activity of 27.4 mM. Values are means ± S.E. (n = 23 cells, 7 preparations).

$a^c_{Cl^-}$	V_a	$\Delta\tilde{\mu}^a_{Cl^-}$	$\Delta\tilde{\mu}^{bl}_{Cl^-}$
23.5 ± 1.4 mM	-30.8 ± 1.1 mV	-10.7 ± 2.2 mV	-71.7 mV

for apical and basolateral cell membranes are shown in Table 5.2. Chloride activity in the cell was 23.5 mM and the $\Delta\tilde{\mu}_{Cl^-}$ for the apical membrane was 10.7 $\pm$ 2.2 mV favoring passive Cl^- entry.

It should be noted at this time that isethionate was used as an anion substitute for Cl^- and to simulate the anion deficit observed in larval hemolymph (Chapter II). Generally, gluconate is used as the anion substitute of choice in experiments in which $a^c_{Cl^-}$ is measured since Cl^- resins tend to be less sensitive to this compound than most other anion substitutes. In experiments in which gluconate replaced isethionate, however, V_{te} hyperpolarized by approximately 10-15 mV and exhibited a continual oscillation of approximately $\pm$ 5.0 mV (data not shown). This observation is consistent with the fact that gluconate is generally more permeable than either Cl^- or many other anion substitutes in certain cells and tissues (see for example, Brown and Saunders, 1977).

Intracellular Cl^- measurements in tissues and cells bathed for prolonged periods in Cl^--free salines give 'apparent' $a^c_{Cl^-}$ values of 4 to 6 mM (e.g. Spring and Kimura, 1978; Baumgarten and Fozzard, 1981; Hanrahan, 1982). This residual Cl^- activity is thought to be due to the presence of interfering anions in the cell and most measurements of $a^c_{Cl^-}$ are assumed to be overestimates of actual values. No attempt was made in the present study to measure this residual anion activity primarily because it was anticipated that the concentration of the major intracellular interfering anion, HCO_3^-, would be altered by removing luminal and bath Cl^-. It must be stressed, however, that any overestimate of $a^c_{Cl^-}$ would only strengthen the major conclusions of this study (see Discussion).

Table 5.2 demonstrates that there is a large $\Delta\tilde{\mu}_{Cl^-}$ at the basolateral membrane of 71.7 mV favoring passive Cl^- exit from the cell. Unlike

the apical Cl^- entry step, however, Cl^- exit at the basolateral cell membrane is electrically silent. Figure 5.17 shows the results of 3 separate experiments in which serosal Cl^- concentration was varied rapidly from a control value of 39 mM to values of 5, 100 or 164 mM. These solution changes had virtually no effect on V_{bl}. The small potential changes which did occur, and which are seen most easily in the lower trace of Figure 5.17, are clearly in the wrong direction to be explained by an electrogenic, basolateral Cl^- exit step.

Data in Figure 5.18 demonstrate that the V_{bl} in anterior rectal cells is primarily a K^+ diffusion potential as is observed in many epithelia. Changes in serosal K^+ concentration alter V_{bl} in a rapid, linear fashion. The slope of the relationship between V_{bl} and serosal K^+ activity (a^s_{K+}) is 54.2 mV/decalog a^s_{K+} and the correlation coefficient is 0.9999 (Fig. 5.18). Decreases in serosal Na^+ concentration from 189.5 to 63 mM had a small, 1-3 mV depolarizing effect on V_{bl} (data not shown).

D. Discussion

1) Cellular Entry and Exit Steps

The results of the present study are summarized in the cellular model shown in Figure 5.19. As demonstrated in Chapters III and IV, HCO_3^- secretion in the anterior rectal salt gland is mediated by a 1:1 exchange of luminal Cl^- for serosal HCO_3^- ions. Data in Figures 5.5 to 5.11 show clearly that experimental conditions which inhibit $J^{CO_2}_{net}$ in this tissue (see Chapter III) cause large hyperpolarizations of V_a and have little effect on V_{bl}. These results are consistent with the hypothesis that HCO_3^- exit at the apical cell membrane is mediated by an electrogenic HCO_3^- or H^+/OH^- transport mechanism.

Figure 5.17 Effects of rapid changes in serosal Cl^- concentration on V_{bl}. Each trace is the result from an experiment conducted on a separate anterior segment preparation. A total number of 8-15 similar experiments were conducted on 2-3 anterior segments.

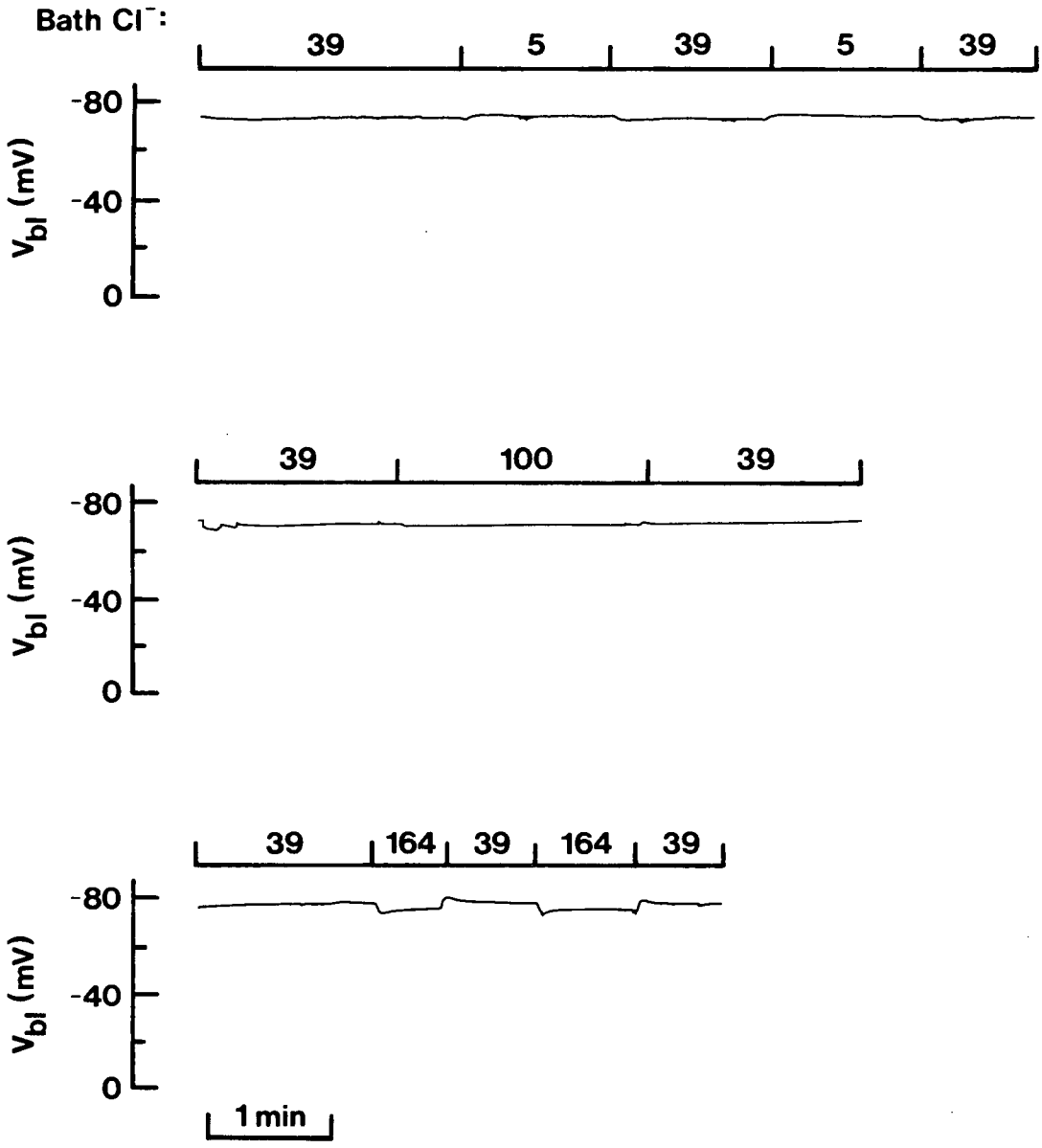
Bath Cl⁻:
39
5
39
5
39
-80
-40
0
V_{bl} (mV)
39
100
39
-80
-40
0
V_{bl} (mV)
39
164
39
164
39
-80
-40
0
V_{bl} (mV)
1 min

Figure 5.18 The upper panel shows the effects of rapid changes in serosal K^+ concentration on V_{bl}. The relationship between the log of the serosal K^+ activity and V_{bl} is shown in the lower panel. Each point is the mean ± S.E. of 10-13 impalements obtained from 4 separate anterior segment preparations. The straight line drawn through the points was determined using the least squares method of linear regression. In all cases the S.E. bar was smaller than the size of the actual point.

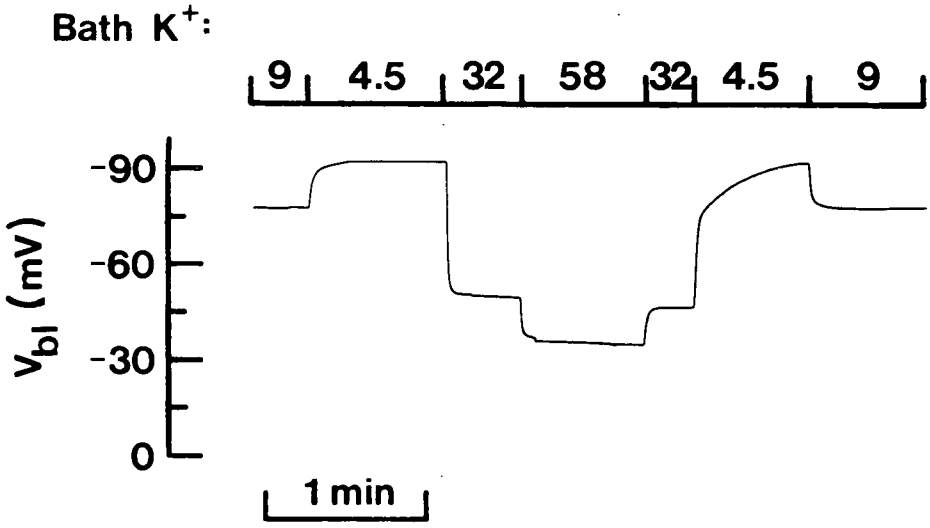
Bath K+:
9
4.5
32
58
32
4.5
9
-90
-60
-30
0
Vbl (mV)
1 min

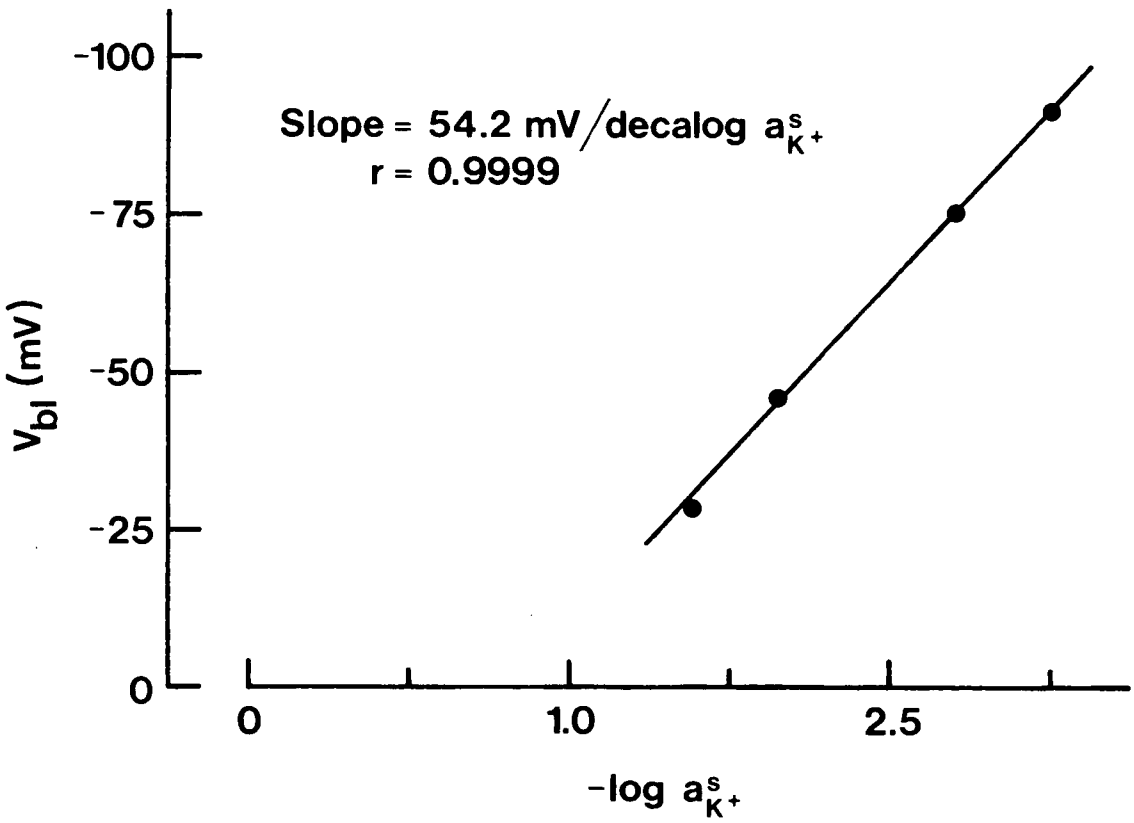
-100
-75
-50
-25
0
Vbl (mV)
Slope = 54.2 mV/decalog a$^s_{K+}$
r = 0.9999
0
1.0
2.5
-log a$^s_{K+}$

Figure 5.19 Tentative cellular model of HCO_3^- and Cl^- entry and exit steps in anterior rectal salt gland cells (c.a. = carbonic anhydrase).

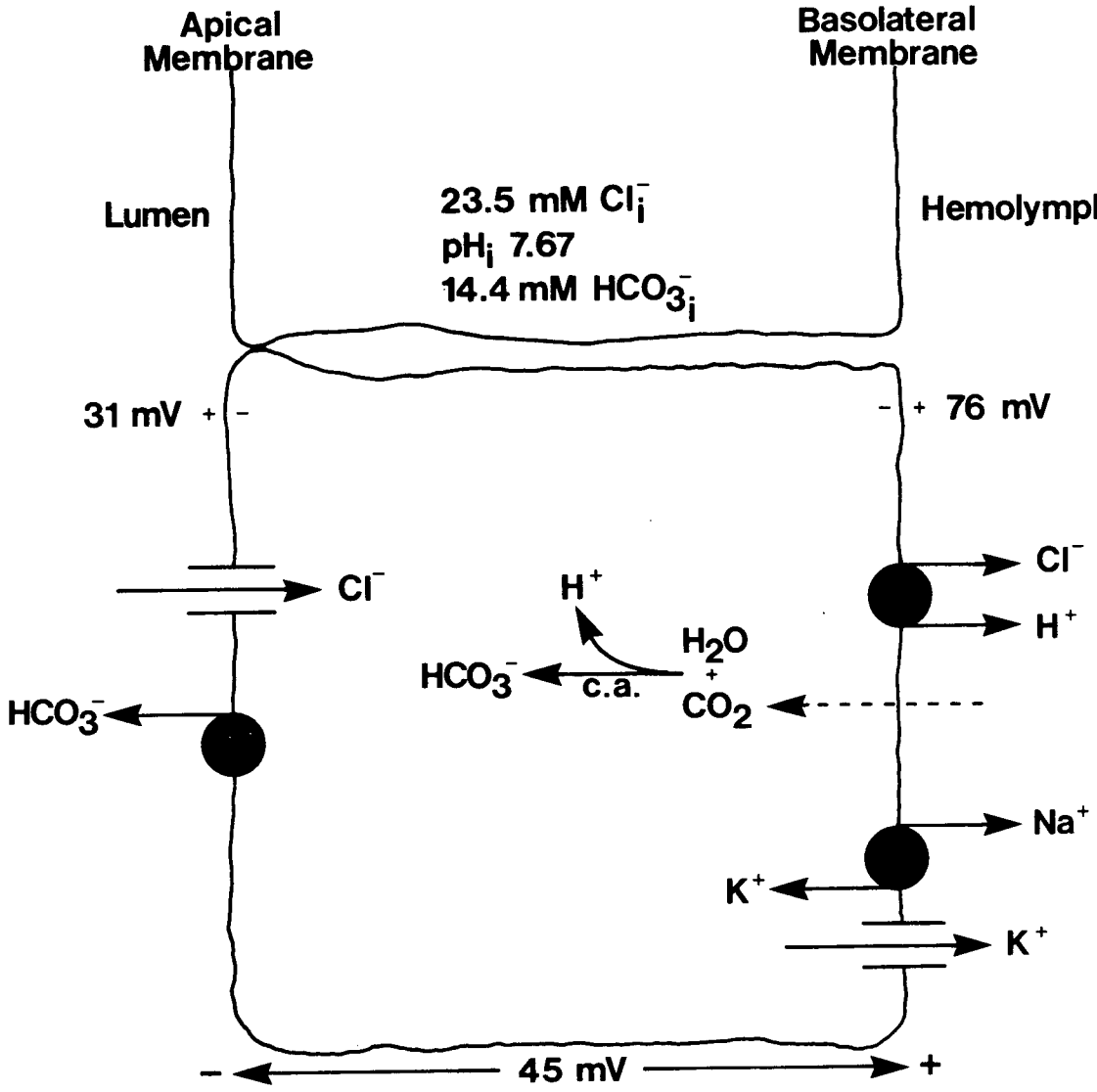
Apical Membrane
Basolateral Membrane
Lumen
23.5 mM Cl^-_i
pH_i 7.67
14.4 mM $HCO_{3_i}^-$
Hemolymph
31 mV + −
− + 76 mV
Cl^-
HCO_3^-
H^+
H_2O
HCO_3^-
c.a.
CO_2
Cl^-
H^+
Na^+
K^+
K^+
45 mV
− +

Recently, Biagi, Kubota, Sohtell and Giebisch (1981) have shown that decreases in serosal HCO_3^- concentration and pH depolarize V_{bl} and inhibit basolateral K^+ conductance in perfused rabbit proximal tubules (see also Steels and Boulpaep, 1976). These changes in K^+ conductance are presumably due to effects of changes in pH_c on basolateral K^+ channels and could suggest falsely a high HCO_3^- permeability of the basolateral cell membrane. Similar effects cannot explain the results in Figures 5.5 to 5.11. Rapid changes in or complete removal of luminal Na^+ or K^+ have little effect on V_a demonstrating that the apical membrane has a very low cation permeability (Fig. 5.13). In addition, the alterations of V_a seen in Figures 5.5 to 5.11 are not due to increasing apical Cl^- conductance. Removal of CO_2 and HCO_3^- from the bath still causes a large depolarization of V_{te} when salt glands are perfused with Cl^--free saline (Fig. 5.14).

Decreases in luminal Cl^- concentration from 164 to 16 mM depolarizes V_a in a rapid, step-wise manner (Fig. 5.15). The relationship between V_a and luminal Cl^- activity is linear with a slope of 42.2 mV/decalog a^l_{Cl}- (Fig. 5.16). These results indicate that the apical membrane has a very high, passive Cl^- conductance. Furthermore, measurement of control a^c_{Cl}- demonstrated that the electrochemical gradient for Cl^- at the apical membrane favors passive entry of Cl^- into the anterior rectal cells (Table 5.2). Taken together, these data suggest strongly that apical Cl^- entry is mediated, at lease in part, by passive, electrodiffusive movement of Cl^- through a Cl^--selective channel.

At luminal Cl^- concentrations below 16 mM, V_a begins to repolarize. Mean V_a in the presence of 4 mM luminal Cl^- was close to 0 mV (see Fig. 5.16). The nature of this repolarization phase is uncertain, but it may be due to an inhibitory effect of low luminal Cl^- concentration on electrogenic

HCO_3^- secretion.

The basolateral cell membrane is the most likely site for a direct 1:1 coupling between Cl^- and HCO_3^- movements. Basolateral Cl^- exit and HCO_3^- entry are both largely electrically silent processes (see Figs. 5.9 to 5.12 and Fig. 5.17). In addition, the Cl^-/HCO_3^- exchange inhibitor DIDS, which inhibits $J_{net}^{CO_2}$ in this tissue (Chapter III), depolarizes V_{te} when when added to the serosal bathing saline (Fig. 5.6).

The anterior rectal cell V_{bl} appears to be primarily a K^+ diffusion potential (Fig. 5.17). The mechanism of cellular K^+ uptake, however, is uncertain at present. Superfusion of the tissue with 1.0 mM serosal ouabain for up to 1 hour had no effect on V_{bl} or V_{te} (data not shown). This may be due to an insensitivity of a putative Na^+/K^+ ATPase to ouabain at room temperature as observed for other insect Na^+/K^+ pumps (reviewed by Anstee and Bowler, 1979). Alternatively, it could simply represent failure of the ouabain to permeate the basement membrane and interact directly with pump sites. Since Na^+/K^+ pumps have been found in a number of insect tissues (see Anstee and Bowler, 1979; Phillips, 1981) and are present in almost all vertebrate epithelia studied in detail, it is tentatively suggested that anterior rectal cell K^+ accumulation is mediated by a basolateral Na^+/K^+ ATPase (see Fig. 5.19).

Experiments using glycodiazine suggest, albeit very indirectly, that basolateral Cl^- exit and HCO_3^- entry may at least partially be mediated by an HCl cotransport or Cl^-/OH^- exchange mechanism. Glycodiazine (sodium glymidine) is a buffer which has a high lipid solubility. The pK_a of glycodiazine (5.7; Ullrich, Radtke and Rumrich, 1971) is similar to that for the CO_2/HCO_3^- equilibrium (6.1) and hence this compound has been used

as a CO_2 and HCO_3^- replacement. In the proximal tubule, it has been shown that glycodiazine is reabsorbed from the tubule lumen at a rate equal to the rate of H^+ secretion (Malnic, Costa Silva, Campiglia, de Mello Aires and Giebisch, 1980). Ullrich et al. (1971) have shown that glycodiazine supports normal isotonic fluid reabsorption in the proximal tubule in the absence of ambient CO_2 and HCO_3^-. Furthermore, renal glycodiazine transport displays many characteristics similar to those of H^+ transport such as Na^+-dependence, inhibitor sensitivity and adaptation to chronic alkalosis (Ullrich, Rumrich and Baumann, 1975). In the pancreas, glycodiazine partially stimulates fluid and solute secretion in the absence of exogenous CO_2 and HCO_3^- (Schulz, 1976, 1981; Schulz and Ullrich, 1979). Since the large glycodiazine molecule (M.W. 308) per se is unlikely to be transported on a membrane carrier, the experiments in the proximal tubule and pancreas have been taken as evidence for the existence of a H^+/OH^- transporter rather than a HCO_3^- carrier involved in transepithelial acid-base movements. For example, in the proximal tubule, reabsorption of HCO_3^- or the glycodiazine anion is dependent upon tubular H^+ secretion and buffer titration followed by passive diffusion of uncharged CO_2 and H_2CO_3 or glycodiazine molecules from lumen to serosa.

In the present study, no attempt was made to investigate glycodiazine transport per se primarily because of the difficulty of obtaining radioactively labelled forms of this compound. The effects of glycodiazine on Cl^- reabsorption and electrophysiology of the anterior salt gland, however, were examined. Figure 5.20 is reproduced in part from the previous chapter and shows that Cl^- reabsorption in the perfused anterior segment is completely inhibited by bilaterally replacing CO_2 and HCO_3^- with an impermeant phosphate or HEPES buffer. When the lipid soluble buffer glycodiazine is used as a CO_2 and HCO_3^- replacement, however, this compound

Figure 5.20 Effects of bilateral CO_2 and HCO_3^- replacement with either a phosphate, HEPES or glycodiazine buffered saline on the change in anterior segment perfusate Cl^- concentration. Values are means + S.E. (n = 5-12). This figure is reproduced in part from Chapter IV.

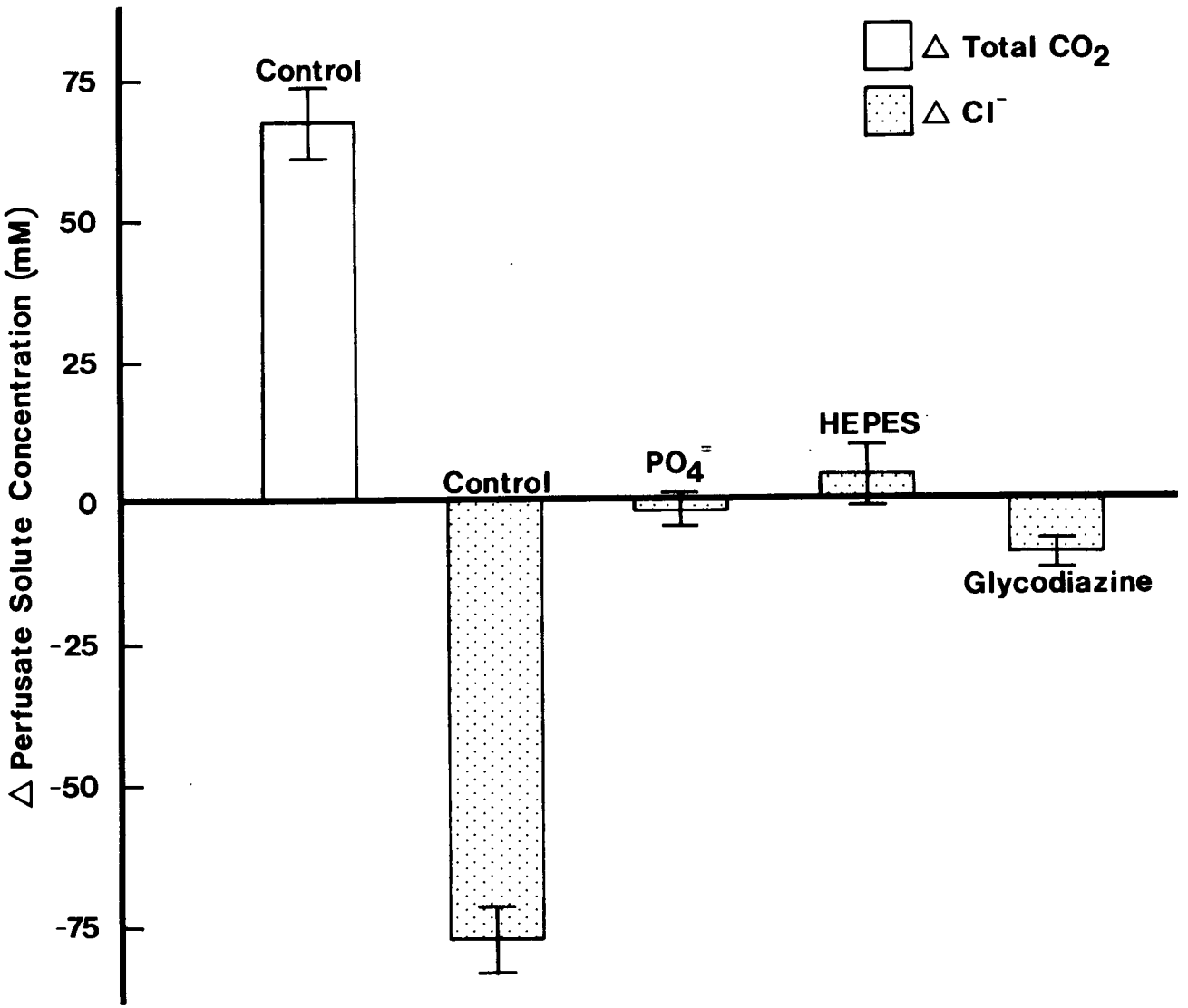
Δ Total CO_2
Δ Cl^-
Control
Control
$PO_4^=$
HEPES
Glycodiazine
75
50
25
0
-25
-50
-75
Δ Perfusate Solute Concentration (mM)

maintains a small and consistent component of Cl^- reabsorption. The change in perfusate Cl^- concentration with glycodiazine was -8.8 $\pm$ 2.8 mM (mean $\pm$ S.E., n = 5) and was significantly different ($0.01 < P < .025$) from zero. In addition, when CO_2 and HCO_3^- are removed from the serosal saline and replaced with glycodiazine, V_{te} rapidly depolarizes and reverses, and the small, positive V_{te} remains stable for at least 60 minutes (Fig. 5.8). When the impermeant HEPES buffer replaces serosal CO_2 and HCO_3^-, however, V_{te} initially depolarizes by 20-30 mV and is then followed by a slow repolarization phase until a new stable V_{te}, 10-15 mV lower than control values, is reached (Fig. 5.7). The nature of this repolarization is uncertain (see Results), but it could be due to changes in intracellular ion concentrations with subsequent changes in a Donnan or Cl^--diffusion potential.

In order for glycodiazine to support Cl^- reabsorption in the anterior salt gland it is necessary to propose the scheme shown in Figure 5.21. Shuttling of protons across the cell membrane would require that both the anionic and undissociated forms of glycodiazine be lipid soluble. Indeed, many weak acid anions are quite permeable to the cell membrane with the anionic form moving down a favorable electrochemical gradient created by the membrane potential and the intracellular dissociation of the uncharged acid (see for example McLaughlin and Dilger, 1980; Roos and Boron, 1981; Boron, 1983). Measurement of V_{bl} during rapid changes in serosal fluid composition suggests indirectly that the glycodiazine anion permeates the cell membrane. Glycodiazine added to the bath either in the presence (18.5 mM glycodiazine plus normal CO_2 and HCO_3^- concentrations; data not shown) or absence (Fig. 5.10) of CO_2 and HCO_3^- causes a small, transient 2-3 mV hyperpolarization of V_{bl}. Replacement of serosal CO_2 and HCO_3^- with the impermeant HEPES buffer, however, causes a small, transient

Figure 5.21 Tentative scheme showing proposed proton shuttling effects of glycodiazine buffer.

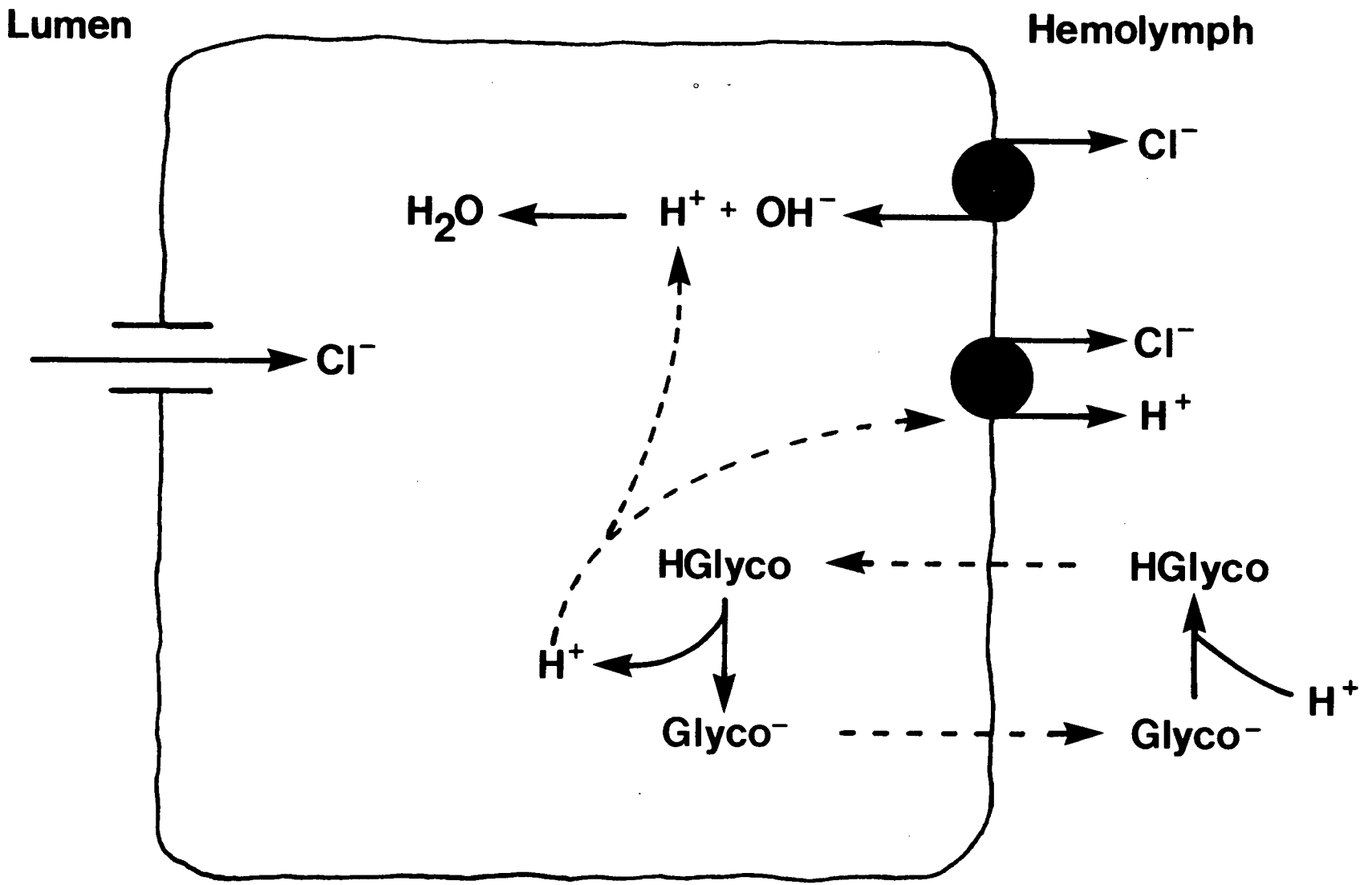
Lumen
Hemolymph
Cl⁻
H₂O
H⁺ + OH⁻
Cl⁻
Cl⁻
H⁺
HGlyco
HGlyco
H⁺
H⁺
Glyco⁻
Glyco⁻

depolarization of V_{bl} (Fig. 5.17) which is consistent with a very small outwardly directed HCO_3^- or inwardly directed H^+ permeability (note that removal of serosal CO_2 and HCO_3^- causes intracellular alkalinization; see Fig. 5.3; Roos and Boron, 1981).

The effects of glycodiazine on Cl^- reabsorption and V_{te} in the anterior segment are admittedly small, but nevertheless support the hypothesis that this compound maintains a component of electrogenic Cl^- reabsorption in the absence of exogenous CO_2 and HCO_3^-. It may be particularly instructive in future investigations to examine the effects of glycodiazine on $J_{net}^{Cl^-}$ and electrophysiology by varying the ratios of charged and uncharged species. In particular, a higher concentration of the undissociated glycodiazine molecule may be more effective in maintaining Cl^- reabsorption by generating a higher rate of proton shuttling.

2) Electrochemical Gradients

In the present study, cellular HCO_3^- concentration was calculated using the Henderson-Hasselbalch equation and by assuming that PCO_2, K_1', CO_2 solubility coefficients and HCO_3^- activity coefficients were the same inside the cell as in free solution. It is uncertain whether these assumptions actually hold <u>in vivo</u>. At present, however, calculation of HCO_3^- concentration provides the best means of estimating intracellular HCO_3^- activity. Given the above assumption it follows that

$$K_{1,o}' = \frac{[H^+]_o[HCO_3^-]_o}{[CO_2]_o} , \qquad (1)$$

$$K_{1,c}' = \frac{[H^+]_c[HCO_3^-]_c}{[CO_2]_c} , \qquad (2)$$

$$K_{1,o}'\,[CO_2]_o = [H^+]_o[HCO_3^-]_o , \qquad (3)$$

$$K_{1,c}' [CO_2]_c = [H^+]_c[HCO_3^-]_c \quad . \qquad (4)$$

Since it was assumed that $K_{1,o}' = K_{1,c}'$ and $[CO_2]_o = [CO_2]_c$ then

$$K_{1,o}' [CO_2]_o = K_{1,c}' [CO_2]_c \quad , \qquad (5)$$

$$[H^+]_o[HCO_3]_o = [H^+]_c[HCO_3^-]_c \quad , \qquad (6)$$

$$\frac{[H^+]_o}{[H^+]_c} = \frac{[HCO_3^-]_c}{[HCO_3^-]_o} \quad , \qquad (7)$$

and therefore $\Delta\tilde{\mu}_{H^+} = \Delta\tilde{\mu}_{HCO_3^-} \quad . \qquad (8)$

Table 5.3 shows the calculated $\Delta\tilde{\mu}_{HCO_3^-}$ for apical and basolateral cell membranes under control conditions. Bicarbonate entry into the cell or the equivalent process at the serosal membrane is against an unfavorable electrochemical gradient of 77.1 mV and therefore must be mediated by an active transport process. It is uncertain at present, however, whether the Cl^-/HCO_3^- exchanger is a primary, ATP-driven pump, or whether it is a secondary active transport process with the basolateral Cl^- electrochemical gradient of 71.7 mV (Table 5.2) energizing active, basolateral HCO_3^- entry. Even if the overestimation of $a^c_{Cl^-}$ which is inherent in microelectrode measurements is ignored, and it is assumed that there is 100% coupling efficiency between Cl^- and HCO_3^- movements, there still does not appear to be sufficient energy stored in the $\Delta\tilde{\mu}^{bl}_{Cl^-}$ to drive HCO_3^- into the cell.

Under control conditions HCO_3^- exit at the apical cell membrane is down a favorable electrochemical gradient of 27.6 mV (Table 5.3). These experiments alone do not demonstrate that apical HCO_3^- transport is normally a downhill process and further studies are needed to determine if $\Delta\tilde{\mu}^{a}_{HCO_3^-}$ favors passive HCO_3^- movement under a variety of experimental conditions.

It is instructive to point out that under conditions which are perhaps more physiological to the salt gland (i.e. the luminal membrane bathed by a strongly hyperosmotic NaCl or $NaHCO_3$-rich fluid; see Chapter II and IV), that it can clearly no longer be assumed that K_1', CO_2 solubility coefficients and HCO_3^- activity coefficients are equivalent in the luminal and intracellular fluids. Therefore, under these conditions $\Delta\tilde{\mu}_{H^+} \neq \Delta\tilde{\mu}_{HCO_3^-}$ and it would be necessary to determine the actual ionic species involved in HCO_3^- secretion before it could be determined that the apical step was active or passive. Data in Table 5.4 illustrate this problem. Measurement of anterior segment cell pH in rectal salt glands bathed by their own secretions or in anterior segments perfused with artificial secretions containing 400 mM HCO_3^- and 40 mM CO_3^{2-} (pH 8.75; Table 5.1) yielded calculated apical, electrochemical gradients which would favor passive H^+ entry into the cell or require the presence of a primary electrogenic HCO_3^- pump in the apical membrane. Since the unequivocal demonstration of H^+/OH^- versus HCO_3^- transport in an intact epithelium is difficult and always subject to question (see for example Al-Awqati, 1978; Malnic, 1980), it may be more fruitful in future investigations to attempt to voltage clamp the anterior segment at various values of V_{te}. Measurement of pH_c and net fluxes of HCO_3^-, CO_3^{2-} and H^+, and calculation of $\Delta\tilde{\mu}_{HCO_3^-}$ under conditions of altered V_{te} may provide a clearer picture than measurement of these parameters under conditions of altered transepithelial chemical gradients (i.e. anterior segments perfused with hyperosmotic NaCl or $NaHCO_3$-rich fluids).

Table 5.3 Calculated HCO_3^- electrochemical gradients for apical and basolateral cell membranes bathed by control serosal and mucosal salines. Net CO_2 flux is from bath to lumen. Negative signs indicate a favorable $\Delta\tilde{\mu}_{HCO_3^-}$ for passive HCO_3^- movement. The $\Delta\tilde{\mu}^{bl}_{HCO_3^-}$ was calculated using the mean V_{bl} of -75.6 mV (see Results). The activity coefficient for intracellular HCO_3^- was assumed to be the same as in the bathing and perfusion salines (i.e. 0.733). Values are means ± S.E. (n = 39 cells, 4 preparations). Note that given the assumptions used in calculating $[HCO_3^-]_c$ (see Discussion) that $\Delta\tilde{\mu}_{HCO_3^-} = \Delta\tilde{\mu}_{H^+}$.

pH_c	$[HCO_3]_c$	$a^c_{HCO_3^-}$	Va	$\Delta\tilde{\mu}^a_{HCO_3^-}$	$\Delta\tilde{\mu}^{bl}_{HCO_3^-}$
7.67 ± 0.03	19.6 ± 1.0 mM	14.4 ± 0.7 mM	-27.3 ± 0.5 mV	-27.6 ± 1.3 mV	77.1 mV

Table 5.4. Intracellular pH and calculated apical membrane electrochemical gradients for H^+ and HCO_3^-. Net HCO_3^- flux is from bath to lumen and net H^+ flux is from lumen to bath. Negative signs indicate a favorable electrochemical gradient for passive ion movement. Secretion pH and HCO_3^- concentration were assumed to be 8.65 and 402 mM, respectively (see Chapter II), for salt glands with luminal membranes bathed by their own secretions. Intracellular K_1', S and HCO_3^- activity coefficients were assumed to be the same as those in the bath. Values are means ± S.E. of 8-14 impalements on 2-3 preparations.

Experiment	pH_c	$[HCO_3^-]_c$	$a^c_{HCO_3^-}$	Va	$\Delta\tilde{\mu}^a_{HCO_3^-}$	$\Delta\tilde{\mu}^a_{H^+}$
Anterior segments perfused with artificial secretion.	7.99 ± 0.02	36.9 ± 1.7 mM	27.1 ± 1.2 mM	-51.2 ± 1.5 mV	8.3 ± 2.5 mV	-7.0 ± 2.5 mV
Rectal salt glands bathed on their luminal surface with their own secretions.	7.84 ± 0.04	29.4 ± 2.6 mM	21.6 ± 1.9 mM	-46.3 ± 1.0 mV	20.9 ± 2.9 mV	-0.6 ± 2.8 mV

In summary, Cl^- enters the apical cell membrane of the anterior salt gland, at least in part, by passive, electrodiffusive movement through a Cl^- selective pathway, and HCO_3^- exits the cell by an active or passive electrogenic transport mechanism. The basolateral cell membrane is the site of direct coupling between Cl^- and HCO_3^- movements via a Cl^-/HCO_3^- exchange or HCl cotransport mechanism. In the last chapter the results of this thesis are summarized and HCO_3^- transport in the anterior salt gland is compared to acid-base transport in vertebrate epithelia and invertebrate single cells.

CHAPTER VI - GENERAL DISCUSSION

Mechanisms of acid and base transport have been studied in a variety of vertebrate gastrointestinal and excretory epithelia, the choroid plexus, and in several types of invertebrate non-epithelial cells. This final chapter is devoted to a comparative discussion of these mechanisms and to a summary of the work in this thesis.

Hydrogen and HCO_3^- transport in gastrointestinal epithelia plays a number of important and specialized roles including providing the proper medium for digestion of foodstuffs, neutralization of gastric acids, protection of the mucosal surface from digestive juices and facilitation of the absorption of nutrients such as NH_3 and volatile fatty acids. In the duct epithelium of the mammalian salivary gland, HCO_3^- is actively secreted in concentrations in excess of 100 mM (reviewed by Young and van Lennep, 1979) and is probably important for maintaining optimal function of salivary digestive enzymes. Studies on the microperfused rat salivary duct have provided evidence for the presence of an apical, electroneutral K^+/H^+ exchange or $KHCO_3$ cotransport mechanism which mediates HCO_3^- secretion (Knauf and Lubcke, 1975; Knauf, Lubcke, Kreutz and Sachs, 1982). The apical K^+/H^+ exchanger has been postulated to be a secondarily active transport process which is coupled to the apical, downhill K^+ gradient maintained by a basolateral Na^+/K^+ ATPase (Knauf et al., 1982). Basolateral HCO_3^- entry into salivary duct cells is thought to be mediated by a passive HCO_3^- conductance and a Na^+/H^+ exchanger (Knauf et al., 1982). It is interesting to note that the labial gland of saturniid moths produces a $KHCO_3$-rich fluid during ecdysis of the adult moth from its cocoon (Kafatos, 1968). Secretion of HCO_3^- is necessary to maintain an alkaline pH for optimal function of the

cocoon-opening enzyme (Kafatos and Williams, 1964) and could conceivably be mediated by a K^+/H^+ exchange mechanism similar to that of the duct epithelium.

The vertebrate gastric mucosa has been one of the most extensively studied acid-base transporting organs and has been the subject of numerous recent review articles (see Sachs, Spenney and Lewin, 1978; Machen and Forte, 1979; Forte, Machen and Obrink, 1980; Sachs, Faller and Rabon, 1982; Diamond and Machen, 1983). It is now fairly well established that luminal acid secretion and generation of transepithelial H^+ gradients of up to 10^7:1 are mediated by a primary, electroneutral H^+/K^+ ATPase mechanism (reviewed by Sachs et al., 1978, 1982; Sachs, Rabon, Stewart, Pierce, Smolka and Saccomani, 1980). These results are, however, difficult to reconcile with experiments in dog stomach and frog gastric mucosa which suggest that H^+ secretion is electrogenic (reviewed by Machen and Forte, 1979; Forte et al., 1980). At present, it appears that the H^+ pump may be capable of operating in either an electrogenic or electroneutral mode depending on the experimental conditions employed.

The process of gastric H^+ secretion necessarily produces intracellular OH^-. This OH^- is neutralized by CO_2 in a carbonic anhydrase-dependent reaction to yield HCO_3^- which exits the basolateral membrane of the oxyntic cell via a Cl^-/HCO_3^- exchange mechanism (Rehm and Sanders, 1975).

Stimulation of gastric acid secretion by hormones is accompanied by spectacular changes in the ultrastructure of the oxyntic cells (see Diamond and Machen, 1983, for an excellent review). In the unstimulated cell, the secretory canaliculi are greatly reduced in volume, apical microvilli are scarce, and the cell cytoplasm is filled with an extensive system of

tubulovesicles. Upon stimulation of the oxyntic cell with a compound such as histamine, however, there is a pronounced expansion of the canaliculi and a dramatic increase in apical microvilli with a concomitant decrease in tubulovesicles. These ultrastructural changes may be associated with insertion of new ion transporters into the apical membrane in a manner similar to that proposed for the apical H^+ pumps of the turtle bladder (Gluck, Cannon and Al-Awqati, 1982; discussed below).

In addition to secreting H^+, the fundic and antral portions of the gastric mucosa are also capable of secreting HCO_3^-. Several studies have suggested that HCO_3^- secretion is an active, electroneutral process which is mediated by a Cl^-/HCO_3^- exchange mechanism located in the luminal membrane of surface cells (reviewed by Flemstrom and Garner, 1982). Gastric HCO_3^- secretion appears to be critically important in alkalinizing an apical mucous layer and unstirred boundary which serves to protect the mucosal epithelium from high intraluminal acidity (Flemstrom and Garner, 1981; see also Powell, 1981).

The mammalian pancreas produces an alkaline secretion containing HCO_3^- concentrations up to 130 mM. This alkaline secretion is necessary to neutralize the highly acidic digestive juice of the stomach before it enters the intestine and to maintain an optimal pH for function of pancreatic enzymes. Generally, it is believed that active HCO_3^- secretion occurs both in the acini and extralobular ducts of the pancreas (reviewed by Schulz and Ullrich, 1979). The actual cellular mechanism of HCO_3^- secretion is uncertain, however, because of the hetergeneous nature of the epithelium and the difficulties associated with isolating the various segments of the pancreas ductal system in vitro. Studies with weak organic acids such as sulfamerazine, glycodiazine, acetate, formate, proprionate and butyrate

(reviewed by Schulz, 1976, 1981; Schulz and Ullrich, 1979; see also Chapter V) suggest that the actual ionic species transported in HCO_3^- secretion is H^+/OH^-. This observation, plus studies on extralobular ducts which demonstrated that application of ouabain to or removal of Na^+ from the serosal bathing medium inhibits HCO_3^- secretion and alters intracellular pH (Swanson and Solomon, 1972, 1975), suggested the presence of Na^+/H^+ exchange in the pancreas. Swanson and Solomon (1975) postulated that apical proton reabsorption was mediated by a primary, ATP-driven Na^+/H^+ exchanger and that basolateral H^+ exit was effected by a Na^+/H^+ exchanger secondarily coupled to the downhill entry of Na^+ into the cell. Two other models have been proposed by Schulz and Ullrich (1979) based on the observed Na^+ dependence and ouabain sensitivity of HCO_3^- transport. These include: 1) a basolateral Na^+/H^+ exchange and a passive, conductive HCO_3^- exit step at the apical membrane similar to that postulated for the basolateral membrane of the rat proximal tubule (see Burckhardt and Fromter, 1980); 2) a secondarily active reabsorption of H^+ coupled to downhill K^+ exit with tight K^+ recycling at the apical membrane and a passive, conductive exit of H^+ at the basolateral cell border. Very little direct experimental evidence exists for any of these models and further studies using more sophisticated technical approaches are clearly needed.

The active secretion of HCO_3^- by the duodenal epithelium of the small intestine is necessary to neutralize gastric acid, protect the intestinal surface, and to provide an optimal alkaline pH for function of pancreatic enzymes. Early studies by Florey, Jennings, Jennings and O'Connor (1939) suggested that HCO_3^- secretion originated in the Brunners gland. Later investigations, however, have shown extensive luminal alkalinization in duodena from species lacking Brunners glands and in duodenal segments

proximal and distal to the Brunners glands in species such as dog, cat, human, guinea pig, rat and rabbit (reviewed by Flemstrom and Garner, 1982). These studies indicate that the surface epithelial cells are the sites of HCO_3^- secretion. Studies on the isolated bullfrog duodenum by Simson, Meshav and Silen (1981a,b) have shown that unstimulated HCO_3^- transport is electrogenic, sensitive to serosal ouabain and dependent upon the presence of Na^+ in the serosal bathing saline. Accordingly, the authors postulated a $NaHCO_3$ cotransport or Na^+/H^+ exchange mechanism to mediate HCO_3^- entry into the cell at the basolateral membrane and a passive, conductive efflux of HCO_3^- at the luminal cell border. Studies on duodenal epithelia exposed to glucagon, however, showed that stimulated HCO_3^- secretion was electroneutral and was inhibited by furosemide and luminal Cl^- removal suggesting the presence of a Cl^-/HCO_3^- exchange mechanism (Flemstrom, Heylings and Garner, 1982). In Amphiuma duodenum, HCO_3^- secretion requires the presence of serosal Na^+ and mucosal Cl^- (White and Imon, 1982) and is inhibited by serosal acetazolamide, ouabain and SITS (Imon and White, 1981). White and Imon (1982) postulate that HCO_3^- enters the cell at the basolateral cell membrane by parallel Na^+/H^+ and Cl^-/HCO_3^- exchangers and exits via an apical conductive pathway.

The vertebrate jejunum is capable of reabsorbing HCO_3^- and acidifying the luminal contents in vivo, however, few studies have examined the actual mechanisms of acidification. Early studies on the human jejunum suggested that HCO_3^- may be reabsorbed by an active, electrically silent Na^+/H^+ exchanger (Fordtran and Rector, 1968; Turnberg, Fordtran, Carter and Rector, 1970). More recently, Imon and White (1983) have provided evidence which indicates that active HCO_3^- reabsorption in Amphiuma jejunum is mediated by a K^+/H^+ exchange or $KHCO_3$ cotransport mechanism.

White and Imon (1983) have also shown that basolateral HCO_3^- exit in jejunal cells is facilitated by an anion exchanger which exchanges internal HCO_3^- for external Cl^-, Br^-, I^-, or SO_4^{2-} in a manner similar to that observed in the erythrocyte membrane (Knauf, 1979).

Although the mammalian ileum has been used extensively as a model for studies of Na^+ and Cl^- transport, relatively few investigations have examined the mechanisms of transepithelial H^+ and HCO_3^- movements. Studies by Hubel (1967, 1969); Turnberg, Bieberdorf, Morawski and Fordtran (1970); and Field, Fromm and McColl (1971) have shown that ileal HCO_3^- secretion is an active process requiring luminal Cl^-, thus suggesting the presence of a Cl^-/HCO_3^- exchanger in this tissue. Sheerin and Field (1975) have presented a very speculative model of ileal HCO_3^- transport which postulates a basolateral Na^+/H^+ exchanger mediating HCO_3^- entry at this membrane and an apical Cl^-/HCO_3^- exchange exit step. Further studies of H^+ and HCO_3^- transport are clearly needed in both the ileal and jejunal intestinal segments.

Secretion of HCO_3^- by the colonic epithelium has been shown to be an active, electroneutral process which is dependent upon the presence of Cl^- in the mucosal bathing saline. These results, plus experiments showing a close reciprocal relationship between net Cl^- and HCO_3^- movements in this tissue, are indicative of a luminal Cl^-/HCO_3^- exchange mechanism (reviewed by Powell, 1979; Schultz, 1981a). Recently, Duffey and Bebernitz (1983) have studied Cl^-/HCO_3^- exchange in rabbit colon using intracellular H^+ and Cl^--selective microelectrodes. Their results demonstrated that apical Cl^- entry was an active transport process that could feasibly be energized by the movement of HCO_3^- down a favorable luminal electrochemical gradient. Emmer and Duffey (1983) have shown that application of serosal

DIDS to the rabbit colon stimulates a HCO_3^-- dependent short-circuit current suggesting that this compound unmasks an electrogenic HCO_3^- secretory process.

Regulation of the acid-base balance of the cerebrospinal fluid (CSF) may be critically important in controlling the function of respiratory neurons which in turn would influence directly extracellular pH and HCO_3^- homeostasis. Unfortunately, relatively few studies have been conducted on the mechanisms of choroid plexus H^+ and HCO_3^- transport, primarily because of the difficulty of isolating and working with this tissue in vitro. Early studies by Siesjo and Kjallquist (1969) suggested that CSF pH was maintained by a passive process. More recently, however, Bledsoe, Eng and Hornbein (1981) have presented good evidence indicating that choroid plexus H^+ transport is mediated by an active mechanism. Based largely on indirect evidence, Wright (1972, 1977) postulated that HCO_3^- secretion in the choroid plexus was mediated by a passive, conductive HCO_3^- exit step at the apical membrane and that HCO_3^- entered the cell via a basolateral Na^+/H^+ exchanger. Saito and Wright (1982, 1983) have provided direct evidence in support of an apical HCO_3^- conductance in the choroid plexus and have shown that HCO_3^- secretion into the CSF may be controlled by hormones which stimulate the adenylate cyclase system.

As described in Chapter I, the gill epithelium of fishes is an important site of acid-base excretion and regulation. Numerous studies have provided strong evidence for the presence of Na^+/H^+, Na^+/NH_4^+ and Cl^-/HCO_3^- exchange mechanisms in the apical membranes of gills from freshwater-adapted fish (reviewed by Evans, 1975, 1980; Potts, 1977; Kirschner, 1979; Evans, Claiborne, Farmer, Mallery and Krasny, 1982). Because of the heterogeneous nature of the branchial epithelium and the

problems associated with *in vitro* gill preparations, however (see for example Karnaky, 1980; Evans *et al.*, 1982), more detailed characterizations of acid and base transport have not been possible. The use of techniques to isolate and possibly culture specific cell types in conjunction with studies on isolated apical and basolateral membrane vesicles from fish gills may be extremely useful in further studies of freshwater branchial H^+/OH^- and HCO_3^- transport steps. The use of the opercular epithelium could also be extremely valuable in investigations of acid-base transport. Opercular skins are composed of the four major cell types which form the salt-transporting epithelium of the gills (Karnaky and Kinter, 1977), and the opercular epithelium can be isolated and short-circuited as a flat sheet in conventional Ussing chambers making pH stat studies feasible. In addition, the use of ion and voltage-selective microelectrodes in the opercular epithelium may provide important insights into cellular entry and exit steps involved in transepithelial acid and base movements.

Exchanges of external Na^+ for internal H^+ or NH_4^+ are also important mechanisms of acid excretion in marine teleosts and elasmobranchs (reviewed by Evans, 1975, 1980, 1982). While this uptake of external Na^+ necessarily imposes an additional ionic load on marine fishes, it is believed to be overridden by the primary need of the animal to regulate its acid-base balance (Evans, 1982). The same techniques discussed above should also be useful in characterizing cellular mechanisms of acid-base transport in seawater teleosts and elasmobranchs.

The amphibian skin is an important site of acid-base excretion and homeostasis, as was discussed in Chapter I. In many respects, the mechanisms of H^+ transport in the *in vitro* frog skin appear to be very similar to that observed in the turtle and toad urinary bladder with an active, electrogenic

H^+ pump located at the apical cell membrane (see for example, Fleming, 1957; Ehrenfeld and Garcia-Romeu, 1977; reviewed by Steinmetz, 1974). In addition, a number of investigators, studying H^+ and HCO_3^- transport in the in vivo frog skin bathed externally by dilute solutions, have provided convincing evidence for the presence of apical Na^+/H^+ and Cl^-/HCO_3^- exchangers which mediate net acid and base excretion (reviewed by Kirschner, 1983).

The turtle urinary bladder has been studied both in its own right and as a model system for the mammalian collecting duct. Numerous studies have shown clearly that H^+ secretion is mediated by a primary, apical, electrogenic H^+ pump (reviewed by Steinmetz, 1974; Malnic and Steinmetz, 1976; Al-Awqati, 1978; Steinmetz and Anderson, 1982). The location of electrogenic H^+ secretion is generally believed to be confined to a small population of mitochondria-rich, carbonic anhydrase-containing cells which make up approximately 10-15% of the bladder epithelium (Schwartz, Rosen and Steinmetz, 1972; Husted, Mueller, Kessel and Steinmetz, 1981). It is interesting to note that direct confirmation of this hypothesis may be possible using the vibrating probe technique which was originally developed to localize ion currents in single cells (Jaffe and Nuccitelli, 1974). More recently, Foskett and Scheffey (1982) have applied this powerful method to the opercular epithelium of a seawater teleost and have provided the first unequivocal evidence that the chloride-cell is the site of active, electrogenic Cl^- secretion in this tissue.

The nature of the OH^-/HCO_3^- efflux or H^+ entry mechanism at the basolateral membrane of the turtle bladder is uncertain at present. Steinmetz and Anderson (1982) have suggested that HCO_3^- efflux may be mediated by a conductive pathway or via a Cl^-/HCO_3^- exchanger (see also

Ehrenspeck and Brodsky, 1976; Cohen, Mueller and Steinmetz, 1978; Fischer, Husted and Steinmetz, 1981).

Several investigations have provided good evidence indicating that H^+ secretion in the bladder is mediated by a H^+-ATPase. Dixon and Al-Awqati (1979) were able to induce ATP synthesis in turtle bladder cells by applying an adverse proton electrochemical gradient to the epithelium (see also Dixon and Al-Awqati, 1980). Further biochemical studies have shown clearly that an electrogenic H^+-ATPase is located in luminal microsomal membrane fractions obtained from the turtle bladder (see for example, Park, Campen, Darrel and Fanestil, 1981; Gluck, Kelly and Al-Awqati, 1982; Youmans, Worman and Brodsky, 1982, 1983; Gluck and Al-Awqati, 1983).

Recent studies have shown important correlations between H^+ secretion and the ultrastructure of the mitochondria-rich cells of the bladder epithelium. These acid secreting cells are characterized by prominent luminal microplicae and by an extensive population of subcellular vesicles located just below the apical plasma membrane. Husted et al. (1981) demonstrated that inhibition of H^+ secretion in the bladder reduced the number of cells having microplicae from 12.7% to 0.5% and suggested that the microplicae represented the active state of the H^+ secreting cell. Stetson and Steinmetz (1982) used ultrastructural morphometry to demonstrate that CO_2-mediated stimulation of H^+ secretion caused a dramatic increase in apical membrane surface area and a decrease in the volume fraction of subcellular vesicles. These studies suggested that the stimulation of H^+ secretion was partially dependent upon fusion of subcellular vesicles with luminal membranes. Gluck et al. (1982; see also Reeves, Gluck and Al-Awqati, 1983) have demonstrated more directly using fluorescence microscopy and intracellular dye techniques that these subcellular vesicles contain H^+

pumps and that vesicle-to-membrane fusion regulates urinary acidification by insertion of new pumps into the apical cell border. The fusion of intracellular vesicles containing specific ion transporters with cell membranes is an exciting discovery and may represent a ubiquitous means of regulating ion and fluid transport in cells and epithelia (see for example Wade, 1980; Karniele, Zarnowski, Hissin, Simpson, Salano, and Cushman, 1982; Lewis and de Moura, 1982; Spring and Ericson, 1982).

The turtle bladder is also capable of alkalinizing the final urine depending upon the acid-base status of the animal (see Cohen, 1980). Studies by Steinmetz and colleagues (Leslie, Schwartz and Steinmetz, 1973; Husted, Cohen and Steinmetz, 1979; Husted and Mahadeva, 1983) suggest that urinary alkalinization is mediated by an electroneutral Cl^-/HCO_3^- exchanger, whereas Brodsky's group (reviewed by Brodsky, Durham and Ehrenspeck, 1980; Satake, Durham and Brodsky, 1981) has postulated an electrogenic HCO_3^- secretory mechanism.

The mechanism of acid excretion in the nephron has been of major interest to renal physiologists since the early micropuncture studies of Montgomery and Pierce (1937) and Gottschalk, Lassiter and Mylle (1960) suggested that the proximal tubule was the major site of filtered HCO_3^- reabsorption. The measurement of intraluminal disequilibrium pH values and transepithelial PCO_2 gradients has provided good evidence indicating that urine acidifiation in the proximal tubule is mediated by H^+ secretion rather than reabsorption of HCO_3^- *per se* (reviewed by Al-Awqati, 1978; Malnic, 1980; Warnock and Rector, 1981). Numerous *in situ* and *in vitro* studies have demonstrated that the bulk of proximal tubule H^+ secretion is mediated by a luminal Na^+/H^+ exchanger as evidenced by the sensitivity of the acidification mechanism to mucosal amiloride and serosal ouabain, and to

its dependence on the presence of Na^+ in the perfusion saline (reviewed by Malnic and Giebisch, 1979; Warnock and Rector, 1979, 1981). In addition, studies on isolated renal membrane vesicles have shown clearly that an electroneutral Na^+/H^+ exchanger is located in the brush-border membrane (reviewed by Murer and Kinne, 1980; Aronson, 1981; Kinne and Kinne-Saffran, 1981).

Several studies have also demonstrated that there is a small component of proximal tubule H^+ secretion which is independent of Na^+ transport (Burg and Green, 1977; McKinney and Burg, 1977b; Chan and Giebisch, 1981). Two indirect studies have suggested that this component may be mediated by an active, electrogenic H^+ pump (Fromter and Gessner, 1975; Bichara, Paillard, Leviel, Prigent and Gardin, 1983). Further studies are needed, however, to confirm this hypothesis.

The mechanism by which HCO_3^- exits the basolateral cell membrane of the proximal tubule is unclear. Microelectrode studies in rat proximal tubule have indicated the presence of a significant basolateral HCO_3^- conductance (Burckhardt and Fromter, 1980). Studies in rabbit proximal tubule suggest that HCO_3^- exits by both a conductive pathway and an electroneutral Cl^-/HCO_3^- exchange (Sasaki and Berry, 1983; see also Biagi, Kubota, Sohtell and Giebisch, 1981). Extensive voltage and ion-selective microelectrode studies by Boron and Boulpaep (1983a,b) have provided a detailed cellular model of H^+ and HCO_3^- transport in Ambystoma proximal tubule. These investigators demonstrated that Na^+/H^+ exchangers were present on both the apical and basolateral cell membranes. In addition, their results indicated the presence of an electrogenic, Na^+-dependent, basolateral HCO_3^- efflux which could be considered as the simultaneous exit of 1 Na^+ and 2 HCO_3^- on a carrier mechanism, or

the electrodiffusive exit of an ion pair such as $NaCO_3^-$. Boron and Boulpaep (1983b) claim that the apical and basolateral Na^+/H^+ exchangers account for intracellular pH regulation and that the basolateral HCO_3^- efflux is the asymmetric component of the system necessary for net transepithelial acid transport. These investigators further claim that urine acidification is secondary to the need of the cell to regulate intracellular pH. It must be noted, however, that proximal tubule urine acidification has never been demonstrated in Ambystoma. As such, this model of acid excretion has been criticized by mammalian renal physiologists. In support of these criticisms, Ives, Yee and Warnock (1983) have provided indirect evidence using renal vesicle preparations which indicates that the Na^+/H^+ exchanger is confined to the luminal membrane of rabbit proximal tubule.

Mammalian collecting tubules are capable in either acidifying (McKinney and Burg, 1977a, 1978a; Lombard, Jacobson and Kokko, 1979; Richardson and Kunau, 1981; DuBose, 1982; Koeppen and Helman, 1982) or alkalinizing (McKinney and Burg, 1977a, 1978b) the final urine depending upon the acid-base status of the animal. The actual mechanisms of H^+ and HCO_3^- transport in the collecting tubule are quite complex and poorly understood at present. Koeppen and Helman (1982; see also Laski, Morgan and Kurtzman, 1983) have recently provided good evidence for an active, electrogenic H^+ secretory mechanism in the rabbit cortical collecting tubule. Studies on the mechanisms of collecting tubule HCO_3^- secretion have suggested very indirectly the presence of an electrogenic HCO_3^- transport and/or an electroneutral Cl^-/HCO_3^- exchange process (reviewed by Berry and Warnock, 1982).

It is interesting to note that the turtle urinary bladder performs many of the same functions as the collecting tubule and has been studied

extensively as a model of the distal nephron. The two major cell types of the turtle bladder, granular and mitochondria-rich cells, are morphologically similar to the principal and intercalated cells of the collecting tubule epithelium (Kaissling and Kriz, 1979). Recently, Al-Awqati (personal communication) has observed a population of intracellular vesicles in the collecting duct which stain with acridine orange in a manner similar to the H^+ pump-containing vesicles in the turtle bladder (Gluck et al., 1982). Thus, both epithelia may possess similar mechanisms for regulating urinary acidification.

As discussed in Chapter III, the only invertebrate epithelium in which H^+ and HCO_3^- transport has been studied is the crustacean gill. Good evidence indicates that acid and base excretion in the branchial epithelium is mediated by Na^+/H^+ and Cl^-/HCO_3^- exchange mechanisms (see Kirschner, Greenwald and Kerstetter, 1973; Ehrenfeld, 1974; Pequeux and Gilles, 1981), although further investigations have not been possible because of the problems associated with studying this tissue in vitro. Detailed cellular mechanisms of H^+ and HCO_3^- transport have, however, been studied in single, non-epithelial invertebrate cells. Indeed, investigations on the snail neuron, squid axon and barnacle muscle fiber have provided the bulk of our current understanding of intracellular pH regulation. Studies by Thomas' group and Boron and co-workers (reviewed by Thomas, 1980, 1982; Roos and Boron, 1981; Boron, 1983) have provided strong evidence for the presence of an acid extrusion mechanism in these cells which requires HCO_3^-, external Na^+ and internal Cl^-, and is blocked almost completely by SITS and other distilbene derivatives such as DIDS and DNDS. Accordingly, it has been postulated that the electroneutral fluxes of Na^+, HCO_3^-, Cl^- and possibly H^+ are all coupled on the same carrier.

Although vertebrate intracellular pH regulatory mechanisms have not been studied as extensively as those in invertebrate cells, it is worth noting that the mechanisms so far proposed only superficially resemble those seen in squid axons, snail neurons and barnacle muscle fibers. In sheep cardiac Purkinjie fibers, Vaughan-Jones (1979, 1982) has postulated a Na^+-independent, Cl^-/HCO_3^- exchange intracellular pH regulatory mechanism. Aickin and Thomas (1977) suggest that acid extrusion in the mouse soleus muscle fiber is mediated by parallel Na^+/H^+ and Cl^-/HCO_3^- exchangers. Clearly, further studies need to be focused on the mechanisms of vertebrate intracellular pH regulation.

One of the major objectives of the work in this thesis was to utilize the salt water mosquito larva, Aedes dorsalis, as a model system in which to study fundamental cellular mechanisms of epithelial H^+ and HCO_3^- transport. As such, this investigation has provided the first detailed study of acid-base regulation in an insect species and the first study of cellular mechanisms of H^+ and HCO_3^- transport in an invertebrate epithelium.

Aedes dorsalis is one of the only organisms capable of inhabiting salt lakes composed almost entirely of high concentrations of $NaHCO_3$ and Na_2CO_3 salts. Under these extreme alkaline conditions the rectal salt gland regulates extracellular HCO_3^- concentration and pH within narrow physiological limits by excreting HCO_3^- against remarkably large electrochemical gradients. In vitro microperfusion experiments have demonstrated clearly that active HCO_3^- secretion is located in the anterior segment of the perfused salt gland and is mediated by a 1:1 exchange of luminal Cl^- for serosal HCO_3^-. Studies with ion and voltage-selective microelectrodes and the anion exchange inhibitor, DIDS, have shown that the

Cl^-/HCO_3^- antiport mechanism is located at the basolateral cell membrane. Chloride entry into the anterior rectal cell at the apical membrane is mediated, at least in part, by passive, electrodiffusive movement of Cl^- through a Cl^--selective pathway or channel. The exit of HCO_3^- from the cell is facilitated by an active or passive, electrogenic HCO_3^- transport mechanism.

The cellular model for anterior segment HCO_3^- secretion shown in Figure 5.19 most closely resembles that proposed for the HCO_3^- secretory mechanism in Amphiuma duodenum (discussed above). White and Imon (1982) postulated a basolateral Cl^-/HCO_3^- exchanger and a passive, conductive HCO_3^- efflux at the apical membrane of the duodenal cells. As in the case for the rectal salt gland, Cl^- reabsorption in the duodenum is mediated by an apical, electrogenic Cl^- entry step. In the duodenum, however, this mechanism appears to be an active Cl^- pump rather than electrodiffusive Cl^- movement as shown for the anterior rectal salt gland in Chapter V.

While the rectal salt gland does not provide a useful model system for investigating some presumably less easily studied epithelium, it clearly provides an excellent tissue in which to study basic membrane physiological processes. The work in this thesis has revealed two important areas which warrant further investigation.

Luminal ion substitution studies in the anterior rectal salt gland have shown that the apical membrane potential is primarily a Cl^- conductance which is partially short-circuited by an electrogenic HCO_3^- transport mechanism. As such, the putative, apical Cl^- channel of the anterior segment is analogous to the Na^+ channel in the Na^+-selective luminal membranes of tight, Na^+ reabsorbing epithelia. Although extensive

studies have been conducted on cation-selective channels from nerve, muscle and epithelial cells, relatively little work has been done on anion-selective channels. White and Miller (reviewed by Miller, 1982) have studied single-channel currents at high time resolution in Torpedo electroplax Cl^- channels reconstituted into planar lipid membranes. These elegant studies have provided the first, and to date, only direct experimental evidence elucidating the molecular mechanisms of a Cl^- diffusion pathway.

Given the high Cl^- selectivity of the apical membrane of anterior rectal cells it is reasonable to suggest that there is a very high density of luminal Cl^- channels in this tissue. Using microsurgical techniques which I have developed during the course of this thesis work, it is possible to expose the apical membrane to the serosal bathing medium and to remove the luminal cuticle. As such, the mechanisms and control of the apical Cl^- channels can feasibly be studied using isolated cell membrane patch-clamp techniques (see Hamill, Marty, Neher, Sakmann and Sigworth, 1981).

An area which has been of major interest to epithelial physiologists in recent years is the nature of the mechanisms by which epithelial cells maintain intracellular homeostasis in the face of rapid, physiologically-induced variations of transepithelial ion and fluid transport. The processes by which cells control cytoplasmic composition have been termed intrinsic or homocellular regulatory mechanisms (Schultz, 1981b). Very little is known about these mechanisms at present and they represent an extremely important area of future epithelial research. One of the most obvious questions which arises from this thesis work is how do the rectal salt gland cells regulate intracellular acid-base balance while simultaneously effecting a large transcellular CO_2 flux and generating remarkable transepithelial HCO_3^- and CO_3^{2-} gradients? Are the

basolateral Cl^-/HCO_3^- exchange and apical, electrogenic HCO_3^- transporter involved in intracellular pH regulation, or does the cell possess additional ion transporters such as Na^+/H^+ exchangers for controlling acid-base balance? If these separate mechanisms exist, how are they controlled? Such questions are of obvious importance in all acid-base transporting epithelia, especially those which utilize electrogenic H^+ and HCO_3^- transport mechanisms. The homogeneous nature of the rectal salt gland epithelium, the large size of the salt gland cells and the ability to isolate this organ completely in vitro makes it an excellent system in which to answer these types of questions, particularly when compared to more structurally complex tissues such as the pancreas, gastric mucosa, turtle bladder and collecting tubule.

REFERENCES

Aickin, C.C. and Thomas, R.C. (1977). An investigation of the ionic mechanism of intracellular pH regulation in mouse soleus muscle fibers. J. Physiol. 273: 295-316.

Al-Awqati, Q. (1978). H^+ transport in urinary epithelia. Am. J. Physiol. 235: F77-F88.

Amman, D., Lanter, F., Steiner, R.A., Schulthess, P., Shijo, Y. and Simon, W. (1981). Neutral carrier based hydrogen ion selective microelectrode for extra- and intracellular studies. Analytical Chem. 53: 2267-2269.

Anstee, J.H. and Bowler, K. (1979). Ouabain-sensitivity of insect epithelial tissue. Comp. Biochem. Physiol. 62A: 763-769.

Aronson, D.S. (1981). Identifying secondary active solute transport in epithelia. Am. J. Physiol. 240: F1-F11.

Atkinson, D.E. and Camien, M.N. (1982). The role of urea synthesis in the removal of metabolic bicarbonate and regulation of blood pH. In "Current Topics in Cellular Regulation" (ed. B.L. Horecker and E.R. Stadtman)Vol. 21, pp. 261-302. New York: Academic Press.

Balagura-Baruch, S. (1971). Renal metabolism and transfer of ammonia. In "The Kidney" (ed. C. Roullier and A.F. Miller) Vol. 3, pp. 253-327. New York: Academic Press.

Baumgarten, C.M. and Fozzard, H.A. (1981). Intracellular chloride activity in mammalian ventricular muscle. Am. J. Physiol. 241: C121-C129.

Benos, D.J. (1982). Amiloride: a molecular probe of sodium transport in tissues and cells. Am. J. Physiol. 242: C131-C145.

Berry, C.A. and Warnock, D.G. (1982). Acidification in the in vitro perfused tubule. Kidney Int. 22: 507-518.

Biagi, B., Kubota, T., Sohtell, M. and Giebisch, G. (1981). Intracellular potentials in rabbit proximal tubules perfused in vitro. Am. J. Physiol. 240: F200-F210.

Bichara, M., Paillard, M., Leviel, F., Prigent, A. and Gardin, J.P. (1983). Na:H exchange and the primary H pump in the proximal tubule. Am. J. Physiol. 244: F165-F171.

Blinn, D.W. (1969). Autoecology of Ctenocladus (Chlorophyceae) in saline environments. Ph.D. thesis, Univ. British Columbia, Vancouver, B.C.

Bledsoe, S.W., Eng, D.Y. and Hornbein, T.F. (1981). Evidence of active regulation of cerebrospinal fluid acid-base balance. J. Appl. Physiol.: Respirat. Environ. Exercise Physiol. 51: 369-375.

Bonner, S., Mann, M.J., Guffanti, A.A. and Krulwich, T.A. (1982). Na^+/solute symport in membrane vesicles from Bacillus alcalophilus. Biochim. Biophys. Acta 679: 315-322.

Boron, W.F. (1983). Transport of H^+ and of ionic weak acids and bases. J. Memb. Biol. 72: 1-16.

Boron, W.F. and Boulpaep, E.L. (1982). Hydrogen and bicarbonate transport by salamander proximal tubule cells. In "Intracellular pH: Its Measurement, Regulation and Utilization in Cellular Functions" (ed. R. Nuccitelli and D.W. Deamer) pp. 253-267. New York: Alan R. Liss, Inc.

Boron, W.F. and Boulpaep, E.L. (1983a). Intracellular pH regulation in the renal proximal tubule of the salamander: Na-H exchange. J. Gen. Physiol. 81: 29-52.

Boron, W.F. and Boulpaep, W.L. (1983b). Intracellular pH regulation in the renal proximal tubule of the salamander: basolateral HCO_3^- transport. J. Gen. Physiol. 81: 53-94.

Boron, W.F. and Fong, P. (1983). Effect of carbonic anhydrase inhibitors on basolateral HCO_3^- transport in salamander proximal tubules. Kidney Intl. 23: 230.

Bradley, T.J. (1976). The mechanism of hyperosmotic urine formation in the recta of saline-water mosquito larvae. Ph.D. thesis, Univ. British Columbia, Vancouver, B.C.

Bradley, T.J. and Phillips, J.E. (1975). The secretion of hyperosmotic fluid by the rectum of a saline-water mosquito larva, Aedes taeniorhynchus. J. Exp. Biol. 63: 331-342.

Bradley, T.J. and Phillips, J.E. (1977a). Regulation of rectal secretion in saline-water mosquito larvae living in waters of diverse ionic composition. J. exp. Biol. 66: 83-96.

Bradley, T.J. and Phillips, J.E. (1977b). The effect of external salinity on drinking rate and rectal secretion in the larvae of the saline-water mosquito Aedes taeniorhynchus. J. exp. Biol. 66: 97-110.

Bradley, T.J. and Phillips, J.E. (1977c). The location and mechanism of hyperosmotic fluid secretion in the rectum of the saline-water mosquito larva Aedes taeniorhynchus. J. exp. Biol. 66: 111-126.

Brodsky, W.D., Durham, J.H. and Ehrenspeck, G. (1980). Bicarbonate and chloride transport in relation to the acidification or alkalinization of the urine. Ann. N.Y. Acad. Sci. 341: 210-224.

Brown, H.M. and Saunders, J.H. (1977). Cation and anion sequences in dark-adapted Balanus photoreceptors. J. Gen. Physiol. 70: 531-543.

Burckhardt, B-Ch. and Frömter, E. (1980). Bicarbonate transport across the peritubular membrane of rat kidney proximal tubule. In "Hydrogen Ion Transport in Epithelia" (ed. I. Schulz, G. Sachs, J.G. Forte and K.J. Ullrich) pp. 277-285. Amsterdam: Elsevier.

Burg, M.B. and Green, N. (1977). Bicarbonate transport by isolated perfused rabbit proximal convoluted tubules. Am. J. Physiol. 233: F307-F314.

Burton, R.F. (1976). Calcium metabolism and acid-base balance in Helix pomatia. In "Perspectives in Experimental Biology" (ed. S. Davies) Vol. 1, pp. 7-16. Oxford: Pergamon Press.

Cameron, J.N. (1978a). Regulation of blood pH in teleost fish. Respir. Physiol. 33: 129-144.

Cameron, J.N. (1978b). Effects of hypercapnia on blood acid-base status, NaCl fluxes, and trans-gill potential in freshwater blue crabs, Callinectes sapidus. J. Comp. Physiol. B. 123: 137-141.

Cameron, J.N. (1979). Effects of inhibitors on ion fluxes, trans-gill potential and pH regulation in freshwater blue crabs, Callinectes sapidus (Rathbun). J. Comp. Physiol. B. 133: 219-225.

Cameron, J.N. (1980). Body fluid pools, kidney function, and acid-base regulation in the freshwater catfish Ictalurus punctatus. J. Exp. Biol. 86: 171-185.

Cameron, J.N. and Batterton, C.V. (1978). Antennal gland function in the freshwater blue crab, Callinectes sapidus: water, electrolyte, acid-base and ammonia excretion. J. Comp. Physiol. B. 123: 143-148.

Cameron, J.N. and Kormanik, G.A. (1982). The acid-base responses of gills and kidneys to infused acid and base loads in the channel catfish, Ictalurus punctatus. J. Exp. Biol. 99: 143-160.

Chamberlin, M.E. (1981). Metabolic studies on locust rectum. Ph.D. thesis, University of British Columbia, Vancouver, B.C.

Chan, Y.L. and Giebisch, G. (1981). Relationship between sodium and bicarbonate transport in the rat proximal convoluted tubule. Am. J. Physiol. 240: F222-F230.

Cheema-Dhadli, S. and Halperin, M.L. (1978). Ammoniagenesis in kidney cortex mitochondria of the rat: Role of mitochondrial dicarboxylate anion transporter. Can. J. Biochem. 56: 23-28.

Cohen, J.J. and Kamm, D.K. (1976). Renal metabolism: relation to renal function. In "The Kidney" (ed. B. Brenner and F.C. Rector, Jr.) 1st ed., Vol. 1, pp. 126-214. Philadelphia: W.B. Saunders Co.

Cohen, L. (1980). HCO_3-Cl exchange transport in the adaptive response to alkalosis by turtle bladder. Am. J. Physiol. 239: F167-F170.

Cohen, L.H., Mueller, A. and Steinmetz, P.R. (1978). Inhibition of the bicarbonate exit step in urinary acidification by a disulfonic stilbene. J. Clin. Invest. 61: 981-986.

Cohen, R.D. and Iles, R.A. (1975). Intracellular pH: measurement, control and metabolic interrelationships. Crit. Rev. Clin. Lab. Sci. 6: 101-143.

Cogan, M.G., Rector, F.C. and Seldin, D.W. (1981). Acid-base disorders. In "The Kidney" (ed. B.M. Brenner and F.C. Rector, Jr.) 2nd ed., Vol. 1, pp. 841-907. Philadelphia: W.B. Saunders Co.

Collatz, K.-G., and Mommsen, T.P. (1974). Die strutktur der emulgierenden substanzen verschiedener invertebraten. J. Comp. Physiol. 94: 339-352.

Coulson, R.A. and Hernandez, T. (1959). Source and function of urinary ammonia in the alligator. Am. J. Physiol. 197: 873-879.

Coulson, R.A. and Hernandez, T. (1961). Renal failure in the alligator. Am. J. Physiol. 200: 893-897.

Craig, R. and Clark, J.R. (1938). The hydrogen ion concentration and buffer value of the blood of larvae of Pieris rapoe (L.) and Heliothis obsoleta (F.). J. Econ. Ent. 31: 51-54.

Dantzler, W.H. (1968). Effect of metabolic alkalosis and acidosis on tubular urate secretion in water snakes. Am. J. Physiol. 215: 747-751.

Dantzler, W.H. (1978). Urate excretion in nonmammalian vertebrates. In "Uric Acid. Handbook of Experimental Pharmacology" (ed. W.N. Kelley and I.M. Weiner) Vol. 51, pp. 185-210. Berlin: Springer-Verlag.

Diamond, J.M. and Machen, T.E. (1983). Impedance analysis in epithelia and the problem of gastric acid secretion. J. Memb. Biol. 72: 17-41.

Dietz, T.H. (1974). Active chloride transport across the skin of the earthworm Lumbricus terrestris. Comp. Biochem. Physiol. A. 49: 251-258.

Dietz, T.H. (1978). Sodium transport in the freshwater mussel, Carunculina texasensis (Lea). Am. J. Physiol. 4(1): R35-R40.

Dietz, T.H. and Alvarado, R.H. (1970). Osmotic and ionic regulation in Lumbricus terrestris L. Biol. Bull. 138: 247-261.

Dietz, T.H. and Alvarado, R.H. (1974). Na and Cl transport across gill chamber epithelium of Rana catesbeiana tadpoles. Am. J. Physiol. 226: 764-770.

Dietz, T.J. and Branton, W.D. (1975). Ionic regulation in the freshwater mussel, Ligumi subrostrata (Say). J. Comp. Physiol. 104B: 19-26.

Dixon, T.E. and Al-Awqati, Q. (1979). Urinary acidification in turtle bladder is due to a reversible proton-translocating ATPase. Proc. Natl. Acad. Sci. 76: 3135-3138.

Dixon, T.E. and Al-Awqati, Q. (1980). H^+/ATP stoichiometry of proton pump of turtle urinary bladder. J. Biol. Chem. 255: 3237-3239.

Dobyan, D.C. and Bulger, R.E. (1982). Renal carbonic anhydrase. Am. J. Physiol. 243: F311-F324.

DuBose, T.D. (1982). Hydrogen ion secretion by the collecting ducts as a determinant of the urine to blood pCO_2 gradient in alkaline urine. J. Clin. Invest. 69: 145-156.

Duffey, M.E. and Bebernitz, G. (1983). Intracellular chloride and hydrogen activities in rabbit colon. Fed. Proc. 42: 1353.

Dugal, L.-P. (1939). The use of calcareous shell to buffer the product of anaerobic glycolysis in Venus mercenaria. J. Cell. Comp. Physiol. 13: 235-251.

Ehrenfeld, J. (1974). Aspects of ionic transport mechanisms in crayfish Astacus leptodactylus. J. Exp. Biol. 61: 57-70.

Ehrenfeld, J. and Garcia-Romeu, F. (1977). Active hydrogen excretion and sodium absorption through isolated frog skin. Am. J. Physiol. 233: F46-F54.

Ehrenfeld, J. and Garcia-Romeu, F. (1978). Coupling between chloride absorption and base excretion in isolated skin of Rana esculenta. Am. J. Physiol. 235: F33-F39.

Ehrenspeck, G. and Brodsky, W.A. (1976). Effects of 4-acetamido-4'-isothiocyano-2,2'-disulfonic stilbene on ion transport in turtle bladders. Biochim. Biophys. Acta 419: 555-558.

Emilio, M.G., Machado, M.M. and Menano, H.P. (1970). The production of a hydrogen ion gradient across the isolated frog skin: quantitative aspects and the effect of acetazolamide. Biochim. Biophys. Acta 203: 394-409.

Emmer, E. and Duffey, M.E. (1983). Inhibition of active chloride absorption in rabbit colon by DIDS. Fed. Proc. 42: 1280.

Evans, D.H. (1975). Ionic exchange mechanisms in fish gills. Comp. Biochem. Physiol. 51A: 491-495.

Evans, D.H. (1980). Kinetic studies of ion transport by fish gill epithelium. Am. J. Physiol. 238: R224-R230.

Evans, D.H. (1982). Mechanisms of acid extrusion by two marine fishes: the teleost, Opsanus beta, and the elasmobranch, Squalus acanthias. J. Exp. Biol. 97: 289-299.

Evans, D.H., Claiborne, J.B., Farmer, L., Mallery, C. and Krasny, E.J. (1982). Fish gill ionic transport: methods and models. Biol. Bull. 163: 108-130.

Ewer, R.F. (1942). On the function of haemoglobin in Chironomus. J. Exp. Biol. 18: 197-205.

Fanelli, G.M. and Goldstein, L. (1964). Ammonia excretion in the neotenous newt, Necturus maculosus (Rafinesque). Comp. Biochem. Physiol. 13: 193-204.

Field, M., Fromm, D. and McColl, I. (1971). Ion transport in rabbit ileal mucosa. I. Na and Cl fluxes and short-circuit current. Am. J. Physiol. 220: 1388-1396.

Fischer, J.L., Husted, R.F. and Steinmetz, P.R. (1981). Role of basolateral anion exchange in urinary acidification of the turtle bladder. Clin. Res. 29: 687A.

Fitzgerrel, W.H. and Vanatta, J.C. (1980). Factors affecting bicarbonate excretion in the urinary bladder of Bufo marinus. Comp. Biochem. Physiol. 66A: 277-281.

Flagg, J.L. and Wilson, T.H. (1977). A protonmotive force as the source of energy for galactoside transport in energy depleted Escherichia coli. J. Memb. Biol. 31: 233-255.

Fleming, W.R. (1957). On the role of hydrogen ion and potassium ion and the active transport of sodium across the isolated frog skin. J. Cell. Comp. Physiol. 49: 129-152.

Flemström, G. and Garner, A. (1982). Gastroduodenal HCO_3^- transport: characteristics and proposed role in acidity regulation and mucosal protection. Am. J. Physiol. 242: G183-G193.

Flemström, G., Heylings, J.R. and Garner, A. (1982). Gastric and duodenal HCO_3^- transport in vitro: effects of hormones and local transmitters. Am. J. Physiol. 242: G100-G110.

Florey, H.W., Jennings, M.A., Jennings, D.A. and Castro, R. (1939). The reactions of the intestine of the pig to gastric juice. J. Pathol. Bacteriol. 49: 105-123.

Florkin, M. and Jeuniaux, Ch. (1964). Hemolymph: composition. In "The Physiology of Insecta" (ed. M. Rockstein) Vol. 3, pp. 109-152. New York: Academic Press.

Fordtran, J.S., Rector, F.C. and Carter, N.W. (1968). The mechanism of sodium absorption in the human small intestine. J. Clin. Invest. 47: 884-900.

Forte, J.G., Machen, T.E. and Obrink, K.J. (1980). Mechanisms of gastric H^+ and Cl^- transport. Ann. Rev. Physiol. 42: 111-1126.

Foskett, J.K. and Scheffey, C. (1982). The chloride cell: definitive identification as the salt-secretory cell in teleosts. Science 215: 164-166.

Frazier, L.W. and Vanatta, J.C. (1971). Excretion of H^+ and NH_4^+ by the urinary bladder of the acidotic toad and the effect of short-circuit current on the excretion. Biochim. Biophys. Acta. 241: 20-29.

Frazier, L.W. and Vanatta, J.C. (1972). Mechanism of acidification of the mucosal fluid by the toad urinary bladder. Biochim. Biophys. Acta. 290: 168-177.

Frazier, L.W. and Vanatta, J.C. (1973). Characteristics of H^+ and NH_4^+ excretion by the urinary bladder of the toad. Biochim. Biophys. Acta. 311: 98-108.

Frazier, L.W. and Vanatta, J.C. (1980). Evidence that catecholamines mediate H^+ and NH_4^+ excretion in toad urinary bladder. Fed. Proc. 39: 739.

Frazier, L.W. and Zachariah, N.Y. (1979). Action of steroids on H^+ and NH_4^+ excretion in the toad urinary bladder. J. Memb. Biol. 49: 297-308.

Frömter, E. and Gessner, K. (1975). Effect of inhibitors and diuretics on electrical potential differences in rat kidney proximal tubules. Pflügers Arch. 357: 209-224.

Frömter, E. and Sato, K. (1976). Electrical events in active H^+/HCO_3^- transport across rat kidney proximal tubular epithelium. In "Gastric Hydrogen Ion Secretion" (ed. D.K. Kasbekar, G. Sachs, W.S. Rehm) Vol. 3, pp. 382-403. New York: Marcel Dekker Inc.

Fujimoto, M. and Kubota, T. (1976). Physiochemical properties of a liquid ion exchanger microelectrode and its application to biological fluid. Jap. J. Physiol. 26: 631-650.

Garcia-Romeu, F. (1971). Anionic and cationic exchange mechanisms in the skin of anurans with special reference to Leptodactylidae in vivo. Phil. Trans. Roy. Soc. B. 262: 163-174.

Garcia-Romeu, F., Salibian, A. and Pezzani-Hernandez, S. (1969). The nature of the in vivo sodium and chloride uptake mechanisms through the epithelium of the Chilean frog Calyptocephalella gayi (Dum. et Bibr., 1841): exchanges of hydrogen against sodium and of bicarbonate against chloride. J. Gen. Physiol. 53: 816-835.

Gluck, S. and Al-Awqati, Q. (1983). Renal H^+ ATPase is an F_0F_1 ATPase different from lysosomal, motochondrial and chromaffin granule pumps. Fed. Proc. 42: 1352.

Gluck, S., Cannon, C. and Al-Awqati, Q. (1982). Exocytosis regulates urinary acidification in turtle bladder by rapid insertion of H^+ pumps into the luminal membrane. Proc. Natl. Acad. Sci. U.S.A. 79: 4327-4331.

Gluck, S., Kelly, S. and Al-Awqati, Q. (1982). The proton translocating ATPase responsible for urinary acidification. J. Biol. Chem. 257: 9230-9233.

Gottschalk, C.W., Lassiter, W.E. and Mylle, M. (1960). Localization of urine acidification in the mammalian kidney. Am. J. Physiol. 198: 581-585.

Green, B. (1969). Water and electrolyte balance in the sand goanna Varanus gouldi (Gray). Ph.D. thesis, University of Adelaide, Australia.

Haines, T.H. (1983). Anionic lipid headgroups as a proton-conducting pathway along the surface of membranes: a hypothesis. Proc. Natl. Acad. Sci. USA 80: 160-164.

Hamill, O.P., Marty, A., Neher, E., Sakmann, B. and Sigworth, F. (1981). Improved patch-clamp techniques for high resolution current rcording from cells and cell-free membrane patches. Pflügers Arch. 391: 85-100.

Hanrahan, J.W. (1982). Cellular mechanism and regulation of KCl transport across an insect epithelium. Ph.D. thesis, University of British Columbia, Vancouver, B.C.

Hastings, E. and Pepper, J.N. (1943). Studies on body fluids of seven orthopterans, their pH, buffering capacity, and effect on solubility of fractionated insecticides. J. Econ. Ent. 36: 857-864.

Hastings, A.B. and Sendroy, J. (1925). The effect of variation in ionic strength on the apparent first and second dissociation constants of carbonic acid. J. Biol. Chem. 65: 445-455.

Heisler, N. (1980). Regulation of acid-base status in fishes. In "Environmental Physiology of Fishes" (ed. M.A. Ali) pp. 123-162. New York: Plenum Press.

Heisler, N. (1982). Transepithelial ion transfer processes as mechanisms for fish acid-base regulation in hypercapnia and lactacidosis. Can. J. Zool. 60: 1108-1122.

Hems, D.A. (1975). Biochemical aspects of renal ammonia formation in metabolic acidosis. Enzyme 20: 1-21.

Henry, R.P., Kormanick, G.A., Smatresk, N.J. and Cameron, J.W. (1981). The role of $CaCO_3$ dissolution as a source of HCO_3^- for the buffering of hypercapnic acidosis in aquatic and terrestrial decapod crustaceans. J. Exp. Biol. 94: 269-274.

Hochachka, P.W. and Somero, G.N. (1973). "Strategies of Biochemical Adaptation." Philadelphia: W.B. Saunders Co.

House, D.G. (1974). Modification of the urine by the cloaca of the desert iguana, Dipsosaurus dorsalis. M.Sc. thesis, University of Wisconsin, Milwaukee.

Hubel, K.A. (1967). Bicarbonate secretion in rat ileum and its dependence on intraluminal chloride. Am. J. Physiol. 213: 1409-1413.

Hubel, K.A. (1969). Effect of luminal chloride concentration on bicarbonate secretion in rat ileum. Am. J. Physiol. 217: 40-45.

Huf, E.G., Parrish, J. and Weatherford, C. (1951). Active salt and water uptake by isolated frog skin. Am. J. Physiol. 164: 137-142.

Husted, R.F. and Mahadeva, V. (1983). Chloride absorption by turtle urinary bladder: effects of luminal pH and luminal HCO_3. Fed. Proc. 42: 1352.

Husted, R.F., Cohen, L.H. and Steinmetz, P.R. (1979). Pathways for bicarbonate transfer across the serosal membrane of turtle urinary bladder: studies with a disulfonic stilbene. J. Memb. Biol. 47: 27-37.

Husted, R.F., Mueller, A.L., Kessel, R.G. and Steinmetz, P.R. (1981). Surface characteristics of carbonic-anhydrase-rich cells in turtle urinary bladder. Kidney Intl. 19: 491-502.

Imon, M.A. and White, J.F. (1981). Intestinal HCO_3^- secretion in Amphiuma measured by pH stat in vitro: relationship with metabolism and transport of sodium and chloride ions. J. Physiol. 314: 429-443.

Imon, M.A. and White, J.F. (1983). Evidence for a relation between HCO_3^- absorption and K^+ uptake from the luminal medium in Amphiuma jejunum. Fed. Proc. 42: 1281.

Ives, H.E., Yee, V.J. and Warnock, D.G. (1983). Na^+/H^+ antiporter of the rabbit proximal tubule is confined to the luminal membrane. Kidney Intl. 23: 233.

Jackson, D.C. and Ultsch, G.R. (1982). Long-term submergence at 3°C of the turtle Crysemys picta belli, in normoxic and severely hypoxic water: II. Extracellular ionic responses to extreme lactic acidosis. J. Exp. Biol. 96: 29-43.

Jaffe, L.F. and Nuccitelli, R. (1974). An ultrasensitive vibrating probe for measuring steady extracellular currents. J. Cell. Biol. 63: 614-628.

Johansen, K., Maloiy, G.M.C. and Lykkeboe, G. (1975). A fish in extreme alkalinity. Resp. Physiol. 24: 159-162.

Kafatos, F.C. (1968). The labial gland: a salt-secreting organ of saturniid moths. J. Exp. Biol. 48: 435-453.

Kafatos, F.C. and Williams, C.M. (1964). Enzymatic mechanism for the escape of certain moths from their cocoons. Science 146: 538-540.

Kaissling, B. and Kriz, W. (1979). Structural analysis of the rabbit kidney. Adv. Anat. Embryol. Cell Biol. 56: 1-121.

Karlmark, B. and Sohtell, M. (1973). The determination of bicarbonate in nanoliter samples. Anal. Biochem. 53: 1-11.

Karnaky, K.J. (1980). Ion-secreting epithelia: chloride cells in the head region of Fundulus heteroclitus. Am. J. Physiol. 238: R185-R198.

Karnaky, K.J. and Kinter, W.B. (1977). Killifish opercular skin: a flat epithelium with a high density of chloride cells. J. Exp. Zool. 199: 355-364.

Karniele, E., Zarnowski, M.J., Hissin, P.J., Simpson, I.A., Salano, L.B. and Cushman, S.W. (1981). Insulin-stimulated translocation of glucose transport system in rat adipose cell. J. Biol. Chem. 256: 4772-4777.

Keilin, D. and Wang, Y.L. (1946). Haemoglobin of Gastrophilus larvae: purification and properties. Biochem. J. 40: 855-866.

Khuri, R.N., Agulian, S.K. and Harik, S.I. (1968). Internal capillary glass microelectrodes with a glass seal for pH, sodium and potassium. Pflügers Arch. 301: 182-186.

Kielland, J. (1937). Individual activity coefficients of ions in aqueous solutions. J. Am. Chem. Soc. 59: 1675-1678.

Kinne, R. and Kinne-Saffran, E. (1981). Membrane vesicles as tools to elucidate epithelial cell function. European J. Cell Biol. 25: 346-352.

Kirschner, L.B. (1979). Control mechanisms in crustaceans and fishes. In "Mechanisms of Osmoregulation in Animals" (ed. R. Gilles) pp. 157-222. New York: John Wiley & Sons.

Kirschner, L.B. (1983). Sodium chloride absorption across the body surface: frog skins and other epithelia. Am. J. Physiol. 244: R429-R443.

Kirschner, L.B., Greenwald, L. and Kerstetter, T.H. (1973). Effect of amiloride on sodium transport across body surfaces of freshwater animals. Am. J. Physiol. 224: 832-837.

Klahr, S. and Schoolwerth, A.C. (1977). Production and excretion of ammonia in health and disease. In "Pathophysiology of the Kidney" (ed. N.A. Kurtzman and M. Martinez-Maldonado) pp. 296-334. Springfield: Thomas.

Knauf, H. and Lubcke, R. (1975). Evidence for Na^+ independent active secretion of K^+ and HCO_3^- by rat salivary duct epithelium. Pflügers Arch. 361: 55-59.

Knauf, H., Lubcke, R., Kreutz, W. and Sachs, G. (1982). Interrelationships of ion transport in rat submaxillary duct epithelium. Am. J. Physiol. 242: F132-F139.

Knauf, P.A. (1979). Erythrocyte anion exchange and the band 3 protein: transport kinetics and molecular structure. In "Current Topics in Membranes and Transport" (ed. F. Bronner and Z. Kleinzeller) Vol. 12, pp. 249-363. New York: Academic Press.

Koeppen, B.M. and Helman, S.I. (1982). Acidifiation of luminal fluid by the rabbit cortical collecting tubule perfused *in vitro*. Am. J. Physiol. 242: F521-F531.

Konings, W.N. and Boonstra, J. (1977). Anaerobic electron transfer and active transport in bacteria. In "Current Topics in Membranes and Transport" (ed. A. Kleinzeller and F. Bronner) Vol. 9, pp. 177-231. New York: Academic Press.

Kormanik, G.A. and Cameron, J.N. (1981). Ammonia excretion in animals that breathe water: a review. Mar. Biol. Letters 2: 11-23.

Krebs, H.A. and Vinay, P. (1975). Regulation of renal ammonia production. Med. Clin. North Am. 59: 595-603.

Krimm, S. and Dwivedi, A.M. (1982). Infrared spectrum of the purple membrane: Clue to a proton conduction mechanism? Science 216: 407-408.

Krogh, A. (1939). "Osmotic Regulation in Aquatic Animals" New York: Cambridge University Press.

Krulwich, T.A. (1982). Bioenergetic problems of alkalophilic bacteria. In "Membranes and Transport" (ed. A.N. Martonosi) Vol. 2, pp. 75-79. New York: Plenum.

Langworthy, T.A. (1982). Lipids of bacteria living in extreme environments. In "Current Topics in Membranes and Transport" (ed. A. Kleinzeller and F. Bronner). Vol. 17, pp. 45-77. New York: Academic Press.

Laski, M.E., Morgan, V.E. and Kurtzman, N.A. (1983). Evidence for voltage dependent acidification in the cortical collecting tubule (CCT) of the rabbit. Kidney Intl. 23: 235.

Leaf, A. (1982). From toad bladder to kidney. Am. J. Physiol. 242: F103-F111.

Leslie, B.R., Schwartz, J.H. and Steinmetz, P.R. (1973). Coupling between Cl^- absorption and HCO_3^- secretion in turtle urinary bladder. Am. J. Physiol. 225: 610-617.

Levenbook, L. (1950a). The physiology of carbon dioxide transport in insect blood. Part I. The form of carbon dioxide present in *Gastrophilus* larva blood. J. exp. Biol. 27: 158-174.

Levenbook, L. (1950b). The physiology of carbon dioxide transport in insect blood. Part III. The buffer capacity of *Gastrophilus* blood. J. exp. Biol. 27: 184-191.

Lewis, R.J., Prince, R.C., Dutton, P.L., Knaff, D.B. and Krulwich, T.A. (1981). The respiratory chain of *Bacillus alcalophilus* and its nonalkalophilic mutant derivative. J. Biol. Chem. 256: 10543-10549.

Lewis, S.A. (1971). Charge properties and ion selectivity of the rectal intima of the desert locust. M.Sc. thesis, University of British Columbia, Vancouver, B.C.

Lewis, S.A. and de Moure, J.L.C. (1982). Incorporation of cytoplasmic vesicles into apical membrane of mammalian urinary bladder epithelium. Nature 297: 685-688.

Lombard, W.E., Jacobson, H.R. and Kokko, J.P. (1979). Collecting duct bicarbonate transport: comparison of cortical and medulllary segments. Kid. Intl. 16: 827.

Long, S. (1982). Acid-base balance and urinary acidification in birds. Comp. Biochem. Physiol. 71A: 519-526.

Long, S. and Giebisch, G. (1979). Comparative physiology of renal tubular transport mechanisms. Yale J. Biol. Med. 52: 525-544.

Ludens, J.H. and Fanestil, D.D. (1972). Acidification of urine by the isolated urinary bladder of the toad. Am. J. Physiol. 223: 1338-1344.

Lykkeboe, G., Johansen, K. and Maloiy, G.M.C. (1975). Functional properties of hemoglobins in the teleost Tilapia grahami. J. Comp. Physiol. 104: 1-11.

Machen, T.E. and Forte, J.G. (1979). Gastric secretion. In "Membrane Transport in Biology" (ed. G. Giebisch, D.C. Tosteson and H.H. Ussing) Vol. IV B, pp. 693-747. Berlin: Springer-Verlag.

Maddrell, S.H.P. (1977). Insect Malpighian tubules. In "Transport of Ions and Water in Animals" (ed. B.L. Gupta, R.B. Moreton, J.L. Oschman and B.J. Wall) pp. 541-569. London: Academic Press.

Maddrell, S.H.P. and Phillips, J.E. (1975). Active transport of sulphate ions by the Malphigian tubules of larvae of the mosquito Aedes campestris. J. Exp. Biol. 62: 367-378.

Maddrell, S.H.P. and Phillips, J.E. (1978). Induction of sulphate transport and hormonal control of fluid secretion by Malpighian tubules of larvae of the mosquito Aedes taeniorhynchus. J. Exp. Biol. 72: 181-202.

Maetz, J. and DeRenzis, G. (1978). Aspects of the adaptation of fish to high external alkalinity: Comparison of Tilapia grahami and T. mossambica. In "Comparative Physiology - Water, Ions and Fluid Mechanics" (ed. K. Schmidt-Nielsen, L. Bolis and S.H.P. Maddrell) pp. 213-228. Cambridge: Cambridge Univ. Press.

Maetz, J., Pagan, P. and DeRenzis, G. (1976). Controversial aspects of ionic uptake in freshwater animals. In "Perspectives in Experimental Biology" (ed. P.S. Davies) Zoology, Vol. 1, pp. 77-92.

Mangum, C.P., Silverthorn, S.U., Harris, J.L., Towle, D.W. and Kroll, A.R. (1976). The relationship between blood pH, ammonia excretion and adaptation to low salinity in the blue crab Callinectes sapidus. J. Exp. Zool. 195: 129-136.

Malnic, G. (1980). CO_2 equilibria in renal tissue. Am. J. Physiol. 239: F307-F318.

Malnic, G. (1981). Cellular mechanisms of urinary acidification. Mineral Electrolyte Metab. 5: 66-82.

Malnic, G. and Giebisch. (1979). Cellular aspects of renal tubular acidification. In "Membrane Transport in Biology" (ed. G. Giebisch, D.C. Tosteson and H.H. Ussing) Vol. IV A, pp. 299-355.

Malnic, G. and Steinmetz, P.R. (1976). Transport processes in urinary acidification. Kidney Intl. 9: 172-188.

Malnic, G., Costa, V.L., Campiglia, S.S., de Mello Aires, M. and Giebisch, G. (1980). Tubular permeability to buffer components as a determinant of net H^+ ion fluxes. In "Current Topics in Membranes and Transport. Vol. 13: Cellular Mechanisms of Renal Tubular Ion Transport." (ed. E.L. Boulpaep) pp. 257-264. New York: Academic Press.

Maloiy, G.M.C., Lykkeboe, G., Johansen, K. and Bamford, O.S. (1978). Osmoregulation in Tilapia grahami: A fish in extreme alkalinity. In "Comparative Physiology - Water, Ions and Fluid Mechanics" (ed. K. Schmidt-Nielsen, L. Bolis and S.H.P. Maddrell) pp. 229-238. Cambridge: Cambridge Univ. Press.

Maren, T.H. (1967). Carbonic anhydrase: chemistry, physiology and inhibition. Physiol. Rev. 47: 595-781.

McGee, L.C. and Hastings, A.B. (1942). The carbon dioxide tension and acid-base balance of jejunal secretions in man. J. Biol. Chem. 142: 893-904.

McKinney, T.D. and Burg, M.B. (1977a). Bicarbonate transport by rabbit cortical collecting tubules: effect of acid and alkali loads in vivo on transport in vitro. J. Clin. Invest. 60: 766-768.

McKinney, T.D. and Burg, M.B. (1977b). Bicarbonate and fluid absorption by renal proximal straight tubules. Kidney Intl. 12: 1-8.

McKinney, T.D. and Burg, M.B. (1978a). Bicarbonate absorption by rabbit cortical collecting tubules in vitro. Am. J. Physiol. 234: F141-F145.

McKinney, T.D. and Burg, M.B. (1978b). Bicarbonate secretion by rabbit cortical collecting tubules in vitro. J. Clin. Invest. 61: 1421-1427.

McLaughlin, S.G.A. and Dilger, J.P. (1980). Transport of protons across membranes by weak acids. Physiol. Rev. 60: 825-863.

Meredith, J. and Phillips, J.E. (1973a). Ultrastructure of the anal papillae of a salt-water mosquito larva, Aedes campestris. J. Insect Physiol. 19: 1157-1172.

Meredith, J. and Phillips, J.E. (1973b). Ultrastructure of anal papillae from a seawater mosquito larva (Aedes togoi Theobald). Can. J. Zool. 51: 349-353.

Meredith, J. and Phillips, J.E. (1973c). Rectal ultrastructure in salt- and freshwater mosquito larvae in relation to physiological state. Z. Zellforsch. 138: 1-22.

Miller, C. (1982). Open-state substructure of single chloride channels from Torpedo electroplax. Phil. Trans. R. Soc. Lond. B 299: 401-411.

Minnich, J.E. (1972). Excretion of urate salts by reptiles. Comp. Biochem. Physiol. 41A: 535-549.

Minnich, J.E. (1979). Reptiles. In "Comparative Physiology of Osmoregulation in Animals" (ed. G.M.O. Maloiy) Vol. 1, pp. 391-641. London: Academic Press.

Mommsen, T.P. (1978a). Digestive enzymes of a spider (Tegenaria atrica Koch) - I. General remarks, digestion of proteins. Comp. Biochem. Physiol. 60A: 365-370.

Mommsen, T.P. (1978b). Digestive enzymes of a spider (Tegenaria atrica Koch) - II. Carbohydrases. Comp. Biochem. Physiol. 60A: 371-375.

Mommsen, T.P. (1978c). Digestive enzymes of a spider (Tegenaria atrica Koch). III. Esterases, phosphatases, nucleases. Comp. Biochem. Physiol. 60A: 377-382.

Mommsen, T.P. (1980). Chitinase and β-N-acetylglucosaminidase from the digestive fluid of the spider, Cupiennius salei. Biochim. Biophys. Acta 612: 361-372.

Montgomery, H. and Pierce, J.A. (1937). The site of acidification of the urine within the renal tubules in amphibia. Am. J. Physiol. 118: 144-152.

Morel, F. and Roinel, M. (1969). Application de la microsonde electronique a l'analyse elementaire quantitative d'echantillons liquides d'un volume inferieur a 10^{-9} l. J. Chim. Physique 66: 1084-1091.

Murer, H. and Kinne, R. (1980). The use of isolated membrane vesicles to study epithelial transport processes. J. Memb. Biol. 55: 81-95.

O'Donnell, M.J., Maddrell, S.H.P. and Gardiner, B.O.C. (1983). Transport of uric acid by the Malpighian tubules of Rhodnius prolixus and other insects. J. Exp. Biol., in press.

Ogden, T.E., Citron, M.C. and Pierantoni, R. (1978). The jet stream microelectrode beveler: an inexpensive way to bevel ultra-fine glass micropipettes. Science 200: 469-470.

Okumura, J.-I. and Tasaki, I. (1968). Urinary nitrogen excretion in fowls fed acid or alkali. J. Nutr. 95: 148-152.

O'Regan, M.G., Malnic, G. and Giebisch, G. (1982). Cell pH and luminal acidification in Necturus proximal tubule. J. Memb. Biol. 69: 99-106.

Park, C.S., Campen, T.J. and Fanestil, D.D. (1981). Is "H^+-ATPase" involved in proton transport in urinary epithelia? Fed. Proc. 40: 374.

Parsons, D.S. (1982). Role of anions and carbonic anhydrase in epithelia. Phil. Trans. R. Soc. Lond. B 299: 369-381.

Pequeux, A. and Gilles, R. (1981). Na^+ fluxes across the isolated perfused gills of the Chinese crab Eriocheir sinensis. J. Exp. Biol. 92: 173-186.

Phillips, J.E. (1961). Rectal absorption of water and salts in the locust and blowfly. Ph.D. thesis, University of Cambridge, England.

Phillips, J.E. (1980). Epithelial transport and control in recta of terrestrial insects. In "Insect Biology in the Future" (ed. M.C. Locke and D.S. Smith) pp. 145-177. New York: Academic.

Phillips, J. (1981). Comparative physiology of insect renal function. Am. J. Physiol. 241: R241-R257.

Phillips, J.E. and Bradley, T.J. (1977). Osmotic and ionic regulation in saline-water mosquito larvae. In "Transport of Ions and Water in Animals" (ed. B.L. Gupta, R.B. Moreton, J.L. Oschman and B.J. Wall) pp. 709-734. New York: Academic Press.

Phillips, J.E. and Dockrill, A.A. (1968). Molecular sieving of hydrophilic molecules by the rectal intima of the desert locust (Schistocerca gregaria). J. Exp. Biol. 48: 521-532.

Phillips, J.E. and Maddrell, S.H.P. (1974). Active transport of magnesium by the Malpighian tubules of the larvae of the mosquito Aedes campestris. J. Exp. Biol. 61: 761-771.

Phillips, J.E. and Meredith, J. (1969). Active sodium and chloride transport by anal papillae of a salt water mosquito larva (Aedes campestris). Nature 222: 168-169.

Phillips, J.E., Bradley, T.J. and Maddrell, S.H.P. (1978). Mechanisms of ionic and osmotic regulation in saline-water mosquito larvae. In "Comparative Physiology - Water, Ions and Fluid Mechanics (ed. K. Schmidt-Nielsen, L. Bolis and S.H.P. Maddrell) pp. 151-171. Cambridge: Cambridge Univ. Press.

Pitts, R.F. (1934). Urinary composition in marine fish. J. Cell. Comp. Physiol. 4: 389-395.

Pitts, R.F. (1948). Renal excretion of acid. Fed. Proc. 7: 418-426.

Pitts, R.F. (1973). Production and excretion of ammonia in relation to acid-base regulation. In "Handbook of Physiology. Renal Physiology" (ed. J. Orloff and R.W. Berliner) sect. 8, pp. 455-496. Washington, D.C.: American Physiological Society.

Potts, W.T.W. (1977). Fish Gills. In "Transport of Ions and Water in Animals" (ed. B.L. Gupta, R.B. Moreton, J.L. Oschman and B.J. Wall) pp. 453-480. London: Academic Press.

Powell, D.W. (1979). Transport in large intestine. In "Membrane Transport in Biology" (ed. G. Giebisch, D.C. Tosteson and H.H. Ussing) Vol. IV B, pp. 781-809. Heidelberg: Springer-Verlag.

Powell, D.W. (1981). Barrier function of epithelia. Am. J. Physiol. 241: G275-G288.

Prager, D.J., Bowman, R.L. and Vurek, G.G. (1965). Constant volume, self-filling nanoliter pipette: construction and calibration. Science 147: 606-608.

Prashad, D.N. and Edwards, N.A. (1973). Phosphate excretion in the laying fowl. Comp. Biochem. Physiol. 46A: 131-137.

Pressley, T.A. and Graves, J.S. (1980). Amiloride-sensitive net ammonium efflux in the blue crab. Fed. Proc. 39: 587.

Prusch, R.D. (1971). The site of ammonia excretion in the blowfly larva Sarcophaga bullata. Comp. Biochem. Physiol. 39A: 761-767.

Prusch, R.D. (1972). Secretion of NH_4Cl by the hindgut of Sarcophaga bullata larva. Comp. Biochem. Physiol. 41A: 215-233.

Prusch, R.D. (1975). Unidirectional ion movements in the hindgut of larval Sarcophaga bullata (Diptera: Sarcophagidae). J. Exp. Biol. 63: 89-101.

Ramsay, J.A. (1956). Excretion by the Malpighian tubules of the stick insect, Dixippus morosus (Orthoptera, Phasmidae): calcium, magnesium, chloride, phosphate and hydrogen ions. J. Exp. Biol. 23: 697-708.

Ramsay, J.A., Brown, R.H.J. and Croghan, P.C. (1955). Electrometric titration of chloride in small volumes. J. Exp. Biol. 32: 822-829.

Randall, D.J. and Wood, C.M. (1981). Carbon dioxide excretion in the land crab (Cardisoma carnifex). J. Exp. Zool. 218: 37-44.

Rector, F.C. (1976). Renal acidification and ammonia production; chemistry of weak acids and bases; buffer mechanisms. In "The Kidney" (ed. B.M. Brenner and F.C. Rector) 1st ed., Vol. 1, pp. 318-343. Philadelphia: W.B. Saunders Co.

Reeves, W., Gluck, S. and Al-Awqati, Q. (1983). Role of endocytosis in H^+ secretion (J_H) regulation by turtle bladder. Kidney Intl. 23: 237.

Rehm, W.S. and Sanders, S.S. (1975). Implications of the neutral carrier Cl^- - HCO_3^- exchange mechanism in gastric mucosa. Ann. N.Y. Acad. Sci. 264: 442-455.

Reite, O.B., Maloiy, G.M.O. and Aasehaug, B. (1974). pH, salinity and temperature tolerance of Lake Magadi Tilapia. Nature 247: 315.

Richardson, R.M.A. and Kunau, R.T. (1981). Bicarbonate reabsorption by the rat papillary collecting duct: effect of acetazolamide. Kidney Intl. 19: 254.

Robertson, D.R. (1972). Influence of the parathyroids and ultimobranchial glands in the frog (Rana pipiens) during respiratory acidosis. Gen. Comp. Endocrinol. Suppl. 3: 421-429.

Robinson, J.R. (1975). "Fundamentals of Acid-Base Regulation," 5th ed. London: Blackwell Scientific Publications.

Robinson, R.A. and Stokes, R.H. (1965). "Electrolyte solutions" 3rd ed. London: Buttersworth.

Roinel, M. (1975). Electron microprobe quantitative analysis of lyophilised 10^{-10} 1 volume samples. J. Microsc. Cell. Biol. 22: 261-267.

Roos, A. and Boron, W.F. (1981). Intracellular pH. Physiological Rev. 61: 296-434.

Sachs, G., Faller, L.D. and Rabon, E. (1982). Proton/hydroxyl transport in gastric and intestinal epithelia. J. Memb. Biol. 64: 123-135.

Sachs, G., Spenney, J.G. and Lewin, M. (1978). H^+ transport: regulation and mechanisms in gastric mucosa and membrane vesicles. Physiol. Rev. 58: 106-173.

Sachs, G., Rabon, E., Stewart, H.B., Peerce, B., Smolka, A. and Saccomani, G. (1980). Gastric glands and vesicles: II. Vesicles. In "Hydrogen Ion Transport in Epithelia" (ed. I. Schulz, G. Sachs, J.G. Forte and K.J. Ullrich) pp. 135-143. Amsterdam: Elsevier.

Saito, Y. and Wright, E.M. (1982). Cyclic-AMP stimulation of HCO_3 secretion by frog choroid plexus. Physiologist 25: 296.

Saito, Y. and Wright, E.M. (1983). Cyclic-AMP stimulation of HCO_3 transport across choroid plexus - a microelectrode study. Fed. Proc. 42: 1283.

Sanders, D. and Slayman, C.C. (1982). Control of intracellular pH: predominant role of oxidative metabolism, not proton transport, in the eukaryotic microorganism Neurospora. J. Gen. Physiol. 89: 377-402.

Sasaki, S. and Berry, C.A. (1983). Mechanism of HCO_3^- exit across the basolateral membrane of rabbit proximal convoluted tubules. Kidney Intl. 23: 238.

Satake, N., Durham, J.H. and Brodsky, W.A. (1981). Reversal of the luminal acidification current by a phosphodiesterase inhibitor in the turtle bladder: evidence for active electrogenic bicarbonate secretion. In "Membrane Biophysics: Structure and Function in Epithelia" (ed. M.A. Dinno and A.B. Gallahan) pp. 13-24. New York: Alan R. Liss.

Satake, N., Durham, J.H. and Brodsky, W.A. (1982). Separate electrogenic pumps for HCO_3^- secretion and reabsorption in turtle bladders. Fed. Proc. 41: 981.

Sauveur, B. (1969). Acidoses metaboliques experimentales chez la poul Pondeuse. I. Action sur l'equilibre acido-basique du sang et l'excretion renale des electrolytes. Ann. Biol. anim. Bioch. Biophys. 9: 379-391.

Scheid, P., Hook, C. and Bridges, C.R. (1981). Diffusion in gas exchange of insects. Fed. Proc. 41: 2143-2145.

Scheide, J.I. and Dietz, T.H. (1982). The effects of independent sodium and chloride depletion on ion balance in freshwater mussels. Can. J. Zool. 60: 1676-1682.

Scherer, N.M. (1977). The function of the anal papillae of saline-water mosquito larvae. M.Sc. thesis, University of British Columbia, Vancouver, B.C.

Schmidt-Nielsen, B. and Skadhauge, E. (1967). Function of the excretory system of the crocodile (Crocodylus acutus). Am. J. Physiol. 212: 973-980.

Schulz, I. (1976). Pancreatic bicarbonate transport. In "Gastric Hydrogen Ion Secretion" (ed. D.K. Kasbekar, G. Sachs and W.S. Rehm) Vol. 3, pp. 363-379. New York: Marcel Dekker Inc.

Schulz, I. (1981). Electrolyte and fluid secretion in the exocrine pancreas. In "Physiology of the Gastrointestinal Tract" (ed. L.R. Johnson) Vol. 2, pp. 795-819. New York: Raven Press.

Schulz, I. and Ullrich, K.J. (1979). Transport processes in the exocrine pancreas. In "Membrane Transport in Biology" (ed. G. Giebisch, D.C. Tosteson and H.H. Ussing) Vol. IV B, pp. 811-852. Berlin: Springer-Verlag.

Schultz, S.G. (1981a). Ion transport by mammalian large intestine. In "Physiology of the Gastrointestinal Tract" (ed. L.R. Johnson) Vol. 2, pp. 991-1002. New York: Raven Press.

Schultz, S.G. (1981b). Homocellular regulatory mechanisms in sodium-transporting epithelia: avoidance of extinction by "flush-through". Am. J. Physiol. 241: F579-F590.

Schultz, S.G. and Curran, P.F. (1970). Coupled transport of sodium and organic solutes. Physiol. Rev. 50: 637-718.

Schwartz, J.H., Rosen, S. and Steinmetz, P.R. (1972). Carbonic anhydrse function and the epithelial organization of H^+ secretion in turtle urinary bladder. J. Clin. Invest. 51: 2653-2662.

Scudder, G.G.E. (1969). The fauna of saline lakes on the Fraser Plateau in British Columbia. Verh. Internat. Verein. Limnol. 17: 430-439.

Sheerin, H.E. and Field, M. (1975). Ileal HCO_3 secretion: relationship to Na and Cl transport and effect of theophyllina. Am. J. Physiol. 228: 1065-1074.

Siesjö, B.K. and Kjallquist, Å. (1969). A new theory for the regulation of the extracellular pH in the brain. Scand. J. Clin. Lab. Invest. 24: 1-9.

Simkiss, K. (1970). Sex differences in the acid-base balance of adult and immature fowl. Comp. Biochem. Physiol. 34: 777-788.

Simson, J.N.L., Merhav, A. and Silen, W. (1981a). Alkaline secretion by amphibian duodenum. I. General characteristics. Am. J. Physiol. 240: G401-G408.

Simson, J.N.L., Merhav, A. and Silen, W. (1981b). Alkaline secretion by amphibian duodenum. II. Short-circuit current and Na^+ and Cl^- fluxes. Am. J. Physiol. 240: G472-G479.

Smith, W.W. (1939). The excretion of phosphate in the dogfish Squalus acanthias. J. Cell. Comp. Physiol. 14: 95-102.

Speight, J. (1967). Acidification of rectal fluid in the locust, Schistocerca gregaria. M.Sc. thesis, University of British Columbia, Vancouver, B.C.

Spring, K.R. and Ericson, A. (1982). Epithelial cell volume modulation and regulation. J. Memb. Biol. 69: 167-176.

Spring, K.R. and Kumura, G. (1978). Chloride reabsorption by renal proximal tubules of Necturus. J. Memb. Biol. 38: 233-254.

Steels, P.S. and Boulpaep, E.L. (1976). Effect of pH on ionic conductances of the proximal tubule epithelium of Necturus and the role of buffer permeability. Fed. Proc. 35: 465.

Steinmetz, P.R. (1974). Cellular mechanisms of urinary acidification. Physiological Rev. 54: 890-956.

Steinmetz, P.R. and Anderson, O.S. (1982). Electrogenic proton transport in epithelial membranes. J. Memb. Biol. 65: 155-174.

Stetson, D.L. and Steinmetz, P.R. (1982). CO_2 stimulation of vesicle fusion in turtle bladder epithelium. Fed. Proc. 41: 1263.

Stobbart, R.H. (1967). The effect of some anions and cations upon the fluxes and net uptake of chloride in the larva of Aedes aegypti (L.), and the nature of the uptake mechanisms for sodium and chloride. J. Exp. Biol. 47: 35-57.

Stobbart, R.H. (1971). Evidence for Na^+/H^+ and Cl^-/HCO_3^- exchanges during independent sodium and chloride uptake by the larva of the mosquito Aedes aegypti (L.). J. Exp. Biol. 54: 19-27.

Stobbart, R.H. and Shaw, J. (1974). Salt and water balance: excretion. In "The Physiology of Insecta" (ed. M. Rockstein) Vol. 5, pp. 362-446. New York: Academic Press.

Stoeckenius, W. (1976). The purple membrane of salt-loving bacteria. Sci. Am. 234: 38-46.

Stoeckenius, W., Lozier, R.H. and Bogomolni, R.A. (1979). Bacteriorhodopsin and the purple membrane of Halobacteria. Biochim. Biophys. Acta 505: 215-278.

Stoff, J.S., Epstein, F.H., Narins, R. and Relman, A.S. (1976). Recent advances in renal tubular biochemistry. Ann. Rev. Physiol. 38: 46-68.

Strange, K., Phillips, J.E. and Quamme, G.A. (1982). Active HCO_3^- secretion in the rectal salt gland of a mosquito larva inhabiting $NaHCO_3$-CO_3 lakes. J. Exp. Biol. 101: 171-186.

Sutton, R.A.L., Quamme, G.A. and Dirks, J.H. (1979). Transport of calcium, magnesium and inorganic phosphate in the kidney. In "Membrane Transport in Biology" (ed. G. Giebisch, D.C. Tosteson and H.H. Ussing) Vol. IV A, pp. 357-412. Heidelberg: Springer-Verlag.

Swanson, C.H. and Solomon, A.K. (1972). Evidence for Na-H exchange in the rabbit pancreas. Nature New Biology 236: 183-184.

Swanson, C.H. and Solomon, A.K. (1973). A micropuncture investigation of the whole tissue mechanisms of electrolyte secretion by the in vitro rabbit pancreas. J. Gen. Physiol. 62: 407-429.

Swanson, C.H. and Solomon, A.K. (1975). Micropuncture analysis of the cellular mechanisms of electrolyte secretion by the in vitro rabbit pancreas. J. Gen. Physiol. 65: 22-45.

Szibbo, C.M. and Scudder, G.G.E. (1979). Secretory activity of the segmented Malpighian tubules of Cencorixa bifida (Hung.) (Hemiptera, Corixidae). J. Insect Physiol. 25: 931-937.

Tannen, R. (1978). Ammonia metabolism. Am. J. Physiol. 235: F265-F277.

Thomas, R.C. (1980). Reversal of the pH_i-regulating system in a snail neuron. In "Current Topics in Membranes and Transport" (ed. E.L. Boulpaep) Vol. 13, pp. 23-29. New York: Academic Press.

Thomas, R.C. (1982). Snail neuron intracellular pH regulation. In "Intracellular pH: Its Measurement, Regulation and Utilization in Cellular Functions" (ed. R. Nuccitelli and D. Deamer) pp. 189-204 New York: Alan R. Liss, Inc.

Topping, M.S. and Scudder, G.G.E. (1977). Some physical and chemical features of saline lakes in central British Columbia. Syesis 10: 145-166.

Truchot, J.-P. (1979). Mechanisms of the compensation of blood respiratory acid-base disturbances in the shore crab, Carcenics maenas (L.). J. Exp. Zool. 210: 407-416.

Turnberg, L.A., Bieberdorf, F.A., Morawski, S.G. and Fordtran, J.S. (1970). Interrelationships of chloride, bicarbonate, sodium and hydrogen transport in the human ileum. J. Clin. Invest. 49: 557-567.

Turnberg, L.A., Fordtran, J.S., Carter, N.W. and Rector, F.C. (1970). Mechanisms of bicarbonate absorption and its relationship to sodium transport in the human jejunum. J. Clin. Invest. 49: 548-556.

Ullrich, K.J., Radtke, H.W. and Rumrich, G. (1971). The role of bicarbonate and other buffers on isotonic fluid absorption in the proximal convolution of the rat kidney. Pflügers Arch. 330: 149-161.

Ullrich, K.J., Rumrich, G. and Baumann, K. (1975). Renal proximal tubular buffer-(glycodiazine) transport. Inhomogencity of local transport rate, dependence on sodium, effect of inhibitors and chronic adaptation. Pflügers Arch. 357: 149-163.

Vanatta, J.C. and Frazier, L.W. (1980). In vivo excetion of NH_4^+ by the skin of Rana pipiens during various states of acid-base balance. Fed. Proc. 39: 739.

Vanatta, J.C. and Frazier, L.W. (1981). The epithelium of Rana pipiens excretes H^+ and NH_4^+ in acidosis and HCO_3^- in alkalosis. Comp. Biochem. Physiol. 68A: 511-513.

Vaughan-Jones, R.D. (1979). Regulation of chloride in quiescent sheep-heart Purkinjie fibers studied using intracellular chloride and pH-sensitive microelectrodes. J. Physiol. 295: 111-137.

Vaughan-Jones, R.D. (1982). Chloride-bicarbonate exchange in the sheep cardiac Purkinjie fibre. In "Intracellular pH: Its Measurement, Regulation, and Utilization in Cellular Functions" (ed. R. Nuccitelli and D. Deamer) pp. 239-252. New York: Alan R. Liss, Inc.

Viera, F.L. and Malnic, G. (1968). Hydrogen secretion by rat renal cortical tubules as studied by an antimony microelectrode. Am. J. Physiol. 214: 710-718.

Vinay, P., Lemieux, G. and Gougoux, A. (1979). Characteristics of glutamine metabolism by rat kidney tubules: a carbon and nitrogen balance. Can. J. Biochem. 57: 346-356.

Vurek, G.G., Warnock, D.G. and Corsey, R. (1975). Measurement of picomole amounts of carbon dioxide by calorimetry. Anal. Chem. 47: 765-767.

Wade, J.B. (1980). Hormonal modulation of epithelial structure. In "Current Topics in Membranes and Transport" (ed. E.L. Boulpaep) Vol. 13, pp. 124-147. New York: Academic Press.

Wolbach, R.A. (1955). Renal regulation of acid-base balance in the chicken. Am. J. Physiol. 181: 149-156.

Wood, C.M. and Caldwell, F.H. (1978). Renal regulation of acid-base balance in a freshwater fish. J. Exp. Zool. 205: 301-307.

Wright, EM. (1972). Mechanisms of ion transport across the choroid plexus. J. Physiol. 226: 545-571.

Wright, E.M. (1977). Effect of bicarbonate and other buffers on choroid plexus Na^+/K^+ pump. Biochim. Biophys. Acta 468: 486-489.

Yoshimura, H., Yata, M., Yuasa, M. and Wolbach, R.A. (1961). Renal regulation of acid-base balance in the bullfrog. Am. J. Physiol. 201: 980-986.

Youmans, S., Worman, H. and Brodsky, W. (1982). ATP-dependent accumulation of protons in membrane vesicles from turtle bladder epithelial cells. Fed. Proc. 41: 981.

Youmans, S.J., Worman, H. and Brodsky, W.A. (1983). ATPase catalyzed proton pumping in plasma membrane vesicles from turtle bladder epithelia. Fed. Proc. 42: 1352.

Young, J.A. and van Lennep, E.W. (1979). Transport in salivary and salt glands. In "Membrane Transport in Biology" (ed. G. Giebisch, D.C. Tosteson and H.H. Ussing) Vol. IV B, pp. 563-692. Berlin: Springer-Verlag.